3 1176 00031 4121

29 APR 1948

NACA TN No. 1404

NATIONAL ADVISORY COMMITTEE FOR AERONAUTICS

TECHNICAL NOTE

No. 1404

COLLECTION OF TEST DATA FOR LATERAL CONTROL WITH FULL-SPAN FLAPS

By Jack Fischel and Margaret F. Ivey

Langley Memorial Aeronautical Laboratory
Langley Field, Va.

FOR REFERENCE

NOT TO BE TAKEN FROM THIS ROOM

Washington
April 1948

LIBRARY COPY

APR 0 1993

LANGLEY RESEARCH CENTER
LIBRARY NASA
HAMPTON, VIRGINIA

NACA LIBRARY
LANGLEY MEMORIAL AERONAUTICAL LABORATORY
Langley Field, Va.

NATIONAL ADVISORY COMMITTEE FOR AERONAUTICS

TECHNICAL NOTE NO. 1404

COLLECTION OF TEST DATA FOR LATERAL CONTROL WITH FULL-SPAN FLAPS

By Jack Fischel and Margaret F. Ivey

SUMMARY

A collection of the available test data on lateral control with full-span flaps is presented. Lateral-control effectiveness and hinge-moment data obtained from two-dimensional, three-dimensional, and flight tests are presented in the form of figures and the data include the characteristics of spoiler devices and ailerons with retractable flaps. The basic data presented on the various flap and aileron combinations should facilitate the design of full-span-flap lateral-control arrangements. A discussion is given of the characteristics of the lateral-control devices considered and of the application of the data to specific airplane design.

INTRODUCTION

One of the problems arising from the increased speed and wing loading of modern airplanes is the difficulty of obtaining high lifts for landing and take-off without impairing lateral control. If conventional aileron arrangements are used to satisfy the lateral-control requirements, the flap span is necessarily limited and the problem of obtaining the lift required for take-off or landing becomes quite important. When full-span flaps are used to obtain the desired lift coefficient for the airplane, the designer is faced with the problem of including and properly locating a lateral-control device on the airplane which will be effective in all flight configurations and have characteristics that will not be deleterious or objectionable.

The purpose of the present paper is to give the most pertinent part of the experimental data on the characteristics of lateral-control devices for use with full-span or almost full-span flaps. The data are, necessarily, greatly condensed and some data have been given in a form different from the original source. Additional information on any particular model may be obtained from the references. (See references 1 to 25 and table I.)

Data on conventional balanced ailerons have been reported previously in reference 26, and a collection of fairly large-chord control-surface data has been given in reference 27.

CLASSIFICATION OF DATA

The data are divided into sections as follows:

A Slot-lip and flap-trailing-edge ailerons

B Spoiler-type ailerons other than slot-lip ailerons

C Ailerons with retractable flaps

The lateral-control arrangements for which data are presented may be considered to consist essentially of only two types – ailerons located at the wing trailing edge (conventional ailerons) and devices located forward of the trailing edge (commonly referred to as "spoiler ailerons") – but the division of the data into the three aforementioned groups has been made for convenience of presentation and is purely arbitrary.

In almost all instances, the aileron designation given to the lateral-control device in the reference paper has been used herein. The flap-trailing-edge ailerons of group A therefore are usually termed plain ailerons (regardless of balance) in the figures and in the text. The designation conventional, ordinary, or standard aileron employed in the figures of groups B and C and in the text refers to the more conventional arrangements in use today of an aileron on the wing trailing edge. This aileron usually spans the outboard part of the wing.

Much of the data presented in group C was obtained on models equipped with duplex flap arrangements (two separate flaps) and since the outboard flap of such arrangements would usually retract into the airfoil contour ahead of the aileron for the flaps-up configuration, the data are representative of retractable-flap aileron arrangements and may be applied in the design of such arrangements.

SYMBOLS

C_L lift coefficient

$C_{m_{c/4}}$ pitching-moment coefficient about quarter chord of wing

$\Delta C_{m_{c/4}}$ increment of pitching-moment coefficient about quarter chord of wing

ΔC_D increment of drag coefficient

C_l' rolling-moment coefficient about axis in plane of symmetry of complete model or airplane, referred to wind axes

C_n' yawing-moment coefficient about axis in plane of symmetry of complete model or airplane, referred to wind axes

C_h hinge-moment coefficient

$C_h = \frac{H}{q_o b_a \bar{c}_a^2}$ for plain and slot-lip ailerons and plate spoilers

$C_h = \frac{H}{q_o M}$ for plug ailerons where M is area moment of top edge about hinge line

$C_h = \frac{H}{q_o R_m t b_s}$ for retractable ailerons

where

R_m mean radius of retractable aileron, feet

t thickness of retractable aileron, feet

b_s span of retractable aileron, feet

C_{l_p} rate of change of rolling-moment coefficient C_l' with helix angle $pb/2V$

c_l section lift coefficient

Δc_l increment of section lift coefficient

Δc_{d_o} increment of section profile-drag coefficient

$c_{m_{c/4}}$ section pitching-moment coefficient about quarter chord of airfoil

c_h section hinge-moment coefficient

$c_h = \frac{h_a}{q_o \bar{c}_a^2}$ for plain and slot-lip ailerons

$c_h = \frac{h}{q_o R_m t}$ for retractable ailerons

P pressure coefficient $\left(\frac{p_l - p_o}{q_o}\right)$

$(v/V)^2$ pressure coefficient $(1 - P)$

c wing chord; also used with subscripts to denote components of wing

$\bar{c}$ chord of a control surface rearward of the hinge axis

b wing span; also used with subscripts to denote components of wing

α angle of attack, degrees

α_o section angle of attack, degrees

$\Delta\alpha$ effective change in angle of attack, degrees

δ deflection, degrees

ϕ angle of roll, degrees

k aileron effectiveness factor, effective change in angle of attack of wing-aileron section per unit aileron deflection $(\Delta\alpha/\Delta\delta)$

A aspect ratio

λ ratio of tip chord to root chord

y_i distance from plane of symmetry to inboard end of flap or lateral-control device, feet

y_o distance from plane of symmetry to outboard end of flap or lateral-control device, feet

q_o free-stream dynamic pressure, pounds per square foot

p_l static pressure at a point on the airfoil, pounds per square foot

p_o free-stream static pressure, pounds per square foot

V true airspeed, feet per second

V_{i_s} service indicated airspeed, miles per hour

v local velocity, feet per second

p rolling angular velocity, radians per second

r yawing angular velocity, radians per second

$pb/2V$ helix angle generated by wing tip in a roll, radians

H	hinge moment of a control surface about hinge axis, foot pounds
h	section hinge moment of a control surface, foot pounds
F_s	stick force, pounds
F_w	wheel force, pounds
M	Mach number
R	Reynolds number
x/c	distance from leading edge of wing to protruding edge of flat-plate spoiler-type ailerons or to chordwise position of emergence from wing of retractable and plug ailerons

Subscripts:

a	aileron
f	flap
f_1	inboard flap
f_2	outboard flap
w	wing
sl	slot lip
sp	spoiler
p	plain, plug, or plate
s	stick
max	maximum

Supplementary information and the test conditions for models and airplanes are given in table I. This table also gives published references and serves as an index to the results presented, because the model or airplane designation is given in the first column of the table and in the upper right-hand corner of each page of model drawings or test results.

CORRECTIONS

The larger part of the data was plotted as taken from the source and the plotting scale for the data is necessarily nonuniform. The data obtained on models A-V and A-VI, B-VII, B-VIII, B-IX, B-XI, and B-XII, and C-III were corrected for jet-boundary effects according to the methods outlined in reference 28 and were plotted as corrected. A reduction of approximately 10 percent in the rolling-moment coefficients of model B-XV was estimated but not applied. Corrections to the data of model C-IV and C-V are unknown because of the uncertainty of end-plate effects. It is not known whether corrections were made to the data of model B-X. Some of the hinge-moment data was given in inch-pounds in the references but was reduced to coefficient form for the present paper.

DISCUSSION

All the lateral-control arrangements for which data are presented herein consist of either a conventional flap-type aileron, some device of the spoiler type, or a combination of both. (See table I and figs. A1 to A33, B1 to B133, and C1 to C49.) The characteristics of flap-type ailerons with flaps retracted, such as the flap-trailing-edge (plain) ailerons of group A and the ailerons of group C, were identical with the aileron characteristics of conventional arrangements and have been summarized previously (references 26 and 29). With full-span flaps deflected the characteristics of these ailerons differed from the characteristics of the ailerons in the flap-retracted condition and are discussed herein in the sections entitled "Slot-Lip and Flap-Trailing-Edge Ailerons" and "Ailerons with Retractable-Type Flaps".

Lateral-control devices located forward of the wing trailing edge are generally termed "spoilers" or "spoiler ailerons". There are four main types of spoiler ailerons - the retractable aileron, which consists of a circular-arc spoiler that usually emerges only from the upper surface of the wing; the plug aileron, which fits into a slot in the wing when in the neutral position and leaves this slot open when deflected upward; the hinged-flap-type spoiler aileron or upper-surface aileron, which lies along and forms part of the wing contour when in the neutral position; and the slot-lip aileron, which also lies along and forms part of the wing contour when in the neutral position and which has a fixed wing slot behind it.

Almost all spoiler-type devices have certain common characteristics that are dependent on the wing, aileron, and flap configuration. When spoilers were located near the wing leading edge, their effectiveness was roughly proportional to the lift coefficient; large rolling moments were provided at large angles of attack. As these devices were moved toward the wing trailing edge, the effectiveness became more nearly independent of lift coefficient (remained almost constant or increased slightly at small angles of attack and decreased at large angles of attack) and became more nearly linear with respect to spoiler projection (figs. A7 to A10, A26, A27, and B18 to B20 and references 2, 8, and 30). Data obtained from both wind-tunnel and flight tests at low values of Mach and Reynolds numbers indicated that small spoiler deflections or projections (of the order of 0.01c or less) generally had little or no effect in producing roll when the wing was not slotted in the spoiler vicinity (figs. A12, B12 to B14, B32 to B39, B44 to B50, B95, B117, B118, and B123). Slotting the wing from the lower to the upper surfaces to the rear of the spoiler improved the rolling effectiveness, particularly at large angles of attack (figs. B44 to B47 and B95 and reference 10), and the linearity with respect to projection (fig. B95) with flaps retracted or deflected. Spoiler controls, especially those located far forward on the wing, were quite effective in the low-speed-flight range near and slightly beyond the stall, because of their pronounced effect in reducing lift or reducing the effective angle of attack over the wing section affected by their action.

Tests of spoiler ailerons at various chordwise locations indicated a perceptible time lag in the rolling response for forward spoiler locations and this time lag decreased as the spoiler was moved rearward. Slotting the wing behind the spoiler further reduced the lag in the response of the airplane to control deflection. At spoiler locations to the rear of about 0.60c, this time lag becomes imperceptible to pilots and hence unobjectionable at low and moderate values of Mach and Reynolds numbers (figs. B27, B28, B80, B82, B100, B112, B113, and B114, and references 2, 9, 14, 16, and 30). (The first part of the curve of the time-response figs. B27 and B28 is indicative of the lag whereas the last part of the curve is indicative of the steady state of roll.) In high-speed flight, time lag may not be noticeable for forward spoiler locations and the use of forward locations would provide increased aileron effectiveness; however, the possibility exists for reversal of effectiveness for small spoiler projections.

Spoilers provide less pitching moment than conventional ailerons (figs. B7, B10, B14, B19, B20, and B69 and reference 31) and hence would be expected to produce lower wing stresses and to have higher reversal speeds. In addition, spoilers provide favorable yawing moments over most of the flight range, except possibly at high angles of attack or lift, where the adverse yaw produced is less than that obtained with conventional ailerons.

The hinge-moment characteristics of spoilers are very unusual over the spoiler deflection range and require special treatment to provide acceptable control forces.

Since spoiler control is obtained through a loss of lift on one wing whereas almost no effect is produced on the other wing, some difficulty may be encountered in raising a wing that had dropped.

This problem is not serious, however, since the axis of rotation with spoiler control is seldom farther outboard than $0.20\frac{b}{2}$ from the plane of symmetry.

Slot-Lip and Flap-Trailing-Edge Ailerons

The test conditions and the results of tests conducted on models and airplanes equipped with slot-lip and flap-trailing-edge ailerons and full-span flaps are given in table I-A and in figures A1 to A33. Data obtained in two-dimensional wind-tunnel tests are shown in figures A1 to A5, three-dimensional wind-tunnel test data are shown in figures A6 to A25, and flight data are presented in figures A26 to A33.

Slot-lip ailerons.- Both wind-tunnel and flight tests of slot-lip ailerons at various chordwise positions have indicated that the most satisfactory position of the slot-lip aileron, from both aerodynamic and structural considerations, is between 0.7c and 0.8c. When slot-lip ailerons are used in conjunction with a slotted flap, a convenient arrangement having satisfactory characteristics consists of a slot-lip aileron located on the lip of the wing slot, ahead of the flap. Because of the physical impossibility of obtaining positive aileron deflections in this position with the flaps retracted, a high differential stick linkage (probably a cam) would be required in the control system.

Wind-tunnel and flight data also indicate that the effectiveness of slot-lip ailerons (figs. A1 to A33) increases with slotted-flap deflection and that these ailerons are very effective at large flap deflections; however, the ailerons are not very effective in the flaps-up condition. The data generally indicate a sharp increase in aileron effectiveness for small and moderate aileron deflections (flaps deflected) with a decreasing increment in effectiveness at larger deflections.

The hinge moments produced by slot-lip ailerons indicate an opening tendency of the aileron near neutral which, coupled with the large differential required, may cause overbalance of the controls. In the flight tests of slot-lip ailerons on a fighter-type airplane (figs. A28 to A33 and reference 5), a spring was introduced into the lateral-control system to counteract the overbalancing tendency of the ailerons. In general, if such adverse hinge-moment effects are encountered, balancing of the control surface or modification of the control linkage probably would result in satisfactory slot-lip-aileron control forces in all flight conditions. If slot-lip ailerons are used on extremely large airplanes, some aerodynamic balance would be required to reduce the large hinge moments at the large aileron deflections.

Flap-trailing-edge ailerons.- When flap-trailing-edge (plain) ailerons were tested in the presence of full-span slotted flaps, the ailerons were necessarily only about 0.10c because of structural considerations and had large spans in order to provide adequate effectiveness (figs. A1 to A33). In the flap-retracted position, the aileron is a narrow-chord long-span aileron. (See reference 26.) In flap-down operation, the aileron effectiveness decreased in the positive aileron-deflection range and generally increased slightly in the negative aileron-deflection range as the flap deflection increased (figs. A3, A5, A14, and A21). A change in the control linkage to provide a greater negative and smaller positive aileron deflection, and probably a greater total aileron deflection, therefore would be desirable to provide adequate lateral control for flap-down operation, if equal up and down deflections were used with flaps up.

The plain ailerons, flaps down, have about the same value for the rate of change of hinge-moment coefficient with aileron deflection as the ailerons with flaps retracted. Plain ailerons also have an upfloating tendency at aileron neutral, flaps deflected. This upfloating tendency, coupled with the differential required for good control, will help to reduce the stick forces but may cause overbalance if the differential for flaps down is too severe. The adverse yawing moments produced by aileron deflection, flaps deflected, were larger than those produced by other lateral controls.

Slot-lip and flap-trailing-edge aileron combination.- The characteristics exhibited by slot-lip and plain ailerons when each is used alone indicate that a lateral-control system consisting of both types of aileron - that is, plain ailerons for flaps-up operation, slot-lip ailerons for flaps-down operation - combines the best qualities of each type. This arrangement requires a mechanism that provides for changing from plain-aileron to slot-lip-aileron operation while extending the flap. Flight tests of such an installation on a fighter-type airplane indicated the adequacy of control provided by this arrangement, particularly in the low-speed range (figs. A28 to A33), and also indicated that some balancing of the ailerons is necessary to provide satisfactory stick-force characteristics over the complete flight range.

Spoiler-Type Ailerons Other Than Slot-Lip Ailerons

Supplementary information and some of the results of various investigations on models equipped with spoiler-type ailerons are given in table I-B and in figures B1 to B133, respectively. Two-dimensional wind-tunnel test data, three-dimensional wind-tunnel test data, and flight data are presented in figures B1 to B14, B15 to B78, and B79 to B133, respectively. Because data were not obtained at small aileron projections in the investigations of models B-II and B-VI, the curves for Δc_l and C_l, respectively, of these models have been faired with dashed lines for these small projections to indicate the probable variations of Δc_l and C_l with projection. These data have been faired thus on the basis of data obtained at small projections in other investigations of similar lateral-control devices.

The spoiler-aileron usually projects above one wing and remains within the airfoil contour or projects slightly below the lower contour on the other wing when the control stick is displaced laterally. When spoilers and conventional ailerons are compared, the fact that the spoiler effectiveness on one wing is comparable to the aileron effectiveness on both wings should therefore be considered. For a given rolling performance the span of the spoiler must therefore be larger than that of a conventional aileron.

Although, as previously indicated, spoiler projections of the order of 0.01c or less produced little or no rolling moment at low Reynolds and Mach numbers, the effectiveness of spoiler controls located at approximately 0.6c or 0.7c usually increased rapidly for projections between 0.02c and 0.07c and increased less rapidly for larger projections. Spoiler data obtained on a low-drag wing at low lift coefficients indicated that an increased rolling moment was provided over the entire projection range and small spoiler projections became more effective as the Mach number increased until shock was obtained (figs. B68 and B69 and reference 13).

Retractable ailerons and hinged-plate-type spoiler ailerons located to the rear of approximately 0.50c were quite effective in the low angle-of-attack range, flaps up, but their effectiveness generally decreased at large angles of attack, probably as a result of flow separation ahead of the spoilers (fig. B14). As previously indicated, slotting the wing behind the spoilers (thus changing the retractable aileron to a plug-type aileron or ventilating the hinged-flap spoiler) improved the effectiveness in the high angle-of-attack range with flaps up (figs. B44 to B47 and B95 and reference 10). Spoiler ailerons generally were more effective with flaps down than in the flap-retracted condition and exhibited a greater effectiveness with slotted flaps than with split flaps (figs. B48 and B49).

The hinge-moment characteristics of spoiler-ailerons generally tend to be somewhat erratic and quite unusual; that is, appreciable moments are provided by the plug-type and hinged-plate-type spoiler ailerons (figs. B30, B76, and B101) and little or no moments are provided by a thin retractable aileron hinged at the center of the spoiler arc (figs. B14, B130, B131, and B133 and references 15 and 16). An appreciable amount of control over the hinge moments, to provide acceptable control forces, can be obtained, however, by such spoiler modifications as varying the thickness of the retractable aileron or installing a plate (hinged or stationary) on top of and normal to the spoiler arc (figs. B33 and B44 to B50), venting or beveling the spoiler (figs. B12 to B14, B57 to B59, and B96), and providing other aerodynamic balance (figs. B110 and B118). With either the hinged plate, the plug, or the thick retractable spoiler ailerons, opening moments were encountered near neutral – an effect produced by the negative pressure existing over the upper surface of the wing (figs. B65 and B66). This condition might be corrected by slotting, venting, or otherwise modifying the spoiler. Control "feel" of the type normally associated with conventional lateral-control surfaces has also been provided by including a short-span conventional aileron, in addition to the spoiler device, in the lateral-control system (figs. B70 to B73 and B124 to B133).

Ailerons with Retractable-Type Flaps

The results of tests and the test conditions of models and airplanes with ailerons in the presence of retractable-type flaps are given in figures C1 to C49 and in table I-C. Three-dimensional wind-tunnel data are presented in figures C1 to C46 and flight data are presented in figures C47 to C49.

When ailerons in the presence of retractable-type flaps were used with duplex flap arrangements, the aileron characteristics obtained with the partial-span inboard flap deflected indicate a slight increase in rolling effectiveness for negative aileron deflections compared with that obtained with flap retracted and an increase in the variation of hinge-moment coefficient with aileron deflection (figs. C8, C9, C11, and C24). Because of the low speed in this attitude, the stick forces should not be critical.

The characteristics of ailerons in the presence of flaps spanning the same part of the wing as the ailerons are affected by the positions and deflections of these flaps and also by the contour of the flap. Wind-tunnel investigations indicated that deflecting a plain split flap in front of an aileron had a blanketing effect on the aileron and resulted in a decrease in rolling effectiveness as well as a decrease in the adverse yaw and the hinge moments (figs. C3 to C11 and C30 to C34). Various tests of balanced split or retractable-type flaps ahead of ailerons showed that this loss in rolling effectiveness decreased when the flap was moved downward away from the wing contour, and also rearward, so as to avoid complete blanketing of the aileron (figs. C15, C22 to C29, and C47 to C49). In general, however, the rolling effectiveness obtained with the outboard flap deflected and located forward of the aileron hinge line was less than that obtained with the flap retracted (figs. C23 and C27).

Locating the flap to the rear of the aileron hinge line and several percent chord below the wing contour increased the effectiveness above that obtained in the flap retracted condition; and the effectiveness of the upgoing aileron was particularly good when the flap was located near and slightly below the aileron trailing edge (figs. C1, C2, and C22 to C29). When the flap is located rearward of the aileron hinge line and in close proximity to the aileron, the positive aileron deflections should be restricted because of the deleterious effects (sudden loss in effectiveness and reversal of hinge-moment slope) obtained. (See reference 22.) This decreased deflection is compensated for in part by the increased effectiveness of the upgoing aileron (figs. C24 and C29 and reference 22). When the flap was moved rearward and deflected, the lift characteristics improved considerably (references 21 and 22), particularly when the configuration of model C-VIII had the flap at the wing trailing edge. An indication of the flap loads on the outboard flap at various flap positions and deflections and at various aileron deflections is given in the pressure-distribution data obtained on model C-V (figs. C16 to C18).

When the flap was located and deflected forward of the aileron hinge and partly blanketed the aileron, the aileron hinge moments indicated a down-floating tendency (figs. C8 to C11, C15, and C21), and this down-floating tendency decreased and became an up-floating tendency as the flap moved rearward (fig. C24 and references 21 and 22). The hinge-moment-coefficient deflection slope generally increased negatively with increased aileron effectiveness, flaps down, and particularly for positive aileron deflections.

The adverse yawing effect usually produced by conventional aileron arrangements was also evident when a flap was employed over the same span as the aileron. This adverse yaw was appreciable when the flap was located near the wing trailing edge and at high values of wing lift coefficient (figs. C24 and C29).

Application of Data to Specific Airplane Design

The data presented herein have not been correlated to provide design charts for full-span flap-aileron installations, as they are intended primarily for illustrating the effects of full-span flaps on various lateral-control devices. Design charts for conventional ailerons, such as the plain ailerons of group A and the ailerons of group C, have been presented in references 29 and 32 to 35, and it is expected that full-span flaps would not prevent use of the charts in aileron design except for aileron effectiveness with flap deflected. When flaps are deflected, experimental data should be used.

Although no design charts have been presented specifically for spoiler-type controls, it is expected and unpublished data indicate that about the same relation exists for the effectiveness of spoiler-type controls as for conventional ailerons with respect to spanwise location of the control device. The values of aileron effectiveness at various spanwise locations given in references 32 and 34 are therefore considered to hold for spoiler ailerons.

In order to find the rolling moment produced by a control, the effective change in the angle of attack produced by a given control deflection (or projection for spoilers) must also be known. Conventional aileron design utilizes the aileron-effectiveness factor k (or $\Delta\alpha/\Delta\delta$) multiplied by the control deflection δ to obtain the angle-of-attack change, but spoiler design cannot employ this simple method because spoiler effectiveness is a complex function of spoiler projection and angle of attack. A chart of effective change in angle of attack $\Delta\alpha$ (or $k\delta$) produced by various spoiler projections should therefore be utilized to obtain $\Delta\alpha$ and provide the rolling moment obtainable with the given control as shown in the following equation $\frac{C_l}{\Delta\alpha} \Delta\alpha = C_l$ where $114.6 \frac{C_l}{\Delta\alpha}$ equals the expression C_{l_δ}/k used in references 32 and 34. This procedure will ultimately give the rolling effectiveness pb/2V of the control by the relation $\frac{pb}{2V} = \frac{C_l}{C_{l_p}}$. The value of C_{l_p} employed is the same as that for an aileron spanning the same part of the wing as the spoiler in question, since C_{l_p} is expected to be the same for spoilers and ailerons. In order to obtain the aforementioned values of $\Delta\alpha$ (or $k\delta$) for a given spoiler-type control, the spoiler geometry, the chordwise location of the spoiler, and the wing profile must be considered as these all affect the values of $\Delta\alpha$.

With regard to spoiler-control stick forces, a number of general facts are known and have been discussed about the hinge moments of slot-lip, flat-plate, plug-type, and retractable-arc-type spoilers and the methods of balancing these control surfaces. Although no design charts exist for balancing these controls, the available spoiler data are considered fairly adequate for preliminary design and indicate possible modifications to obtain acceptable control forces.

Langley Memorial Aeronautical Laboratory
National Advisory Committee for Aeronautics
Langley Field, Va., September 22, 1947

REFERENCES

1. Wenzinger, Carl J., and Bamber, Millard J.: Wind-Tunnel Tests of Three Lateral-Control Devices in Combination with a Full-Span Slotted Flap on an N.A.C.A. 23012 Airfoil. NACA TN No. 659, 1938.

2. Shortal, Joseph A.: Wind-Tunnel and Flight Tests of Slot-Lip Ailerons. NACA Rep. No. 602, 1937.

3. Rogallo, Francis M., and Spano, Bartholomew S.: Wind-Tunnel Investigation of a Plain and a Slot-Lip Aileron on a Wing with a Full-Span Slotted Flap. NACA ACR, April 1941.

4. Rogallo, F. M., and Schuldenfrei, Marvin: Wind-Tunnel Investigation of a Plain and a Slot-Lip Aileron on a Wing with a Full-Span Flap Consisting of an Inboard Fowler and an Outboard Slotted Flap. NACA ARR, June 1941.

5. Wetmore, Joseph W., and Sawyer, Richard H.: Flight Tests of F2A-2 Airplane with Full-Span Slotted Flaps and Trailing-Edge and Slot-Lip Ailerons. NACA ARR No. 3L07, 1943.

6. Wenzinger, Carl J.: Wind-Tunnel Investigation of the Aerodynamic Balancing of Upper-Surface Ailerons and Split Flaps. NACA Rep. No. 549, 1935.

7. Weick, Fred E., and Wenzinger, Carl J.: Wind-Tunnel Research Comparing Lateral Control Devices, Particularly at High Angles of Attack. XII - Upper-Surface Ailerons on Wings with Split Flaps. NACA Rep. No. 499, 1934.

8. Shortal, J. A.: Effect of Retractable-Spoiler Location on Rolling- and Yawing-Moment Coefficients. NACA TN No. 499, 1934.

9. Wenzinger, Carl J., and Rogallo, Francis M.: Wind-Tunnel Investigation of Spoiler, Deflector, and Slot Lateral-Control Devices on Wings with Full-Span Split and Slotted Flaps. NACA Rep. No. 706, 1941.

10. Rogallo, Francis M., and Swanson, Robert S.: Wind-Tunnel Development of a Plug-Type Spoiler-Slot Aileron for a Wing with a Full-Span Slotted Flap and a Discussion of Its Application. NACA ARR, Nov. 1941.

11. Rogallo, F. M., and Spano, Bartholomew S.: Wind-Tunnel Investigation of a Spoiler-Slot Aileron on an NACA 23012 Airfoil with a Full-Span Fowler Flap. NACA ARR, Dec. 1941.

12. Lowry, John G., and Liddell, Robert B.: Wind-Tunnel Investigation of a Tapered Wing with a Plug-Type Spoiler-Slot Aileron and Full-Span Slotted Flaps. NACA ARR, July 1942.

13. Laitone, Edmund V.: An Investigation of the High-Speed Lateral-Control Characteristics of a Spoiler. NACA ACR No. 4C23, 1944.

14. Clousing, L. A., Lehr, Robert R., and O'Sullivan, William J.: Full-Scale Wind-Tunnel and Flight Tests of a Fairchild XR2K-1 Airplane with a Zap Flap and Upper-Surface Aileron-Wing Installation. NACA ARR, March 1942.

15. Soulé, H. A., and McAvoy, W. H.: Flight Investigation of Lateral Control Devices for Use with Full-Span Flaps. NACA Rep. No. 517, 1935.

16. Wetmore, J. W.: Flight Tests of Retractable Ailerons on a Highly Tapered Wing. NACA TN No. 714, 1939.

17. Baker, Paul S.: The Development of a New Lateral-Control Arrangement. NACA ARR, Oct. 1941.

18. Platt, Robert C., and Shortal, Joseph A.: Wind-Tunnel Investigation of Wings with Ordinary Ailerons and Full-Span External-Airfoil Flaps. NACA Rep. No. 603, 1937.

19. Wenzinger, Carl J., and Ames, Milton B., Jr.: Wind-Tunnel Investigation of Rectangular and Tapered N.A.C.A. 23012 Wings with Plain Ailerons and Full-Span Split Flaps. NACA TN No. 661, 1938.

20. Harris, Thomas A., and Purser, Paul E.: Wind-Tunnel Investigation of Plain Ailerons for a Wing with a Full-Span Flap Consisting of an Inboard Fowler and an Outboard Retractable Split Flap. NACA ACR, March 1941.

21. Rogallo, F. M., and Lowry, John G.: Wind-Tunnel Investigation of a Plain Aileron and a Balanced Aileron on a Tapered Wing with Full-Span Duplex Flaps. NACA ARR, July 1942.

22. Rogallo, F. M., Lowry, John G., and Fischel, Jack: Wind-Tunnel Investigation of a Full-Span Retractable Flap in Combination with Full-Span Plain and Internally Balanced Ailerons on a Tapered Wing. NACA ARR No. 3H23, 1943.

23. Graham, Robert R., and Ashworth, C. Dixon: Tests in the 19-Foot Pressure Tunnel of a 1/2.75-Scale Model of the F4U-1 Airplane with Several Balanced Elevators, Full-Span Flaps, and Droppable Gas Tank. NACA ACR, Oct. 1942.

24. Rogallo, Francis M., and Swanson, Robert S.: Wind-Tunnel Tests of a Twin-Engine Model to Determine the Effect of Direction of Propeller Rotation on the Static-Stability Characteristics. NACA ARR, Jan. 1943.

25. Williams, W. C.: A Flight Investigation of Internally Balanced Sealed Ailerons in the Presence of a Balanced Split Flap. NACA ARR, May 1942.

26. Rogallo, F. M.: Collection of Balanced-Aileron Test Data. NACA ACR No. 4A11, 1944.

27. Sears, Richard I.: Wind-Tunnel Data on the Aerodynamic Characteristics of Airplane Control Surfaces. NACA ACR No. 3L08, 1943.

28. Swanson, Robert S., and Toll, Thomas A.: Jet-Boundary Corrections for Reflection-Plane Models in Rectangular Wind Tunnels. NACA Rep. No. 770, 1943.

29. Langley Research Department: Summary of Lateral-Control Research. (Compiled by Thomas A. Toll.) NACA TN No. 1245, 1947.

30. Weick, Fred E., and Shortal, Joseph A.: Development of the N.A.C.A. Slot-Lip Aileron. NACA TN No. 547, 1935.

31. Purser, Paul E., and McKinney, Elizabeth G.: Comparison of Pitching Moments Produced by Plain Flaps and by Spoilers and Some Aerodynamic Characteristics of an NACA 23012 Airfoil with Various Types of Aileron. NACA ACR No. L5C24a, 1945.

32. Pearson, Henry A., and Jones, Robert T.: Theoretical Stability and Control Characteristics of Wings with Various Amounts of Taper and Twist. NACA Rep. No. 635, 1938.

33. Ames, Milton B., Jr., and Sears, Richard I.: Determination of Control-Surface Characteristics from NACA Plain-Flap and Tab Data. NACA Rep. No. 721, 1941.

34. Gilruth, R. R., and Turner, W. N.: Lateral Control Required for Satisfactory Flying Qualities Based on Flight Tests of Numerous Airplanes. NACA Rep. No. 715, 1941.

35. Pearson, Henry A., and Aiken, William S., Jr.: Charts for the Determination of Wing Torsional Stiffness Required for Specified Rolling Characteristics or Aileron Reversal Speed. NACA Rep. No. 799, 1944.

Table I.– Supplementary Information Regarding Tests of Models and Airplanes Having Full-Span Flaps

A– Slot-Lip and Flap-Trailing-Edge Ailerons

Model or Airplane: Designation	Model or Airplane: Plan form of surface	Typical aileron section	Airfoil section: Root	Airfoil section: Tip	A	λ	Aileron location and chord: Plain aileron $\frac{y_i}{b/2}$	Plain aileron $\frac{y_o}{b/2}$	Plain aileron c_a/c	Slot-lip aileron $\frac{y_i}{b/2}$	Slot-lip aileron $\frac{y_o}{b/2}$	Slot-lip aileron c_a/c	Hinge location fraction of c	Flap location and chord: $\frac{y_i}{b/2}$	$\frac{y_o}{b/2}$	c_f/c	Type of test	Air flow characteristics	Published reference
A-I	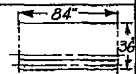		NACA 23012		∞	---	---	---	0.10	---	---	0.10	0.727	---	---	0.2566 slotted	Two dimensional	$R=2.19\times10^6$ $M=0.11$	1
A-II	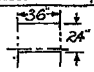	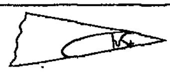	NACA 66,2-216		∞	---	---	---	.10	---	---	---	---	---	---	.30 slotted	Two dimensional	$R=6\times10^6$ $M=0.14$	
A-III	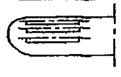	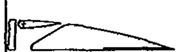	Clark Y		6.0	1.00	---	---	---	.35	.85	.10 (approx)	.10 .30 .55 (approx)	0	.85	.20 (approx) split	Full-span wing model	$R=.61\times10^6$ $M=0.11$	2
A-IV	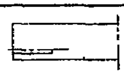		NACA 23012		6.0	1.00	---	---	---	.63	1.00	.10	.727	0	1.00	.2566 slotted	Full-span wing model	$R=.61\times10^6$ $M=0.11$	
A-V	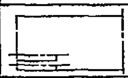		NACA 23012		4.0	1.00	.63	1.00	.10	.63	1.00	.10	.727	0	1.00	.2566 slotted	Semispan wing model	$R=1.44\times10^6$ $M=0.055$	3
A-VI	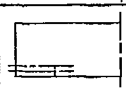		NACA 23012		4.0	1.00	.63	1.00	.10	.63	1.00	.10	.80	0 .63	.63 1.00	.30 Fowler .30 slotted	Semispan wing model	$R=1.44\times10^6$ $M=0.055$	4
A-VII	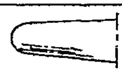		NACA 23018	NACA 23009	5.88	.66	.34	.903	.10 (approx)	.428	.819	.10 (approx)	.75 (approx)	.12	.94	.25 (approx) slotted	Complete model	$R=.57\times10^6$ $M=0.11$	
A-VIII	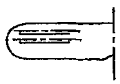		NACA 2412		6.0	1.00	---	---	---	.41	.89	.10	.20 .45	.09	.91	.20 split	Full-scale complete model and flight	$R=2.9\times10^6$ $M=0.08$ ------	2
A-IX	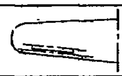	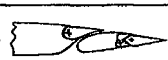	NACA 23018	NACA 23009	5.8	.65	.338	.903	.10 (approx)	.411	.808	.10 (approx)	.73 (approx)	.13 (approx)	.95 (approx)	.25 (approx) slotted	Flight	------	5

NATIONAL ADVISORY COMMITTEE FOR AERONAUTICS

Table I.– Supplementary Information Regarding Tests of Models and Airplanes Having Full-Span Flaps—Continued

B – Spoiler - Type Ailerons (Other Than Slot-Lip Ailerons)

Model or Airplane: Designation	Model or Airplane: Plan form of surface	Typical aileron section	Airfoil section: Root	Airfoil section: Tip	A	λ	Flap location and chord: $\frac{y_i}{b/2}$	Flap: $\frac{y_o}{b/2}$	Flap: c_f/c	Spoiler location and chord: $\frac{y_i}{b/2}$	Spoiler: $\frac{y_o}{b/2}$	Spoiler: c_s/c	Chordwise spoiler location, x/c	Aileron location and chord: $\frac{y_i}{b/2}$	Aileron: $\frac{y_o}{b/2}$	Aileron: c_a/c	Type of test	Air flow characteristics	Published reference
B-I	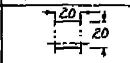	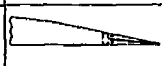	Clark Y		∞	---	---	---	0.15 split	---	---	0.15	1.00	---	---	---	Two dimensional	$R=1.22\times10^6$ $M=0.11$	6
B-II	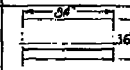	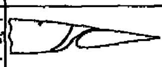	NACA 23012		∞	---	---	---	.2566 slotted	---	---	---	.73	---	---	---	Two dimensional	$R=2.19\times10^6$ $M=0.11$	1
B-III	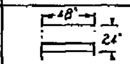		NACA 0009		∞	---	---	---	---	---	---	---	.65	---	---	---	Two dimensional	$R=1.42\times10^6$ $M=0.10$	
B-IV	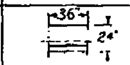	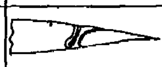	NACA 66(215)-216		∞	---	---	---	.25 slotted	---	---	---	.75	---	---	---	Two dimensional	$R=2.5, 6.0\times10^6$ $M=0.11$ and 0.18	
B-V	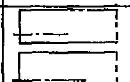	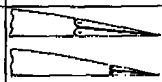	Clark Y		6	1	0	1.00	.25 split .15 split	.60 .40	1.00 1.00	.25 .15	1.00 1.00	---	---	---	Full-span wing model	$R=0.61\times10^6$ $M=0.11$	7
B-VI	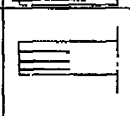	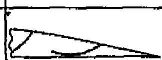	Clark Y		6	1	0	1.00	.20 split	.50	1.00	---	.30 .60 .833	---	---	---	Full-span wing model	$R=0.61\times10^6$ $M=0.11$	8
B-VII	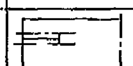	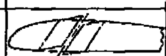	Clark Y-15		4	1	0	1.00	.20 split	.63	1.00	.11	.40 .25	.63	1.00	.15	Semispan wing model	$R=1.44\times10^6$ $M=0.055$	
B-VIII	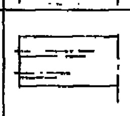	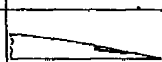	Clark Y-15		4	1	---	---	---	.63 .63 .33	1.00 1.00 .53	.10 .10 .10	.40 .90 .40	.63	1.00	.15	Semispan wing model	$R=1.44\times10^6$ $M=0.055$	
B-IX	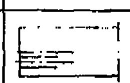	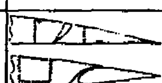	Clark Y-15 NACA 23012		4	1	0	1.00	.20 split .2566 slotted	.63 .63	1.00 1.00	--- .10	.72 and .75 .72 .50 and .60	.63 ---	1.00 ---	.15 ---	Semispan wing model	$R=1.44\times10^6$ $M=0.055$	9
B-X		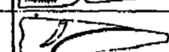							.50 Blackburn	.73	1.00	---	.61	---	---	---	Three dimensional	Unknown	
B-XI	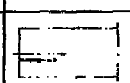		NACA 23012		4		0	1.00	.2566 slotted	.63	1.00	---	.655 .67 .685 .70	---	---	---	Semispan wing model	$R=1.44\times10^6$ $M=0.055$	10
B-XII	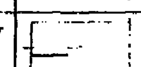		NACA 23012		4	1	0	1.00	.30 Fowler	.63	1.00	---	.685	---	---	---	Semispan wing model	$R=1.44\times10^6$ $M=0.055$	11
B-XIII	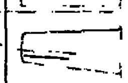		NACA 23015.5 (approx)	NACA 23006.25 (approx)	5.6	.6	0	.98	.207 slotted	.54	.98	---	.75	---	---	---	Semispan wing model	$R=1.54, 2.05\times10^6$ $M=0.08$ and 0.11	12
B-XIV	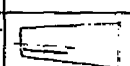	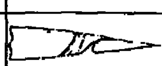	NACA 23015.5 (approx)	NACA 23008.25 (approx)	5.6	.6	0	.98	.207 slotted	.54	.98	---	.75	---	---	---	Semispan wing model	$R=2.05\times10^6$ $M=0.11$	

NATIONAL ADVISORY COMMITTEE FOR AERONAUTICS

Table I.– Supplementary Information Regarding Tests of Models and Airplanes Having Full-Span Flaps–Continued

B - Spoiler-Type Ailerons (Other Than Slot-Lip Ailerons) - Concluded

Model or Airplane: Designation	Model or Airplane: Plan form of surface	Typical aileron section.	Airfoil section: Root	Airfoil section: Tip	A	λ	Flap location and chord: $y_i/(b/2)$	Flap location and chord: $y_o/(b/2)$	Flap location and chord: c_f/c	Spoiler location and chord: $y_i/(b/2)$	Spoiler location and chord: $y_o/(b/2)$	Spoiler location and chord: c_s/c	Chordwise spoiler location x/c	Aileron location and chord: $y_i/(b/2)$	Aileron location and chord: $y_o/(b/2)$	Aileron location and chord: c_a/c	Type of test	Air flow characteristics	Published reference
B-XV			NACA 66,2-118	NACA 66(2x15)-116	6.28	0.33	---	---	---	0.50	0.91	---	0.75	---	---	---	Semispan wing model	R=7.7 to 13.7x10^6 M=0.3 to 0.725	13
B-XVI			NACA 66(215)-216	NACA 66,2-215	10.38	.398	0	0.888	0.25 slotted	.48	.88	---	.75	.888	.996	.20	Complete model	Unknown	
B-XVII			Z-115 or modified N-71		7.71	1.00	0	.974	.376 Zap	.392	.974	.196	.90	---	---	---	Full-scale complete model and flight	R=2.36x10^6 M=.08 -------	14
B-XVIII			N-22		5.59	1.00	.10	1.00	.20 split	.454	.953	---	.78	.09	.92	.18	Flight	-------	15
			NACA 2412		6.3	1.00	.13	.92	.20 split	.088	.92	.136	1.00	---	---	---			
B-XIX			NACA 23015	NACA 23009	10	.2	0	1.00	.23 inboard .20 outboard	.572	.899	---	.74	---	---	---	Flight	-------	16
B-XX			Piercy .20c thick max. thickness at .40c	Piercy .15c thick	6.7	.625	0	.92	.157 (approx) split	.37 (approx)	.92 (approx)	---	.70	---	---	---	Flight	-------	
B-XXI			NACA 23015	NACA 23009	4.9	.67	0	.625	.23 slotted	.51	.92	.10	.78	.63	.95	.20 (approx)	Flight	-------	17
B XXII			NACA 23015	NACA 23009	4.9	.67	0	.625	.23 slotted	.51	.92	.10	.78	.63	.95	.17 (approx)	Flight	-------	
B-XXIII			NACA 23015	NACA 23009	4.9	.67	0	.625	.23 slotted	.51	.92	.10	.78	.63	.95	.20 (approx)	Flight	-------	
B-XXIV			Zap .1725c thick	Zap .12c thick	6.3	.51	0	.98	.41 Zap	.39	.96	---	.79 (approx.)	---	---	---	Flight	-------	
B-XXV			Zap .1725c thick	Zap .12c thick	6.3	.51	0	.98	.41 Zap	.39	.96	---	.72 .70	---	---	---	Flight	-------	
B-XXVI			Zap .15c thick	Zap .13c thick	6.7	.55 (approx)	0	.83	.20 (approx) slotted	.49	.83	---	.72	.83	.96	.17	Flight	-------	

NATIONAL ADVISORY COMMITTEE FOR AERONAUTICS

Table I.–Supplementary Information Regarding Tests of Models and Airplanes Having Full-Span Flaps–Concluded.

C–Ailerons with Retractable-Type Flaps.

NATIONAL ADVISORY COMMITTEE FOR AERONAUTICS

Model or airplane: Designation	Model or airplane: Plan form of surface	Typical aileron section	Airfoil section: Root	Airfoil section: Tip	A	λ	Flap location and chord, Inboard flap: $\frac{y_i}{b/2}$	Inboard flap: $\frac{y_o}{b/2}$	Inboard flap: c_f/c	Outboard flap: $\frac{y_i}{b/2}$	Outboard flap: $\frac{y_o}{b/2}$	Outboard flap: c_f/c	Aileron location and chord: $\frac{y_i}{b/2}$	Aileron: $\frac{y_o}{b/2}$	Aileron: c_a/c	Type of test	Air flow characteristics	Published reference
C-I			NACA 23012		6.0	1.00	0	1.00	0.2	----	----	----	0	1.00	0.12	Full-span wing model	$R=0.61 \times 10^6$ $M=0.11$	18
C-II			NACA 23012		6.0 6.0	1.00 .20	0 0	1.00 1.00	.20 split .20 split	----	----	----	0 .40	1.00 1.00	.10 .15	Full-span wing model	$R=0.61 \times 10^6$ $M=0.11$	19
C-III			NACA 23012		4.0	1.00	0	.63	.30	.63	1.00	.20 split	.63	1.00	.15	Semispan wing model	$R=1.44 \times 10^6$ $M=0.055$	20
C-IV and C-V	End plate		Davis .16c thick		8.1	1.00	0	.565	.30	.565	.976	.20	.565	.976	.15	Semispan wing model	$R=2.25 \times 10^6$ $M=0.16$	
C-VI	Tunnel wall		NACA 63(420)-422	NACA 63(420)-517	11.09	.25	0	.57	.24 (approx) slotted	.59	.96	.20 (approx) split	.59	.97	.15 (approx)	Partial-span wing model	$R=8.9 \times 10^6$ $M=0.17$	
C-VII			NACA 23015.5 (approx)	NACA 23008.25 (approx)	5.6	.60	0	.58	.207 slotted	.58	.98	.19 (approx) split	.58	.98	.155	Semispan wing model	$R=1.54 \times 10^6$ $M=0.08$	21
C-VIII			NACA 23015.5 (approx)	NACA 23008.25 (approx)	5.6	.60	0	.98	.207 split	----	----	----	0	.98	.08	Semispan wing model	$R=2.05, 1.54 \times 10^6$ $M=0.11$ and 0.08	22
C-IX			NACA CYH (modified)		5.88	.657	0	.585	.25 slotted	.585	.96 (approx)	.20 split	.585	.96 (approx)	.18 (approx)	Complete model	$R=.20 \times 10^6$ $M=0.05$	
C-X			NACA 23018	NACA 23009	5.3	.67	0	.57	.26 (approx) slotted	.57	.94	.20 split	.57	.94	.20 (approx)	Complete model	$R=2.6 \times 10^6$ $M=0.13$	23
C-XI			Conventional		7.8	.40	0	.626	.202 slotted	.626	.939	.234 split	.626	.939	.192	Complete model	$R=.73, .365 \times 10^6$ $M=0.11$ and 0.055	24
C-XII			Davis .229c thick	Davis .093c thick	12.82	.325	0	.60	.142 Fowler .172	.60	.96	.204 split	.60	.96	.152	Complete model	$R=2.6, 3.2 \times 10^6$ $M=0.11$ and 0.13	
C-XIII			NACA 23014.7 (approx)	NACA 23009	6.16	.292	0	.45	.21 slotted	.45	.97	.20	.45	.97	.15	Complete model	$R=.56, .75 \times 10^6$ $M=0.08$ and 0.11	
C-XIV			NACA 23014.7 (approx)	NACA 23009	5.88	.397	0	.44	.20 slotted	.45	.97	.20	.44	.97	.15	Complete model	$R=.6, .8 \times 10^6$ $M=0.08$ and 0.11	
C-XV			NACA 23012		7.2	1.00	0	.56	.20 Fowler	.56	.94	.20 split	.56	.94	.20	Flight	--------	25

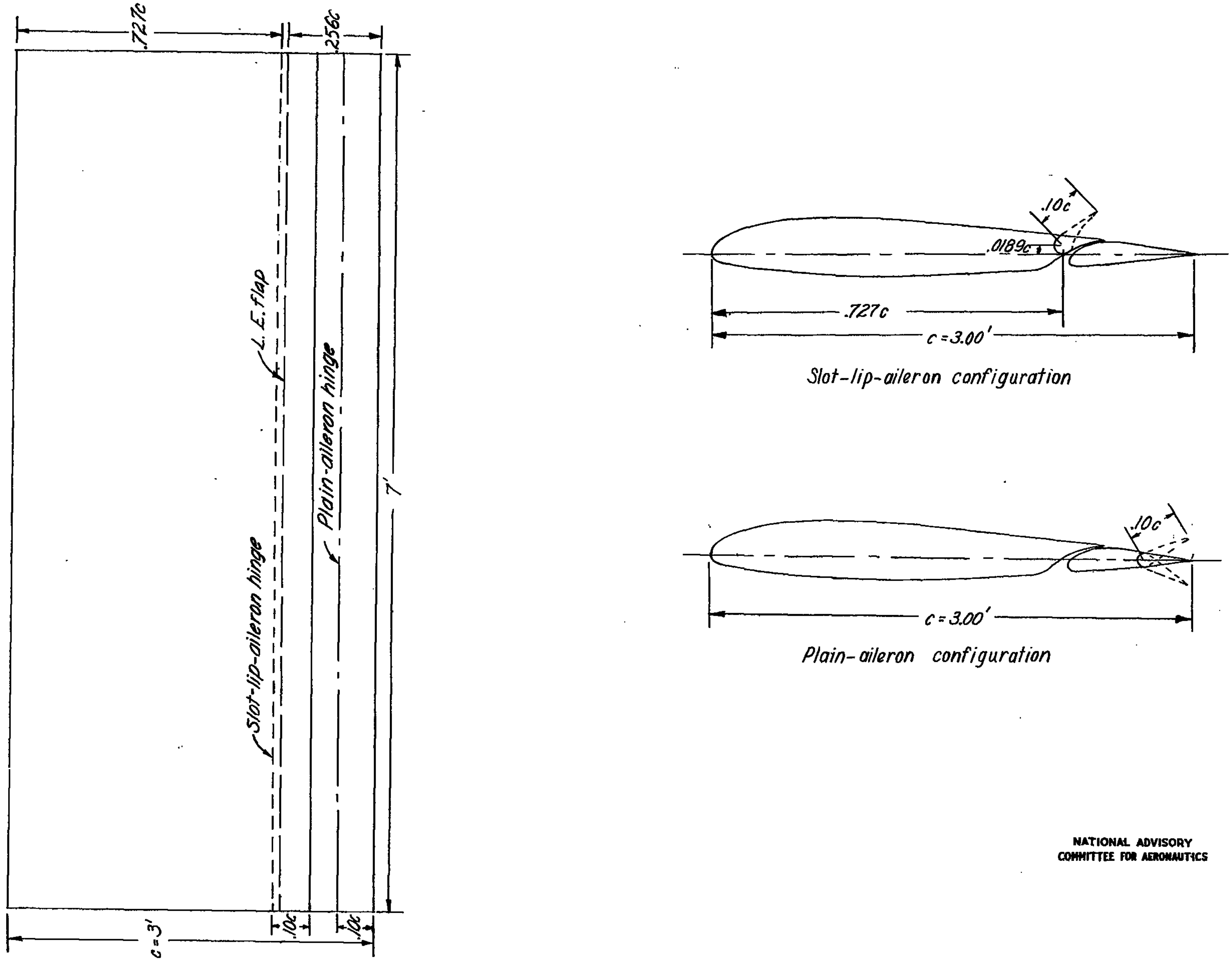

NATIONAL ADVISORY
COMMITTEE FOR AERONAUTICS

Figure A1.- Plan form and sections of the 3- by 7-foot NACA 23012 airfoil tested with a slotted flap and slot-lip and plain ailerons in the Langley 7- by 10-foot tunnel.

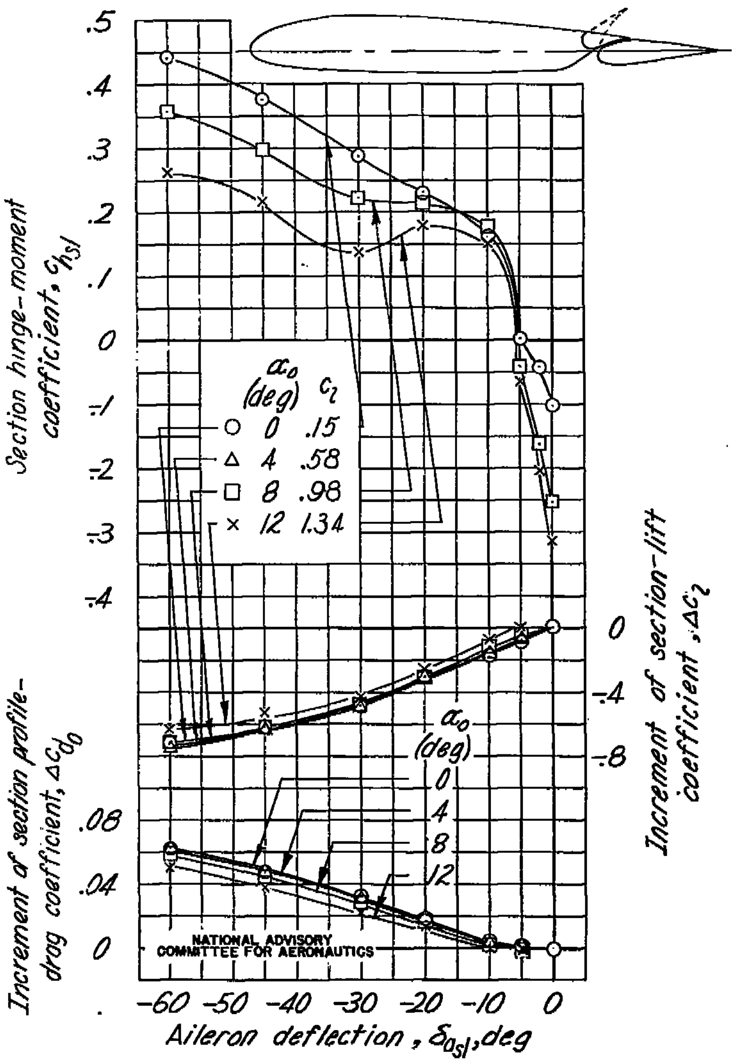

(a) δ_f, 0°.

Figure A2.- Effect of slot-lip-aileron deflection on the section aerodynamic characteristics of an NACA 23012 airfoil equipped with a full-span slotted flap.

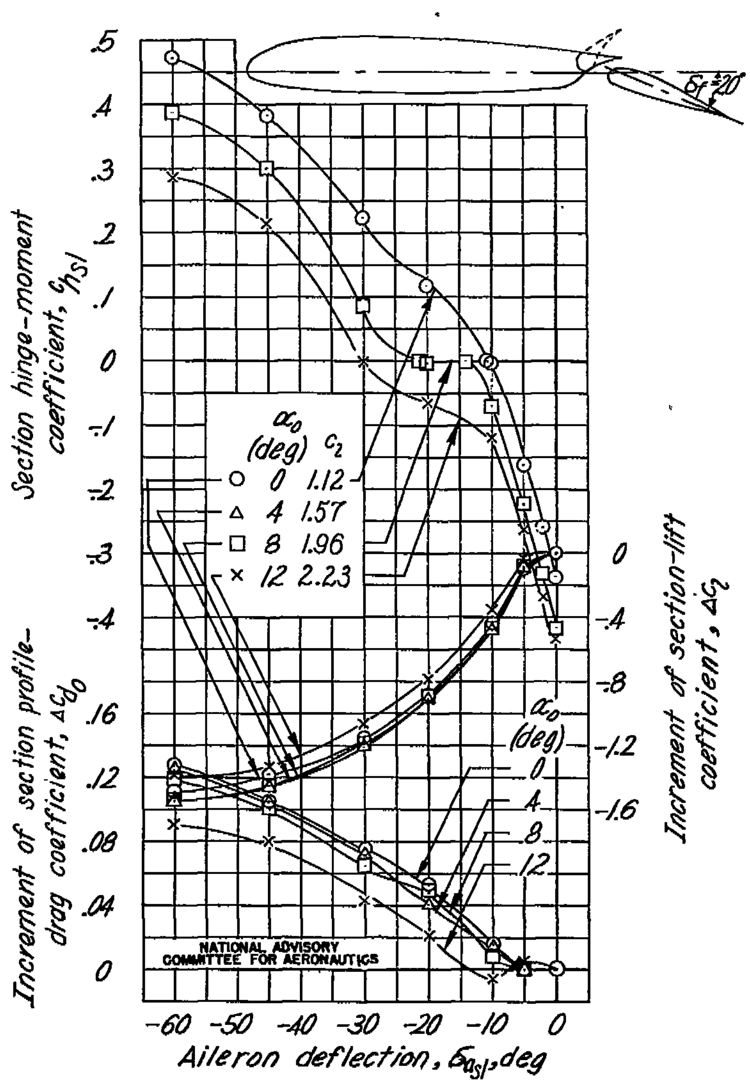

(b) δ_f, 20°.

Figure A2.- Continued.

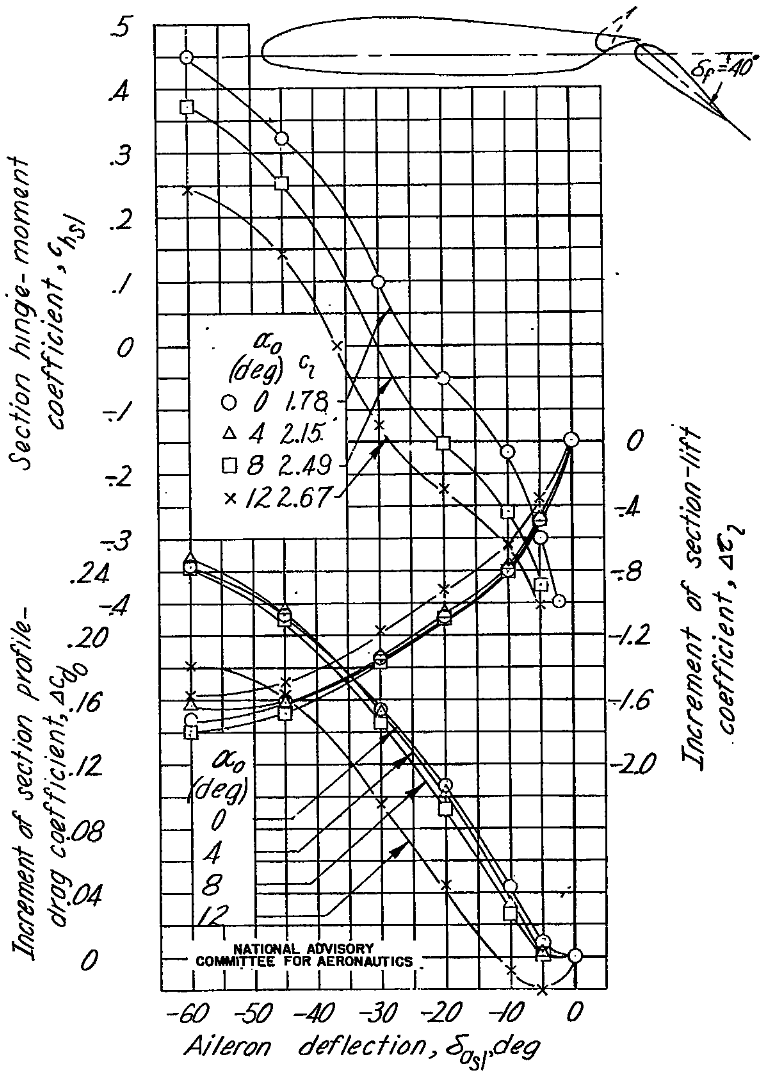

(c) δ_f, 40°.

Figure A2.- Concluded.

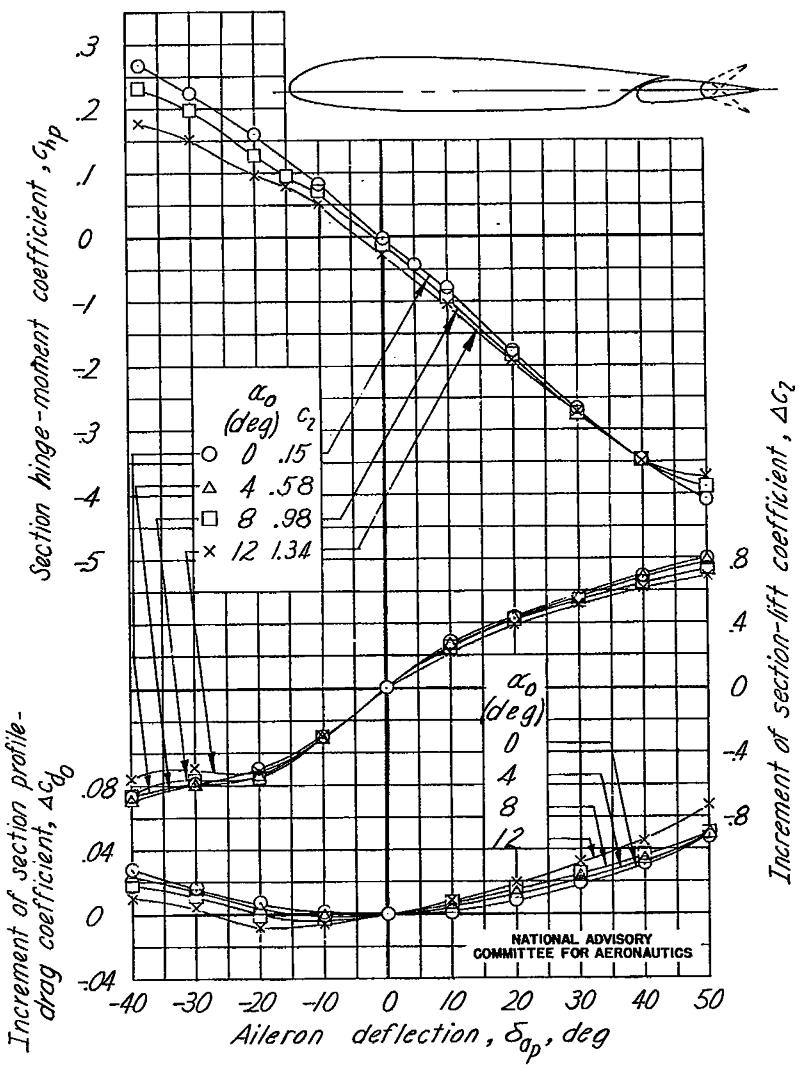

(a) δ_f, 0°.

Figure A3.- Effect of plain aileron deflection on the section aerodynamic characteristics of an NACA 23012 airfoil equipped with a full-span slotted flap.

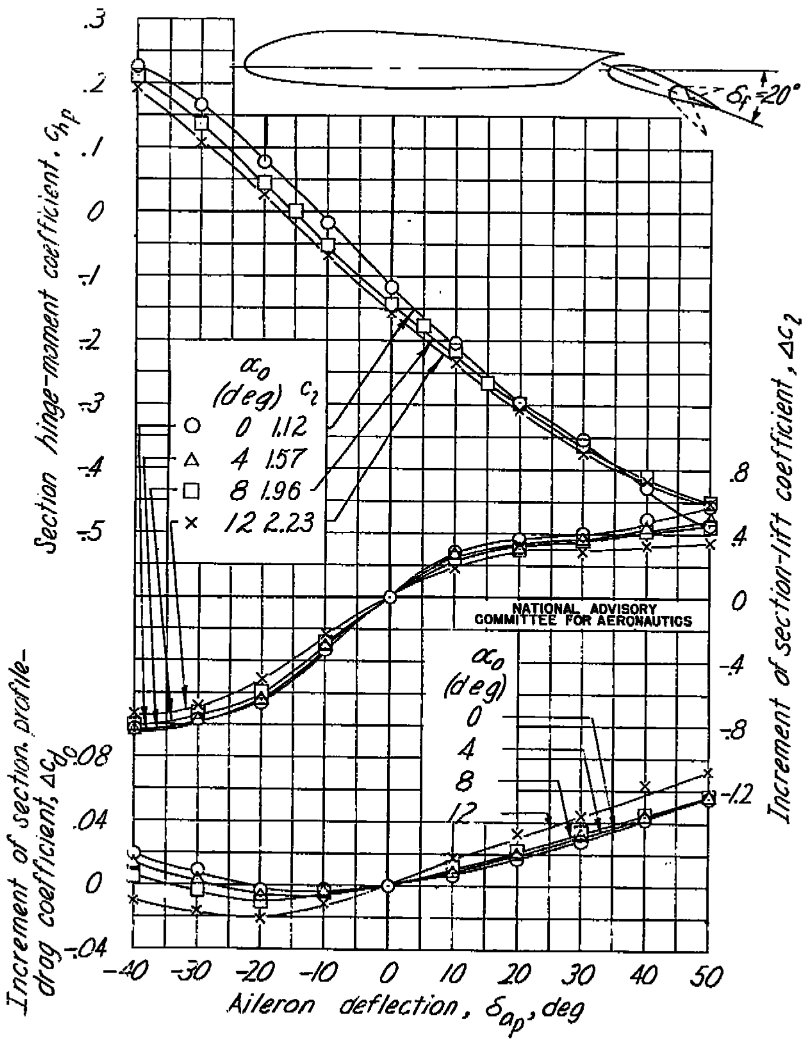

(b) δ_f, 20°.

Figure A3.- Continued.

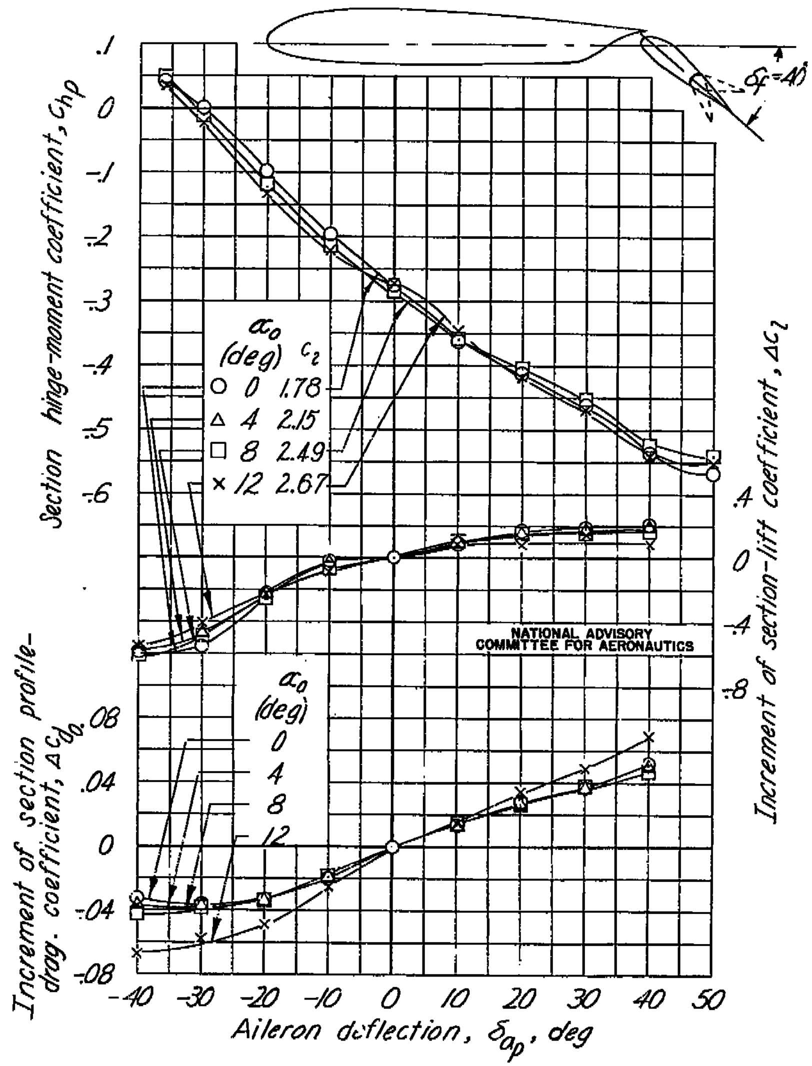

(c) δ_f, 40°.

Figure A3.- Concluded.

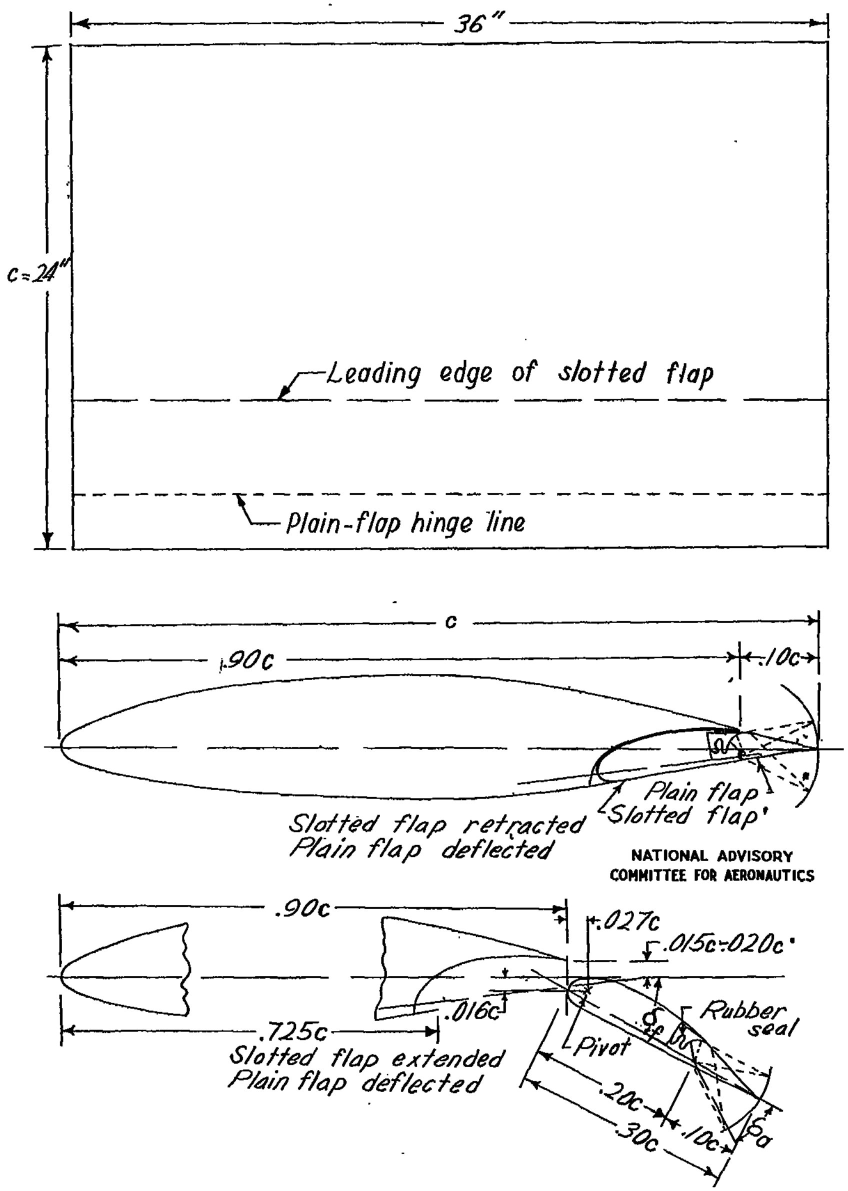

Figure A4.- Plan form and sections of an NACA 66,2-216, a = 0.6 airfoil with a slotted and plain flap as tested in Langley two-dimensional low-turbulence tunnel.

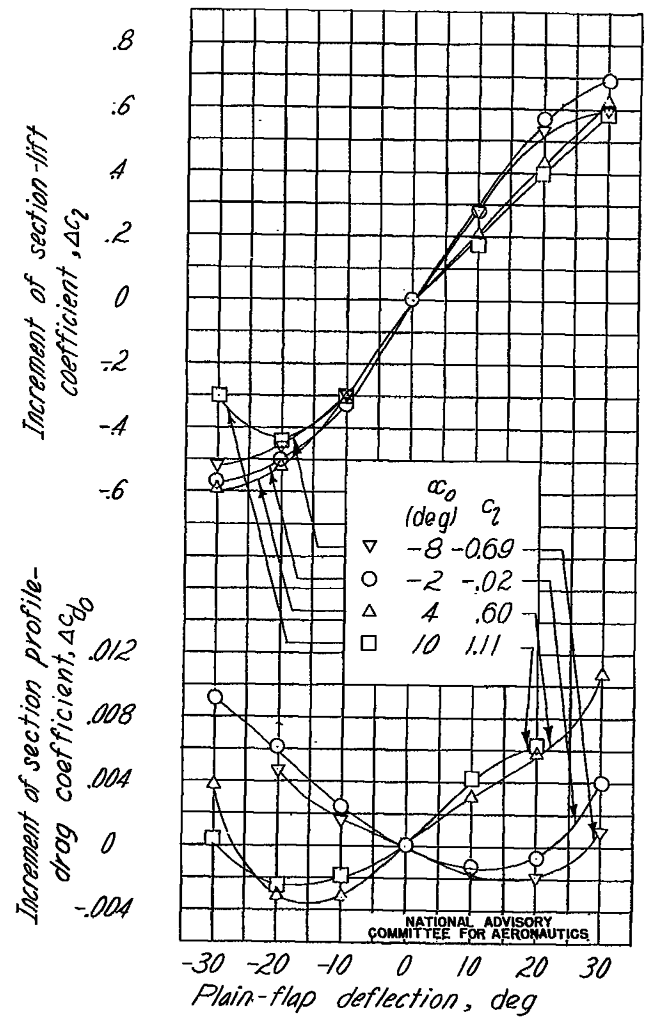

(a) Slotted flap retracted, $\delta_f = 0°$.

Figure A5.- Effect of plain flap deflection on the lift characteristics of an NACA 66,2-216, a = 0.6 airfoil with 0.30c slotted and 0.10c plain flap.

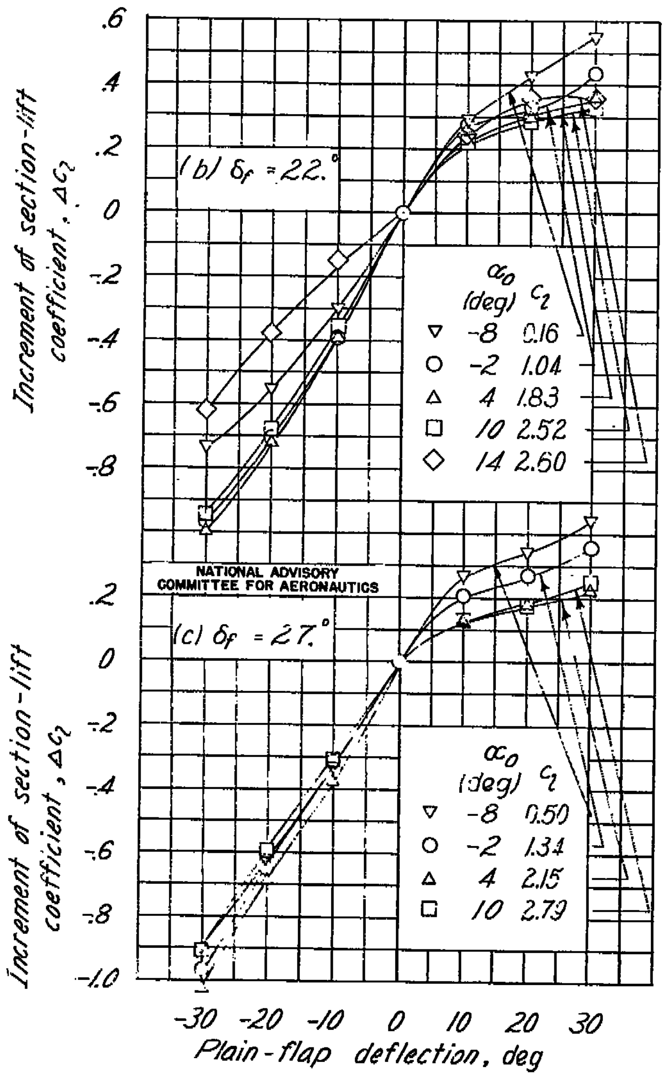

Figure A5.- Continued.

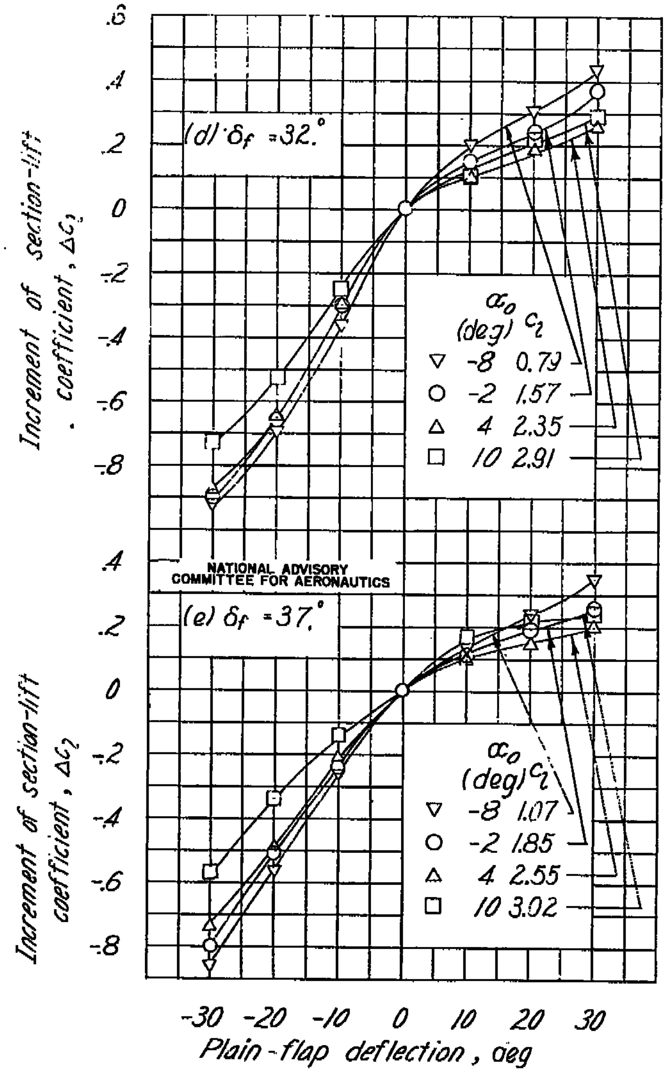

Figure A5.- Concluded.

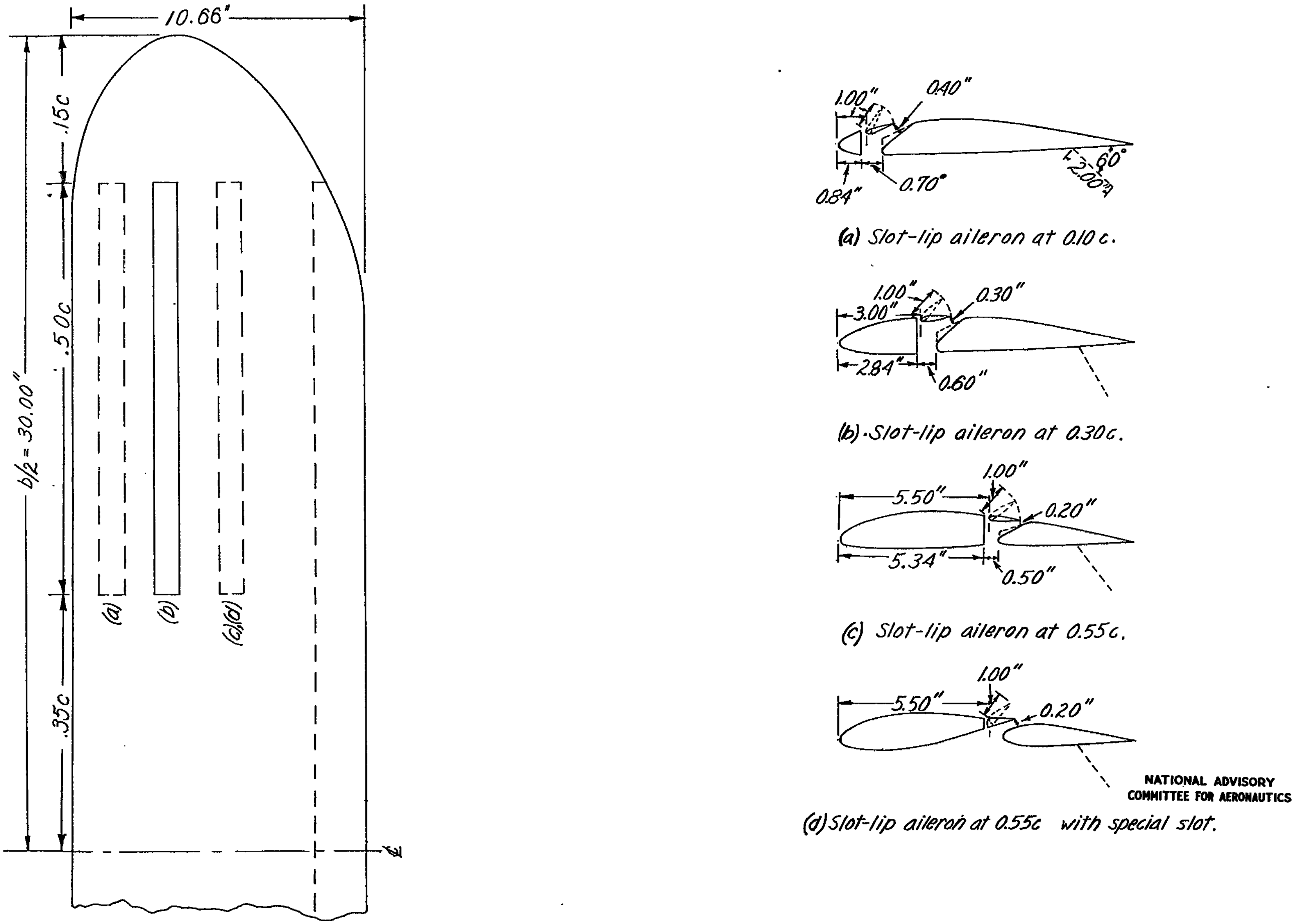

Figure A6.- Plan form and sections of the Clark Y wing tested with slot-lip ailerons and full-span split flaps in the Langley 7- by 10-foot tunnel.

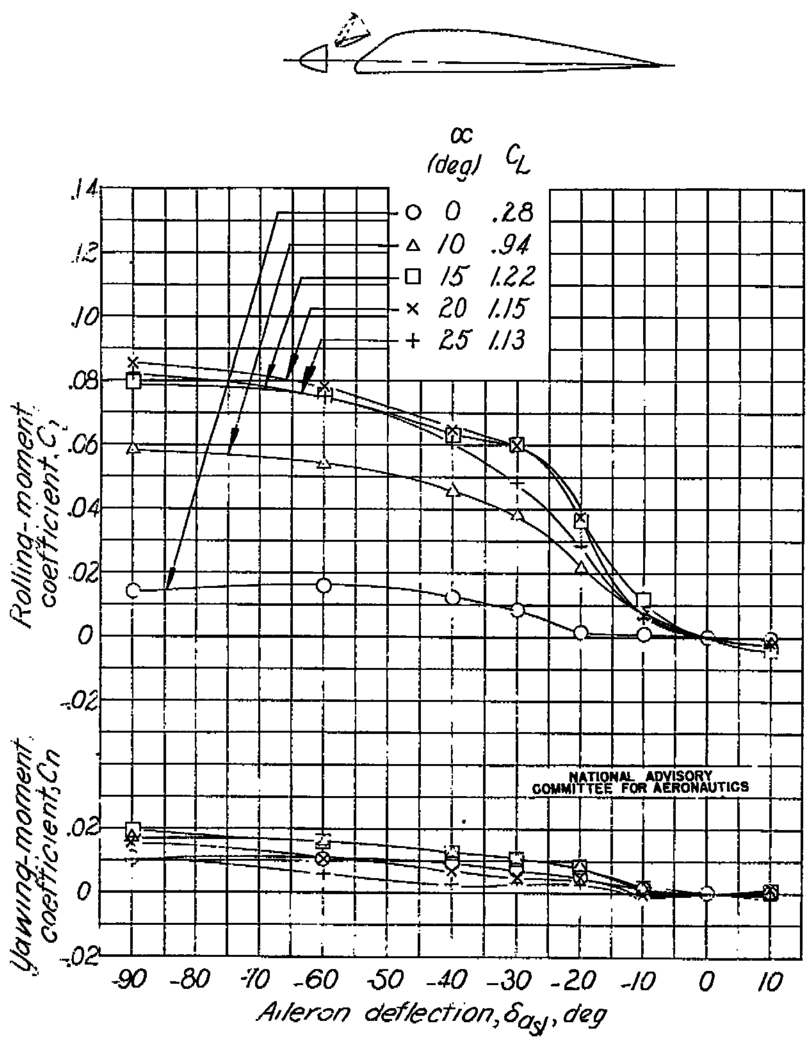

(a) δ_f, 0°.

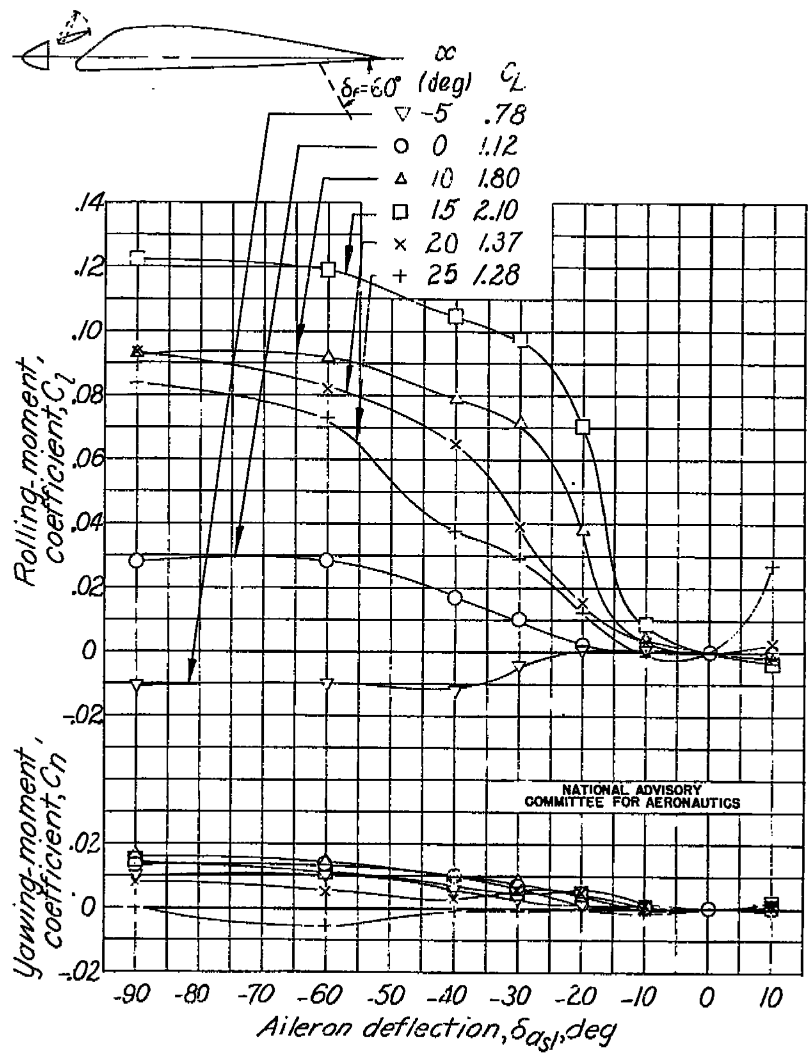

(b) δ_f, 60°.

Figure A7.- Concluded.

Figure A7.- Rolling-moment and yawing-moment coefficients of the Clark Y wing due to slot-lip ailerons at 0.10c.

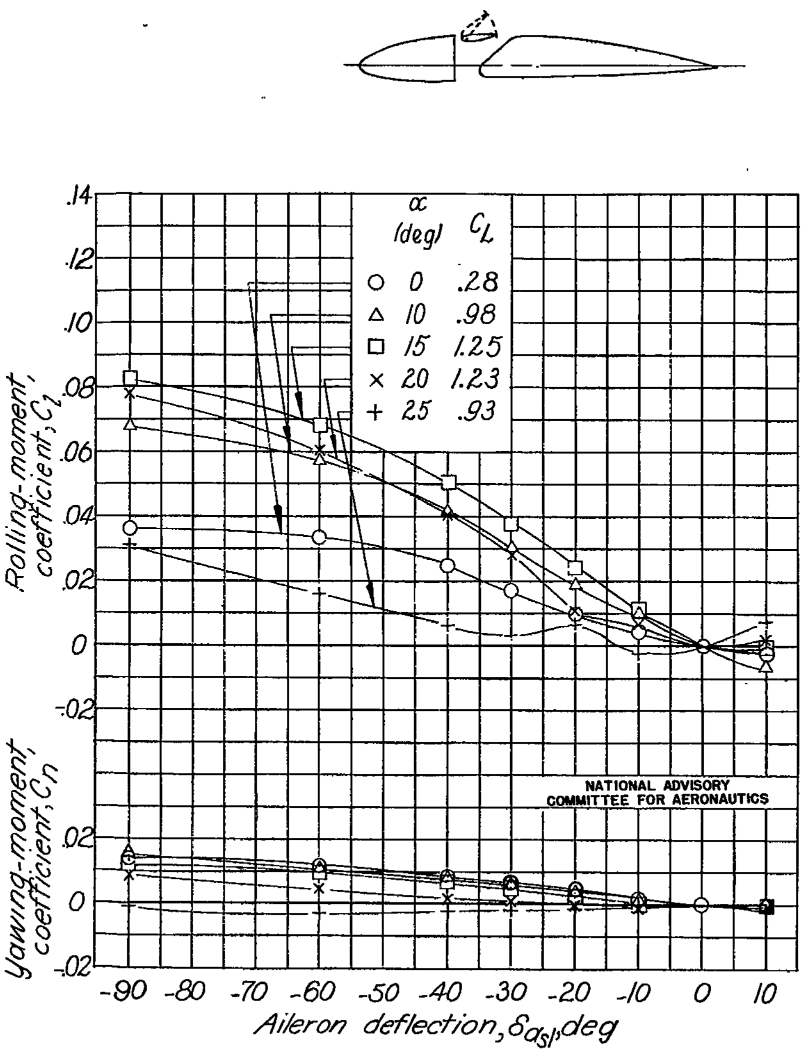

(a) δ_f, 0°.

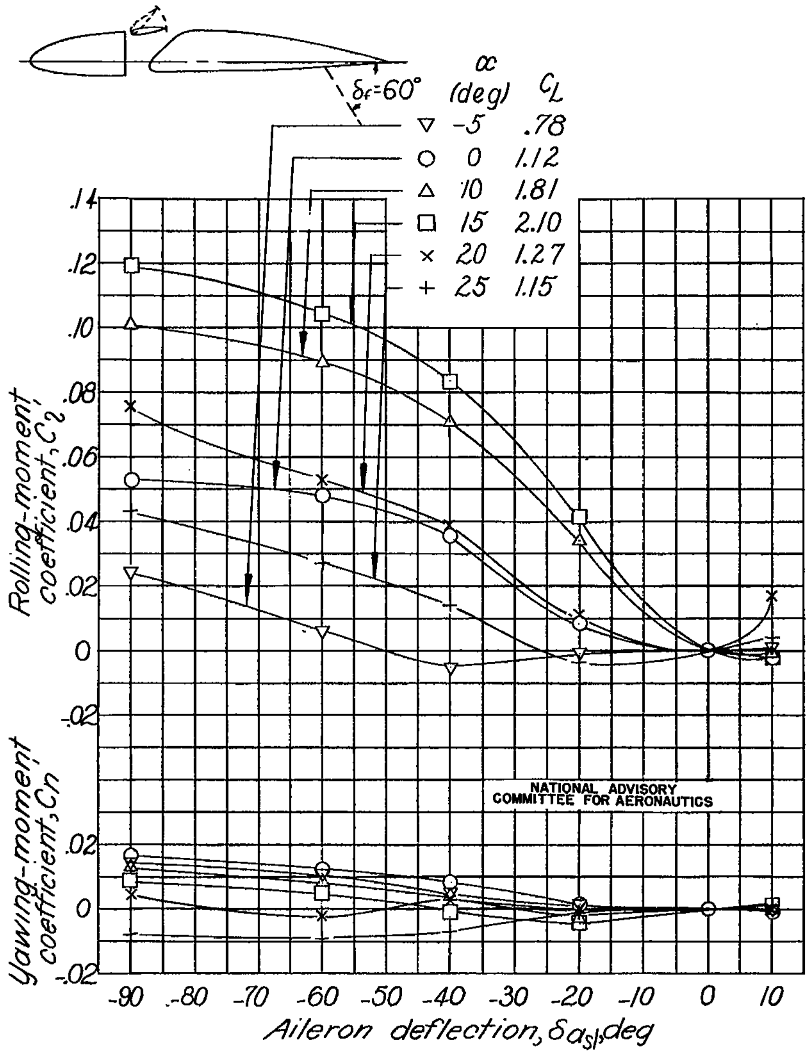

(b) δ_f, 60°.

Figure A8.- Concluded.

Figure A8.- Rolling-moment and yawing-moment coefficients of the Clark Y wing due to slot-lip ailerons at 0.30c.

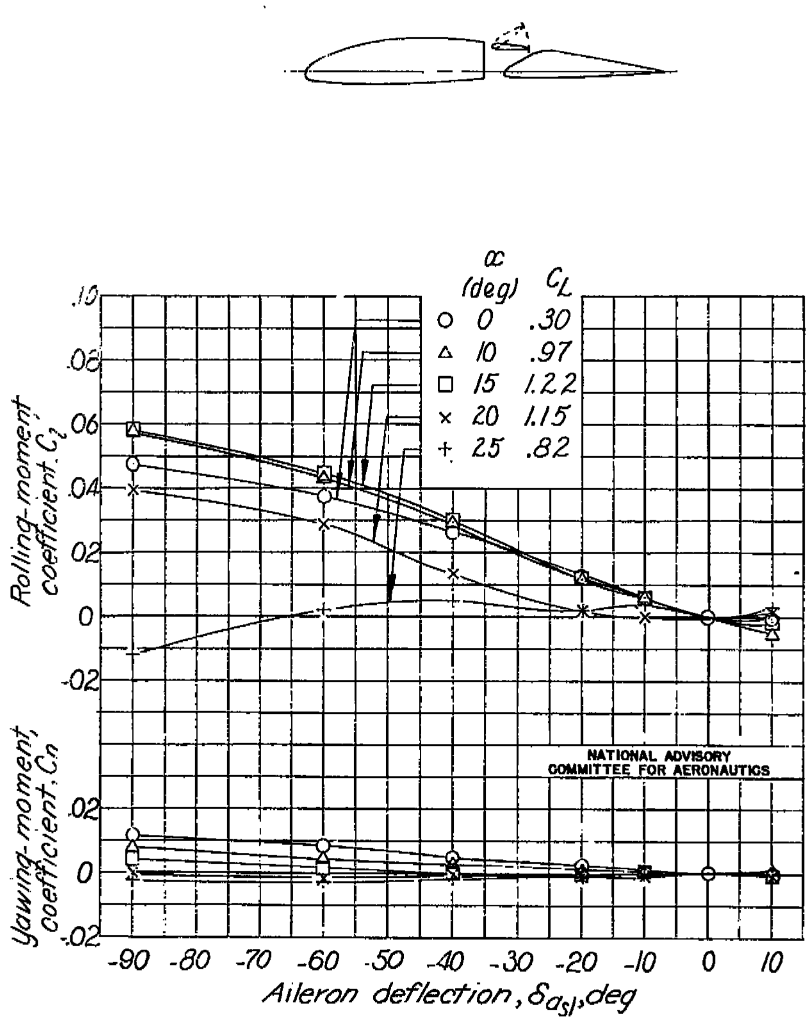

(a) δ_f, 0°.

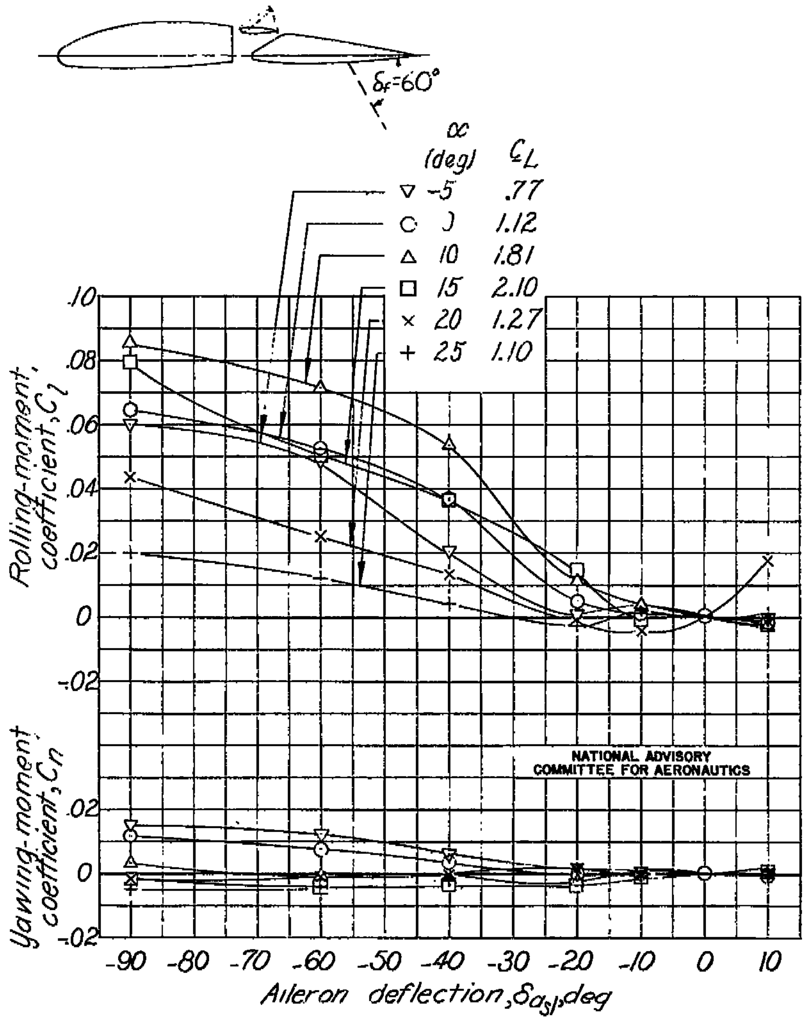

(b) δ_f, 60°.

Figure A9.- Rolling- and yawing-moment coefficients of the Clark Y wing due to slot-lip ailerons at 0.55c.

Figure A9.- Concluded.

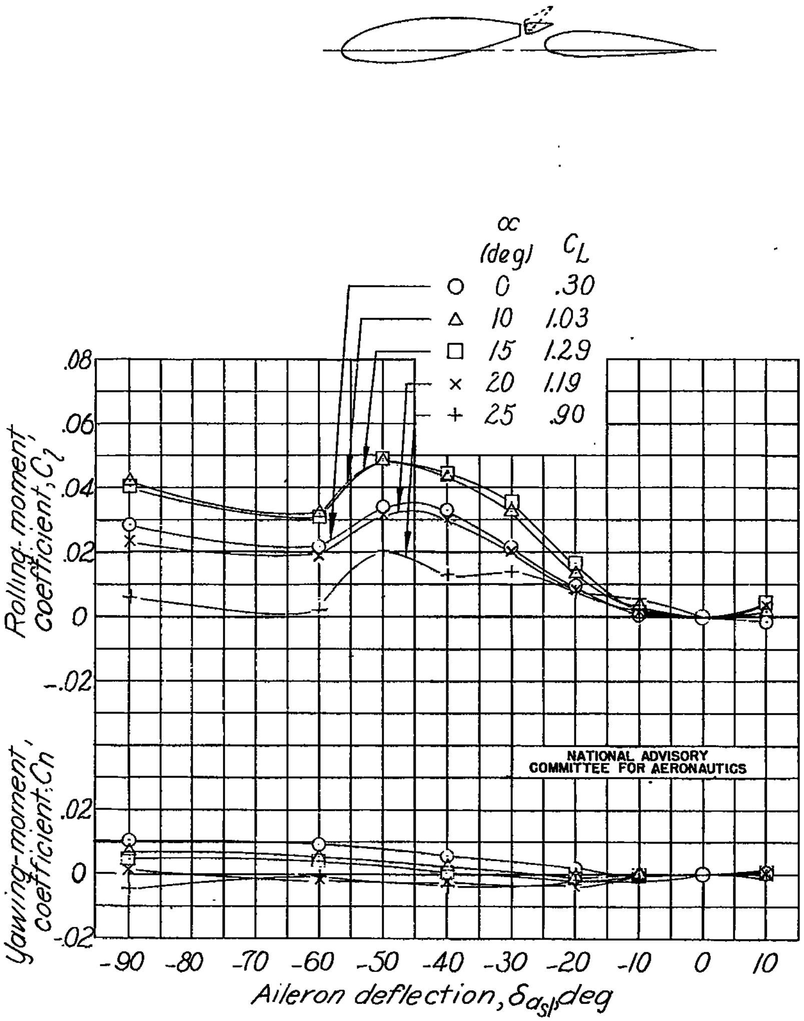

(a) δ_f, 0°.

Figure A10.- Rolling- and yawing-moment coefficients of the Clark Y wing due to slot-lip ailerons at 0.55c with a special slot.

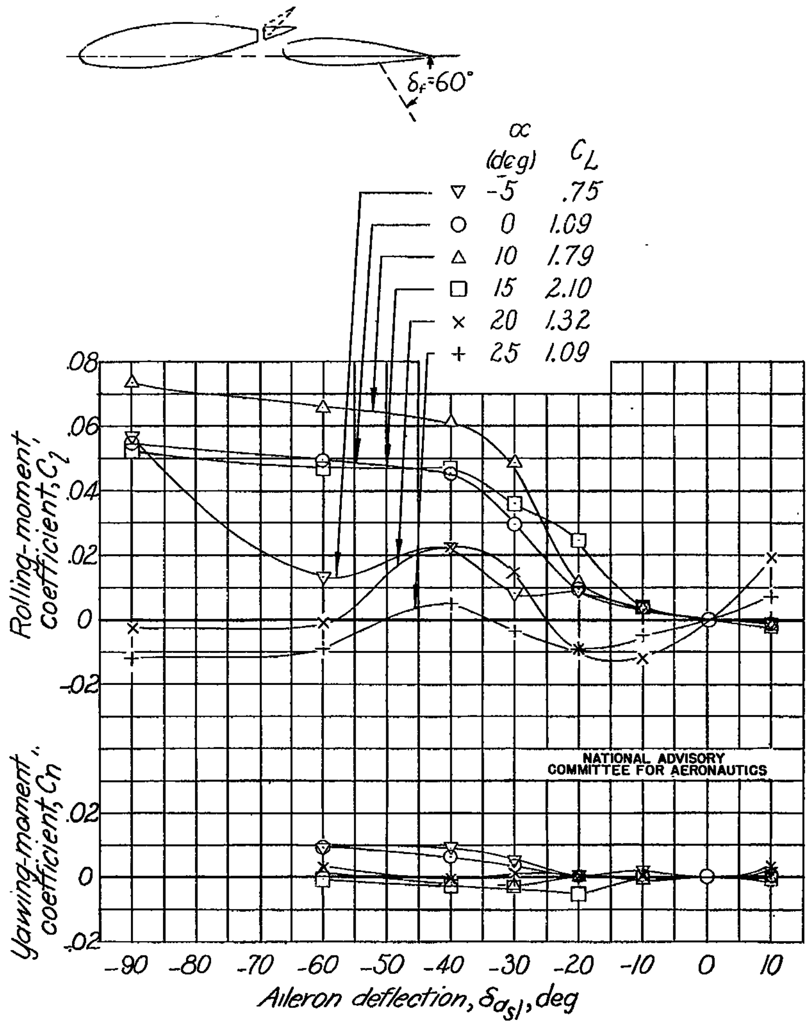

(b) δ_f, 60°.

Figure A10.- Concluded.

Model A-IV

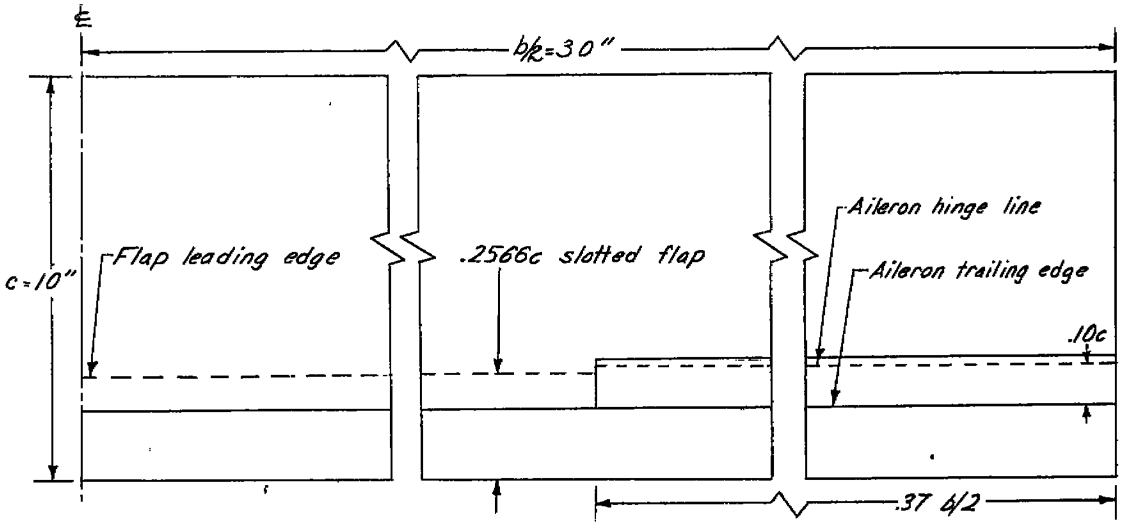

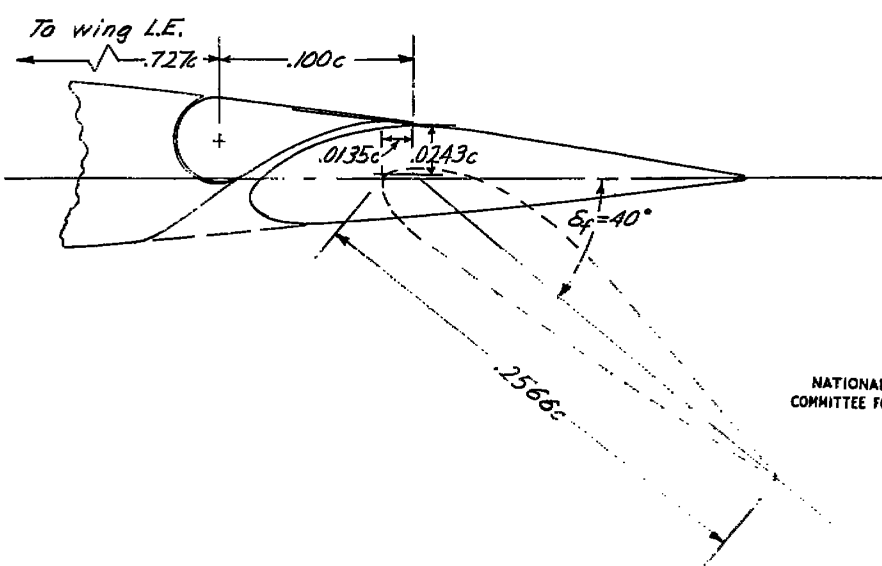

NATIONAL ADVISORY COMMITTEE FOR AERONAUTICS

Figure A11.- Plan form and section of the 10- by 60-inch NACA 23012 wing tested with a full-span slotted flap and a slot-lip aileron in the Langley 7- by 10-foot tunnel.

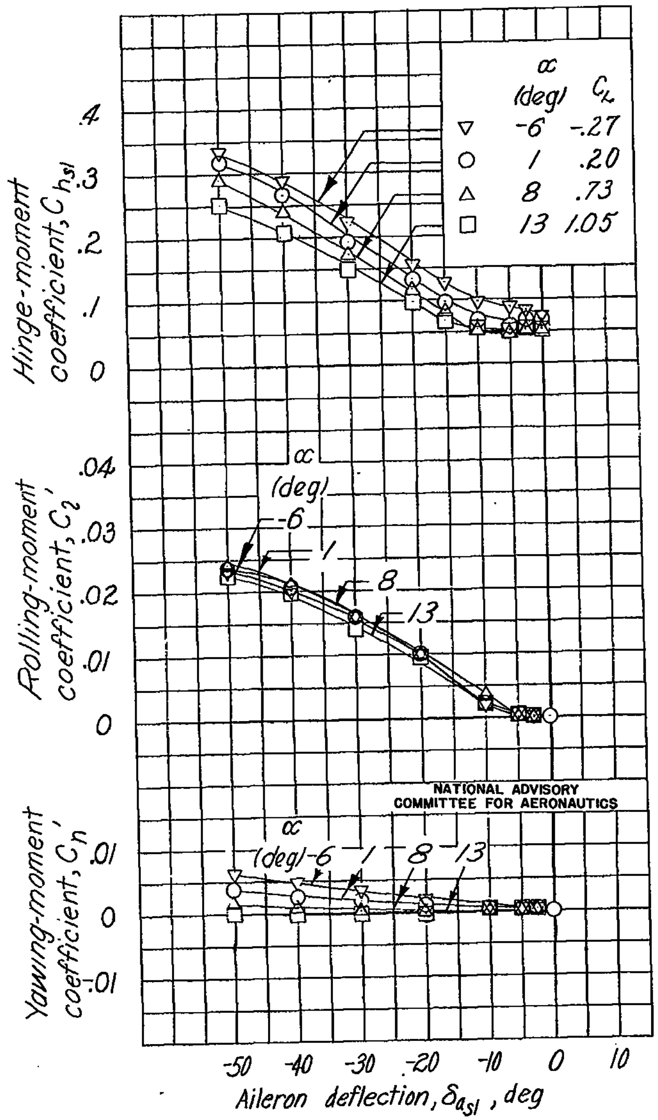

(a) δ_f, 0°.

Figure A12.- Rolling-, yawing-, and hinge-moment characteristics of the 10- by 60-inch wing equipped with full-span slotted flaps and a slot-lip aileron.

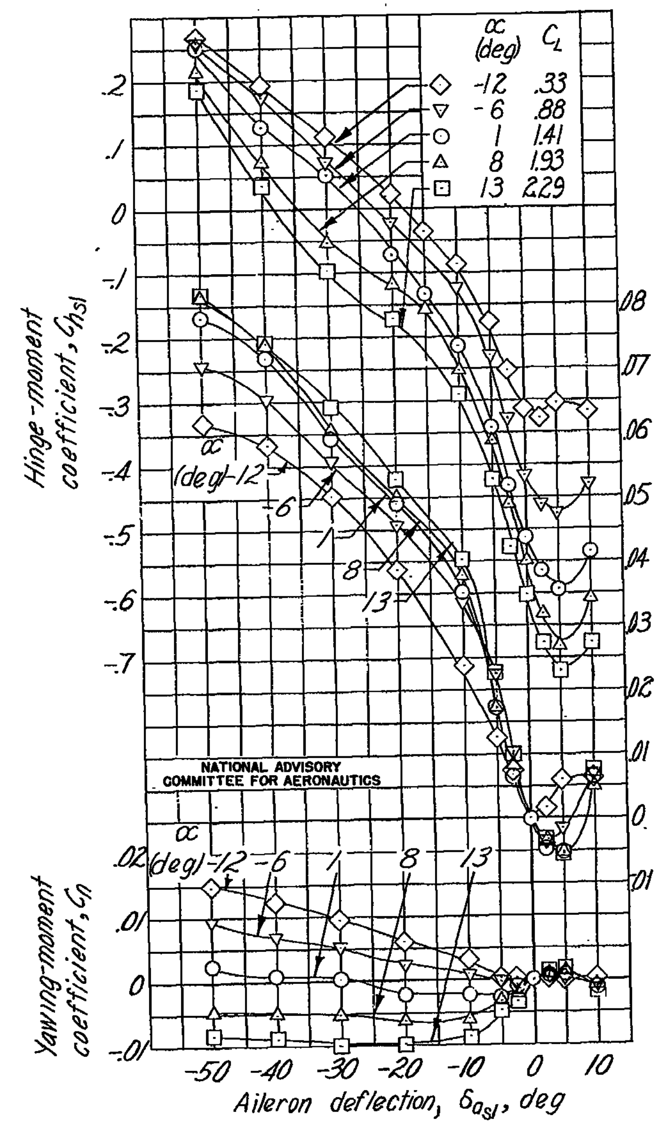

(b) δ_f, 40°.

Figure A12.- Concluded.

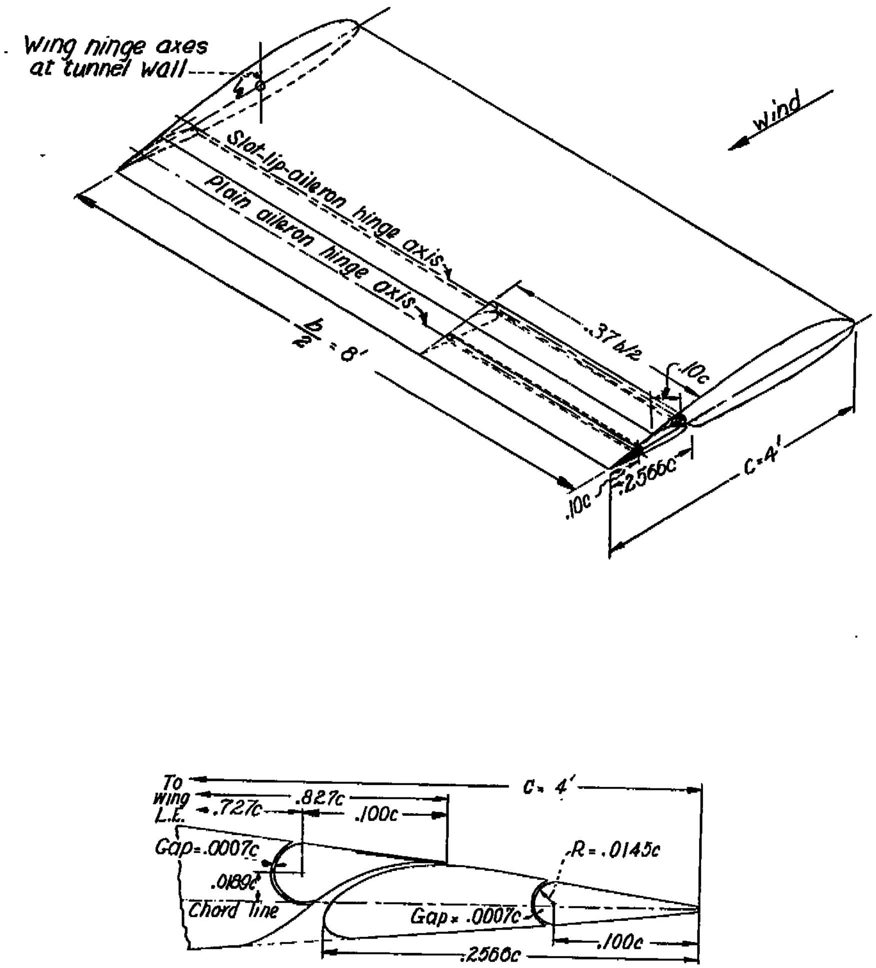

Figure A13.- Diagram of test setup and a section of the 4- by 8-foot NACA 23012 semispan wing tested with a 0.2566c full-span slotted flap and 0.10c by 0.37 b/2 slot-lip and plain ailerons in the Langley 7- by 10-foot tunnel.

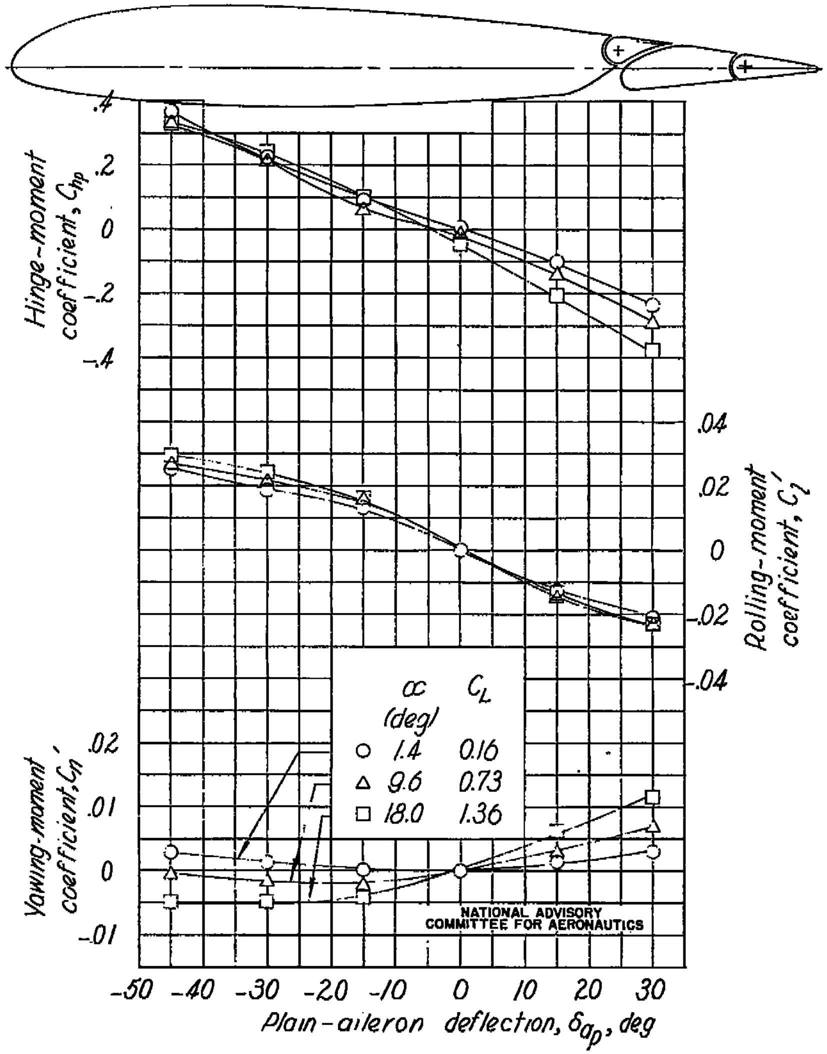

(a) Flap retracted, slot closed.

Figure A14.- Effect of plain-aileron deflection on the aerodynamic characteristics of the 4- by 8-foot NACA 23012 semispan wing equipped with a 0.2566c full-span slotted flap and 0.10c by 0.37 b/2 slot-lip and plain ailerons. $\delta_{a_{s_1}} = 0^\circ$.

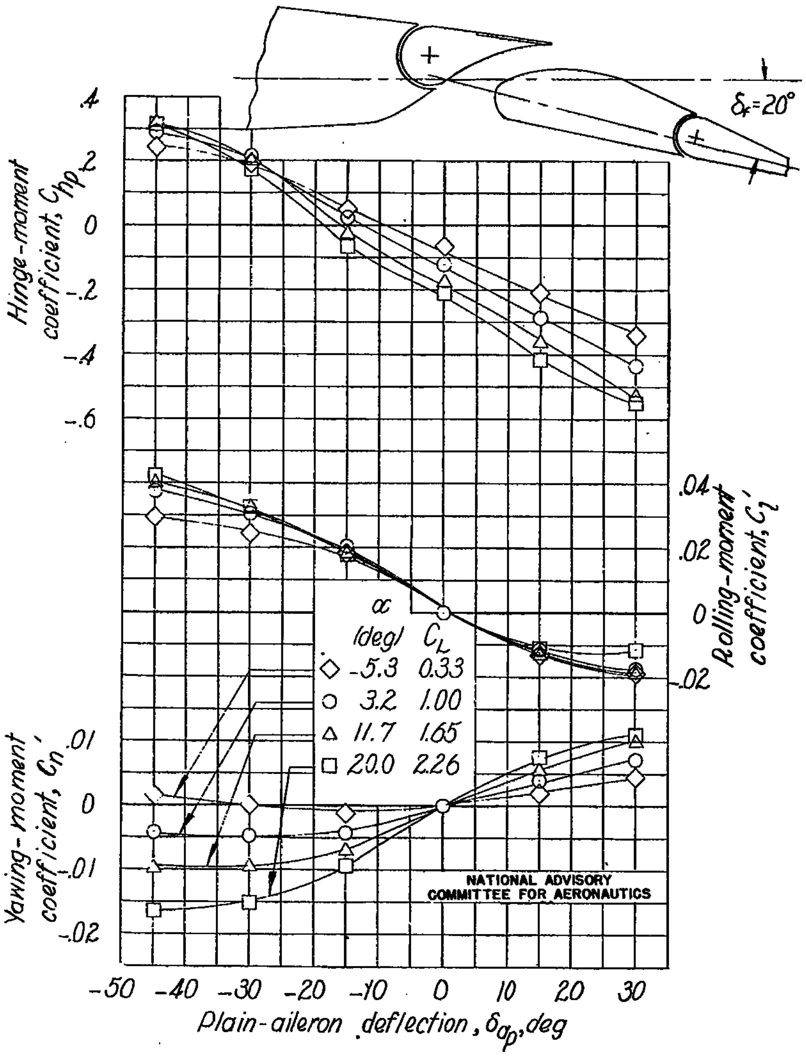

(b) δ_f, 20°.

Figure A14.- Continued.

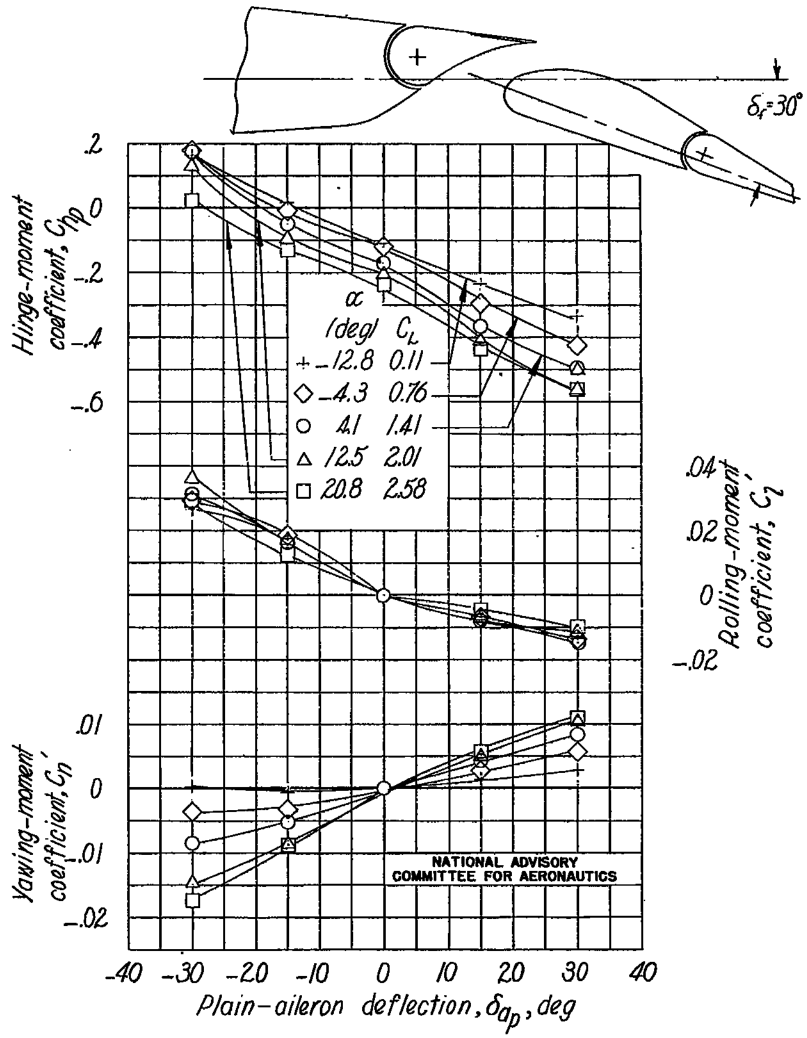

(c) δ_f, 30°.

Figure A14.- Concluded.

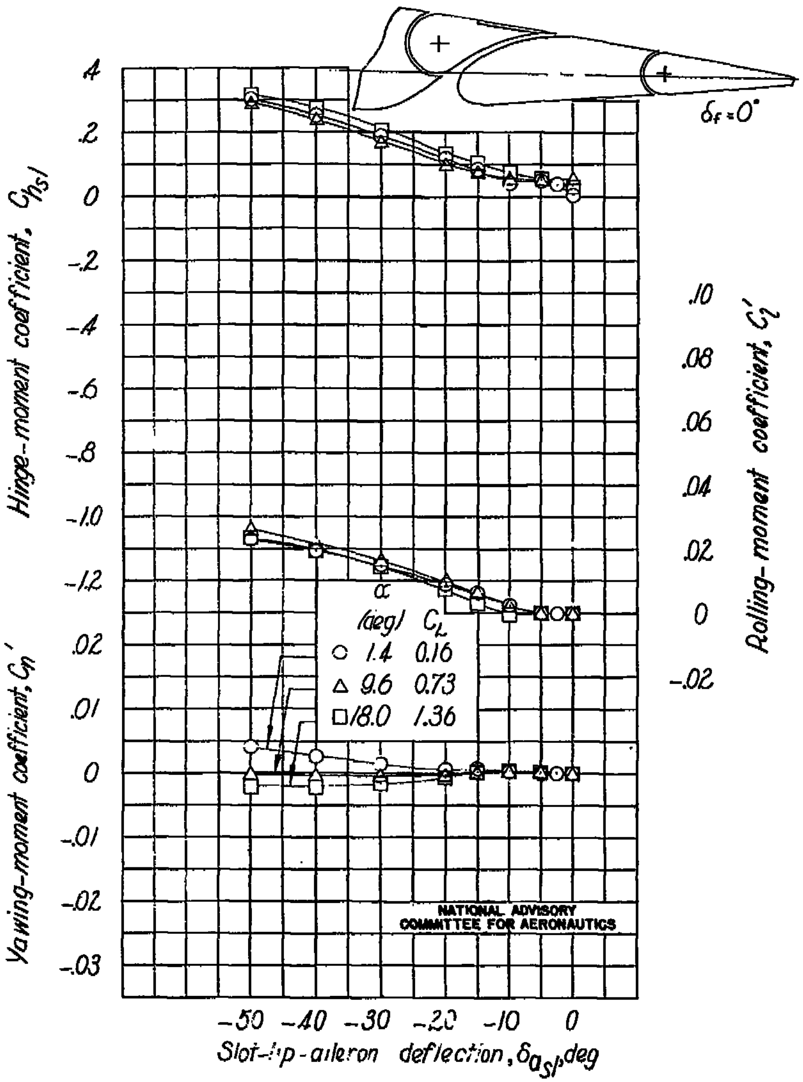

(a) δ_f, 0°.

Figure A15.- Effect of slot-lip-aileron deflection on the aerodynamic characteristics of the 4- by 8-foot NACA 23012 semispan wing equipped with a 0.2566c full-span slotted flap and 0.10c by 0.37 b/2 slot-lip and plain ailerons. δ_{a_p}, 0°.

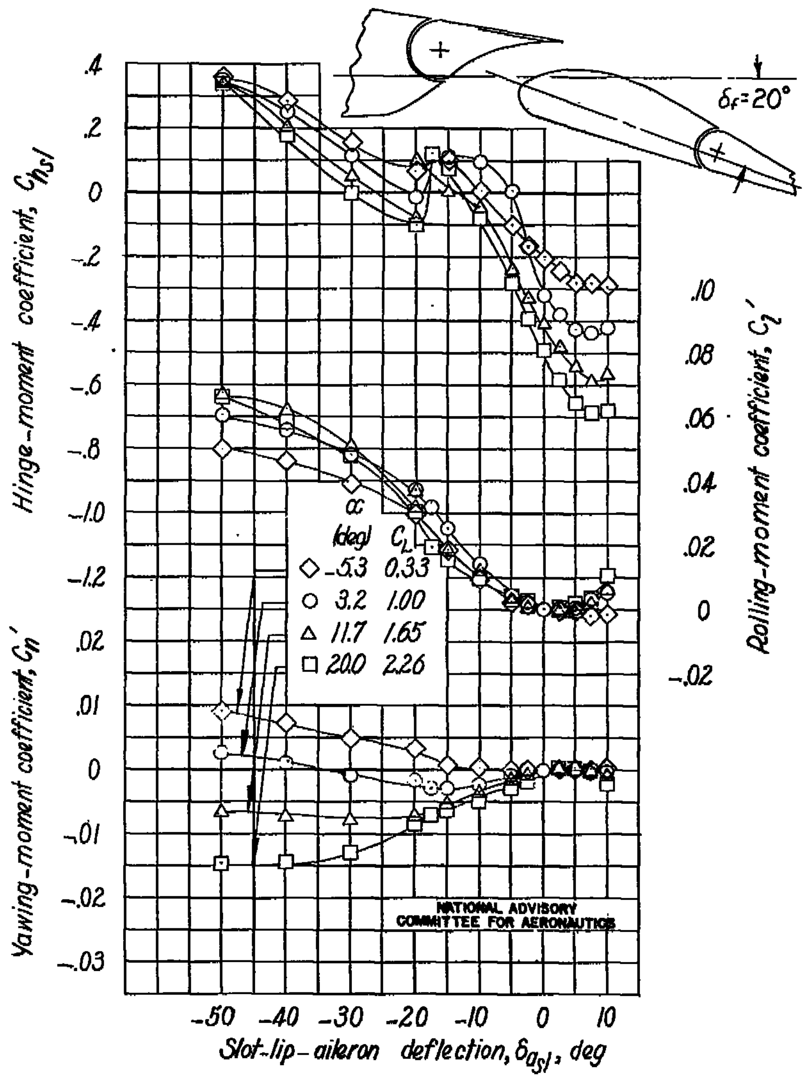

(b) δ_f, 20°.

Figure A15.- Continued.

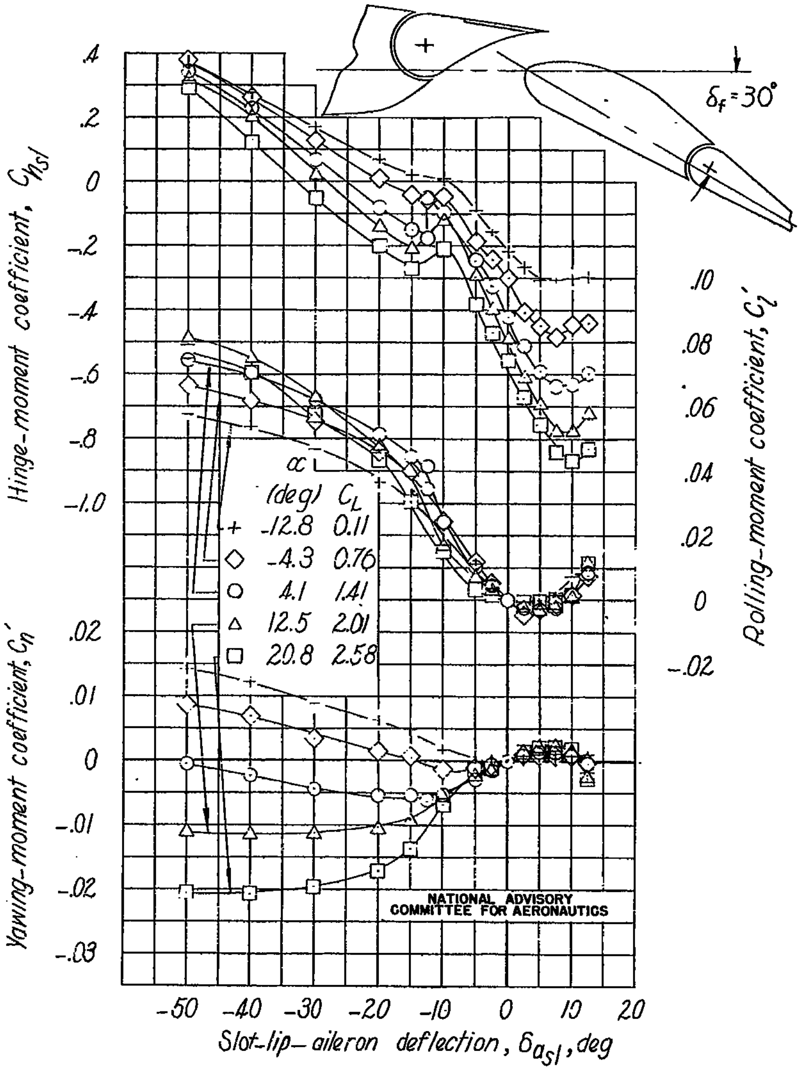

(c) δ_f, 30°.

Figure A15.- Continued.

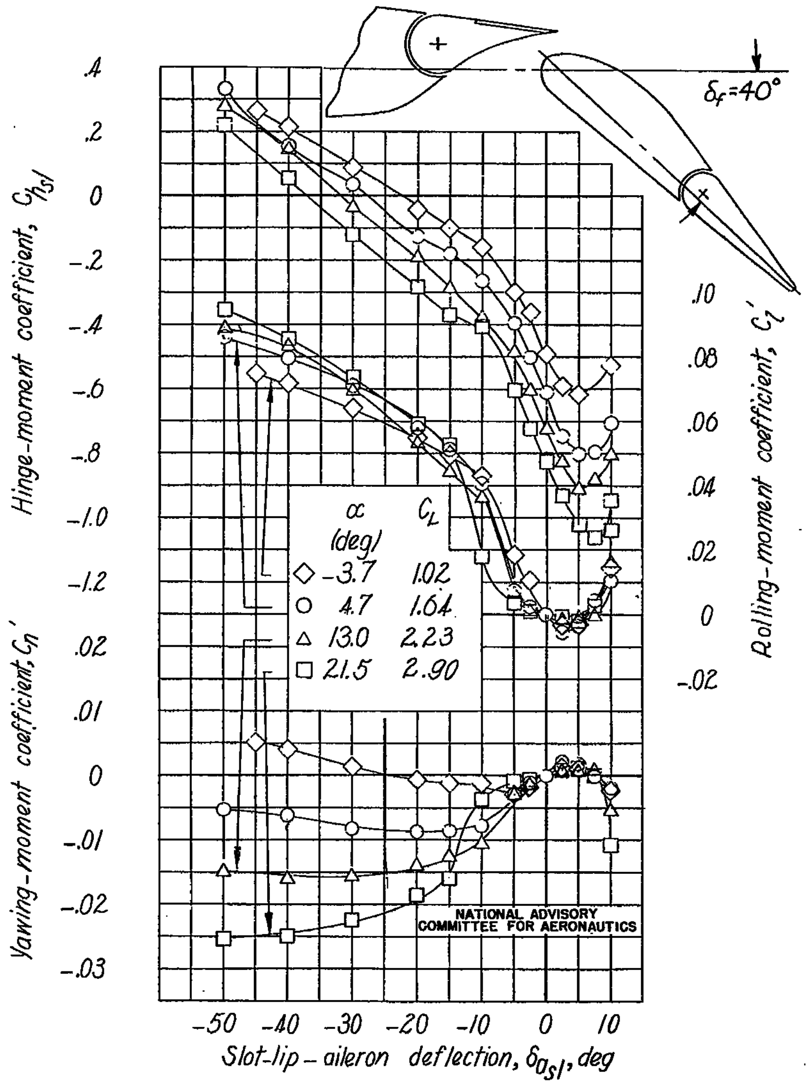

(d) δ_f, 40°.

Figure A15.- Continued.

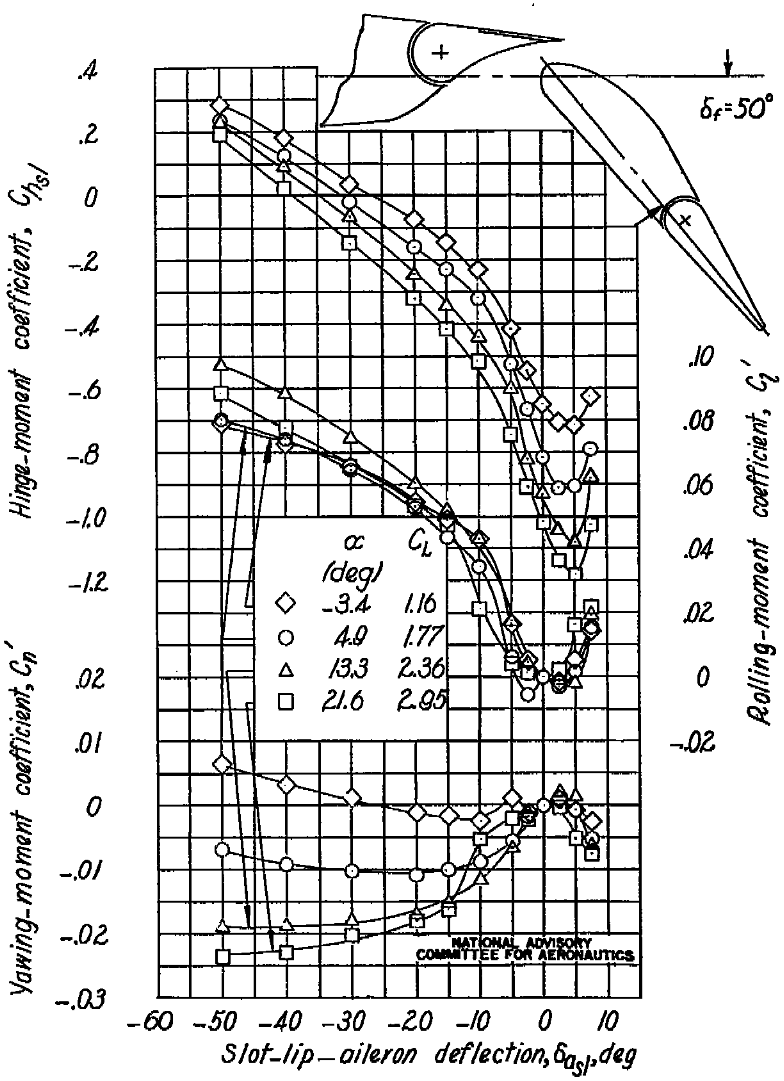

(e) δ_f, 50°; flap nose located 0.005c ahead of lip and 0.015c below lip.

Figure A15.- Continued.

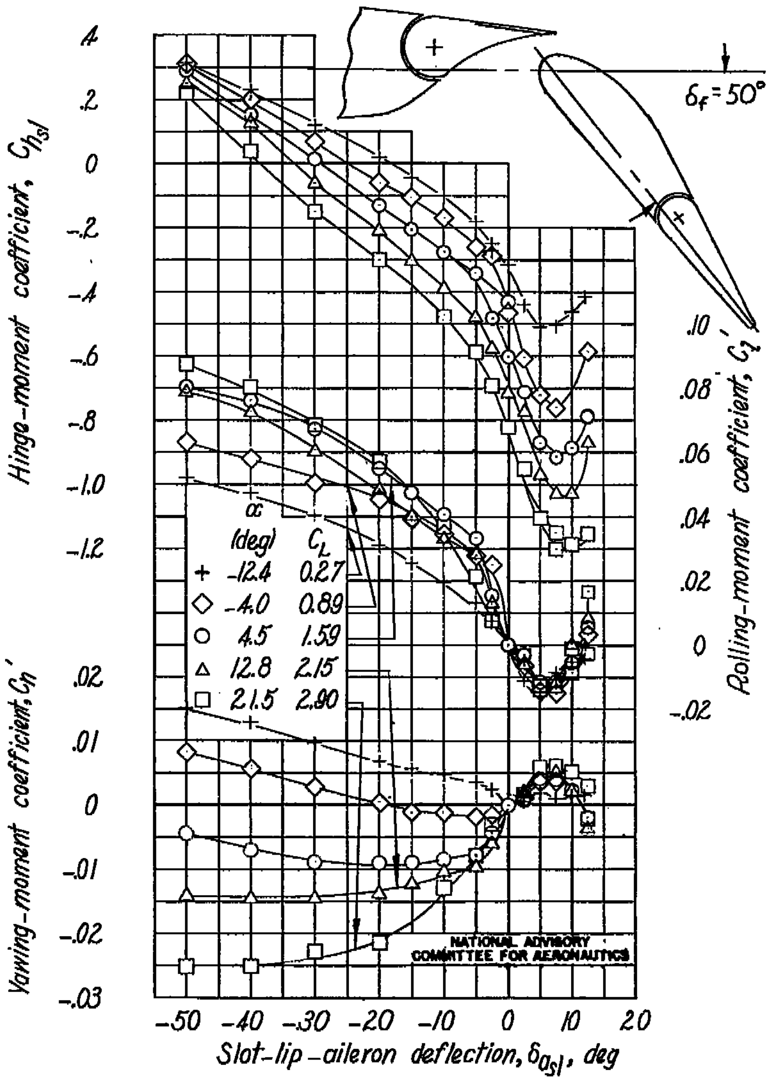

(f) δ_f, 50°; flap-nose located 0.005c ahead of lip and 0.025c below lip.

Figure A15.- Concluded.

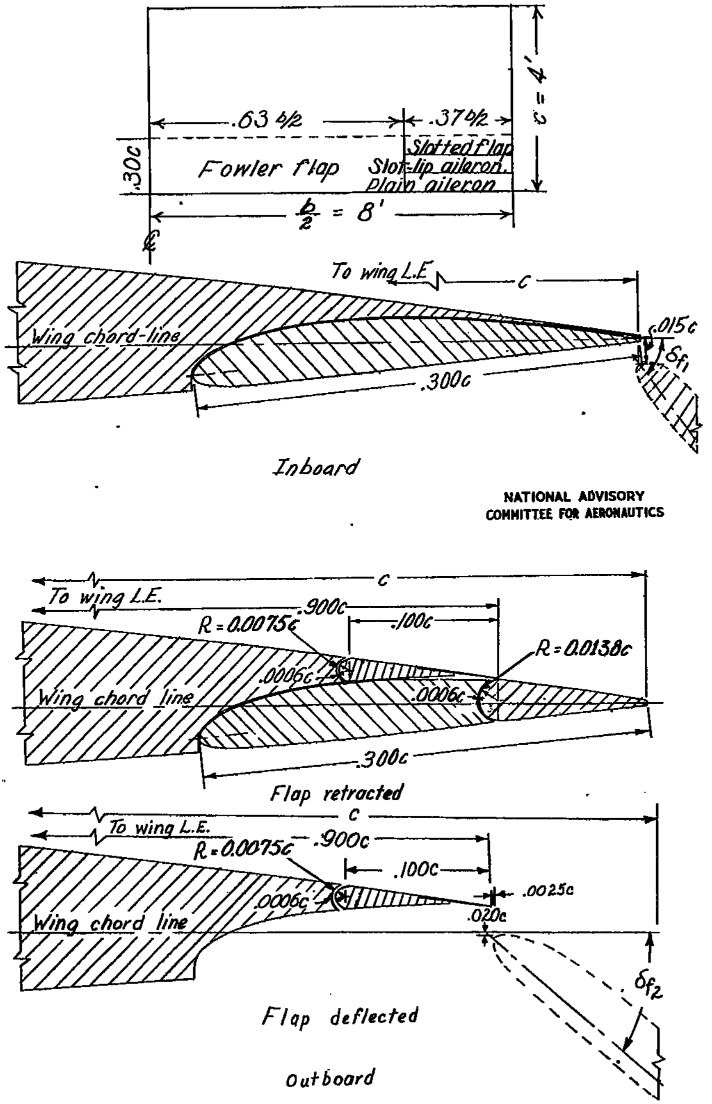

Figure A16.- Plan form and sections of the 4- by 8-foot NACA 23012 semispan wing equipped with 0.37 b/2 modified slotted flap outboard and a 0.63 b/2 Fowler flap inboard with 0.37 b/2 sealed slot-lip and plain ailerons. Tested in the Langley 7- by 10-foot wind tunnel.

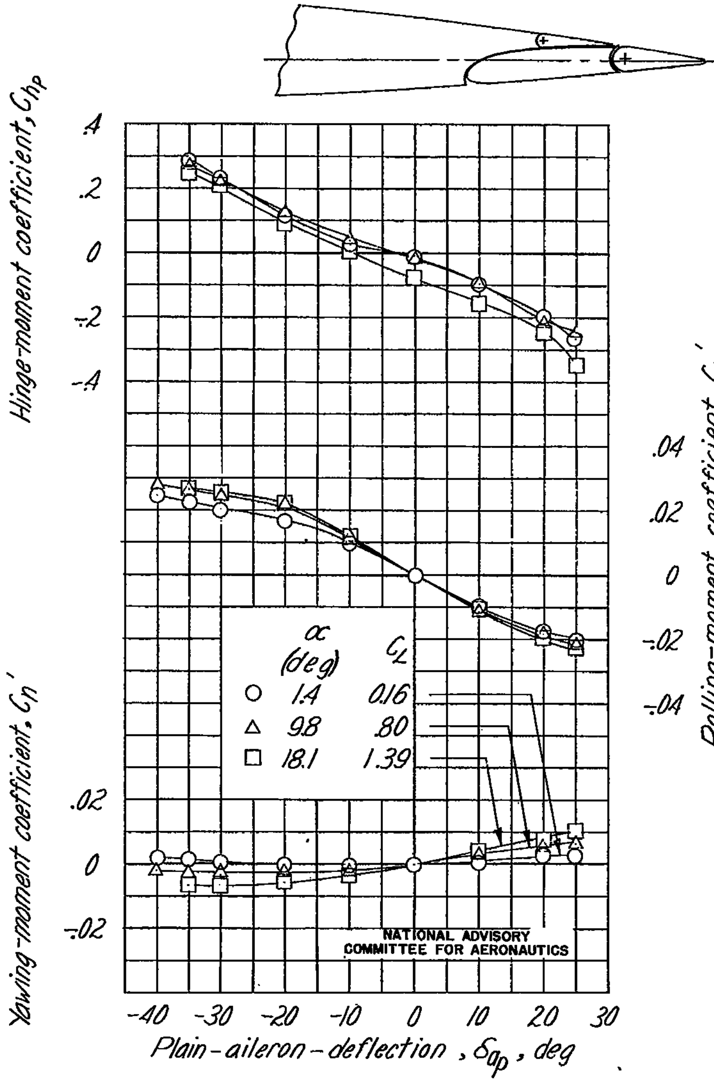

(a) δ_{f_1}, 0°; δ_{f_2}, 0°.

Figure A17.- Effect of sealed-plain-aileron deflection on the aerodynamic characteristics of the NACA 23012 wing.

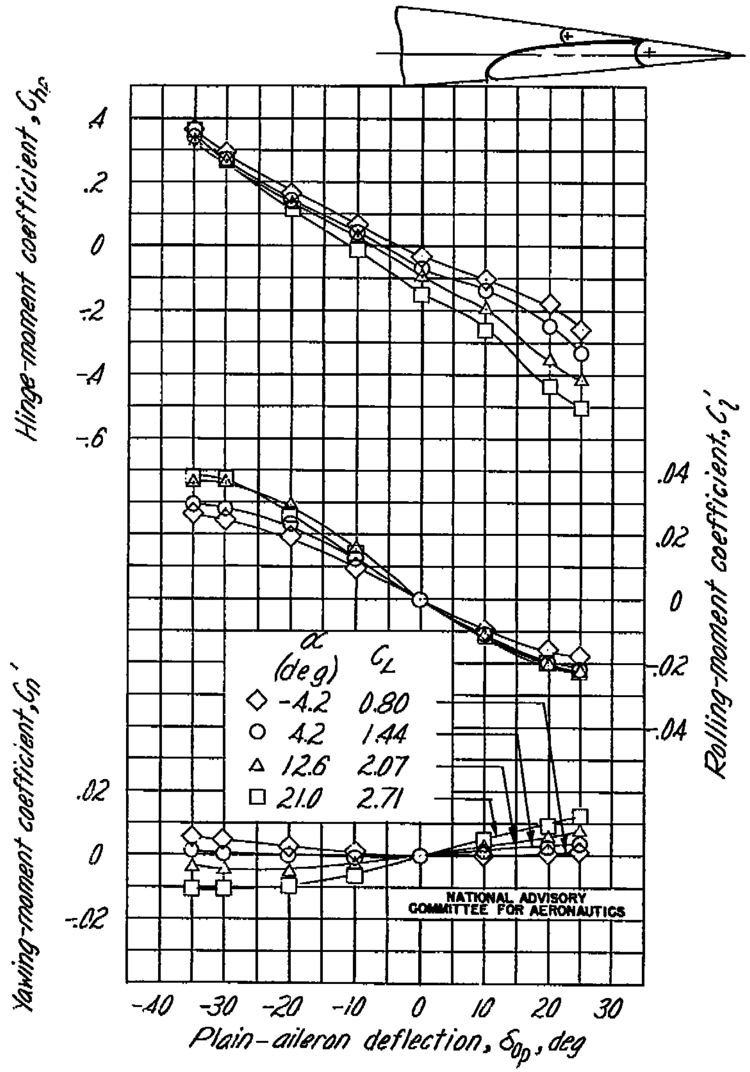

(b) δ_{f_1}, 40°; δ_{f_2}, 0°.

Figure A17.- Continued.

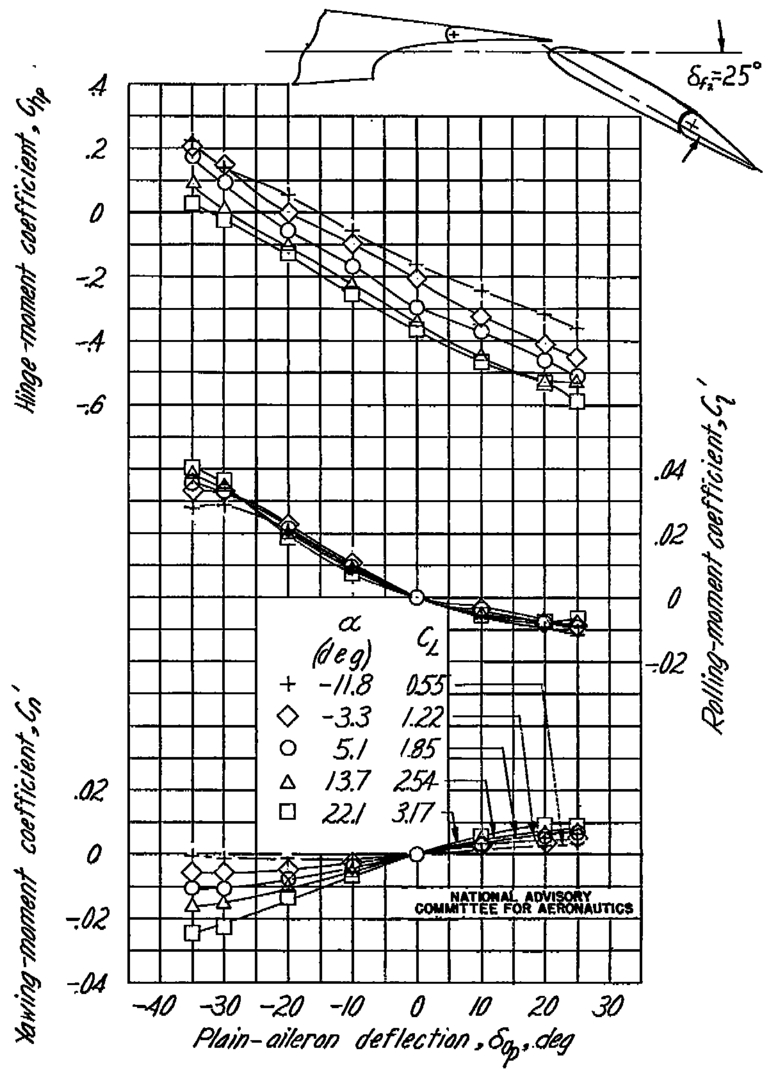

(c) δ_{f_1}, 40°; δ_{f_2}, 25°.

Figure A17.- Concluded.

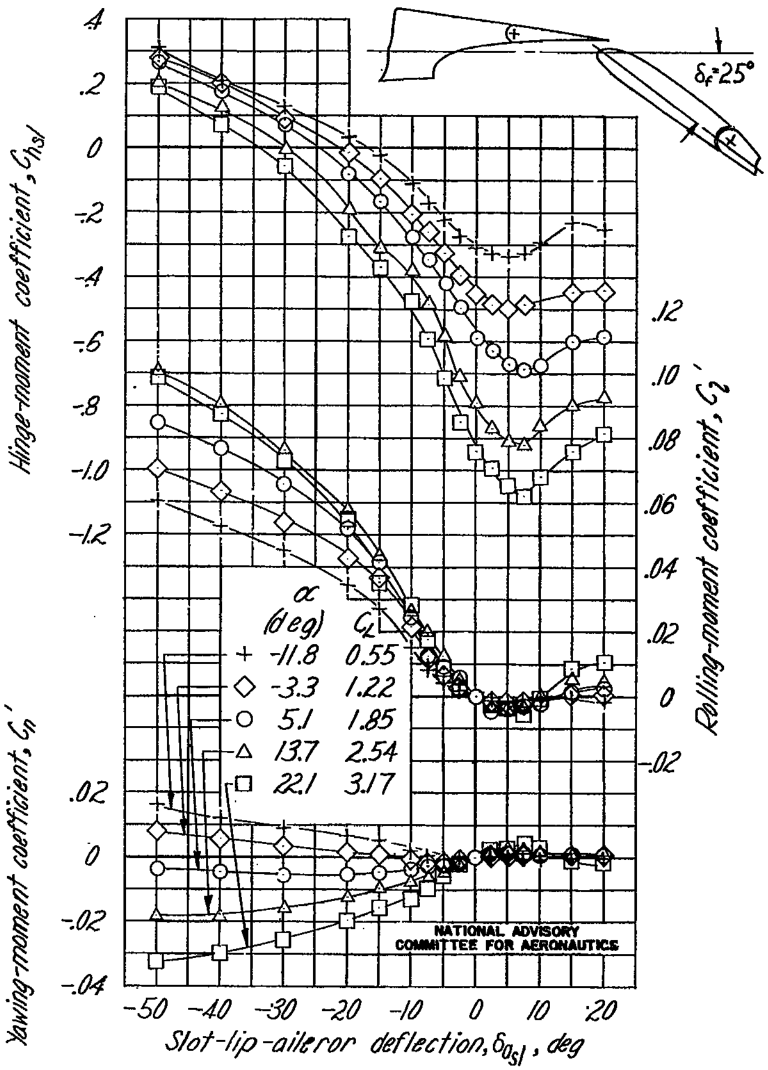

(a) δ_{f_1}, 40°; δ_{f_2}, 25°.

Figure A18.- Effect of sealed slot-lip-aileron deflection on the aerodynamic characteristics of the NACA 23012 wing.

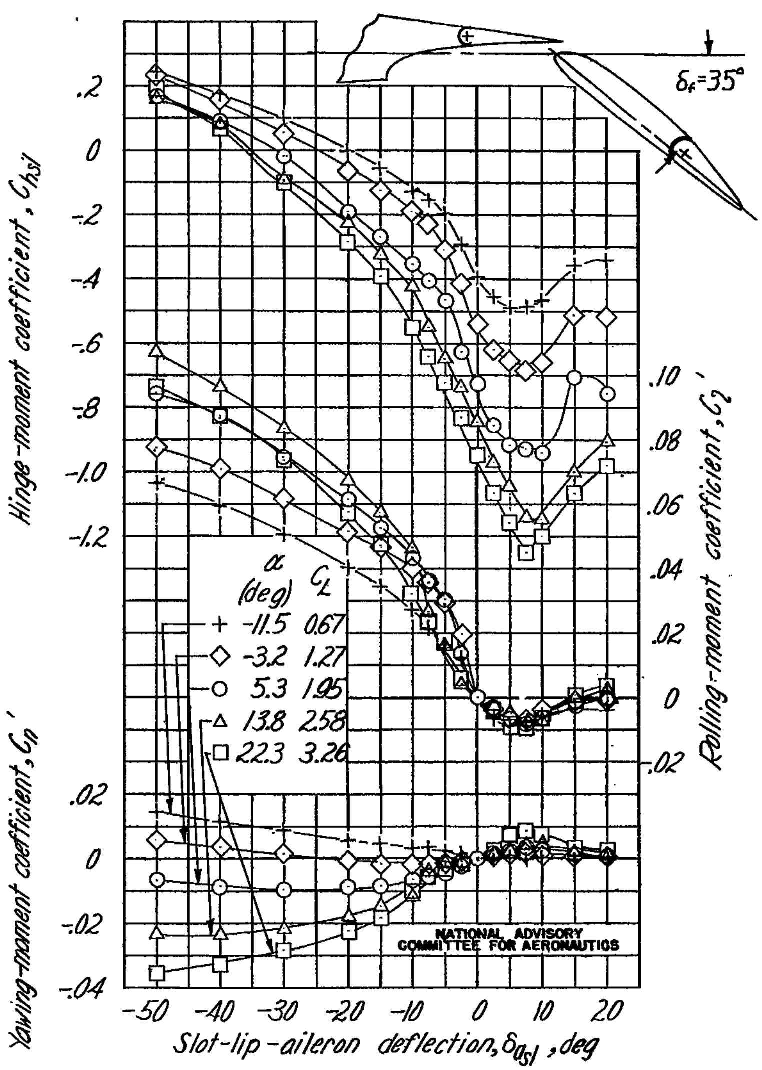

(b) δ_{f_1}, 40°; δ_{f_2}, 35°.

Figure A18.- Concluded.

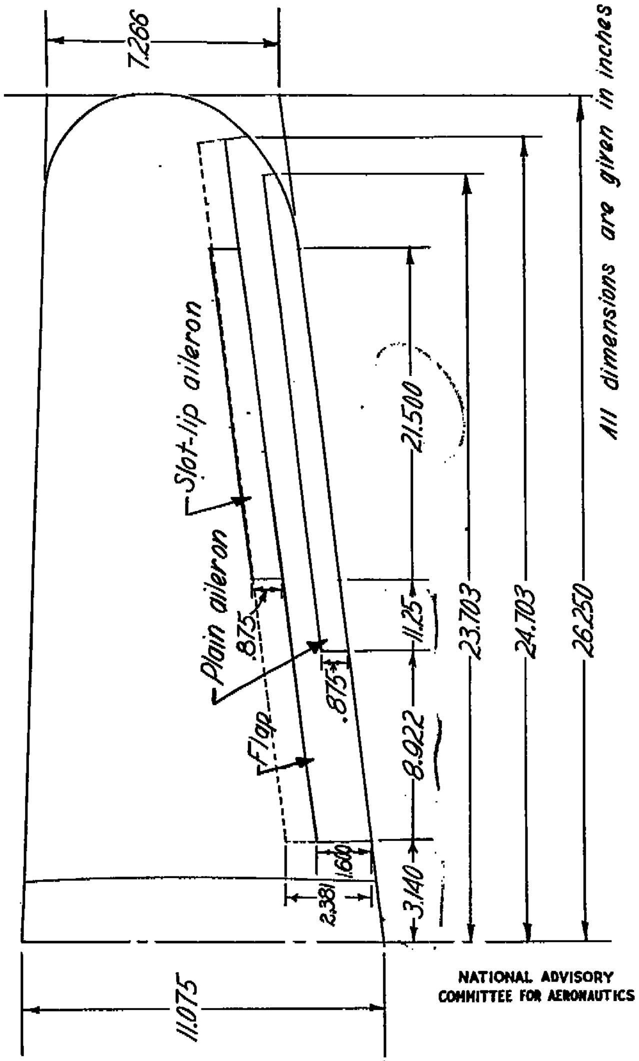

Figure A19.- Plan form of the tapered semispan wing on a $\frac{1}{8}$-scale model of a fighter-type airplane tested in the Langley 7- by 10-foot tunnel.

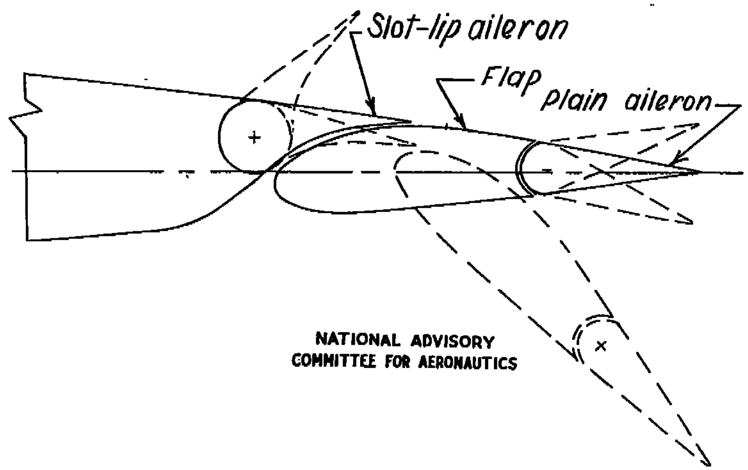

Figure A20.- Sectional view of the wing showing the slotted flap and plain and slot-lip ailerons.

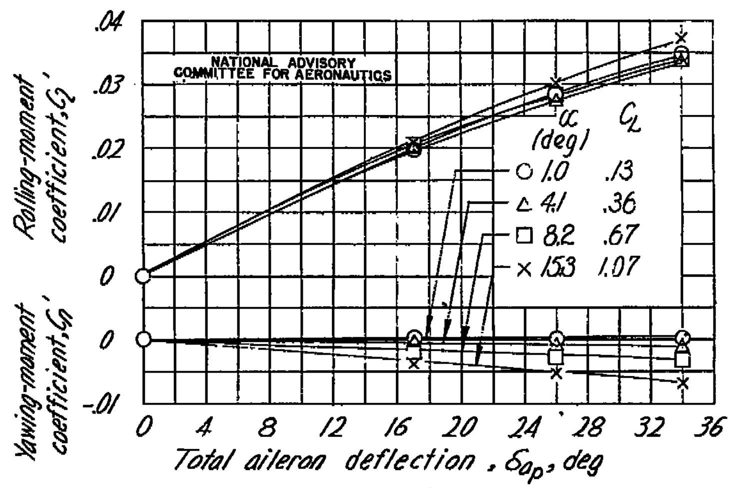

(a) Flap retracted.

Figure A21.- Effect of plain aileron deflection on the yawing- and rolling-moment coefficients of the $\frac{1}{8}$-scale model of a fighter-type airplane. $\delta_{a_{sl}}$, 0°. $\delta_{a_{p(right)}} = \delta_{a_{p(left)}}$.

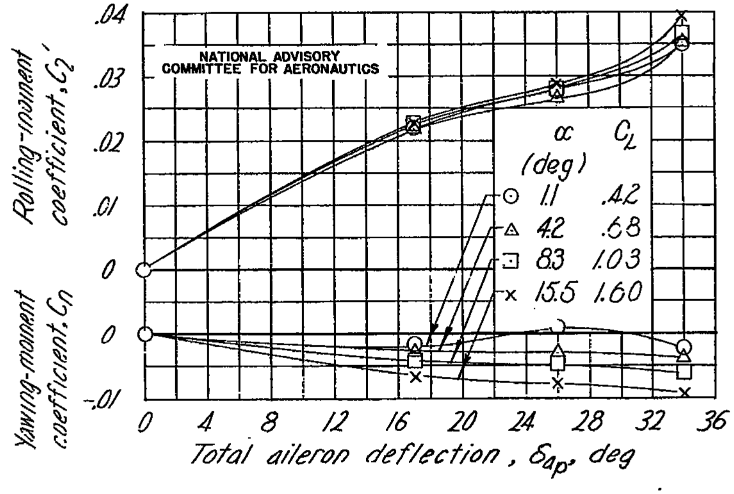

(b) δ_f, 10°.

Figure A21.- Continued.

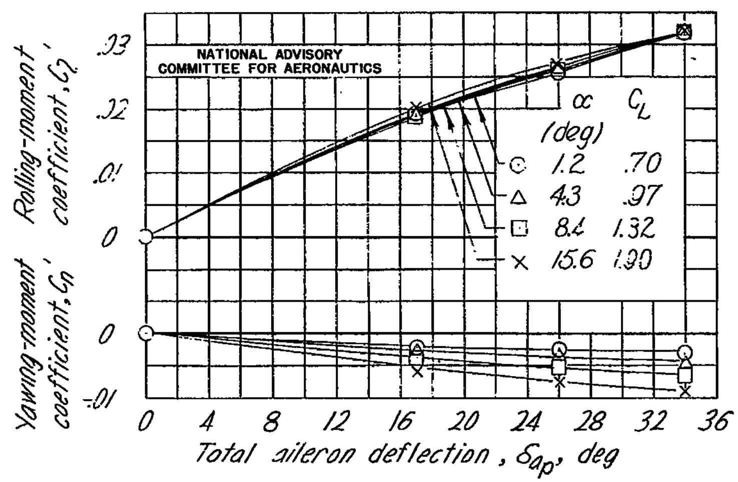

(c) δ_f, 20°.

Figure A21.- Continued.

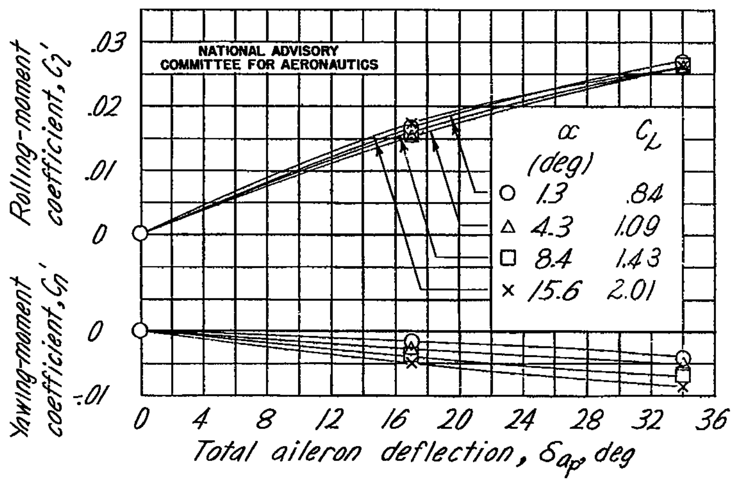

(d) δ_f, 30°.

Figure A21.- Continued.

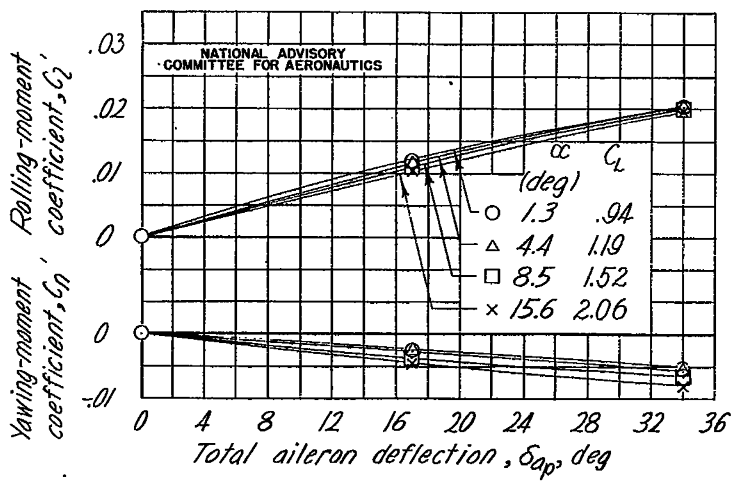

(e) δ_f, 40°

Figure A21.- Concluded.

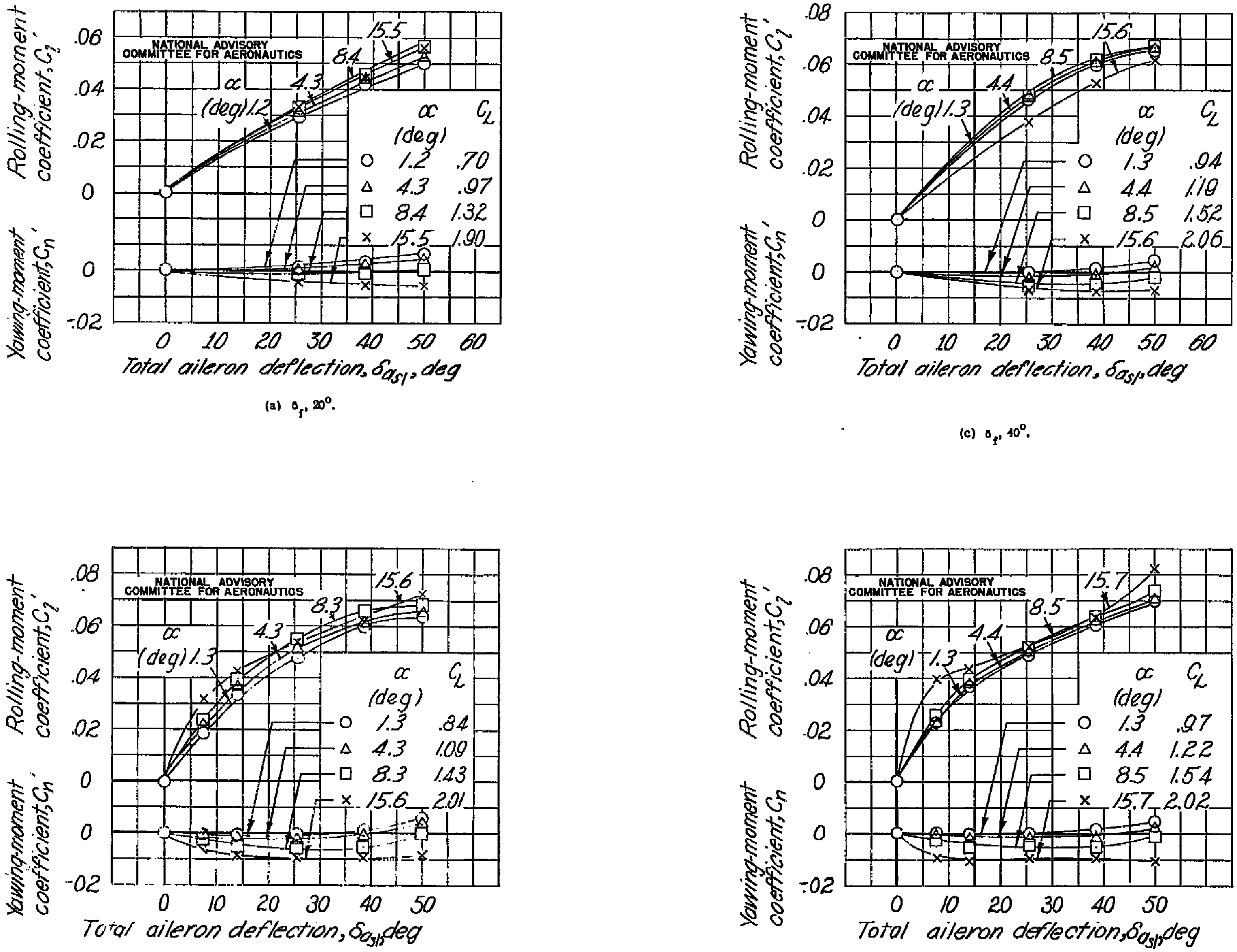

(a) δ_f, 20°.

(c) δ_f, 40°.

(b) δ_f, 30°.

(d) δ_f, 50°.

Figure A22.- Effect of sl[illegible] aileron deflection on the rolling- and yawing-moment coefficients of the $\frac{1}{8}$-scale model of a fighter-type airplane. δ_{a_t}, 0°. (See fig. [illegible] for aileron-stick differential.)

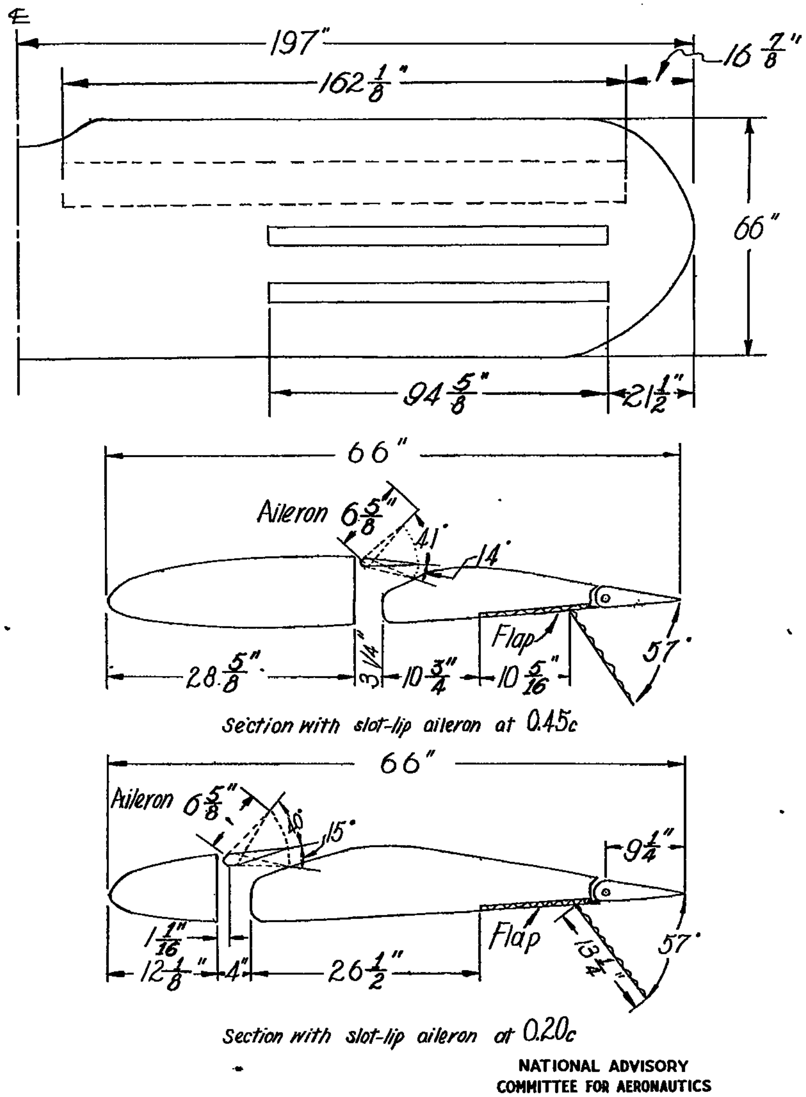

Figure A23.- Plan form of semispan wing and profile of wing sections of the Fairchild 22 airplane tested with slot-lip ailerons and full-span split flaps in the Langley full-scale tunnel and in flight.

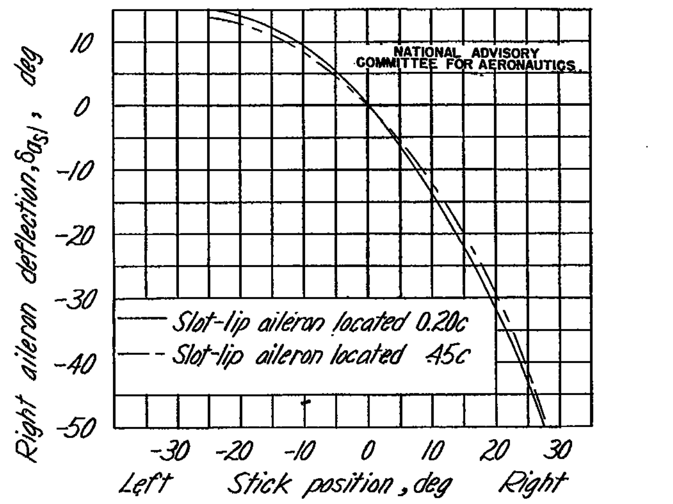

Figure A24.- Variation of stick position with slot-lip aileron deflection for the Fairchild 22 airplane.

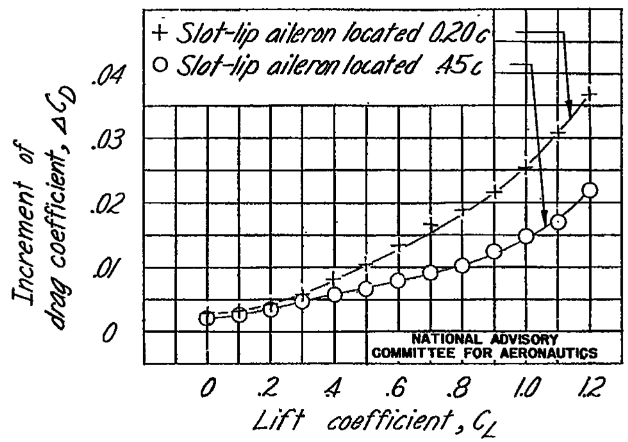

Figure A25.- Increase in drag due to slot-lip ailerons on the Fairchild 22 airplane in the Langley full-scale tunnel. Airspeed, 56 miles per hour.

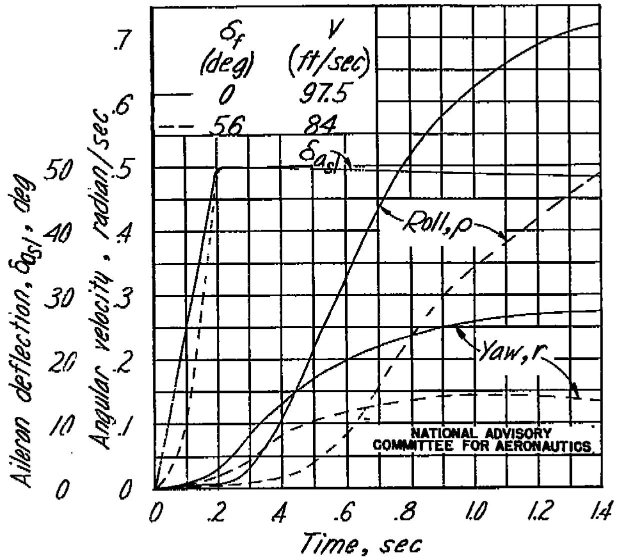

(a) Slot-lip ailerons at 0.20c.

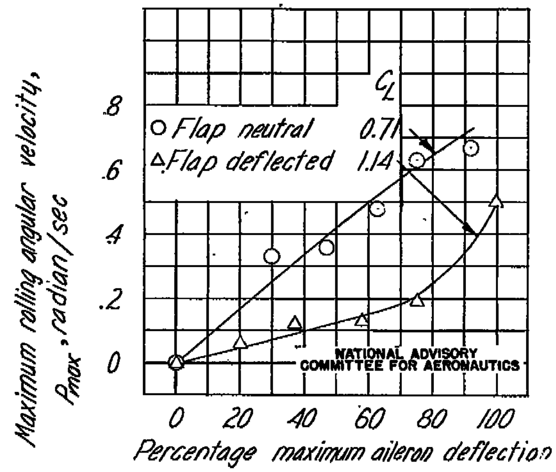

(a) Slot-lip ailerons at 0.20c.

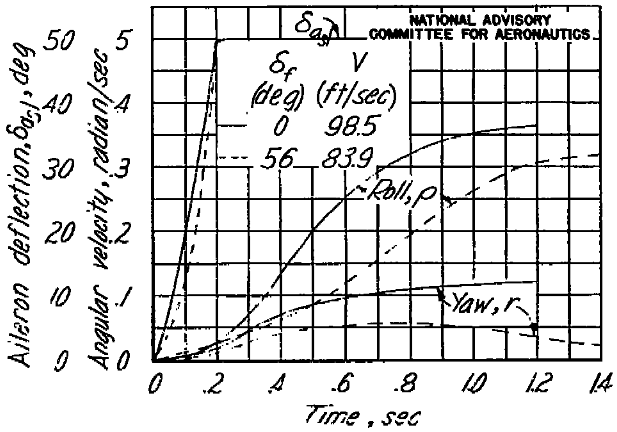

(b) Slot-lip ailerons at 0.45c.

Figure [illegible].- Time history of airplane motion with abrupt slot-lip aileron deflection on the Fairchild 22 airplane in flight.

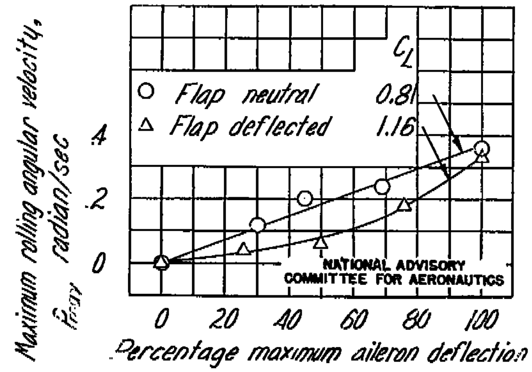

(b) Slot-lip ailerons at 0.45c.

Figure [illegible].- Variation of maximum rolling angular velocity with aileron deflection for slot-lip ailerons on the Fairchild 22 airplane in flight.

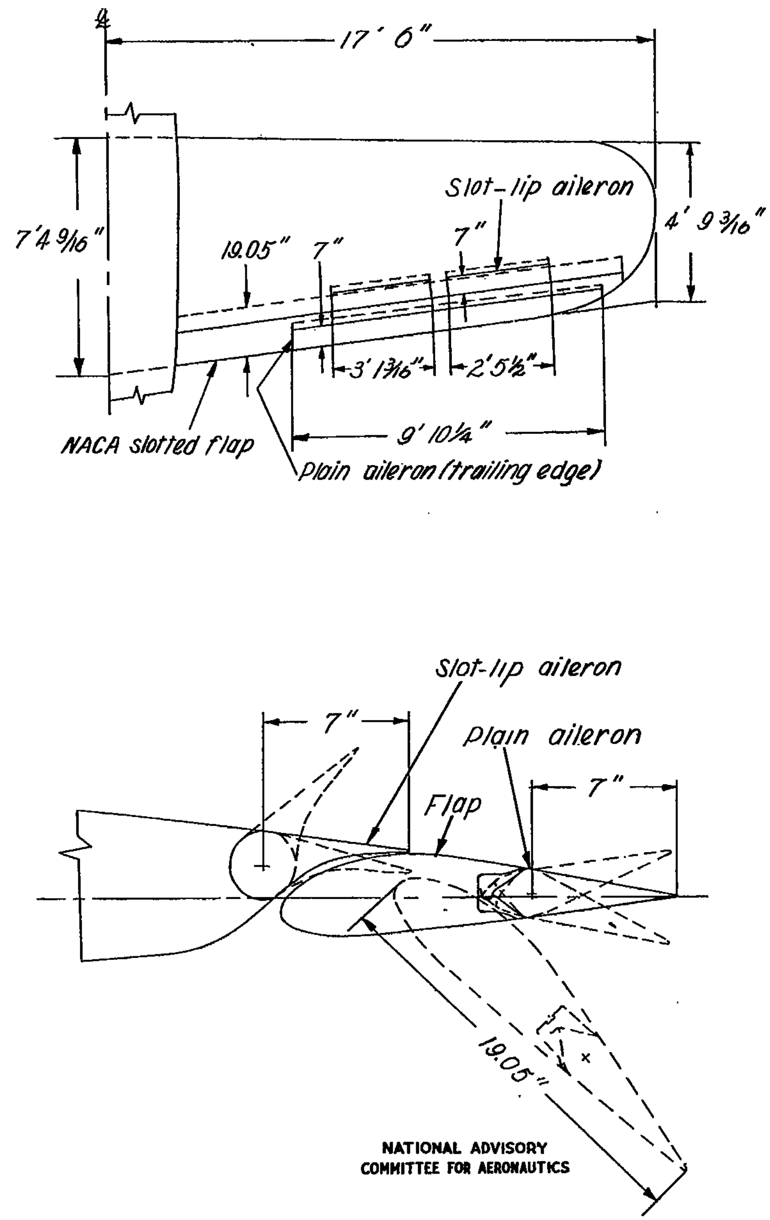

Figure A28.- Plan form and section of the wing of a fighter-type airplane tested in flight at Langley with full-span slotted flaps, internally balanced trailing-edge ailerons, and slot-lip ailerons.

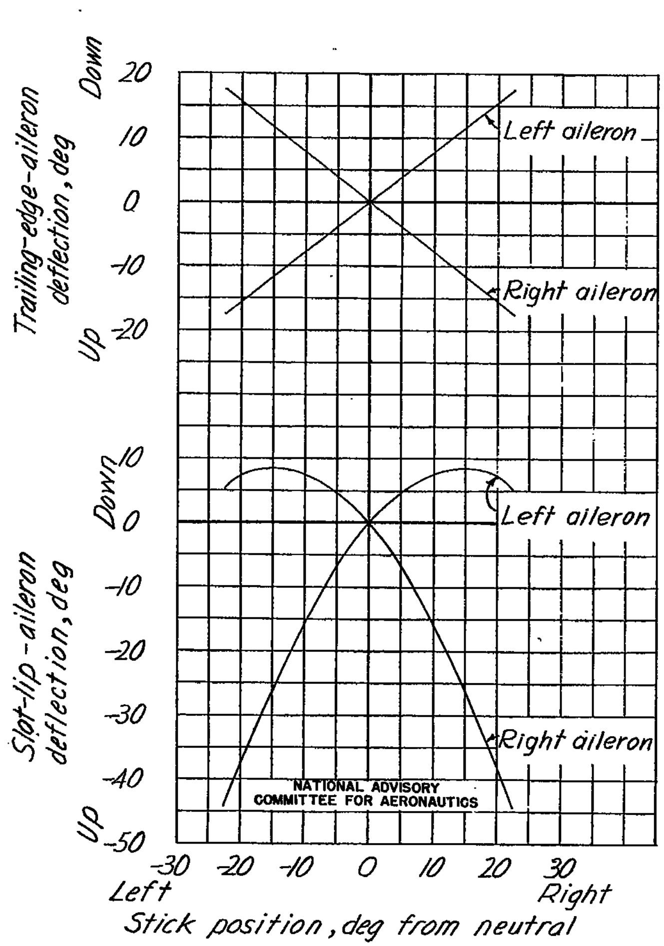

Figure A29.- Relation between trailing-edge and slot-lip-aileron deflections and stick position. Stick length, 19.0 inches.

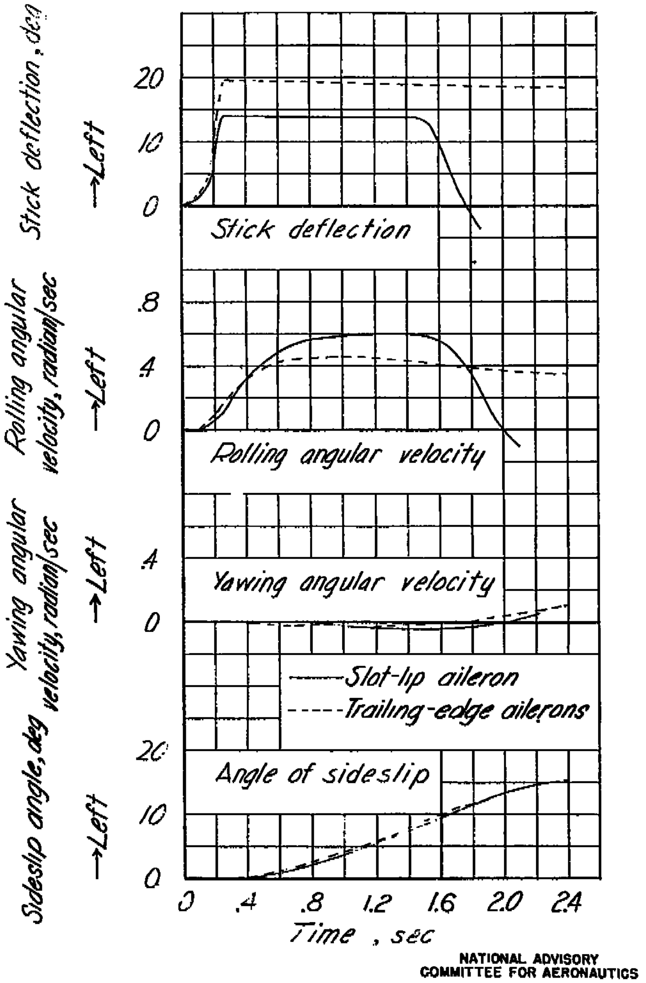

Figure A30.- Comparison of motion of a fighter-type airplane resulting from abrupt application of slot-lip ailerons and of flap trailing-edge ailerons. Level-flight power. For slot-lip ailerons: flap setting, 50°; V_{i_s}, 84 miles per hour. For trailing-edge ailerons: flap setting 0°; V_{i_s}, 90 miles per hour.

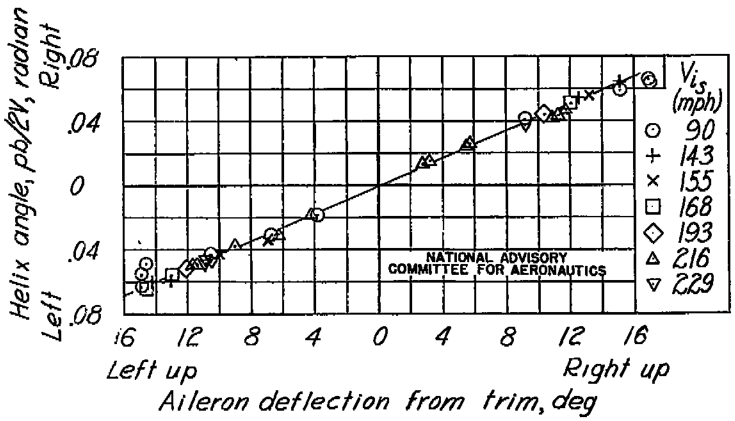

Figure A31.- Variation of wing-tip helix angle (pb/2V) with aileron deflection. Internally-balanced flap trailing-edge ailerons deflected; slot-lip ailerons neutral; level-flight power.

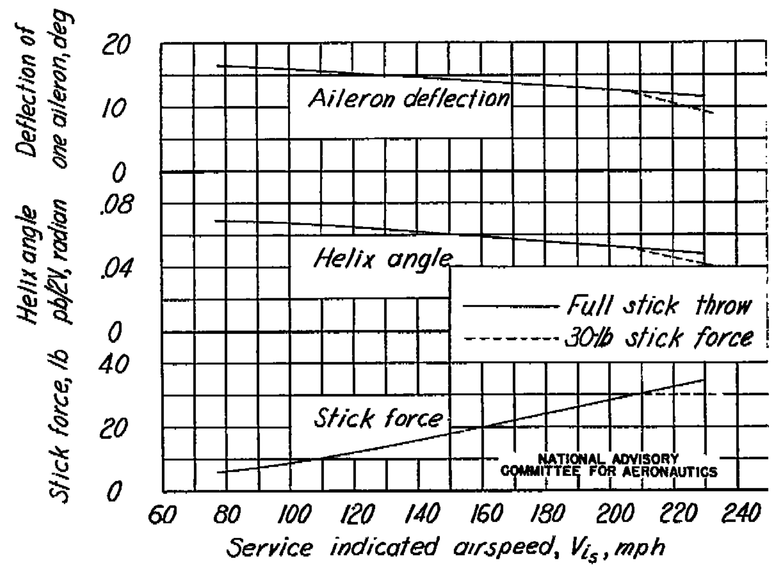

Figure A32.- Variation of aileron deflection, effectiveness and stick force with airspeed for full stick throw or 30-pound stick force. Internally balanced flap trailing-edge ailerons deflected; slot-lip ailerons neutral; level-flight power.

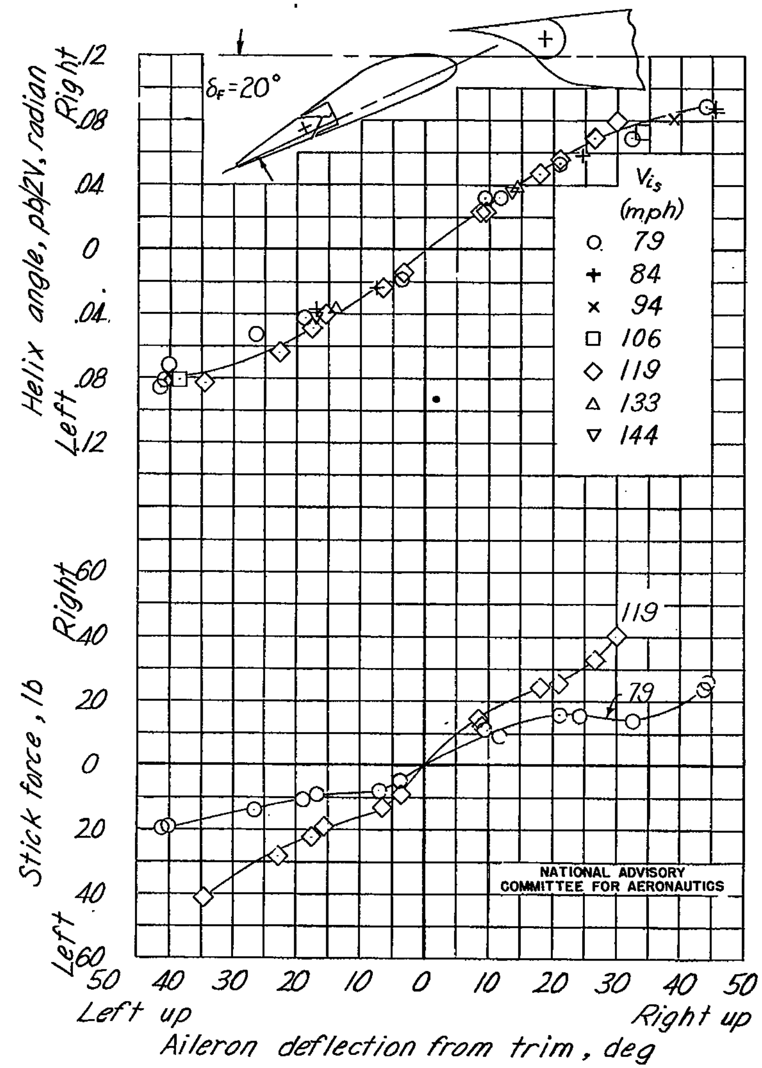

(a) Flap selector setting, 20°.

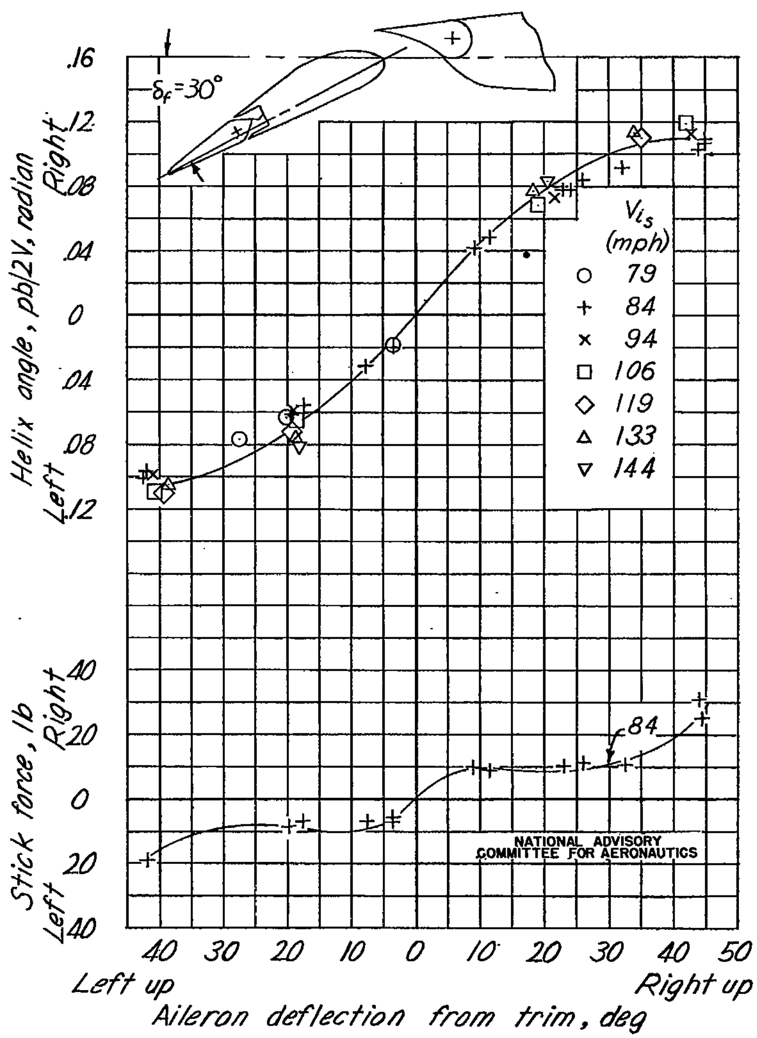

(b) Flap selector setting, 30°.

Figure A33.- Continued.

Figure A33.- Variation of wing-tip helix angle (pb/2V) and stick force with deflection of upgoing slot-lip aileron; flap trailing-edge ailerons neutral; level-flight power.

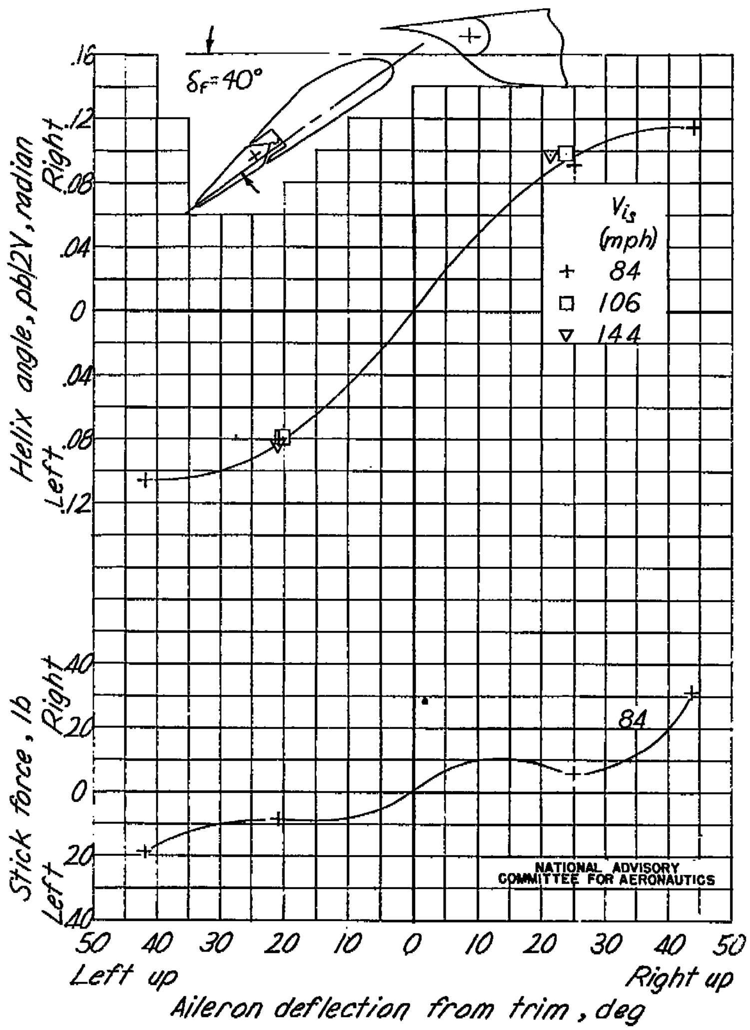

(c) Flap selector setting, 40°.

Figure A33.- Continued.

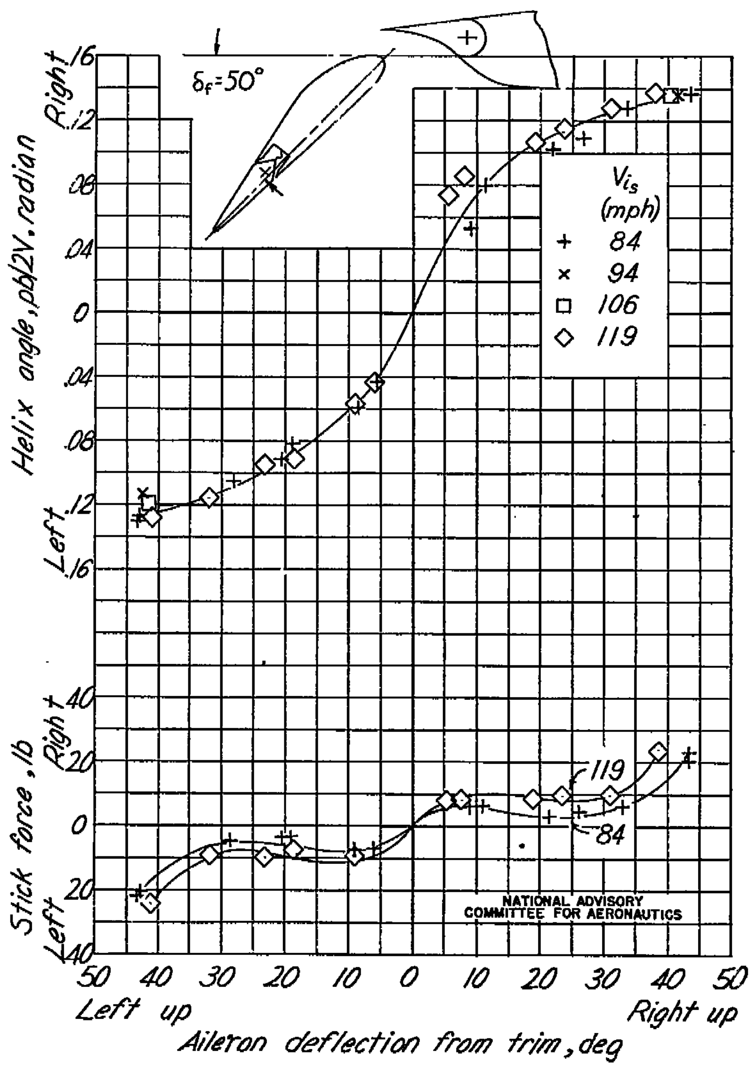

(d) Flap selector setting, 50°.

Figure A33.- Concluded.

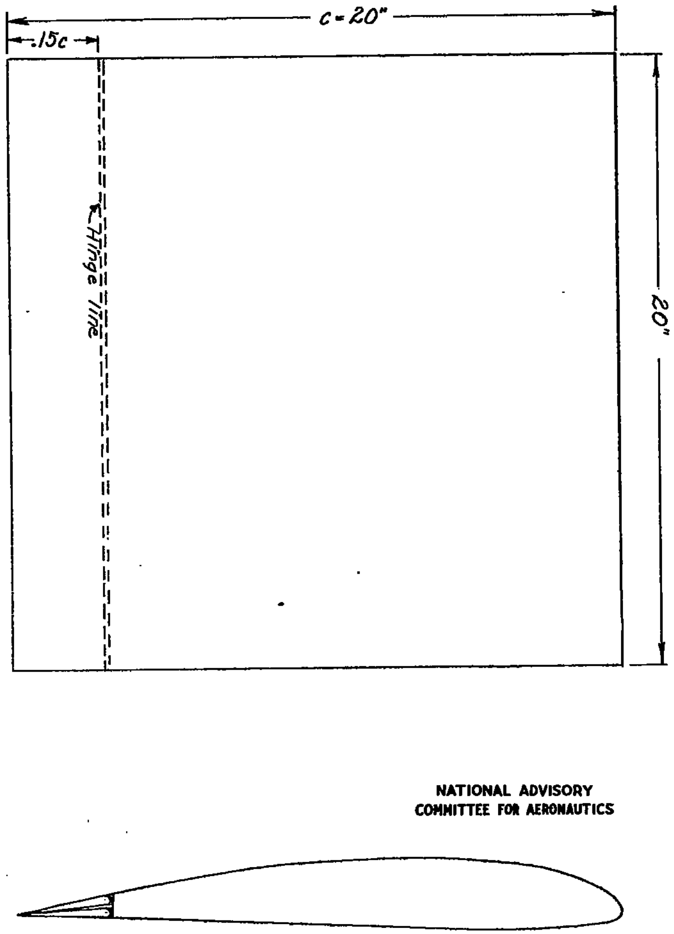

Figure B1.- Plan form and section of the Clark Y airfoil tested in the Langley 7- by 10-foot tunnel.

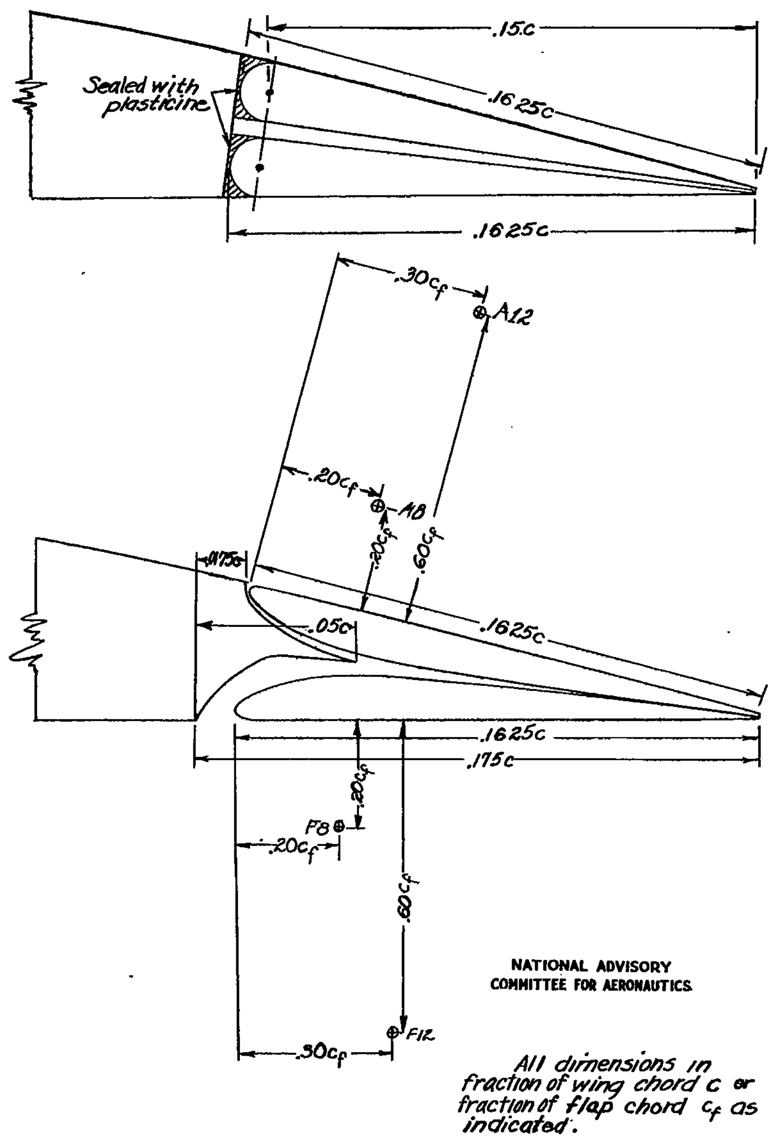

Figure B2.- Section of unbalanced upper-surface aileron and unbalanced split flap and section of balanced upper-surface aileron and balanced split flap with A, aileron axes, and F, flap axes tested.

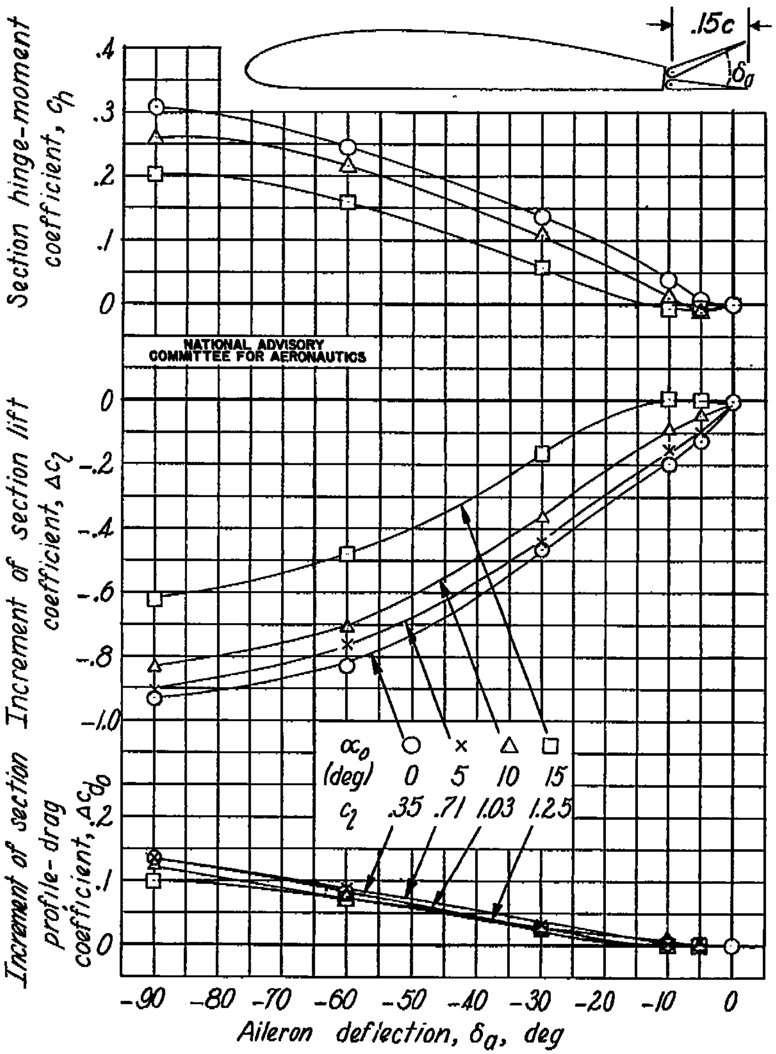

(a) Flap neutral.

Figure B3.- Characteristics of the unbalanced upper-surface aileron on the Clark Y airfoil.

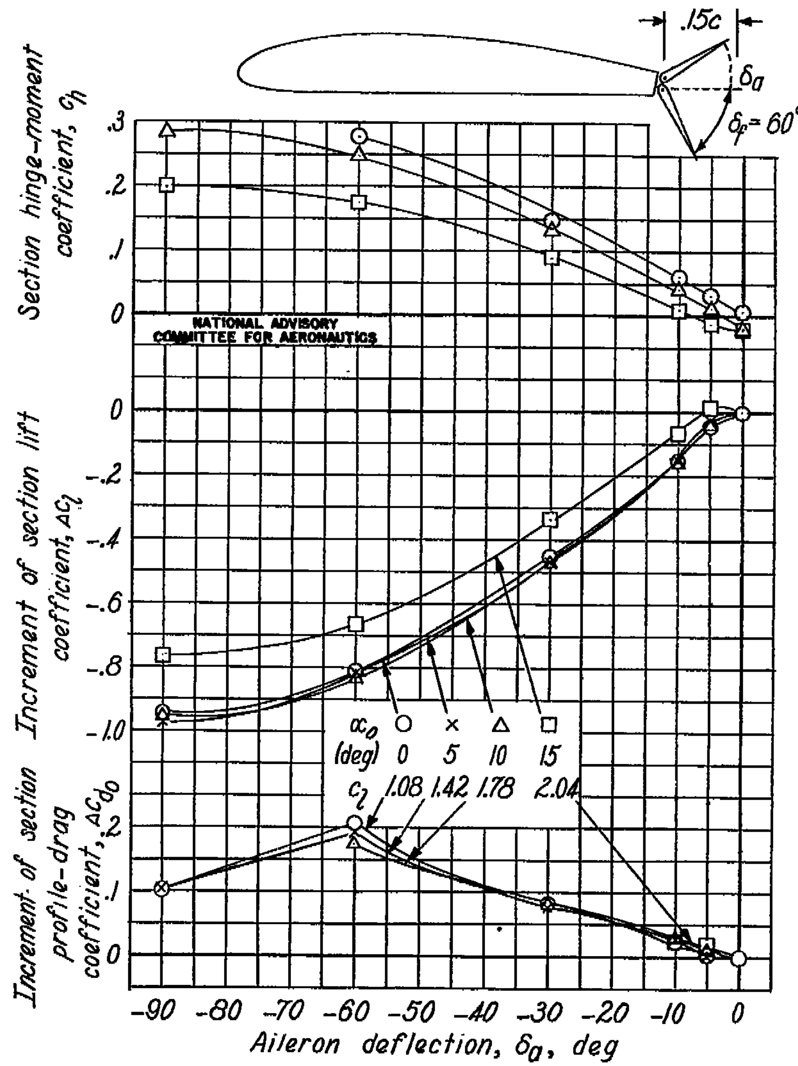

(b) Flap down 60°.

Figure B3.- Concluded.

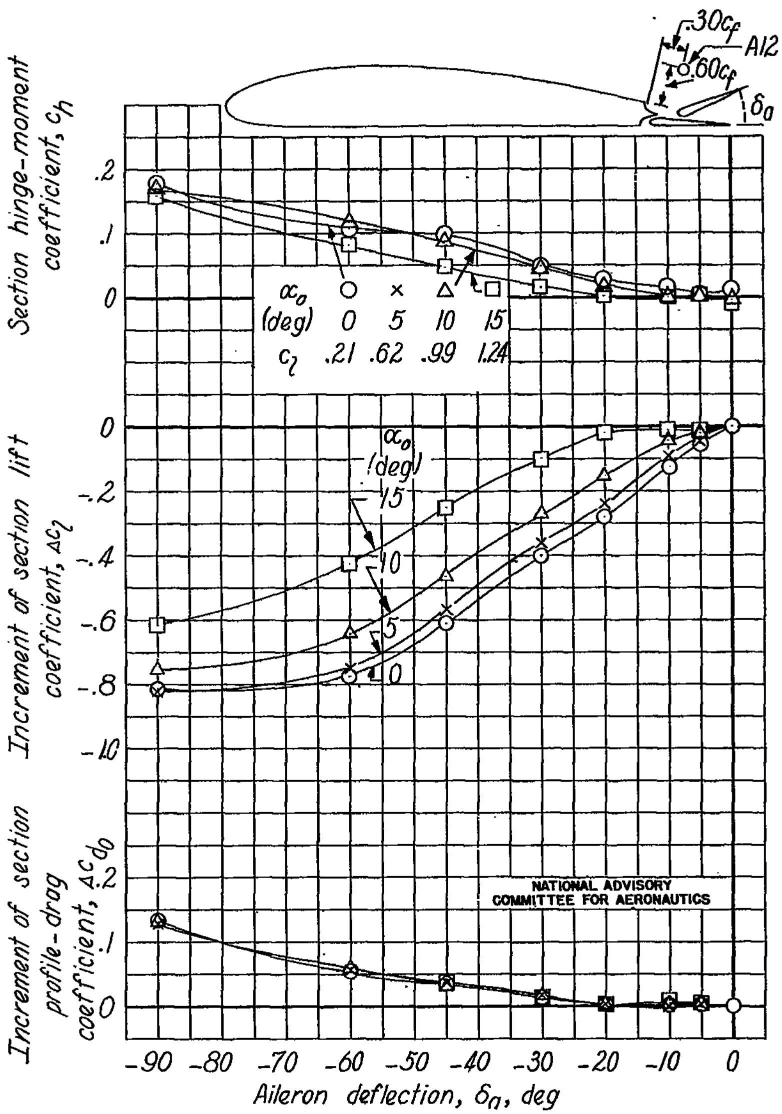

(a) Flap neutral.

Figure B4.- Characteristics of the balanced upper-surface aileron at axis A12 on the Clark Y airfoil.

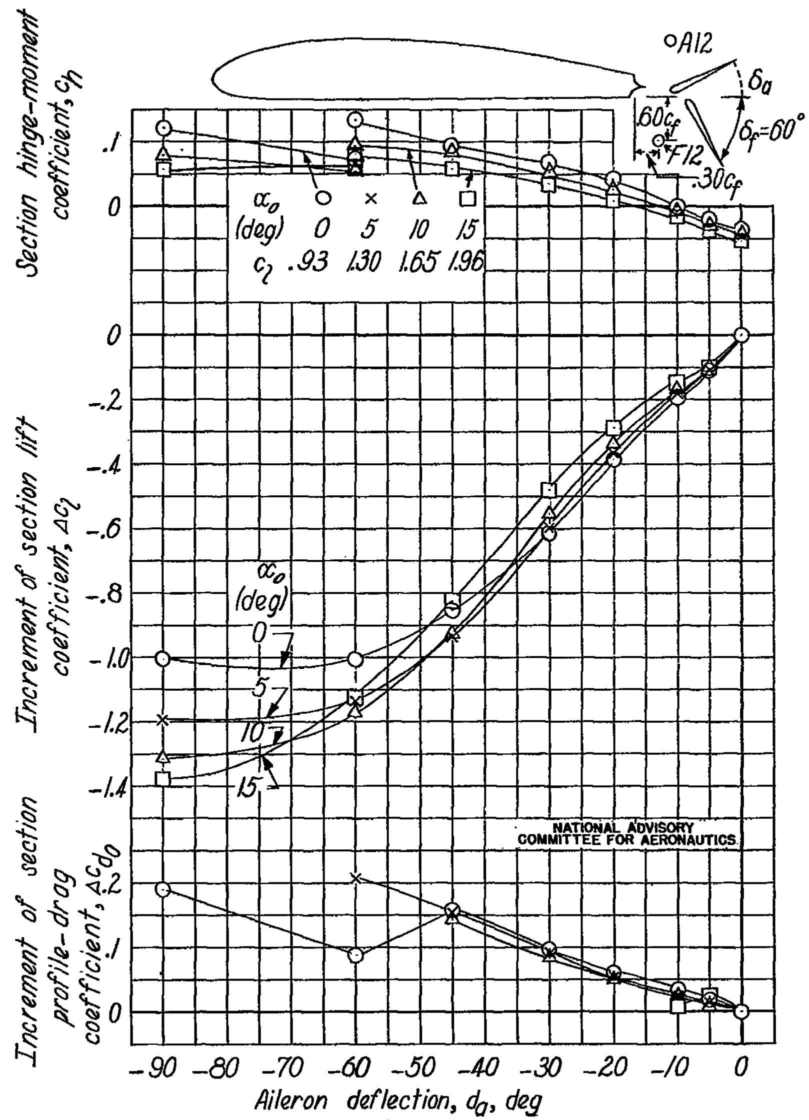

(b) Flap down 60° at axis F12.

Figure B4.- Concluded.

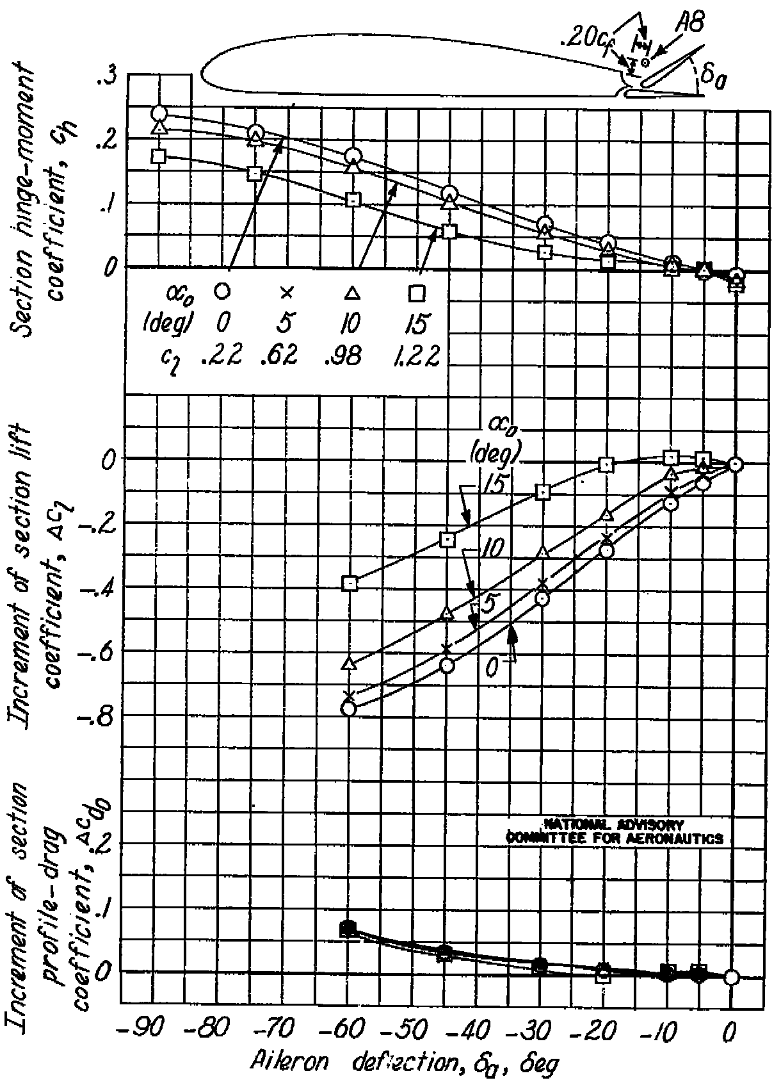

(a) Flap neutral.

Figure B5.- Characteristics of the balanced upper-surface aileron at axis A 8 on the Clark Y airfoil.

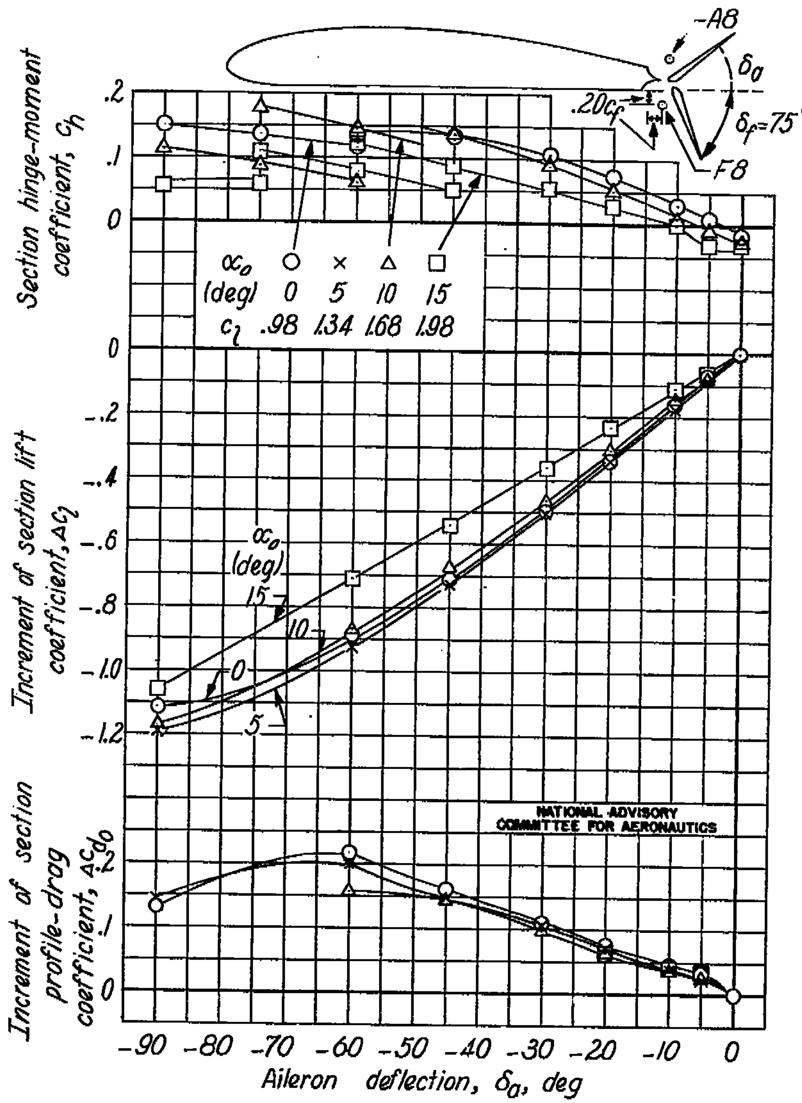

(b) Flap down 75° at axis F8.

Figure B5.- Concluded.

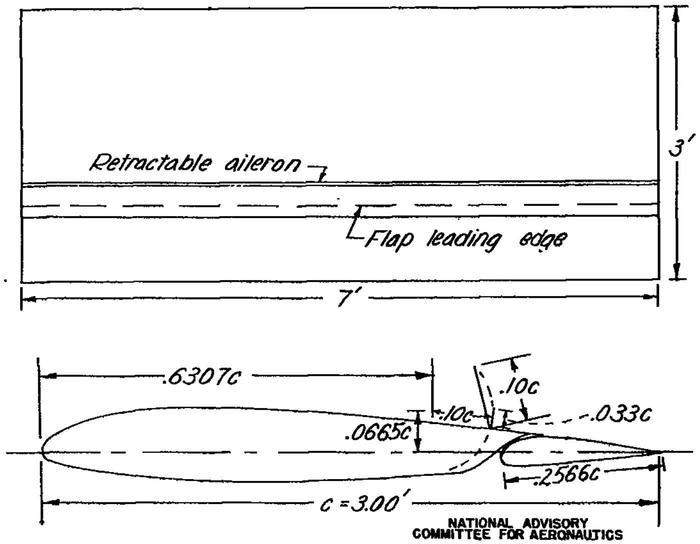

Figure B6.- Plan form and section of the NACA 23012 airfoil with a retractable aileron and a full-span slotted flap tested in the Langley 7- by 10-foot tunnel.

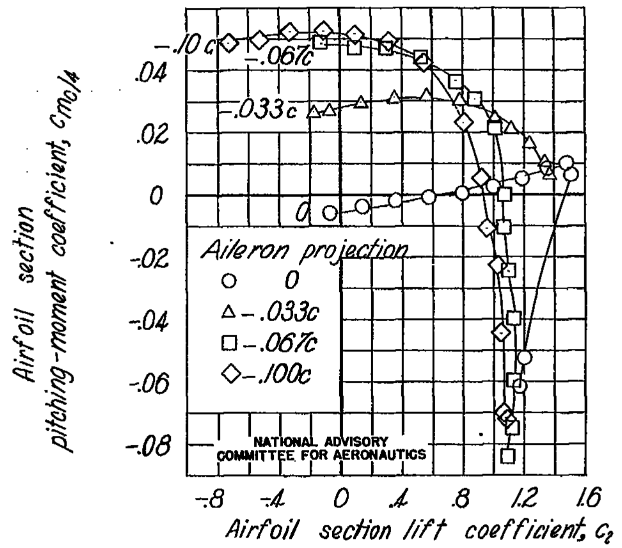

Figure B7.- Section pitching-moment characteristics of the NACA 23012 airfoil due to various aileron projections.

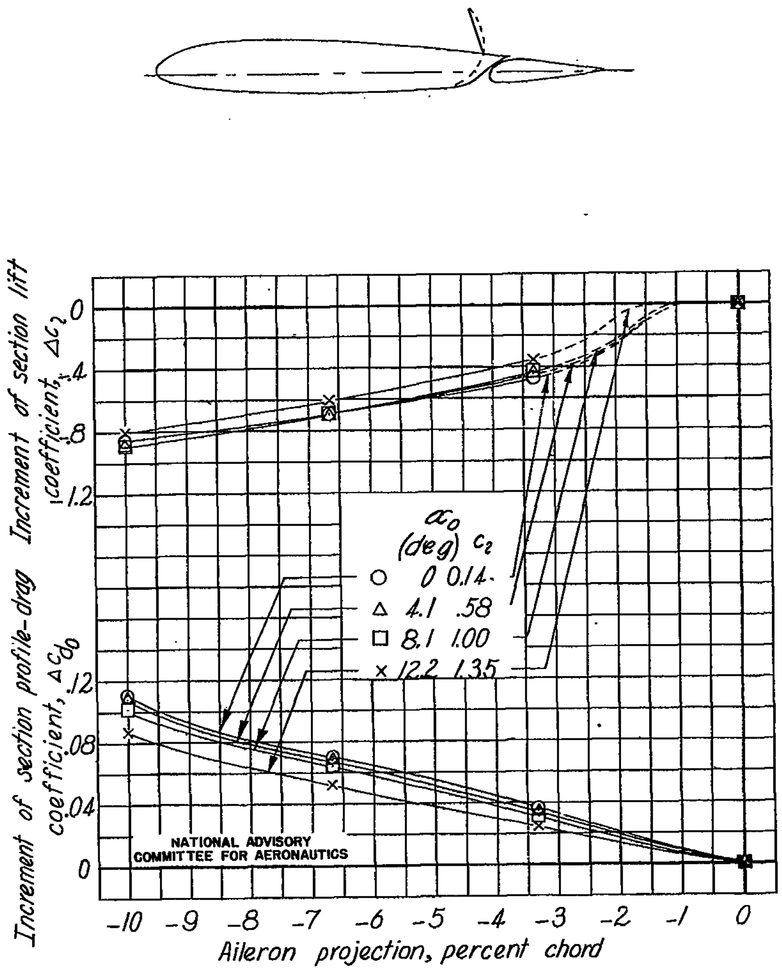

(a) δ_f, 0°.

Figure B8.- Aerodynamic characteristics of the NACA 23012 airfoil at various aileron projections.

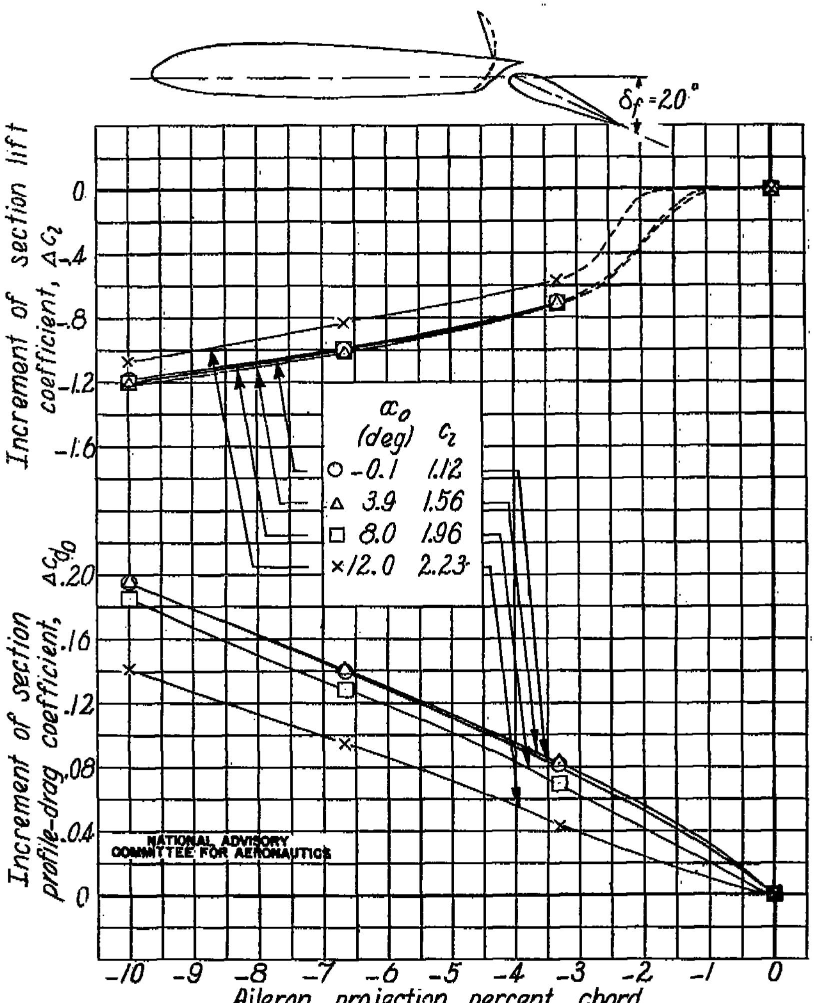

(b) δ_f, 20°.

Figure B8.- Continued.

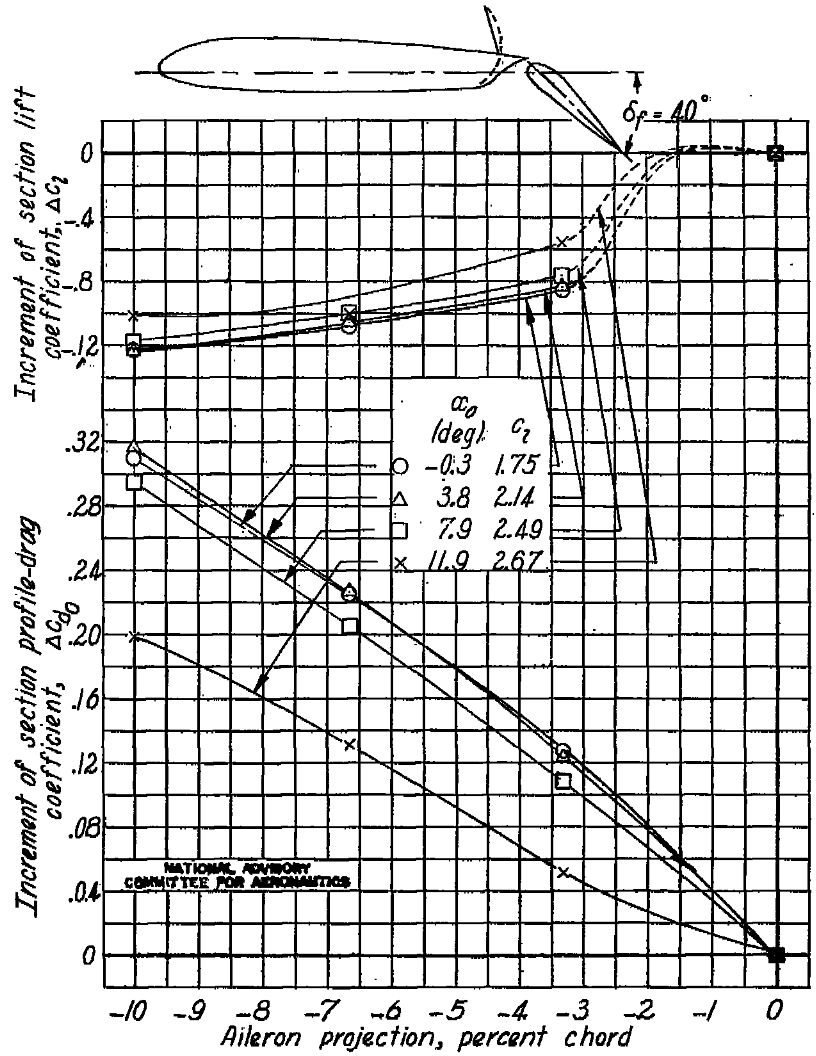

(c) δ_f, 40°.

Figure B8.- Concluded.

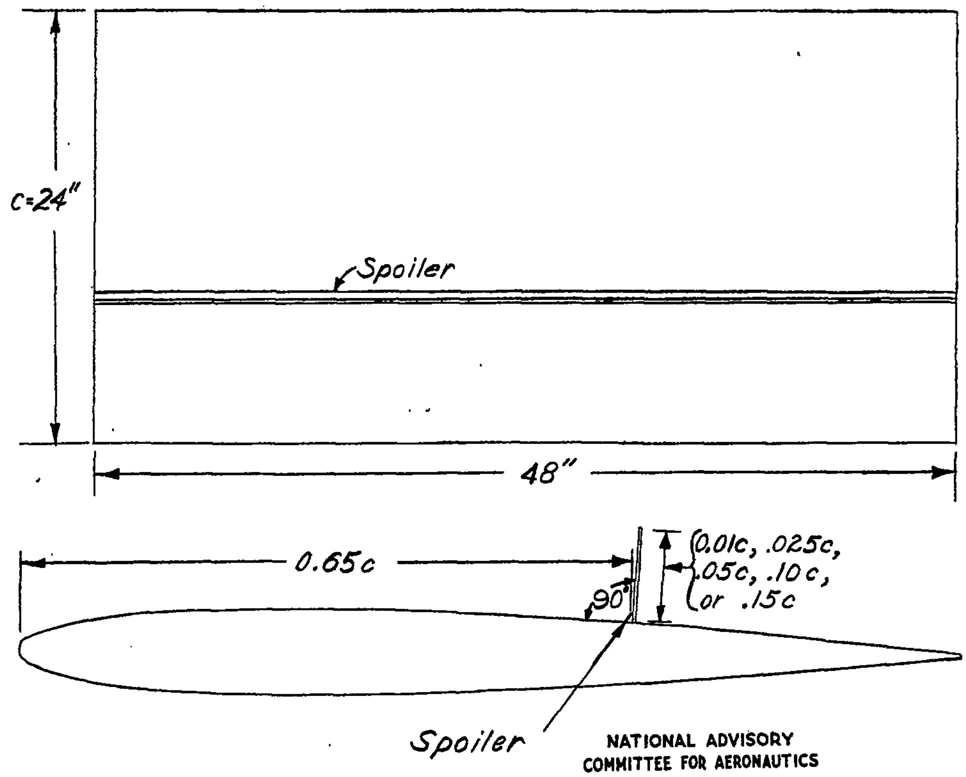

Figure B9.- Plan view and section of the NACA 0009 airfoil showing size and location of spoilers, as tested in the Langley 4- by 6-foot vertical tunnel.

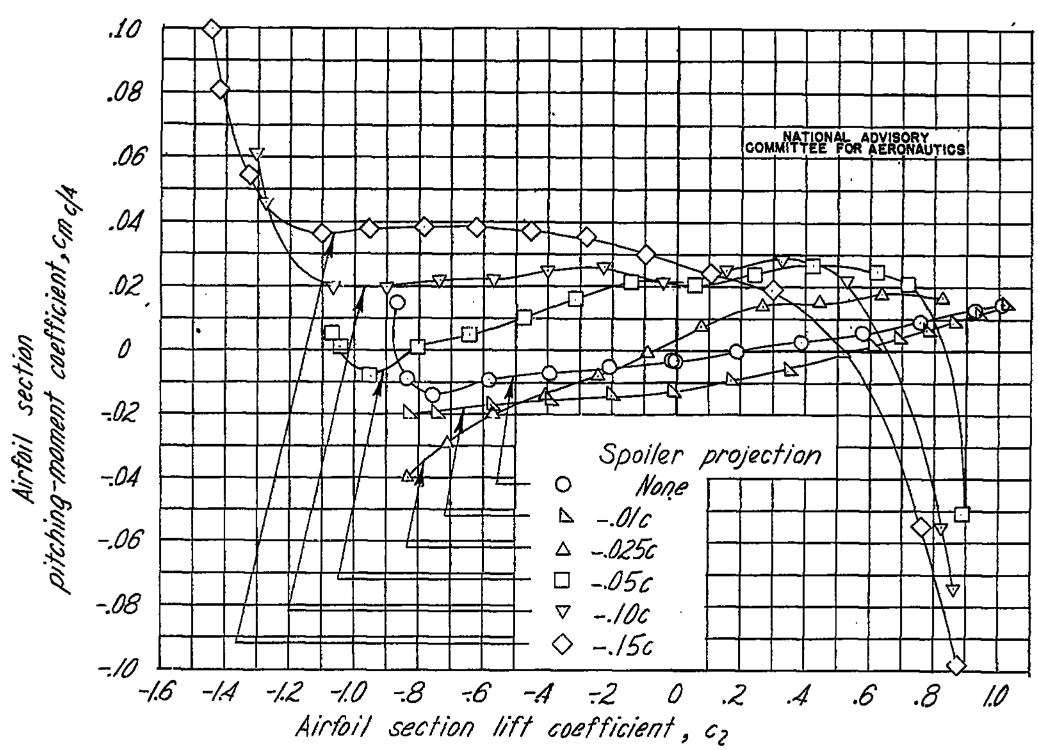

Figure B10.- Effect of spoiler projection on the airfoil section pitching-moment characteristics of the NACA 0009 airfoil.

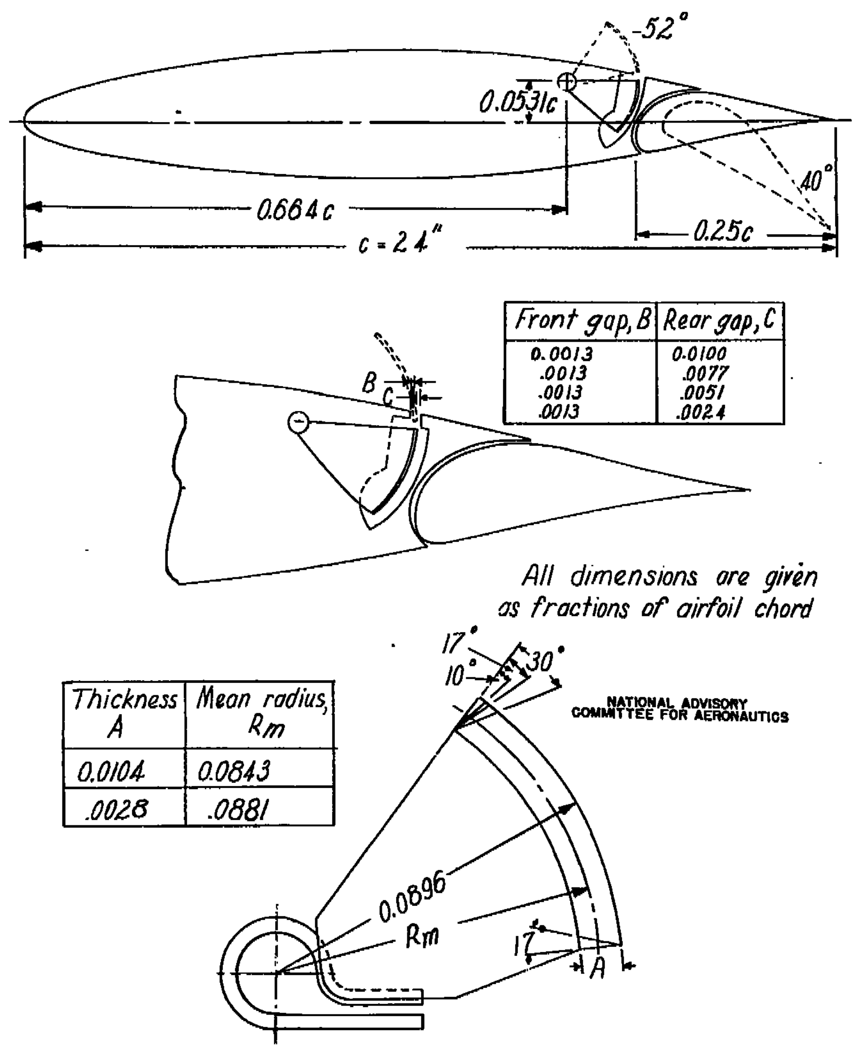

Front gap, B	Rear gap, C
0.0013	0.0100
.0013	.0077
.0013	.0051
.0013	.0024

Thickness A	Mean radius, Rm
0.0104	0.0843
.0028	.0881

Figure B11.- Section details of the NACA 66(215)-216 airfoil tested with spoiler ailerons and a 0.25c slotted flap in the Langley two-dimensional low-turbulence pressure tunnel.

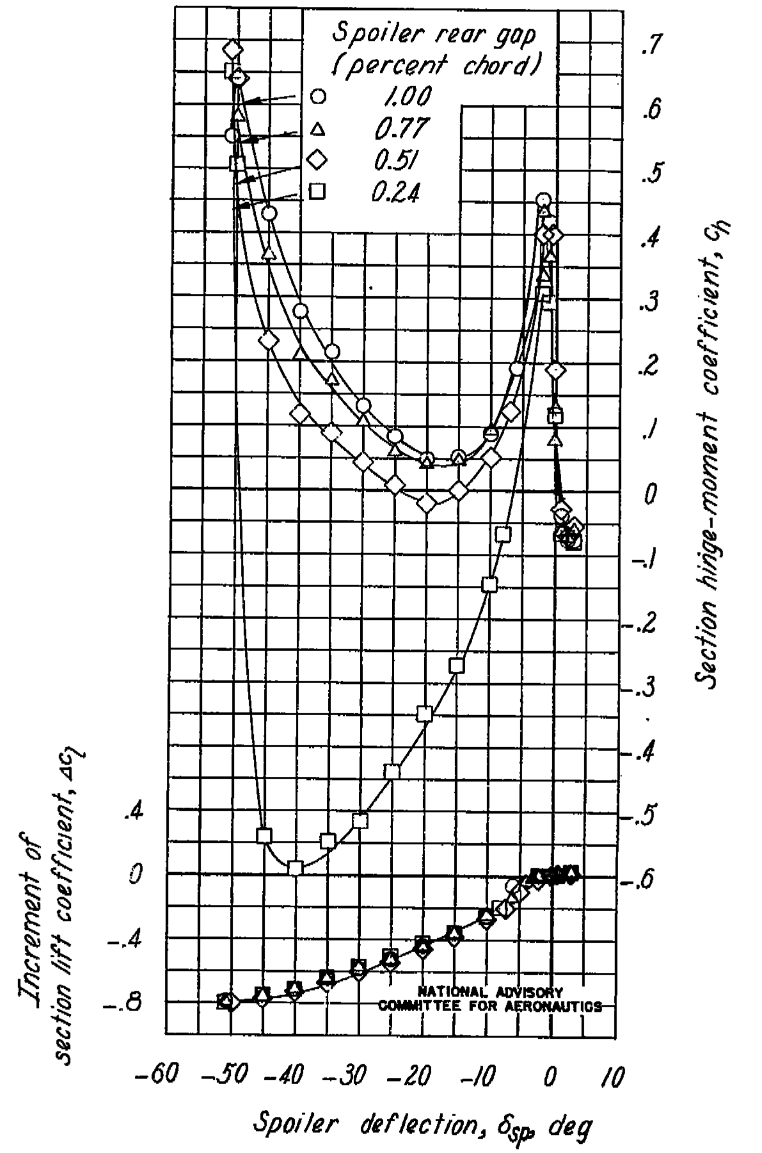

(a) α_o, 0°; c_l, 0.12; δ_f, 0°.

Figure B12.- Effect of spoiler deflection and spoiler rear-gap width on the section lift and hinge-moment characteristics of the NACA 66(215)-216 airfoil. Spoiler thickness, 0.0104c. Spoiler bevel, 0°.

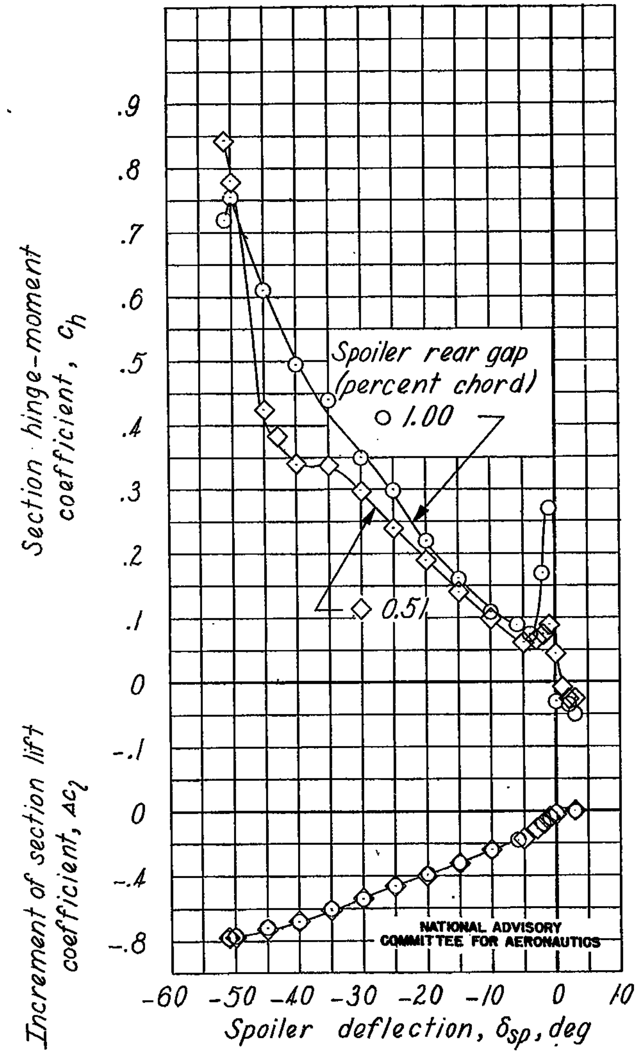

(b) α_o, 7.1°; C_l, 0.76; δ_f, 0°.

Figure B12.- Continued.

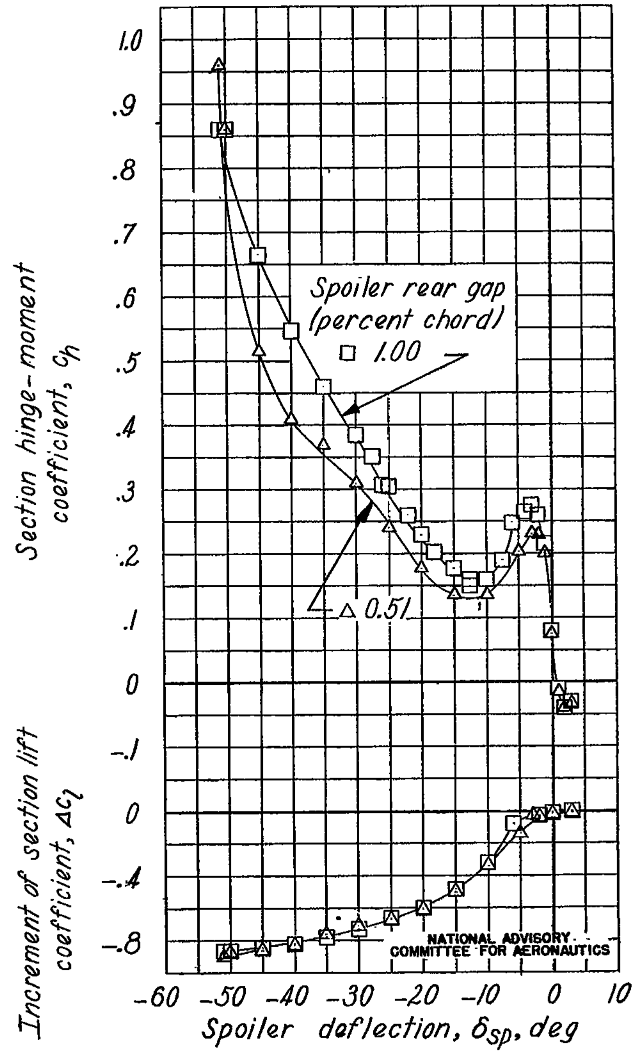

(c) α_o, 7.1°; C_l, 2.02; δ_f, 40°.

Figure B12.- Concluded.

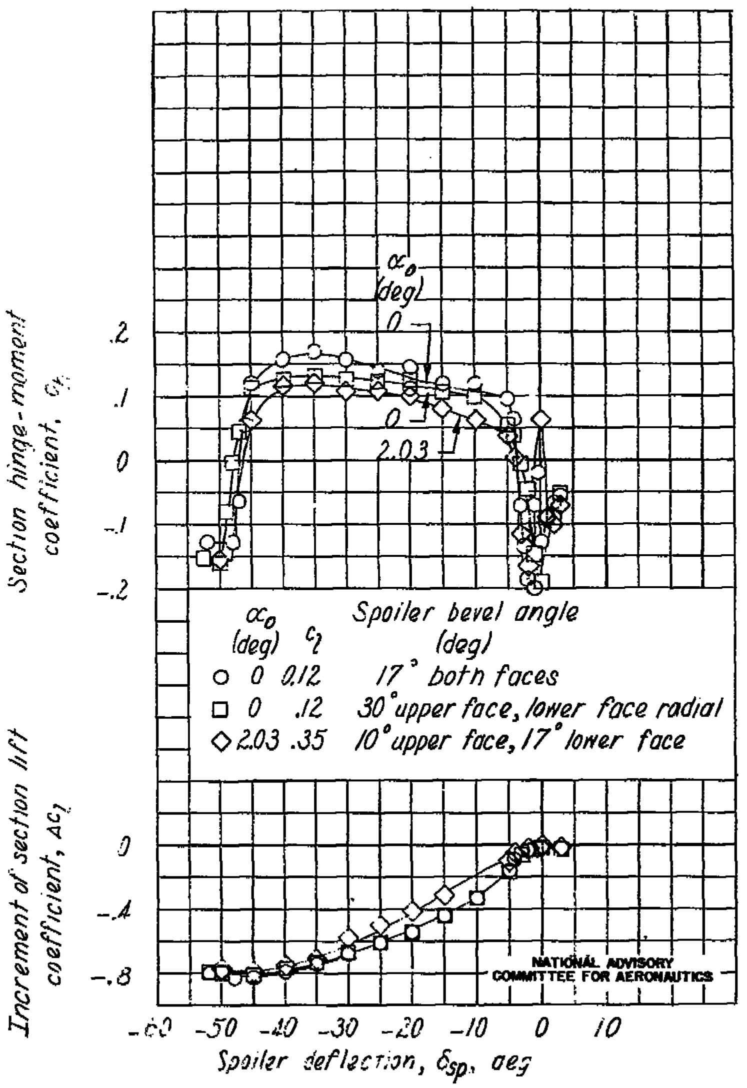

Figure B13.- Effect of spoiler deflection and spoiler bevel angle on the section lift and hinge-moment characteristics of the NACA 66(215)-216 airfoil. δ_f, 0°. Spoiler thickness, 0.0028c; spoiler upper face smooth.

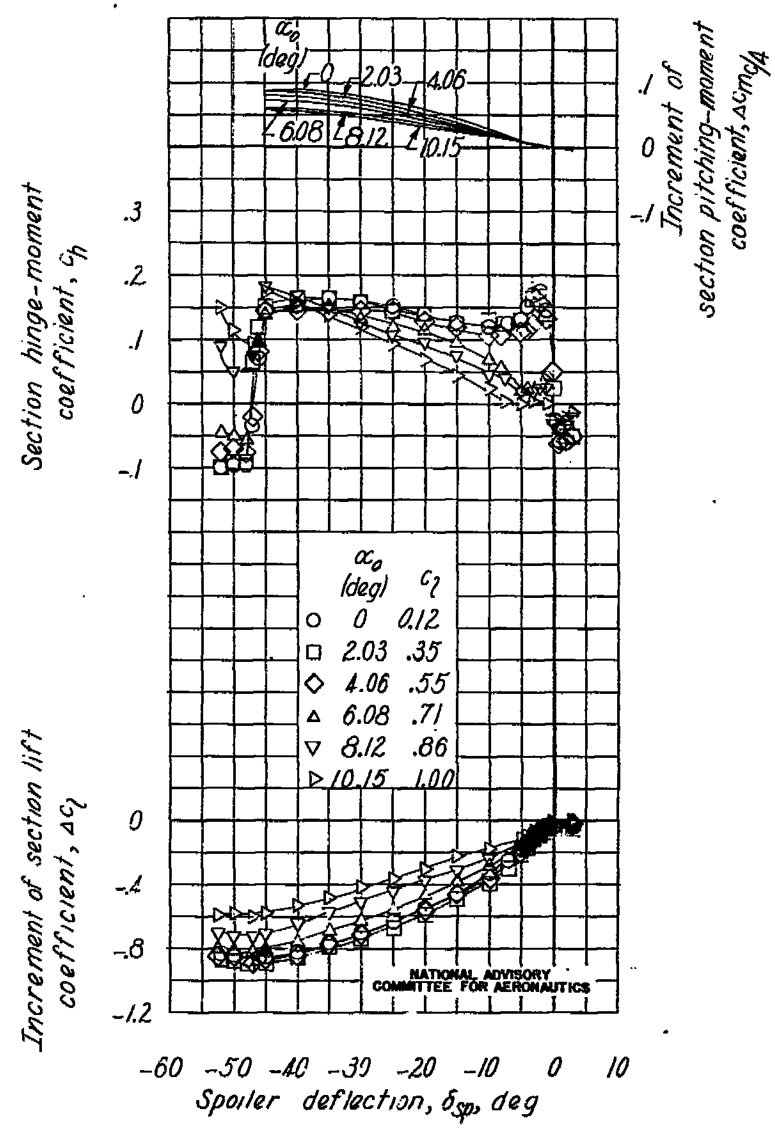

(a) δ_f, 0°.

Figure B14.- Effect of spoiler deflection on the section lift, pitching-moment, and hinge-moment characteristics of the NACA 66(215)-216 airfoil. Spoiler thickness, 0.0028c; forward gap, 0.0013c; rear gap, 0.0100c; spoiler beveled 17° on both faces. Roughness on upper surface.

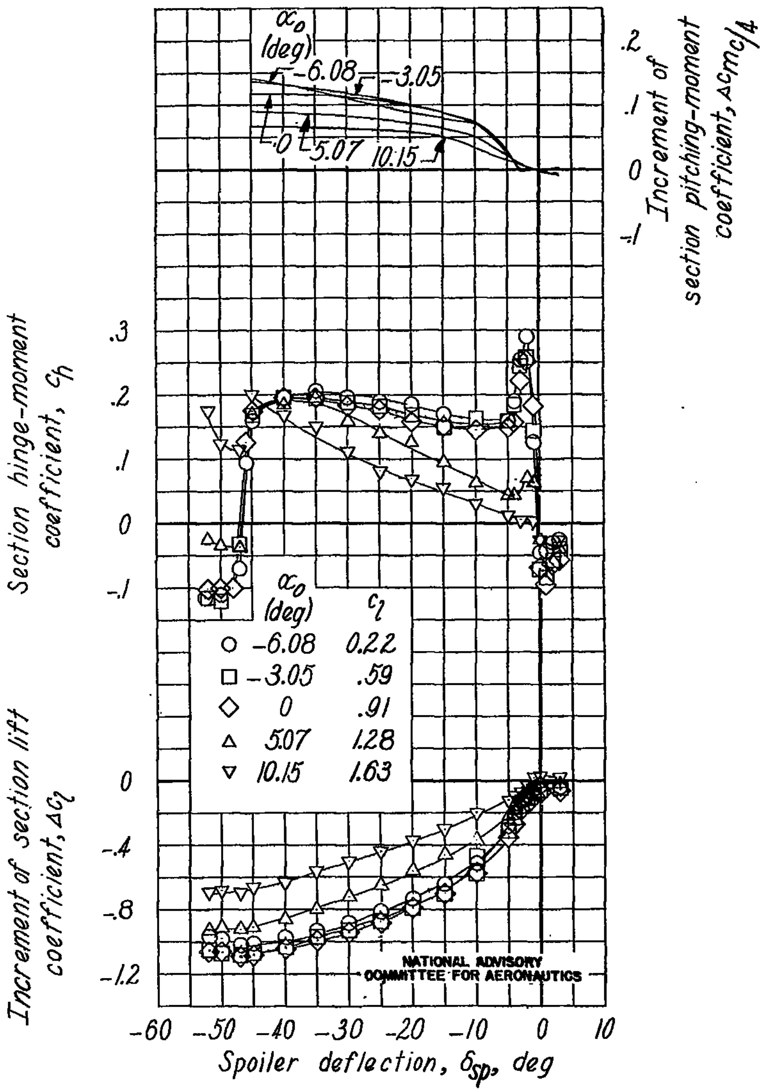

(b) δ_f, 20°.

Figure B14.- Continued.

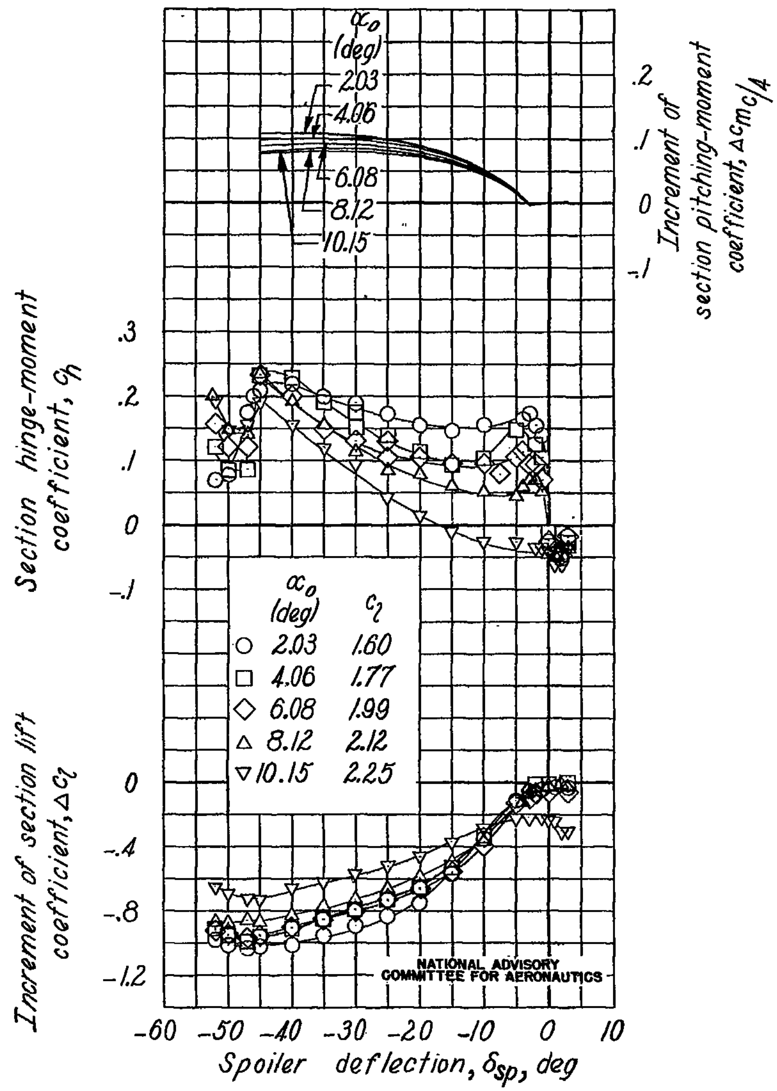

(c) δ_f, 40°.

Figure B14.- Concluded.

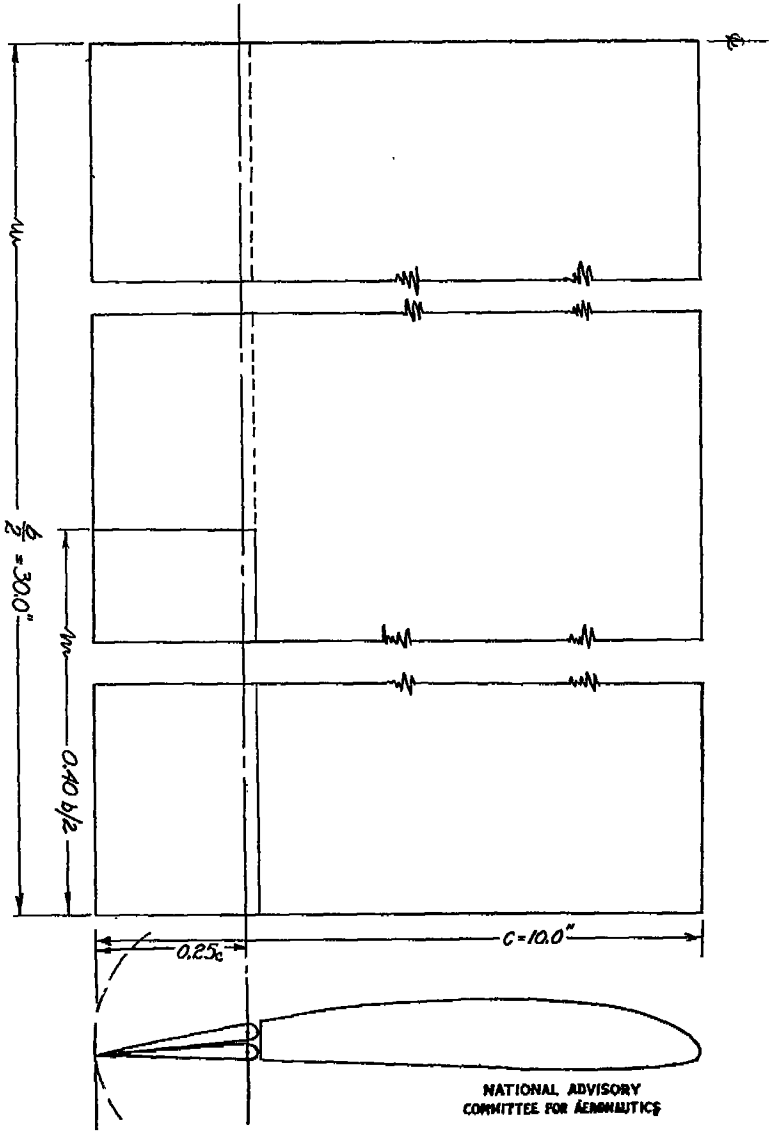

(a) 0.25c flap and aileron.

Figure B15.- Plan forms and sections of the 10- by 60-inch Clark Y wing with upper-surface ailerons and full-span split flaps. Tested in the Langley 7- by 10-foot tunnel.

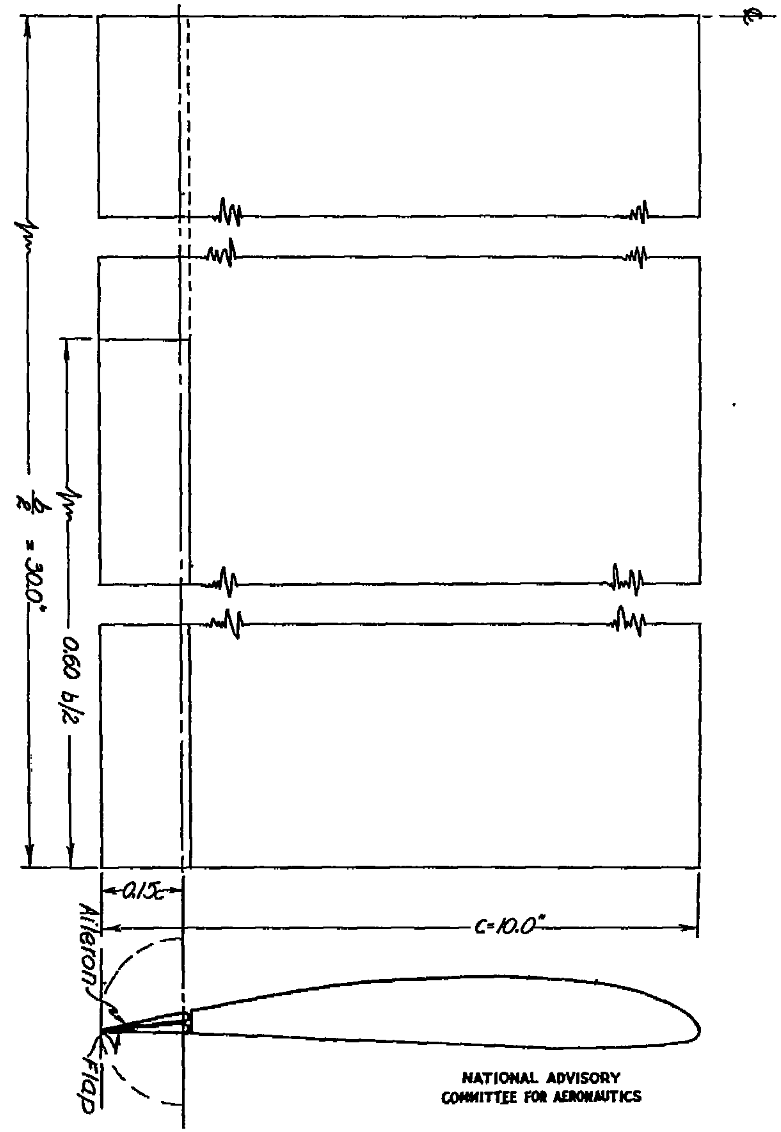

(b) 0.15c flap and aileron.

Figure B15.- Concluded.

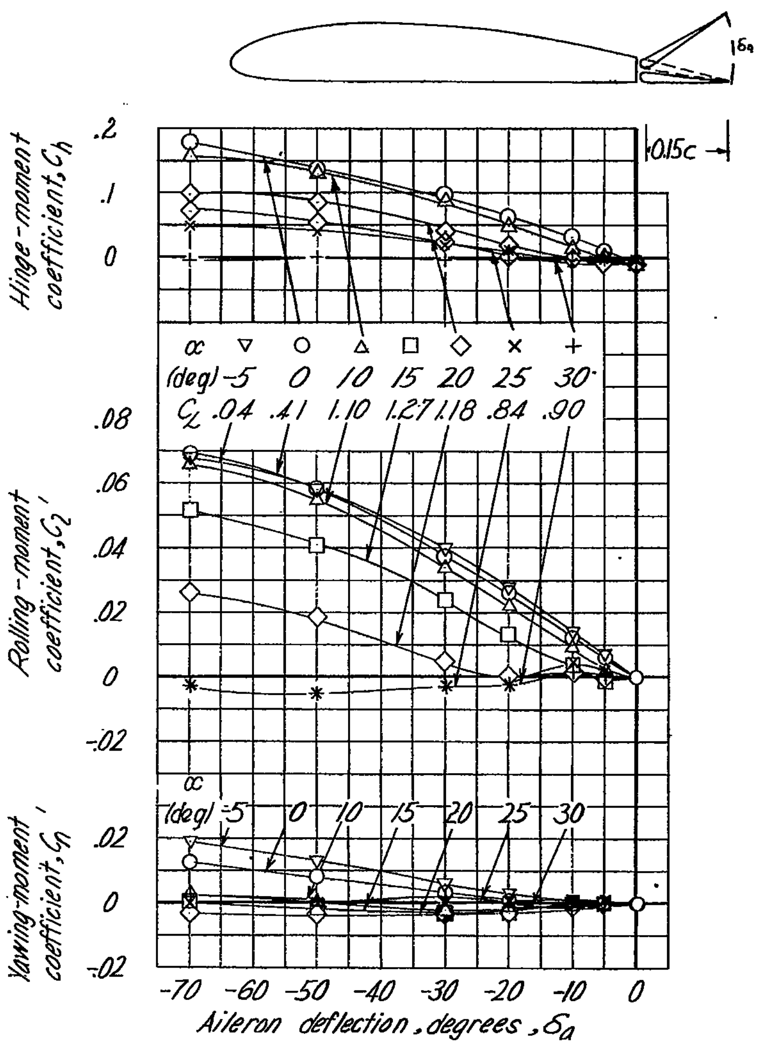

(a) Split flap neutral.

Figure B16.- Aileron characteristics of the 0.15c upper-surface aileron on the Clark Y wing.

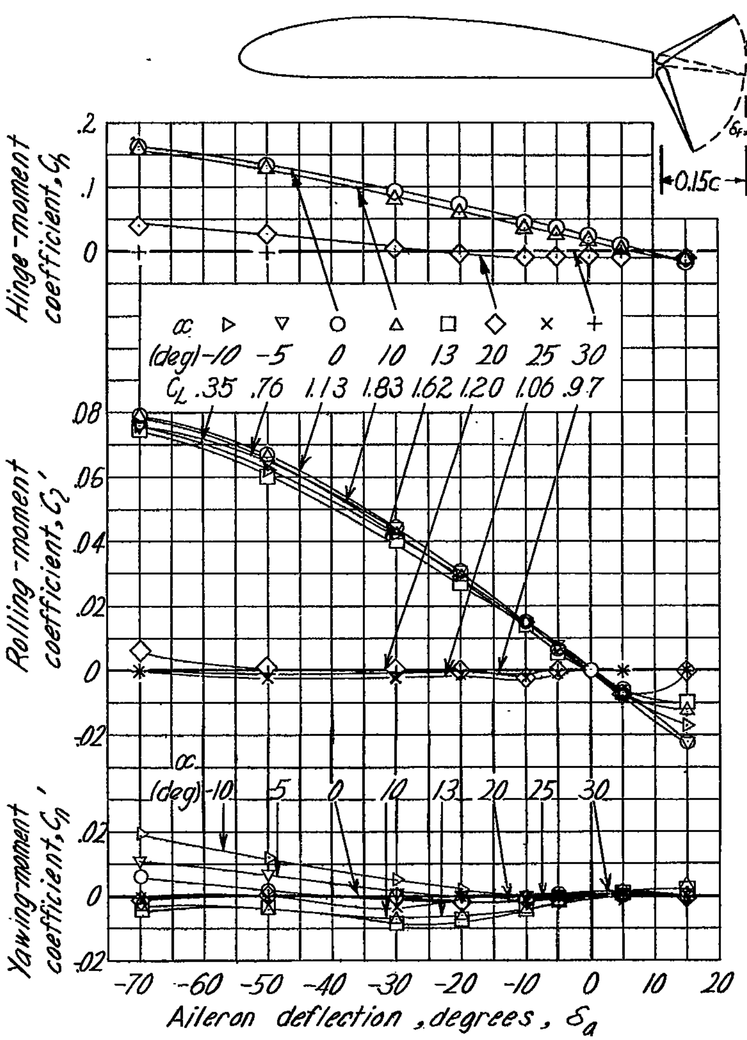

(b) δ_f, 60°.

Figure B16.- Concluded.

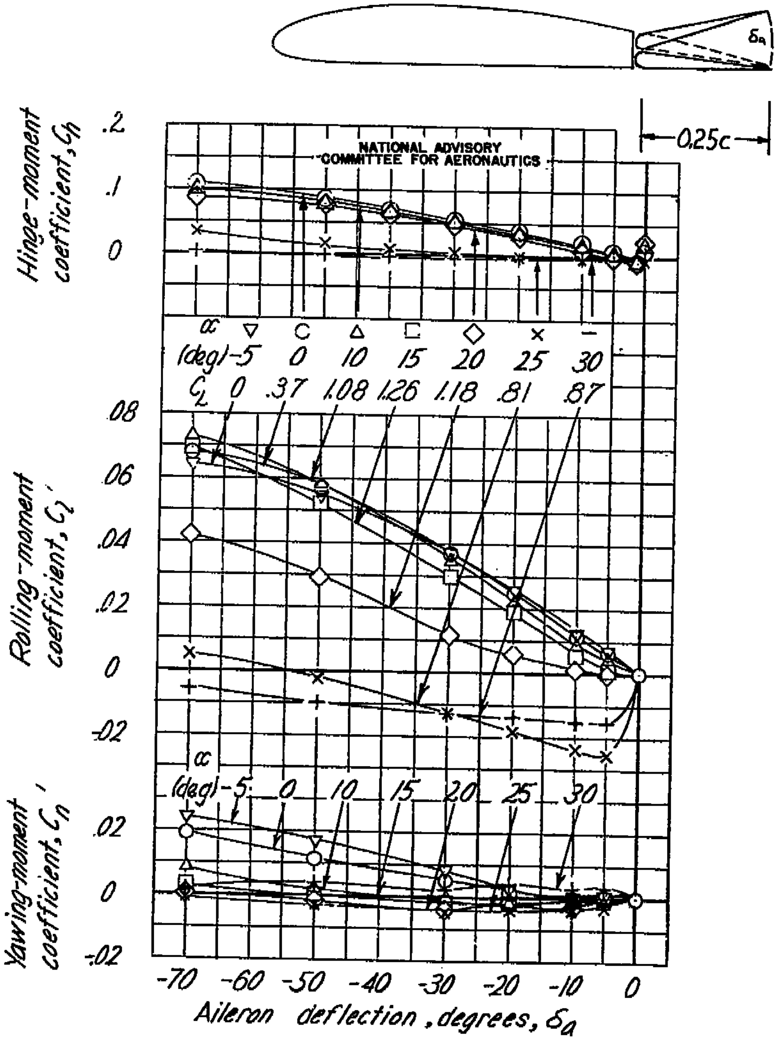

(a) Split flap neutral.

Figure B17.- Aileron characteristics of the 0.25c upper-surface aileron on the Clark Y wing.

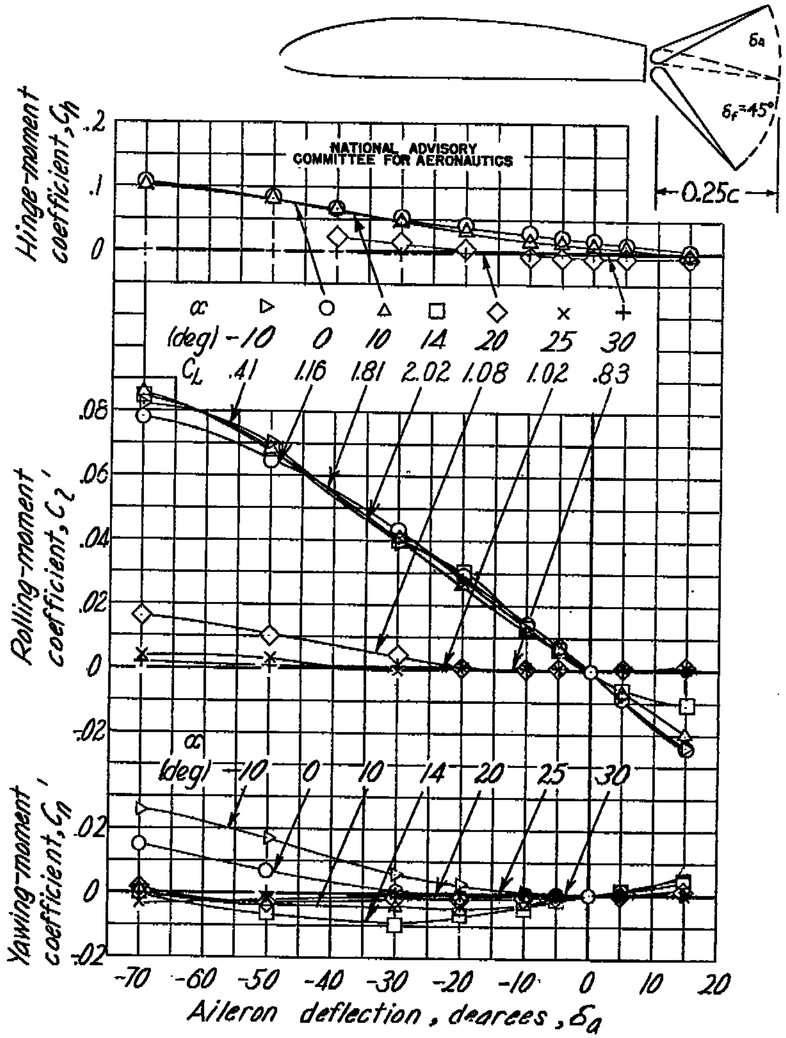

(b) δ_f, 45°.

Figure B17.- Concluded.

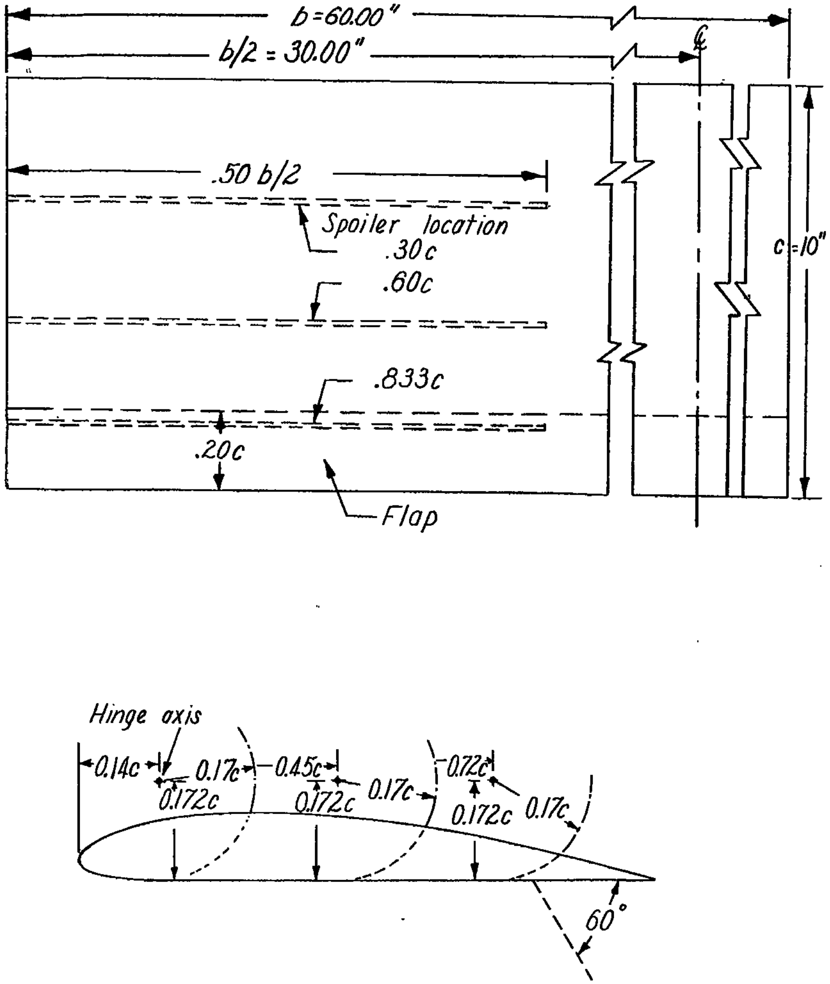

Figure B18.- Plan form and section of the Clark Y wing tested with 0.50 b/2 retractable spoiler at various chordwise locations and a 0.20c full-span split flap. Langley 7- by 10-foot tunnel.

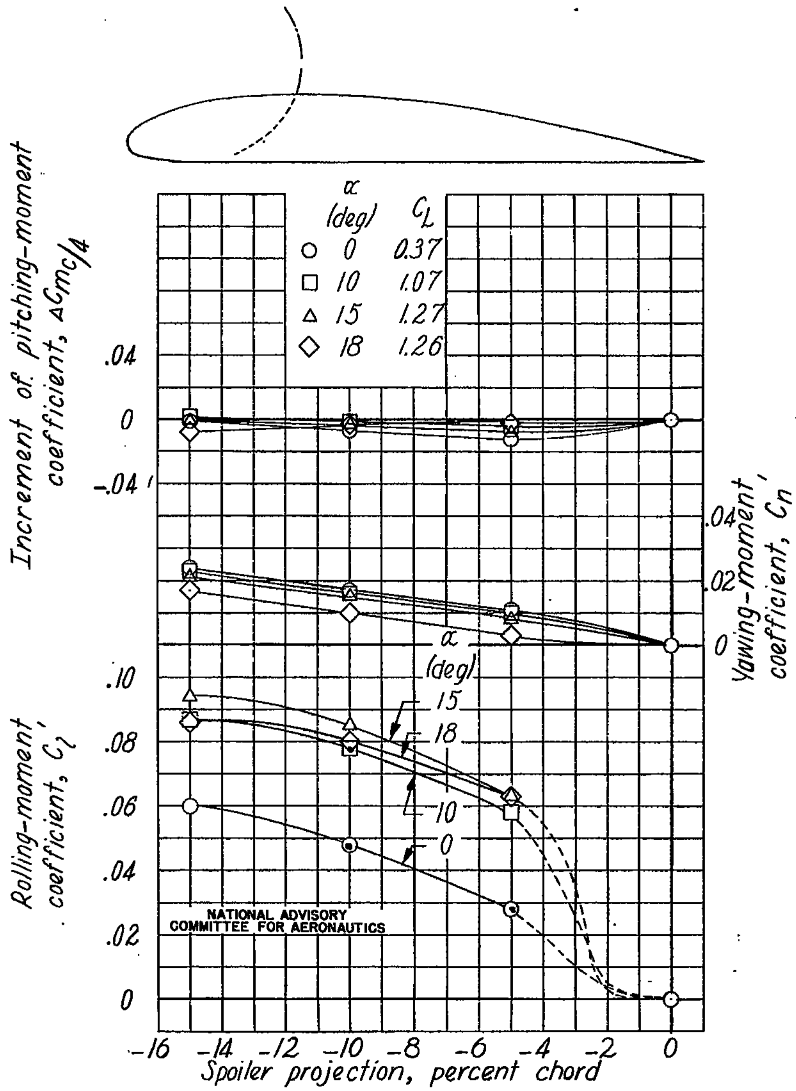

(a) Spoiler located at 0.30c.

Figure B19.- Rolling-, yawing-, and pitching-moment characteristics of the Clark Y wing due to retractable spoiler projection. Flap retracted.

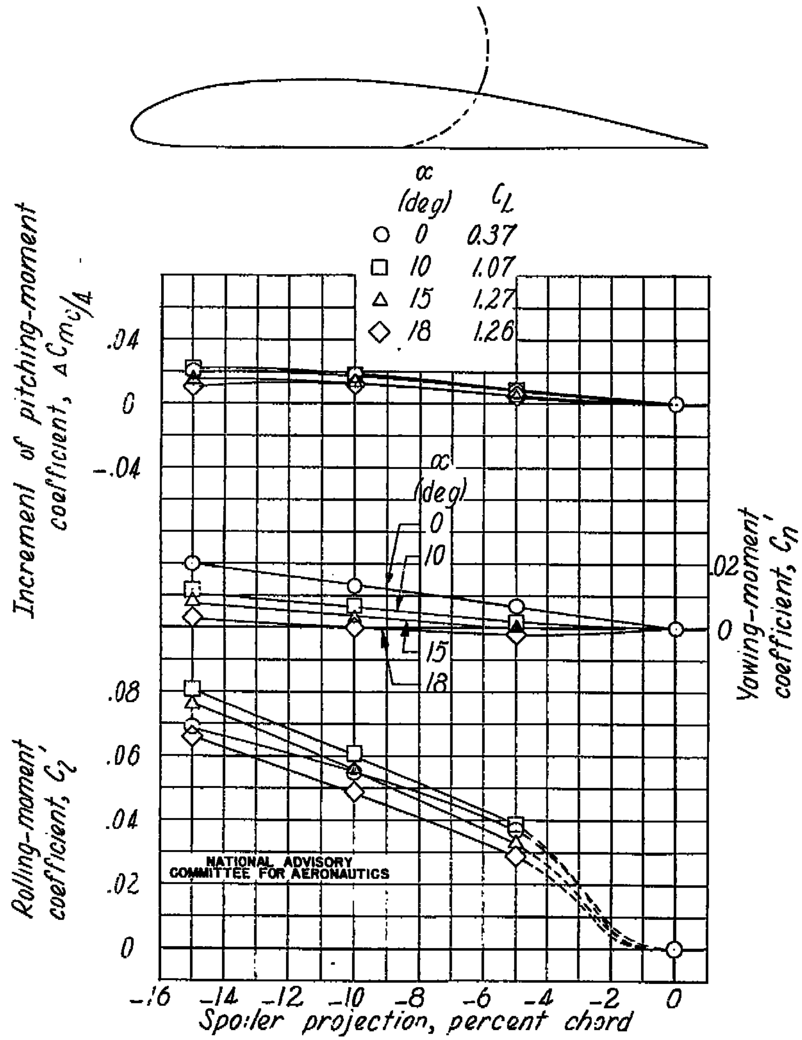

(b) Spoiler located at 0.80c.

Figure B19.- Continued.

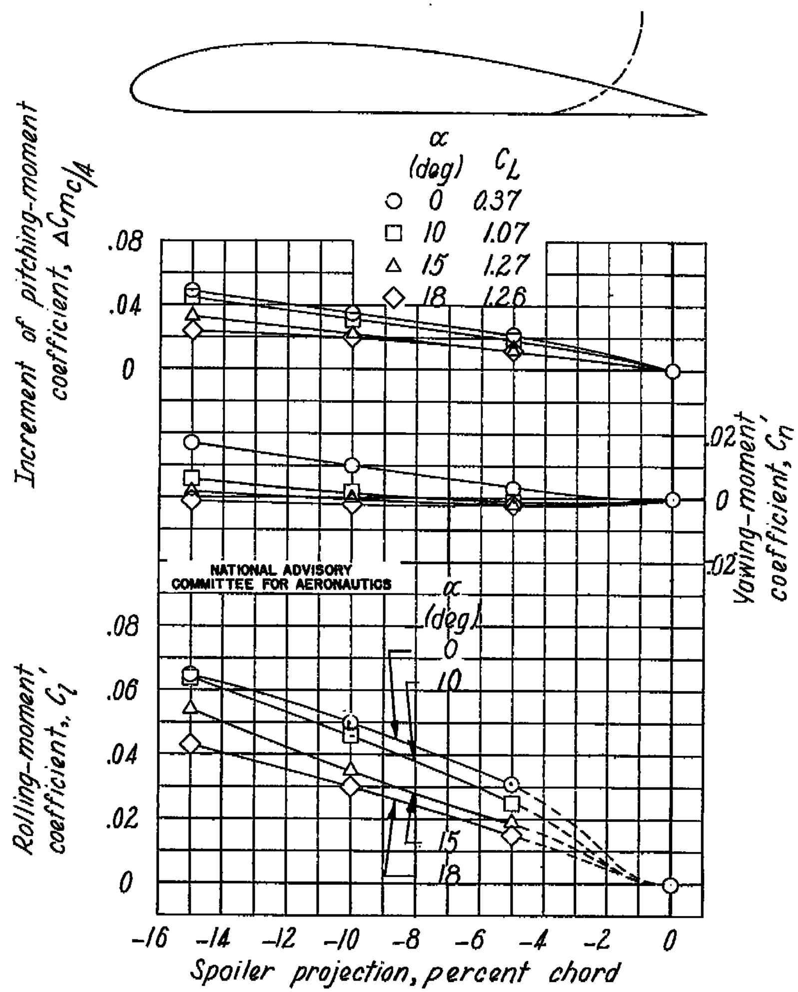

(c) Spoiler located at 0.833c.

Figure B19.- Concluded.

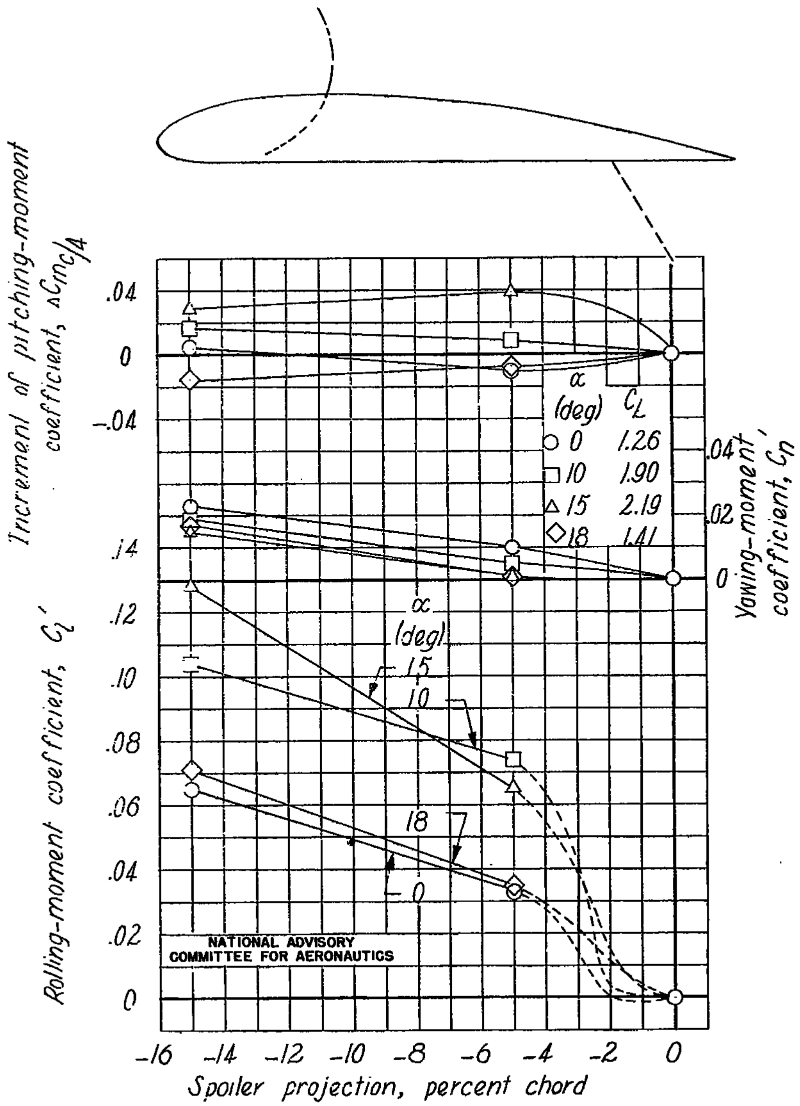

(a) Spoiler located at 0.30c.

Figure B20.- Rolling-, yawing-, and pitching-moment characteristics of the Clark Y wing due to retractable spoiler projection. Flap deflected 60°.

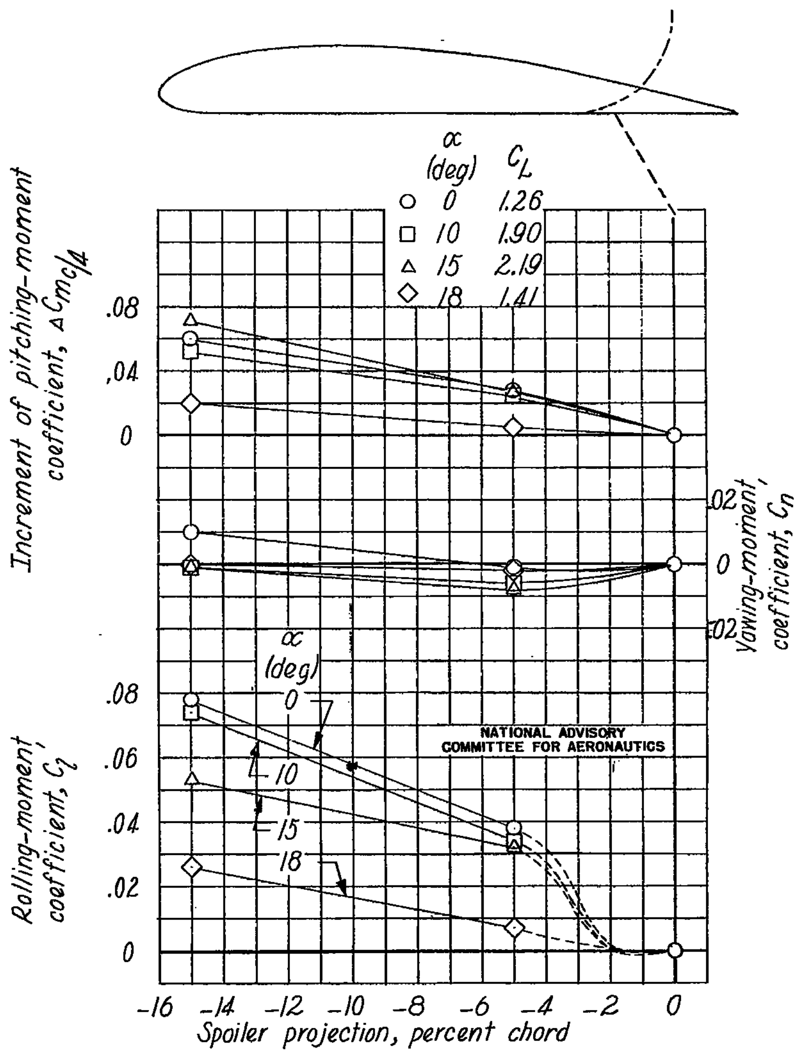

(b) Spoiler located at 0.833c.

Figure B20.- Concluded.

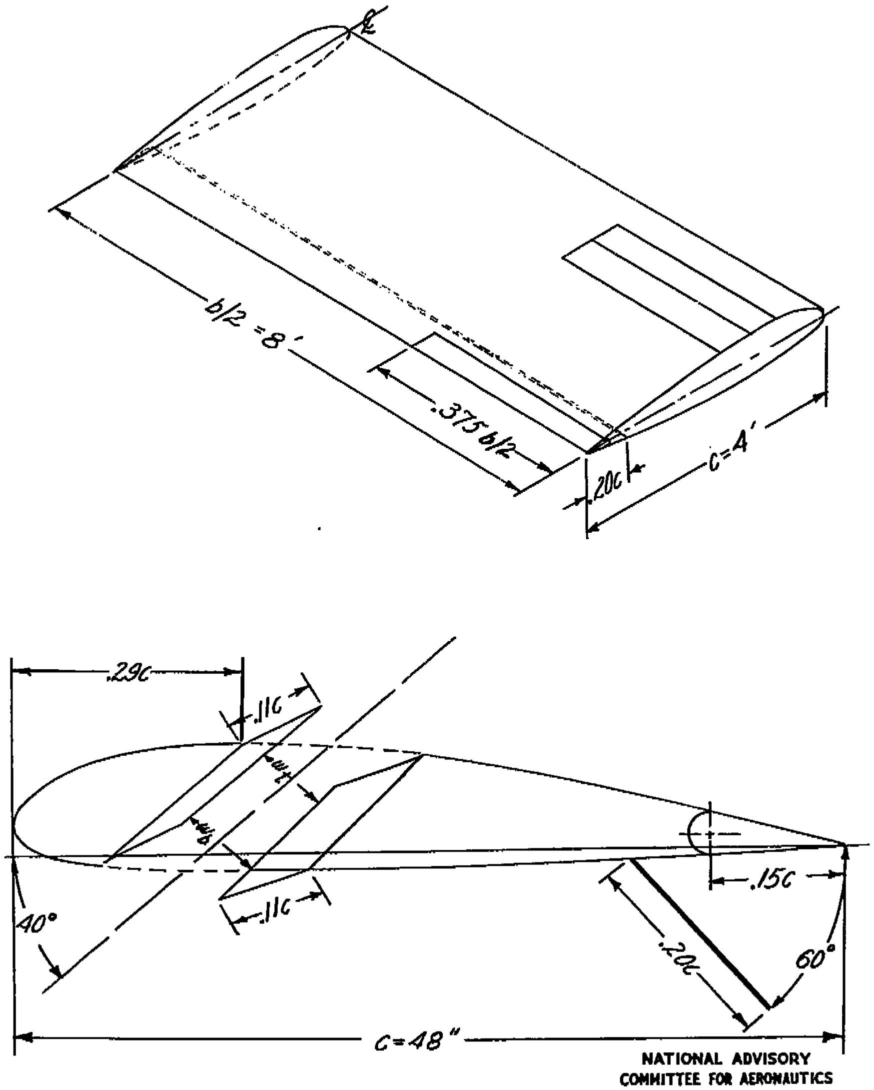

Figure B21.- Plan form and section of the 4- by 8-foot Clark Y-15 wing tested in the Langley 7- by 10-foot tunnel with spoilers, a plain sealed aileron, and a full-span split flap.

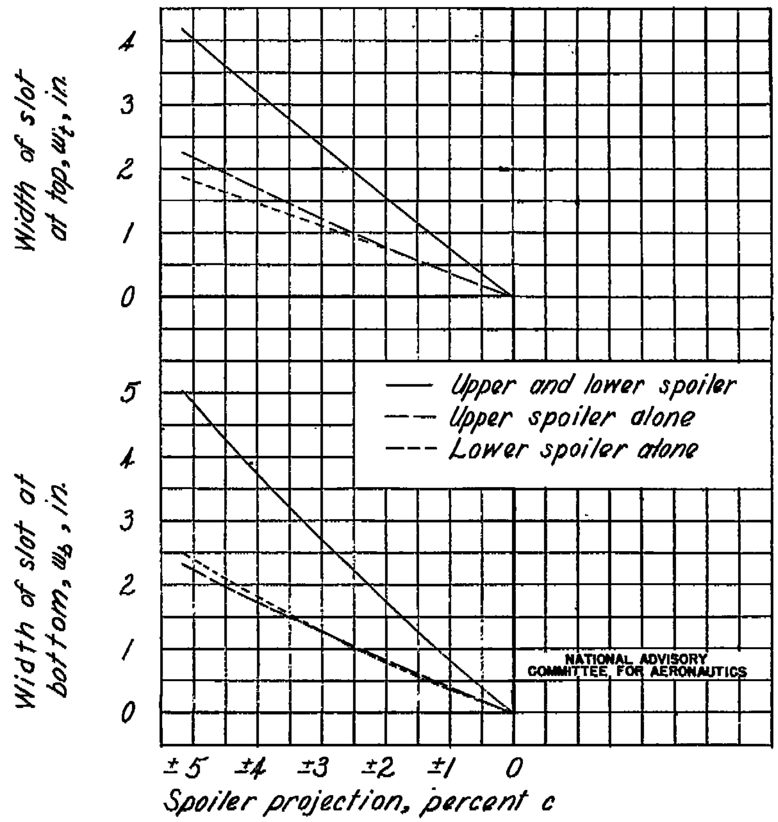

Figure B22.- Variation of spoiler-slot width with spoiler projection.

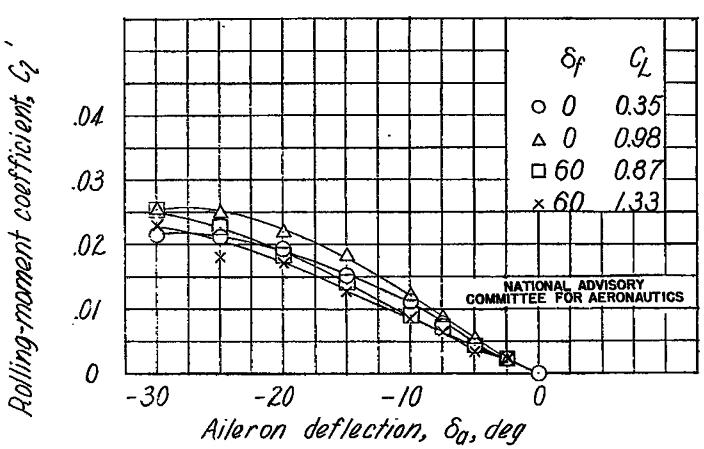

Figure B23.- Variation of rolling-moment coefficient with plain sealed aileron deflection on the Clark Y-15 airfoil.

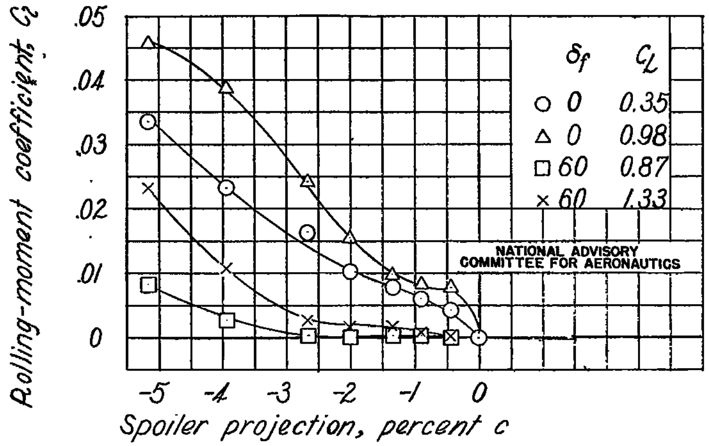

(b) Upper spoiler projection.

Figure B24.- Continued.

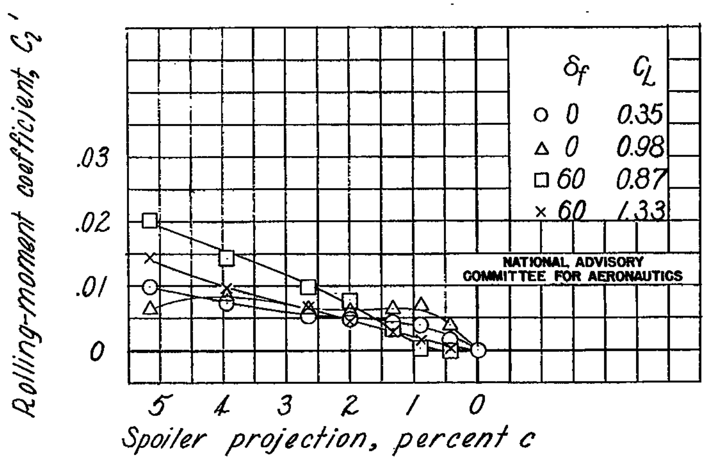

(a) Lower spoiler projection.

Figure B24.- Variation of rolling-moment coefficient with spoiler projection on the Clark Y-15 wing.

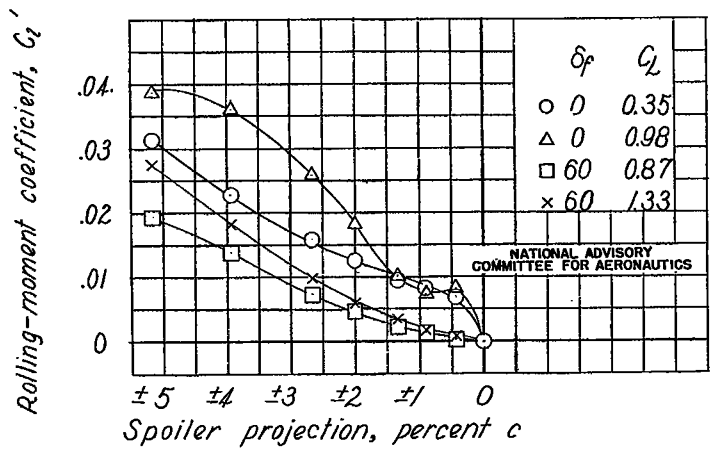

(c) Upper and lower spoiler projection.

Figure B24.- Concluded.

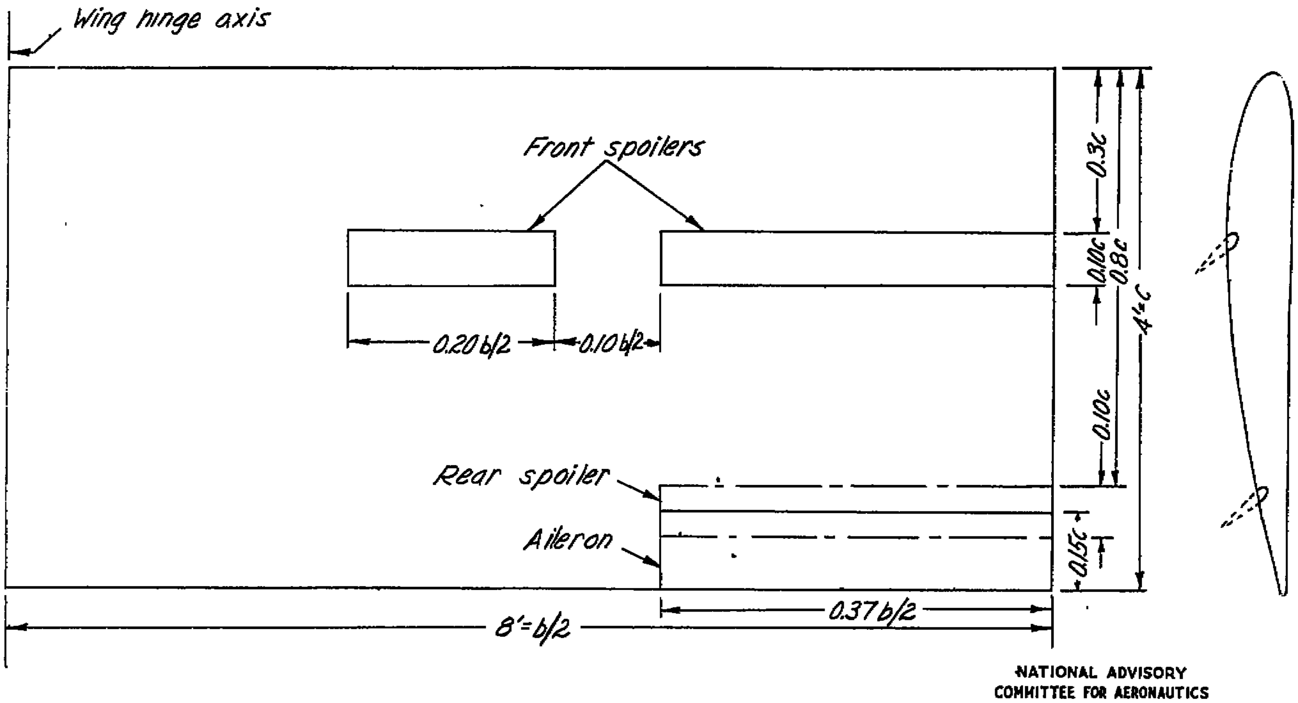

Figure B25.- Plan form and section of the Clark Y-15 semispan wing. Tested in the Langley 7- by 10-foot tunnel.

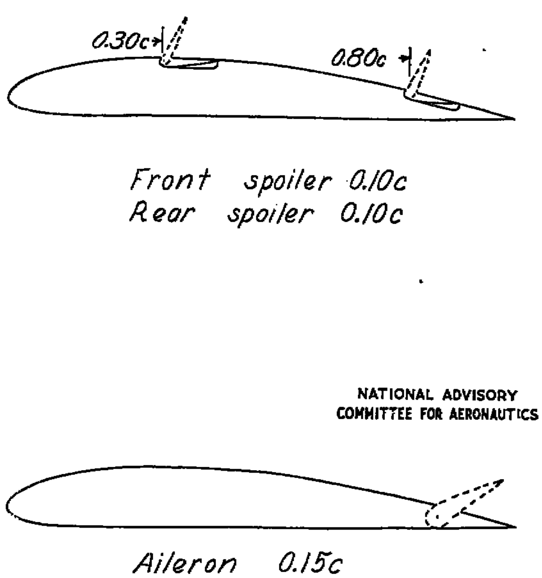

Figure B26.- Sections of Clark Y-15 wing showing the spoilers and aileron.

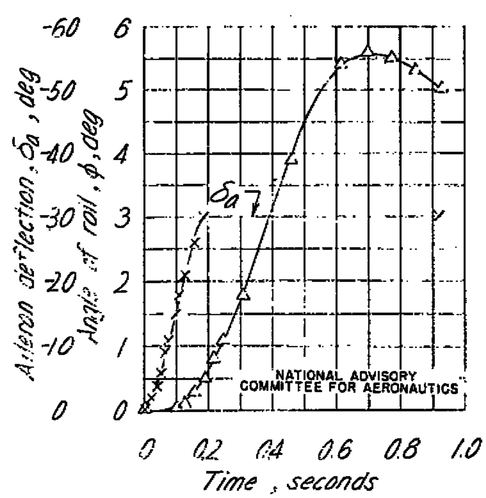

Figure B27.- Time history of wing motion due to ordinary aileron deflection; C_L, 1.02. (Wing restrained in roll by means of a spring.)

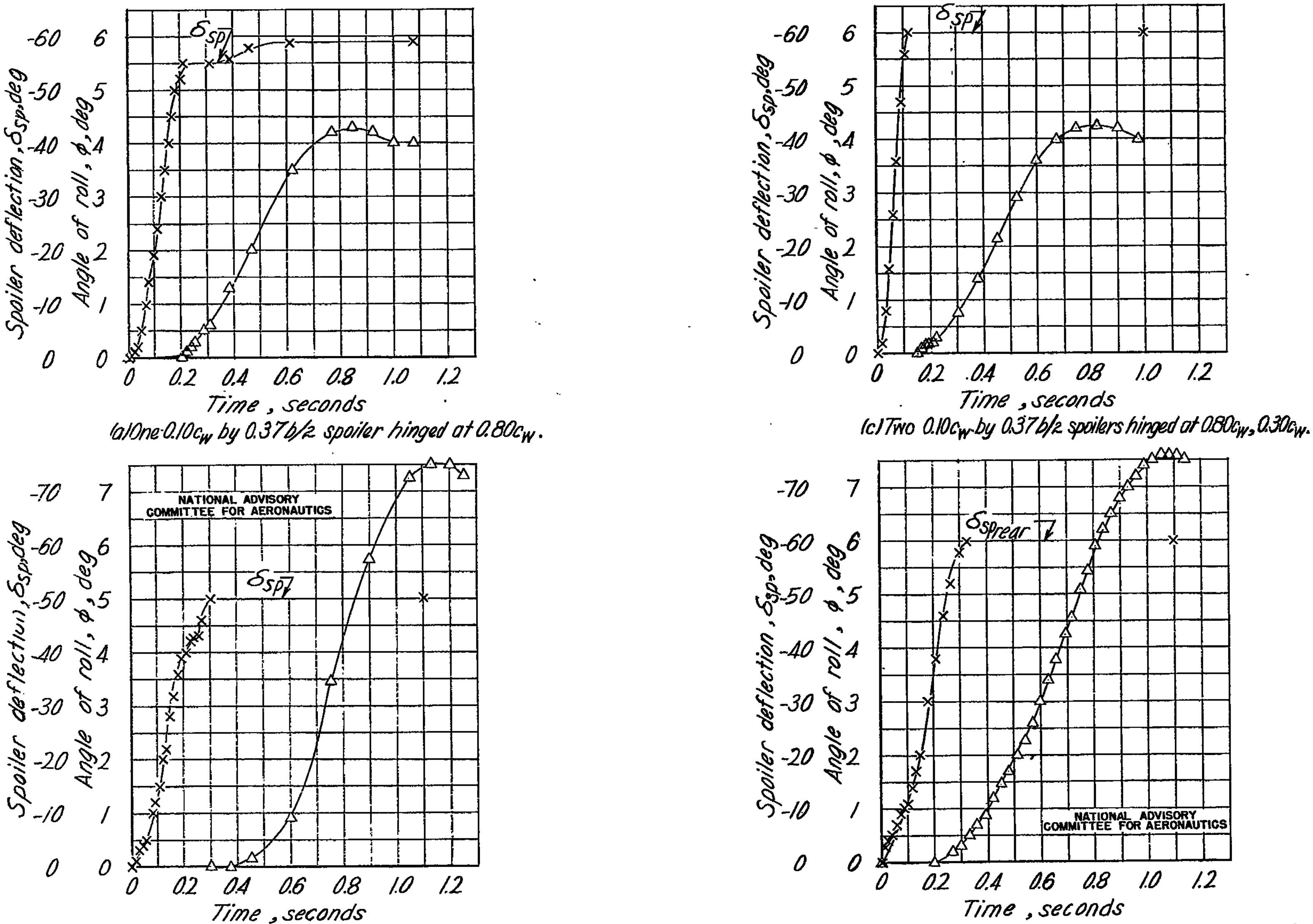

(a) One 0.10c_W by 0.37b/2 spoiler hinged at 0.80c_W.

(b) One 0.10c_W by 0.37b/2 spoiler hinged at 0.30c_W.

(c) Two 0.10c_W by 0.37b/2 spoilers hinged at 0.80c_W, 0.30c_W.

(d) One 0.10c_W by 0.37b/2 spoiler hinged at 0.80c_W and one 0.10c_W by 0.20b/2 spoiler hinged at 0.30c_W inset 0.47b/2.

Figure B28.- Time history of wing motion due to spoiler deflection; semispan of Clark Y-15 wing; C_L, 1.02. (Wing restrained in roll by means of a spring.)

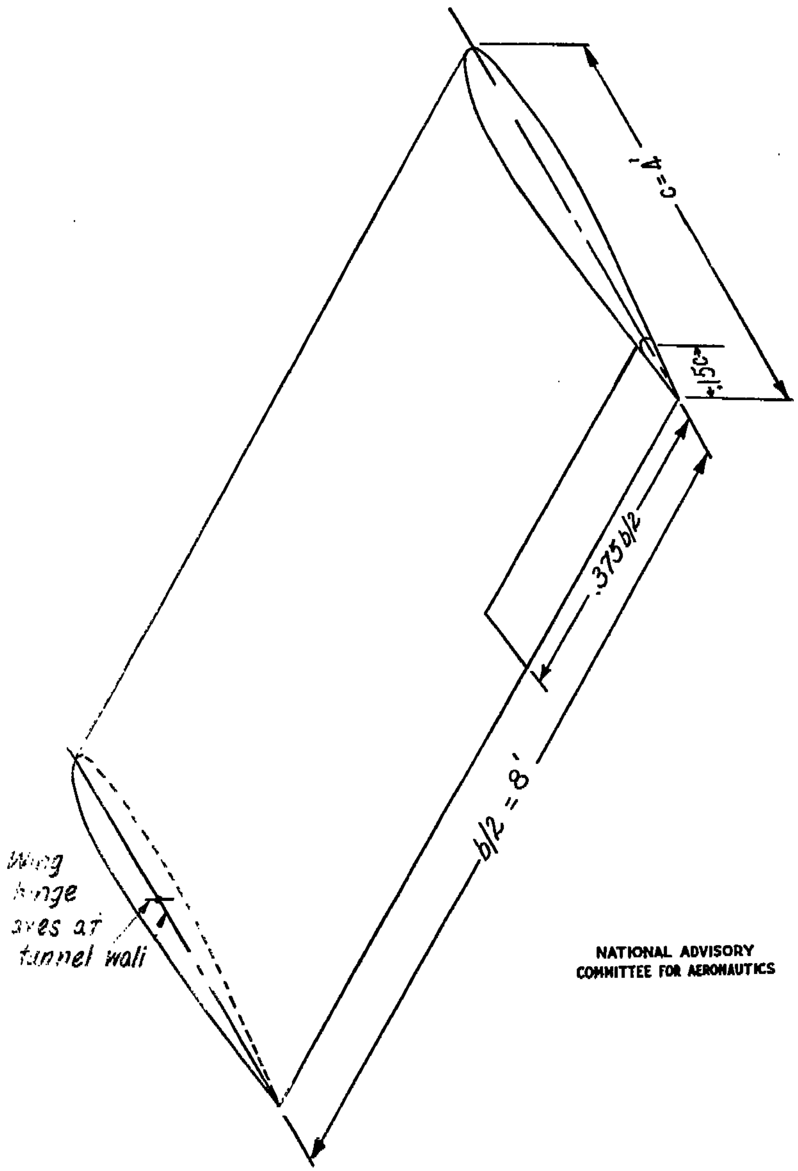

Figure B29.- Schematic diagram of the 4- by 8-foot wing semispan tested in the Langley 7- by 10-foot tunnel. Span of all lateral-control devices, 3 feet.

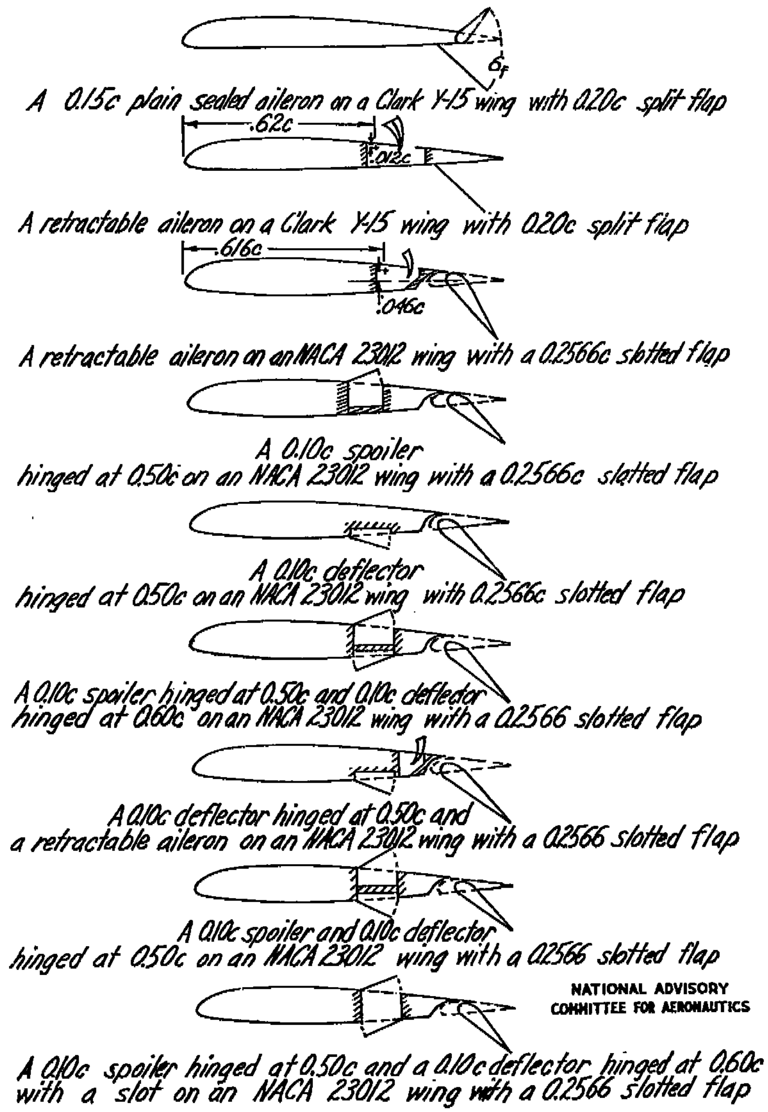

Figure B30.- Sections of the 4- by 8-foot wing showing the various types of spoilers and flaps tested.

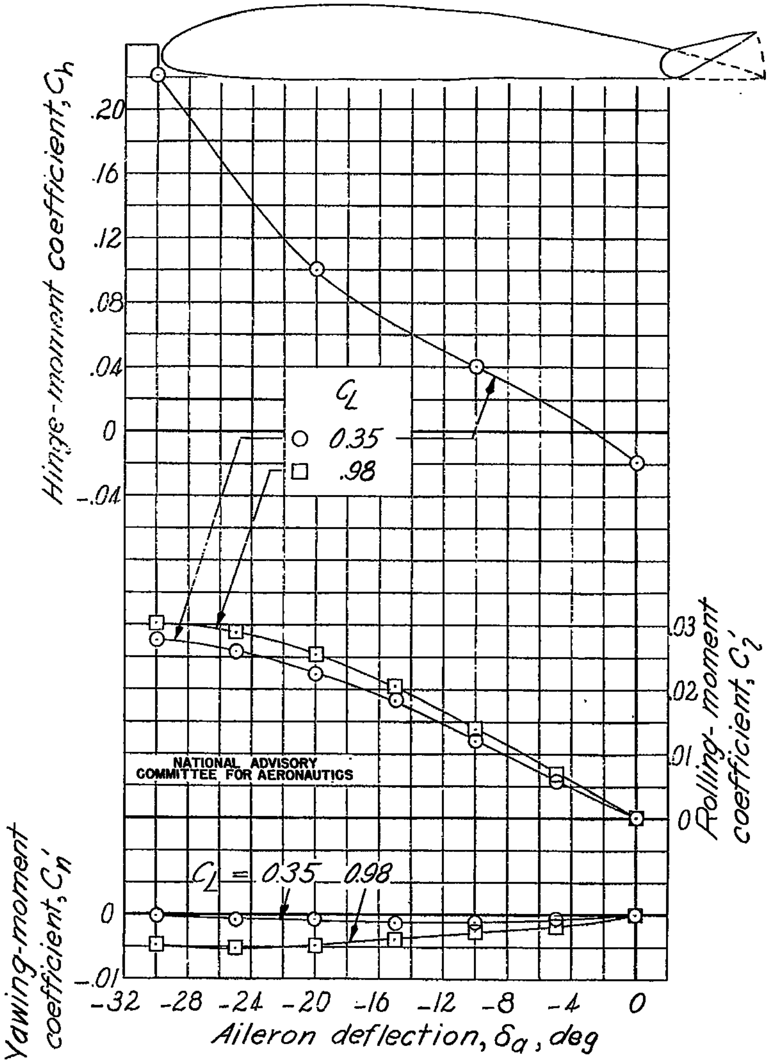

(a) Flap removed.

Figure B31.- Aileron characteristics of a 0.15c plain sealed aileron on a Clark Y-15 wing with a 0.20c full-span split flap.

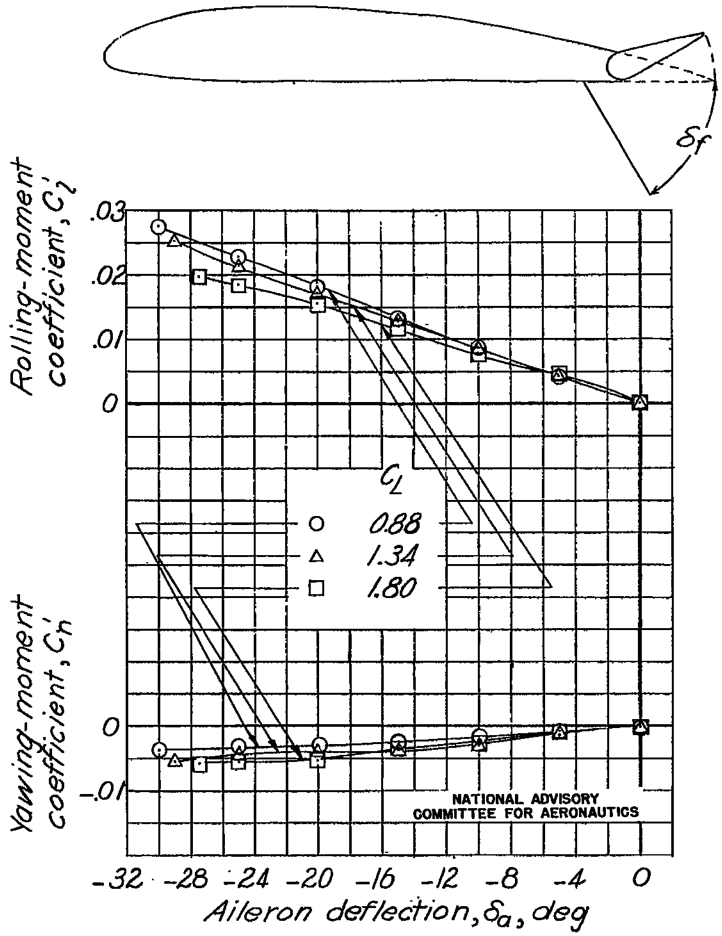

(b) δ_f, 60°.

Figure B31.- Concluded.

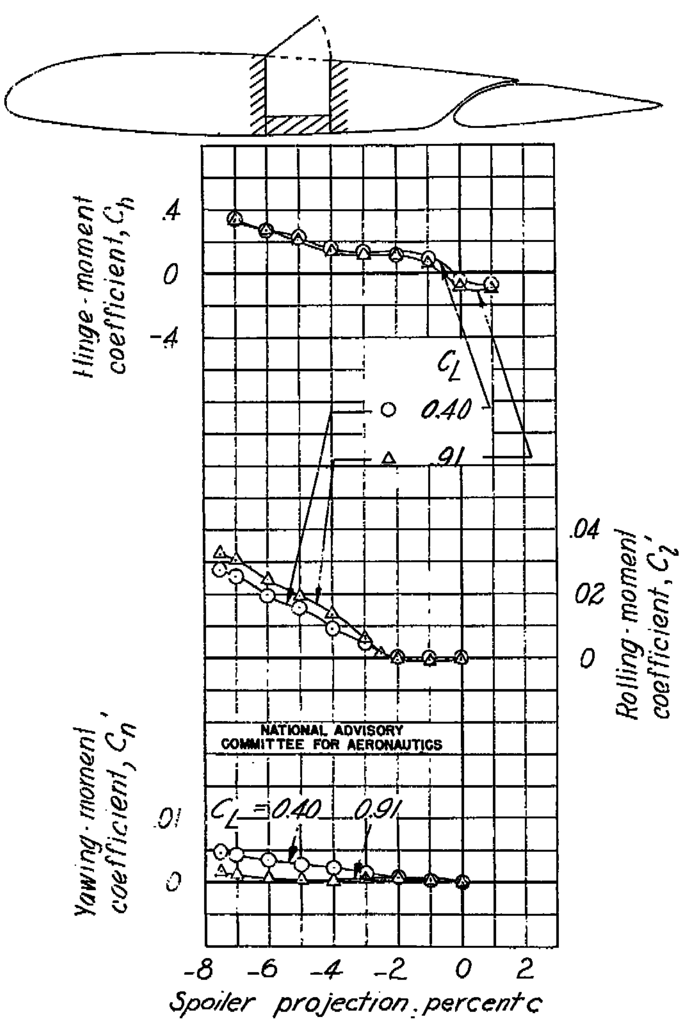

(a) δ_f, 0°.

Figure B32.- Aileron characteristics of a 0.10c spoiler hinged at 0.80c on an NACA 23012 wing with a 0.2566c full-span slotted flap.

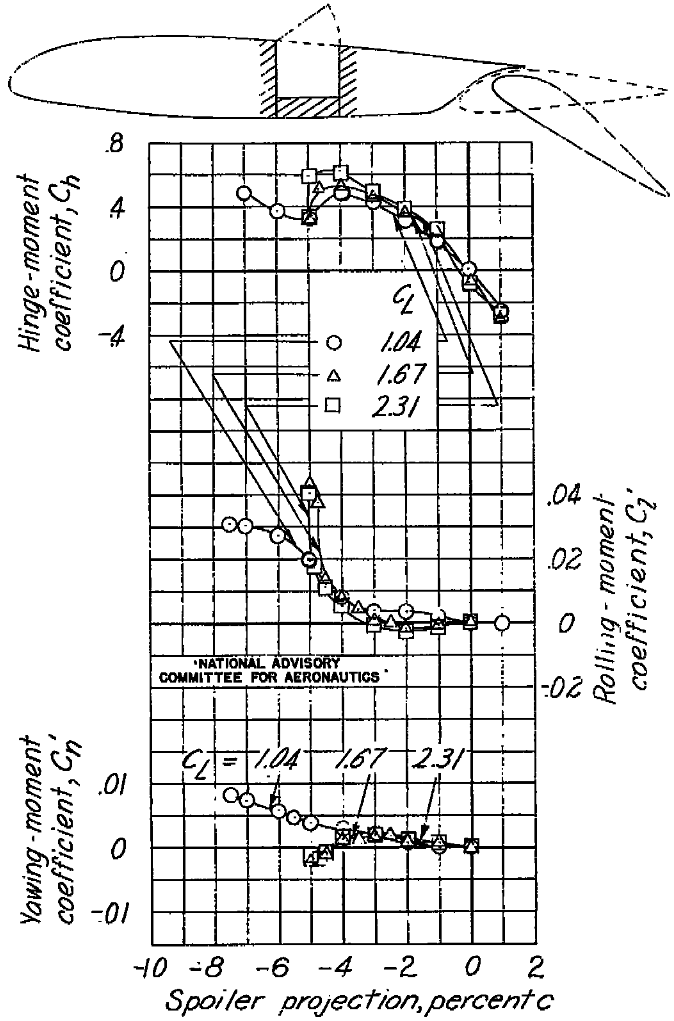

(b) δ_f, 40°.

Figure B32.- Concluded.

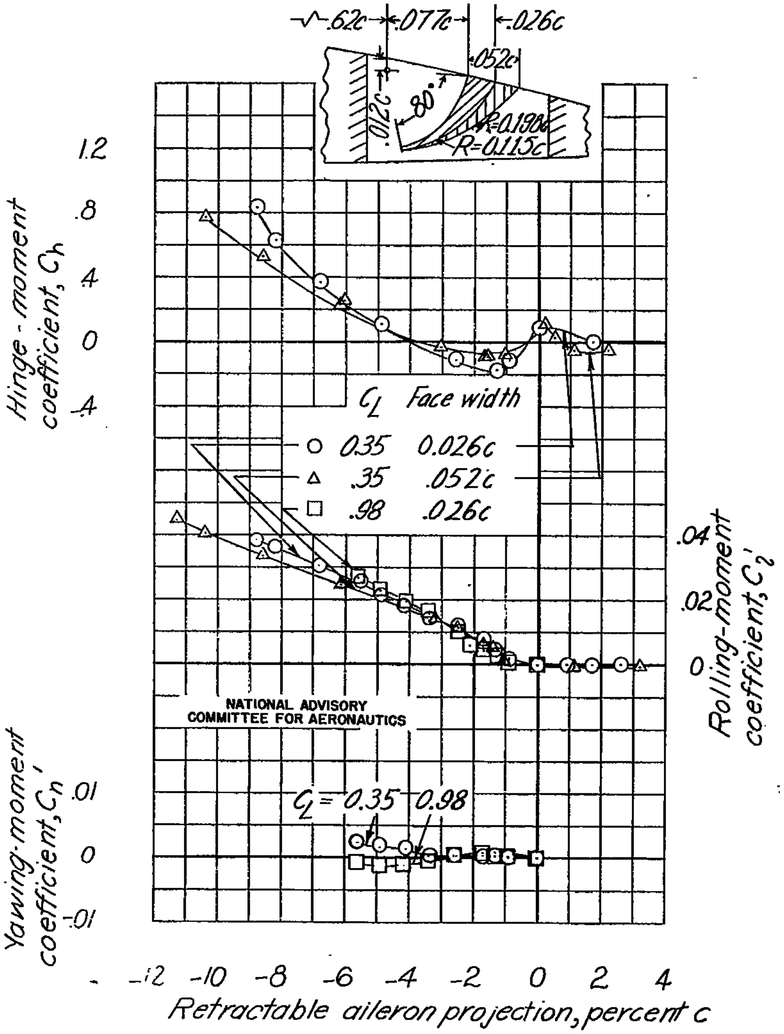

(a) Flap removed.

Figure B33.- Aileron characteristics of a retractable aileron on a Clark Y-15 wing with a 0.20c full-span split flap.

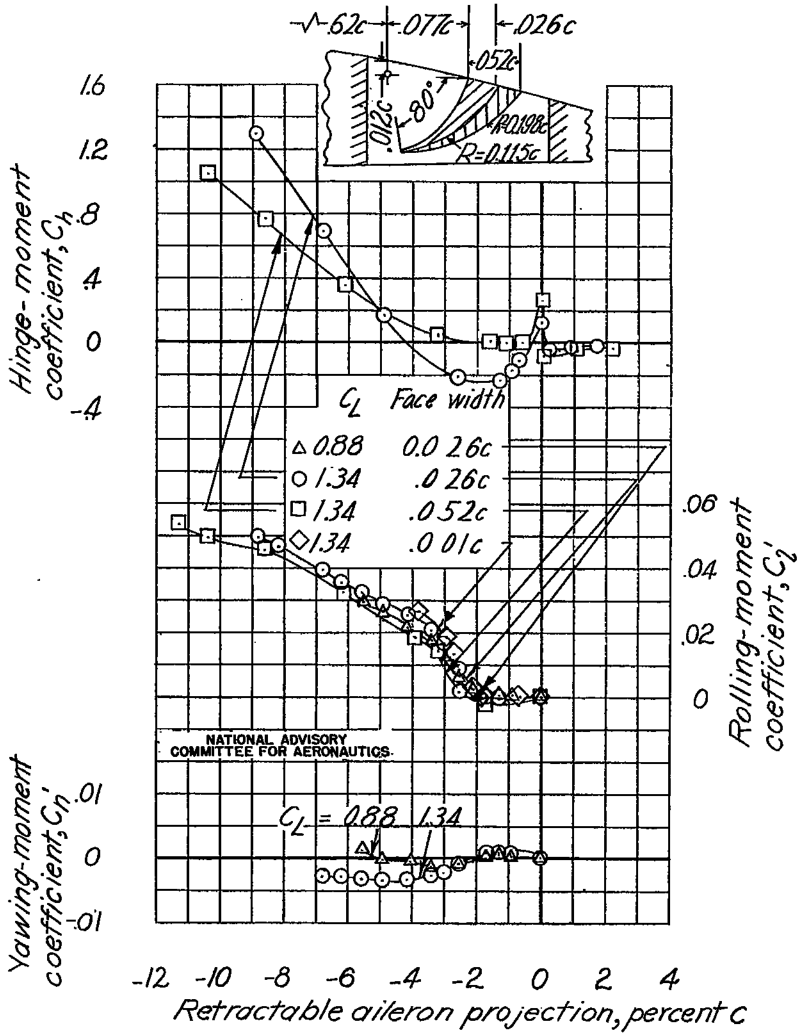

(b) δ_f, 60°.

Figure B33.- Concluded.

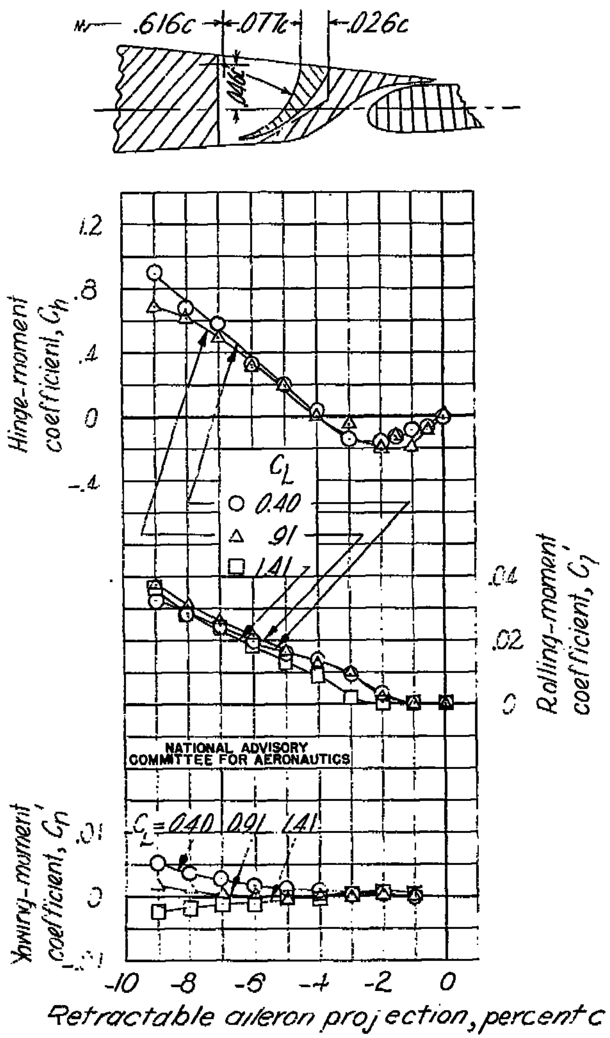

(a) δ_f, [illegible].

Figure B34.- Aileron characteristics of a retractable aileron on an NACA 23012 wing with a 0.2566c full-span slotted flap.

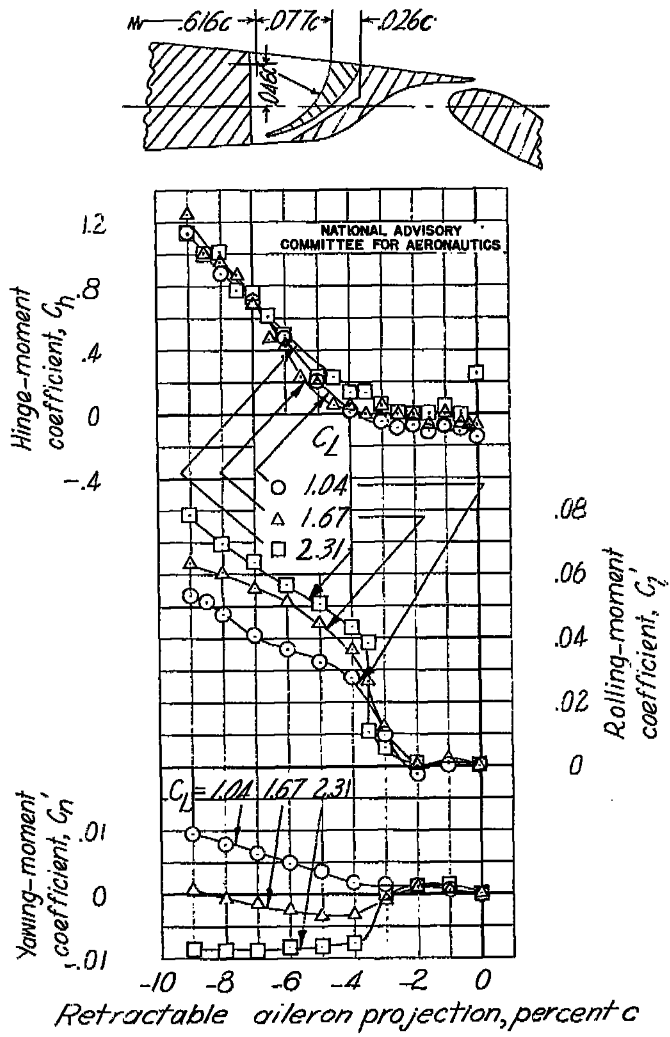

(b) δ_f, 40°.

Figure B34.- Concluded

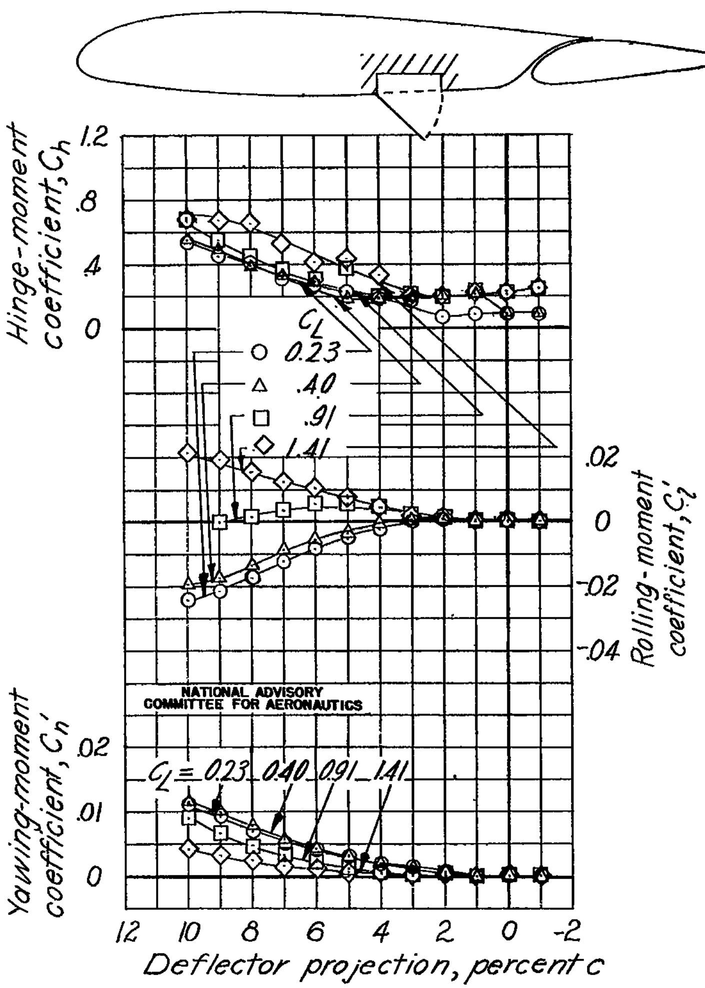

(a) δ_f, 0°.

Figure B35.- Aileron characteristics of a 0.10c deflector hinged at 0.50c on an NACA 23012 wing with a 0.2566c full-span slotted flap.

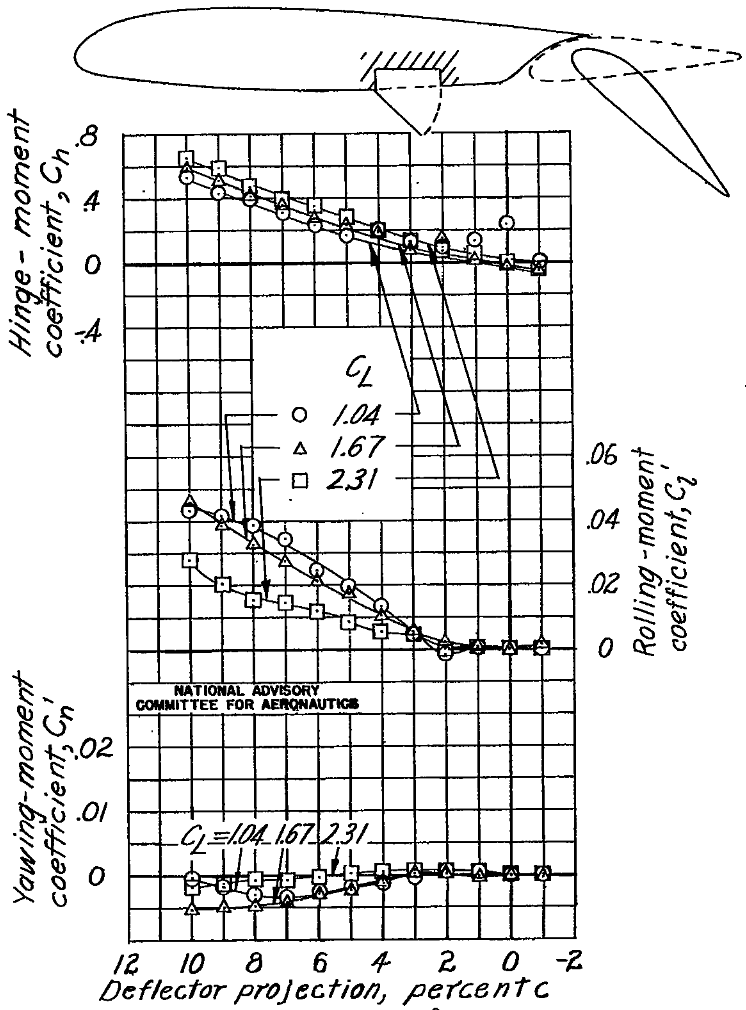

(b) δ_f, 40°.

Figure B35.- Concluded.

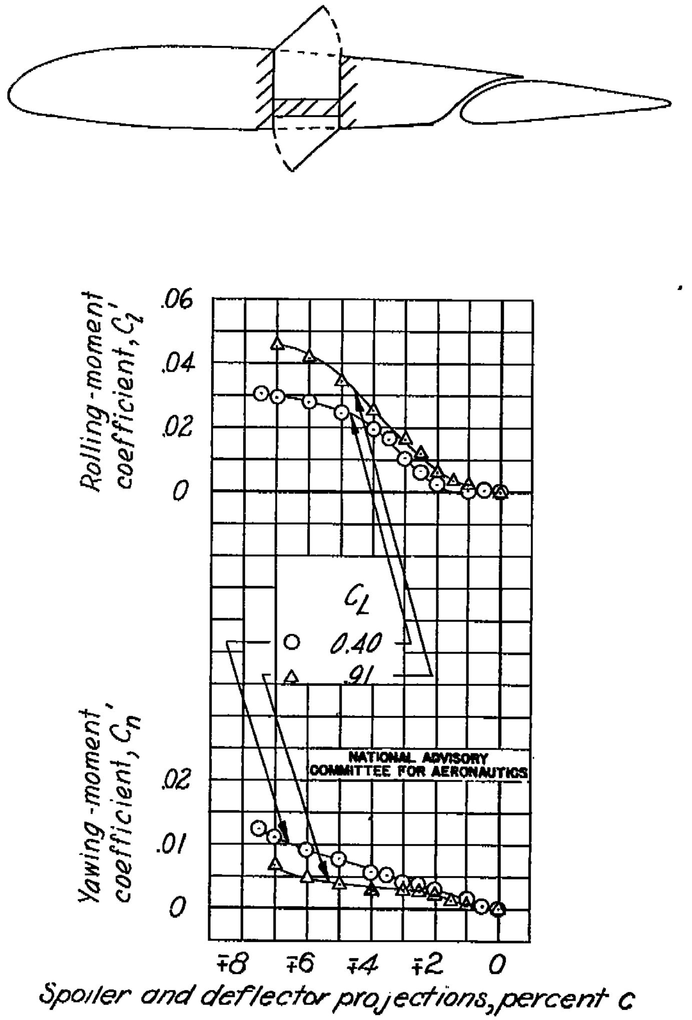

(a) δ_f, 0°.

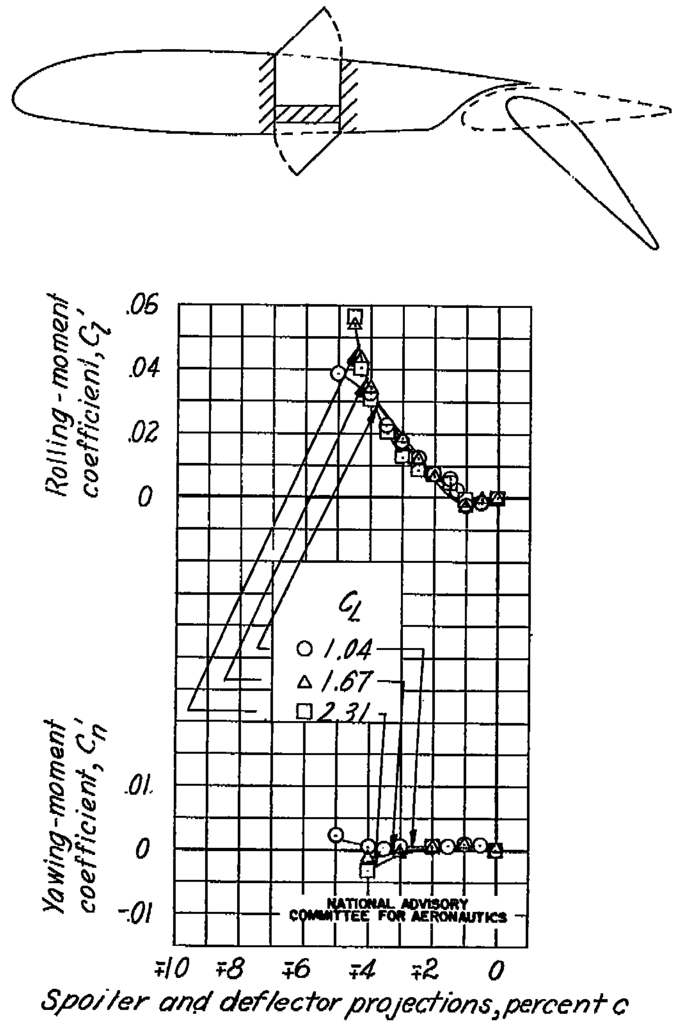

(b) δ_f, 40°.

Figure B36.- Aileron characteristics of a 0.10c spoiler and a 0.10c deflector on an NACA 23012 wing with a 0.2566c full-span slotted flap; spoiler hinged at 0.50c; deflector hinged at 0.60c.

Figure B36.- Concluded.

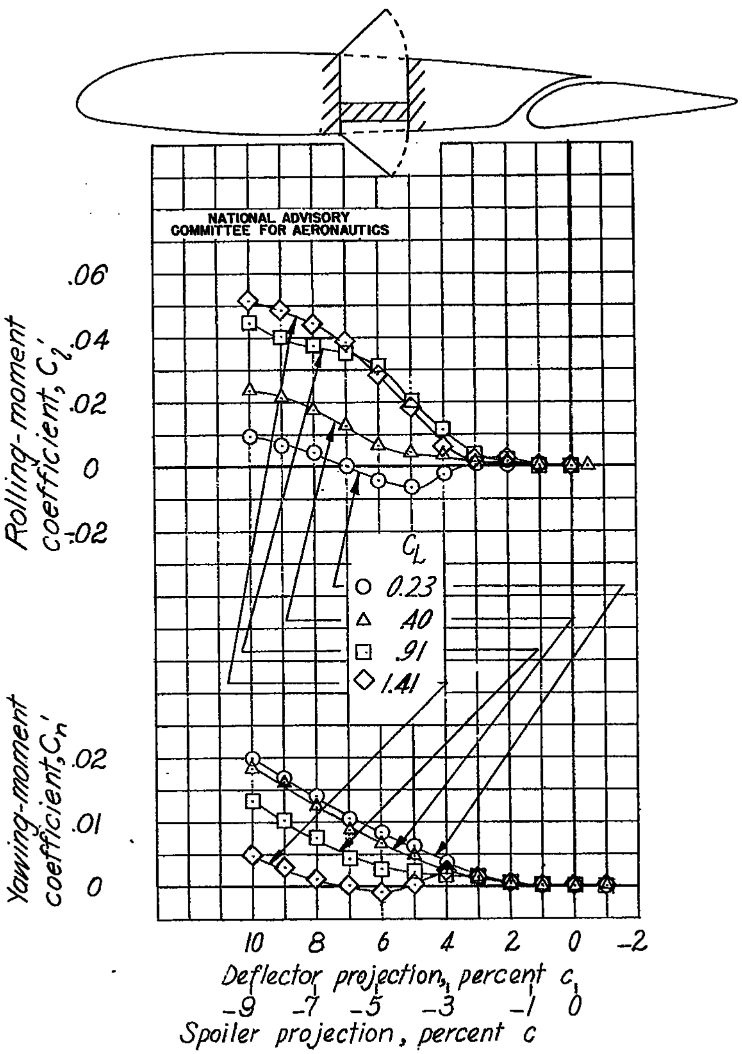

(a) δ_f, 0°.

Figure B37.- Aileron characteristics of a 0.10c spoiler and a 0.10c deflector on an NACA 23012 wing with a 0.2566c full-span slotted flap; spoiler and deflector hinged at 0.50c.

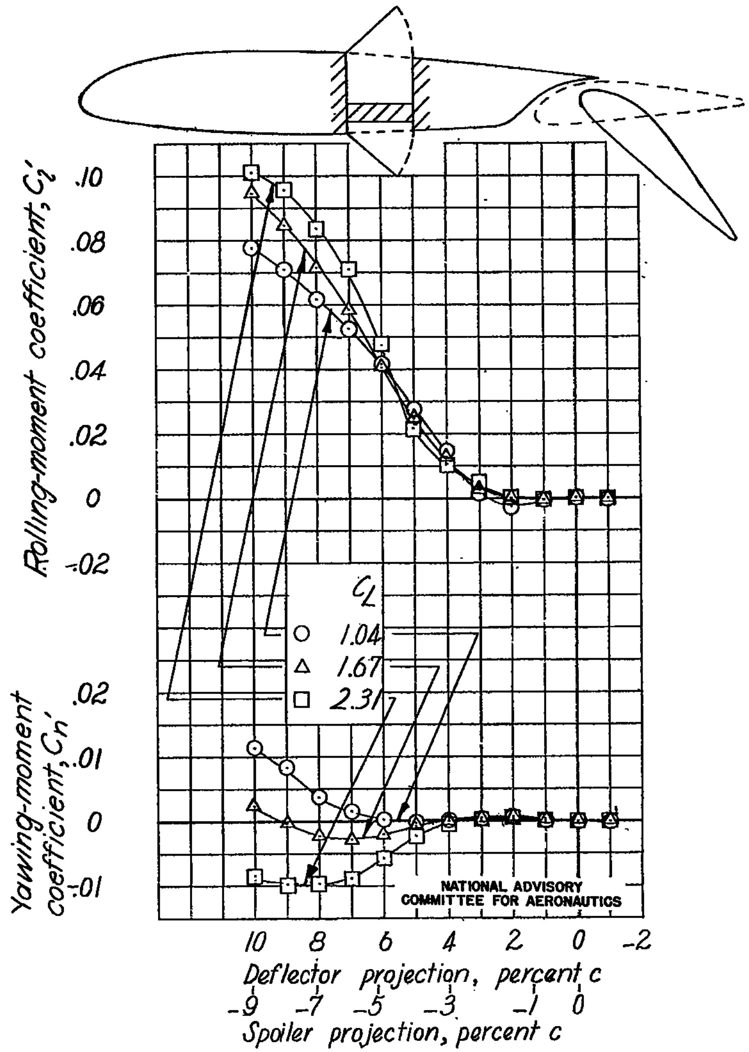

(b) δ_f, 40°.

Figure B37.- Concluded.

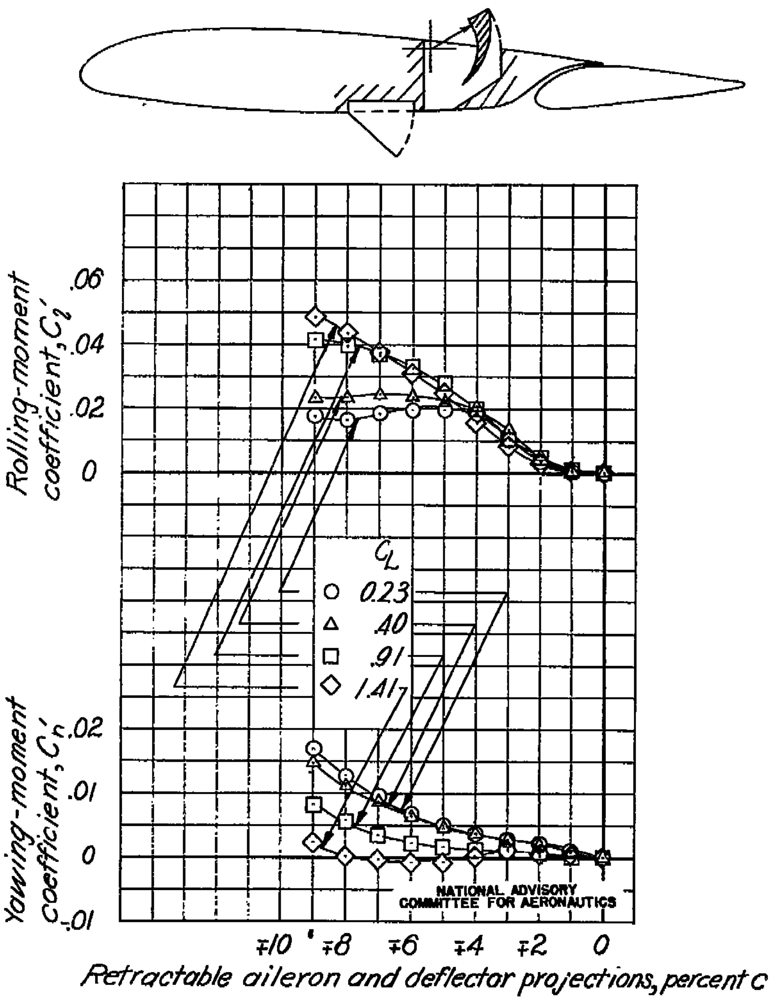

(a) δ_f, 0°.

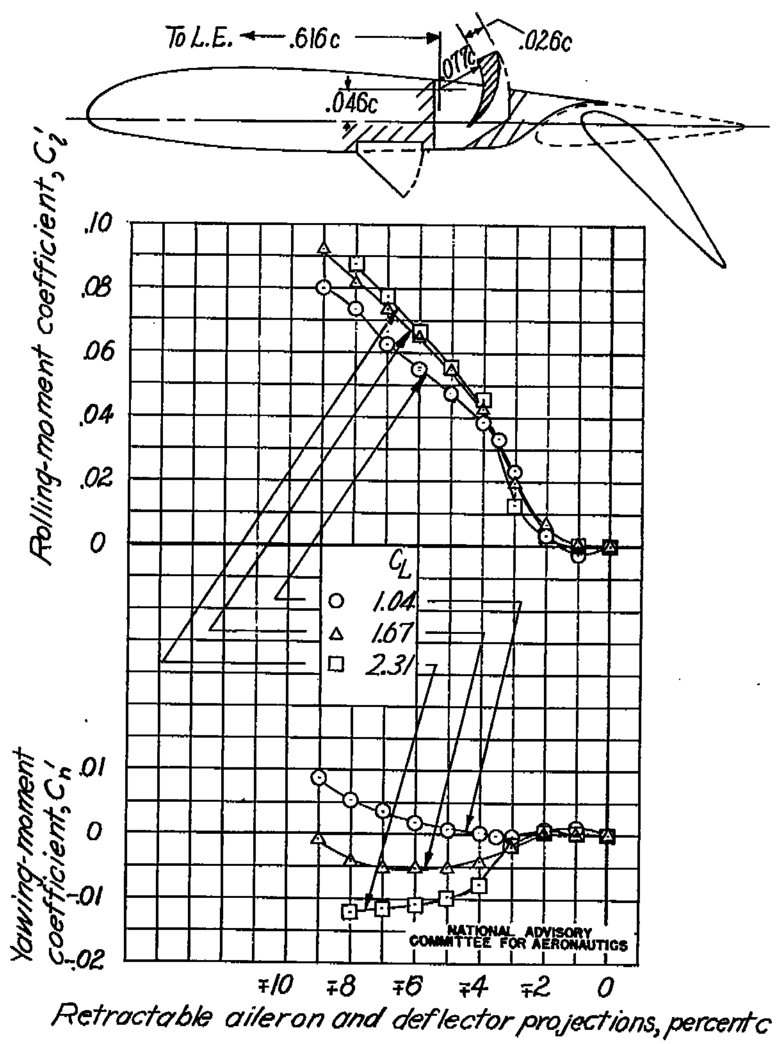

(b) δ_f, 40°.

Figure B38.- Aileron characteristics of a 0.10c deflector hinged at 0.50c and a retractable aileron on an NACA 23012 wing with a 0.2566c full-span slotted flap, projection ratio of aileron to deflector, 1:1.

Figure B38.- Concluded.

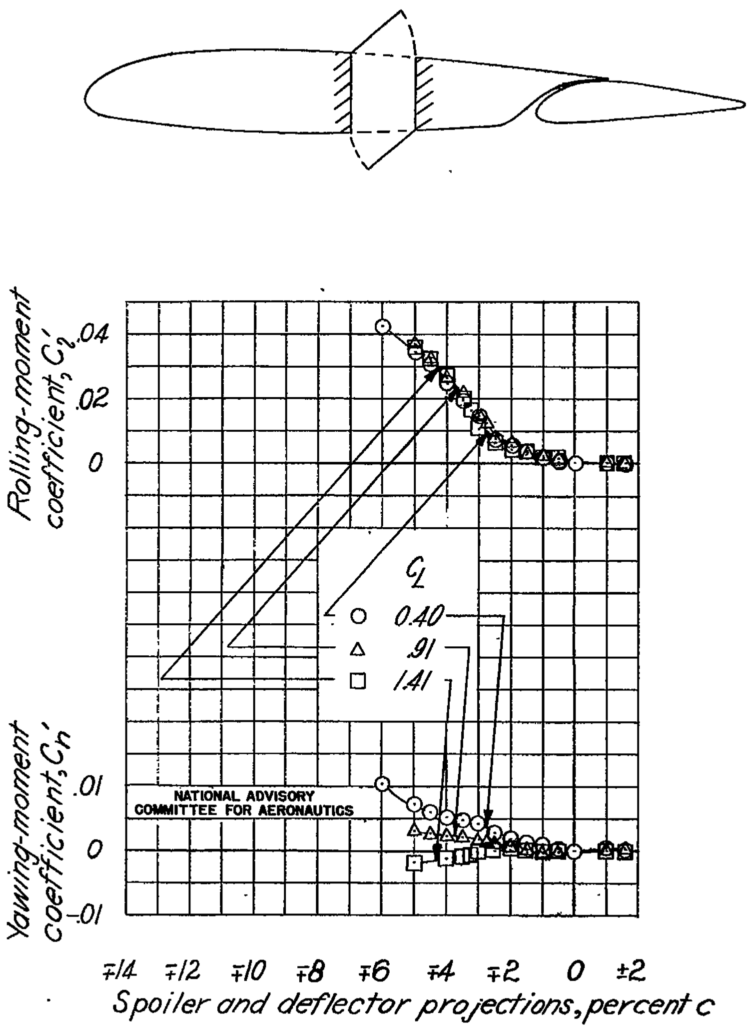

(a) δ_f, 0°.

Figure B39.- Aileron characteristics of a 0.10c spoiler and a 0.10c deflector with a slot on an NACA 23012 wing with a 0.2566c full-span slotted flap; spoiler hinged at 0.50c; deflector hinged at 0.60c; projection ratio of spoiler to deflector, 1:1.

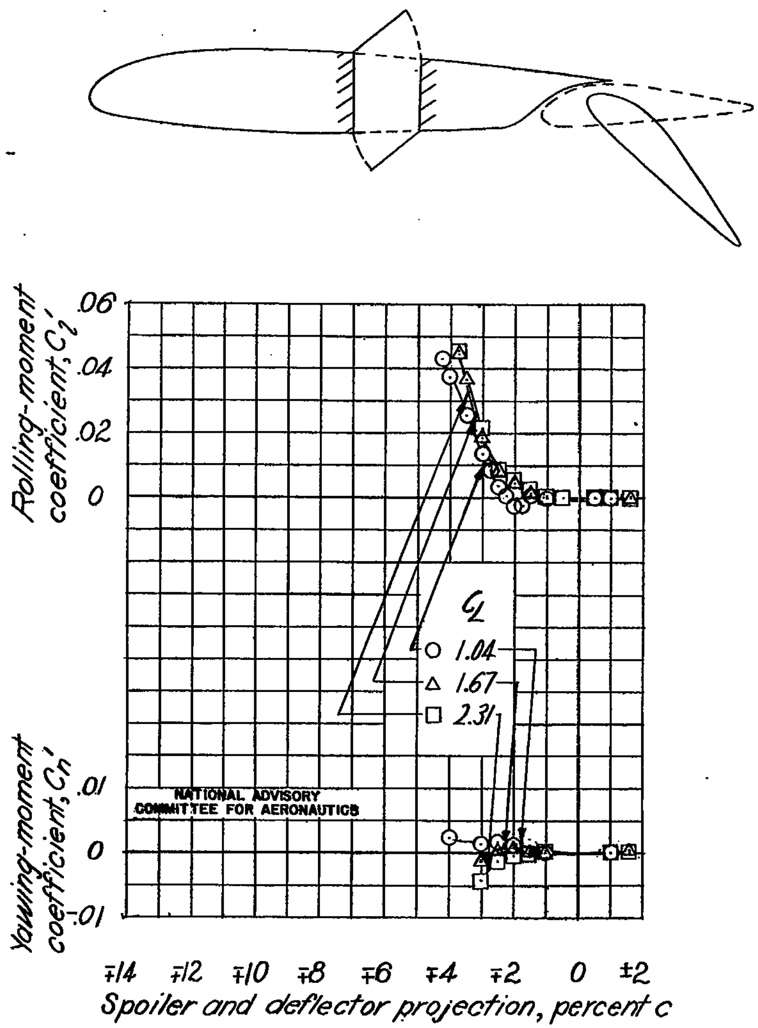

(b) δ_f, 40°.

Figure B39.- Concluded.

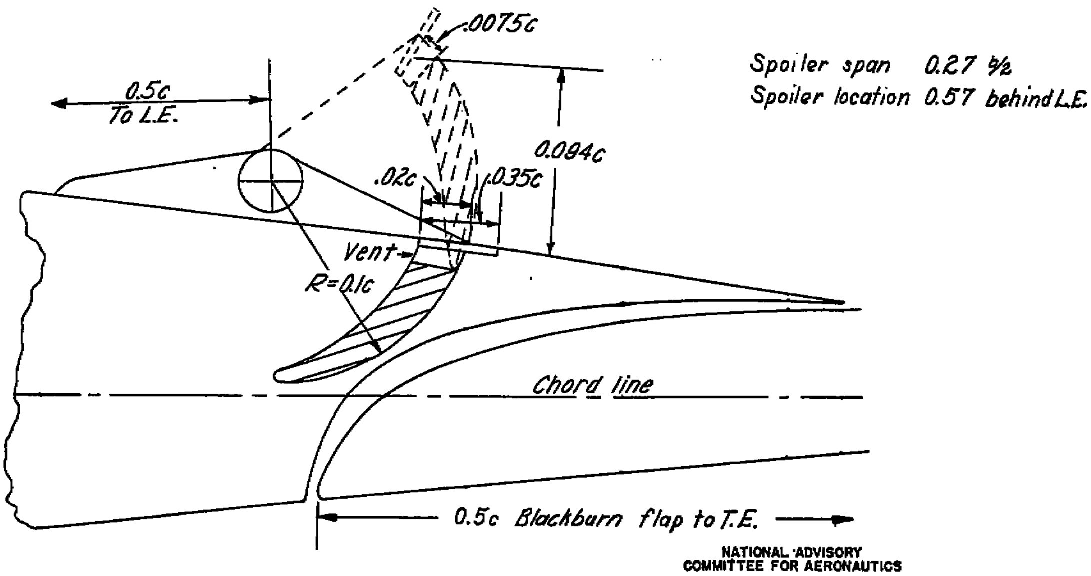

Figure B40.- Drawing of Blackburn retractable arc spoiler tested in the Blackburn wind tunnel.

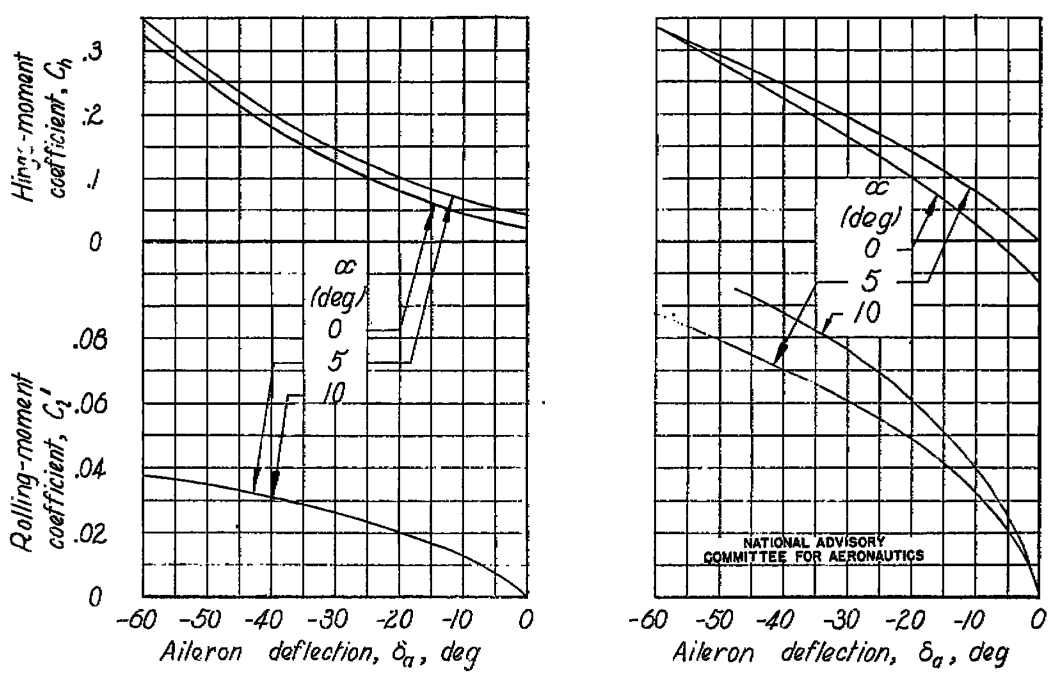

(a) Flaps retracted.

(b) Flaps deflected 45°.

Figure B41.- Rolling and hinge-moment characteristics of airfoil equipped with Blackburn retractable arc spoiler.

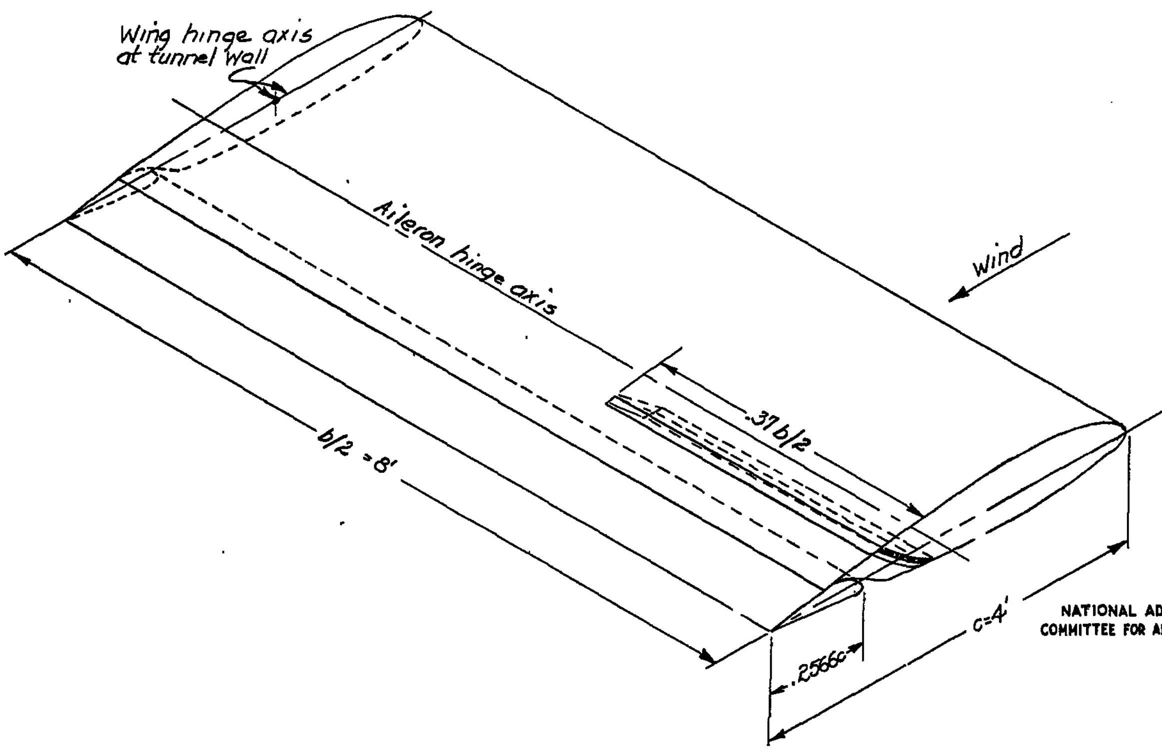

Figure B42.- Schematic diagram of the 4- by 8-foot NACA 23012 semispan wing tested in the Langley 7- by 10-foot tunnel.

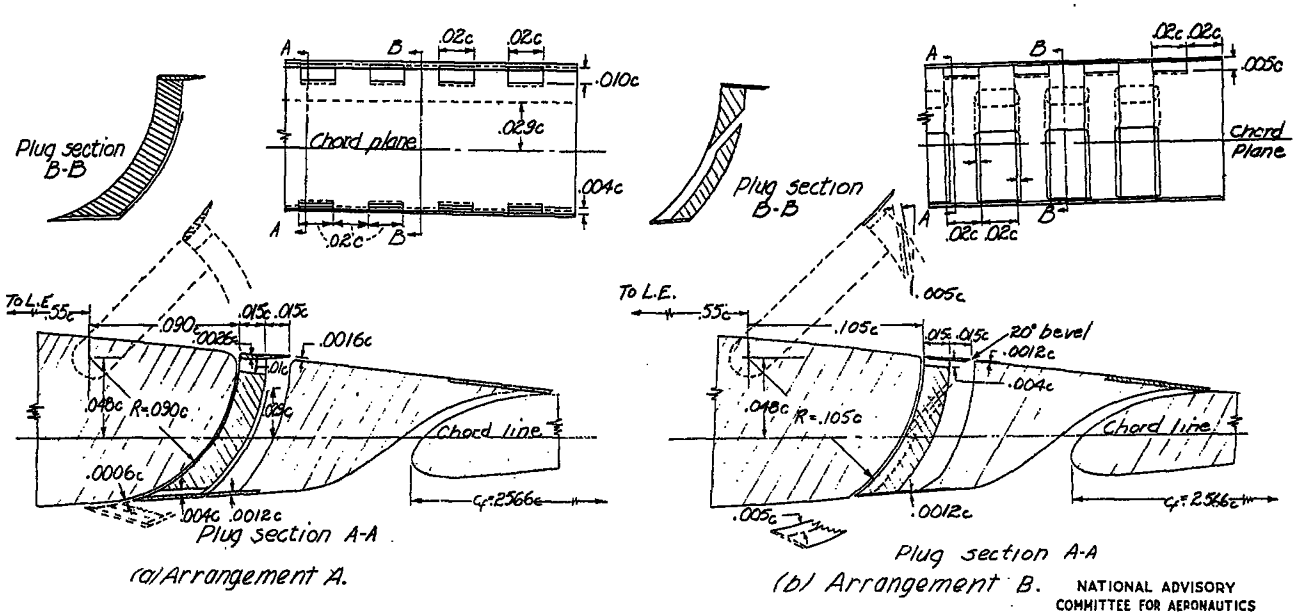

Figure B43.- Detail of plugs used on the 0.37 b/2 plug-type aileron on the NACA 23012 wing with a 0.2566c full-span slotted flap.

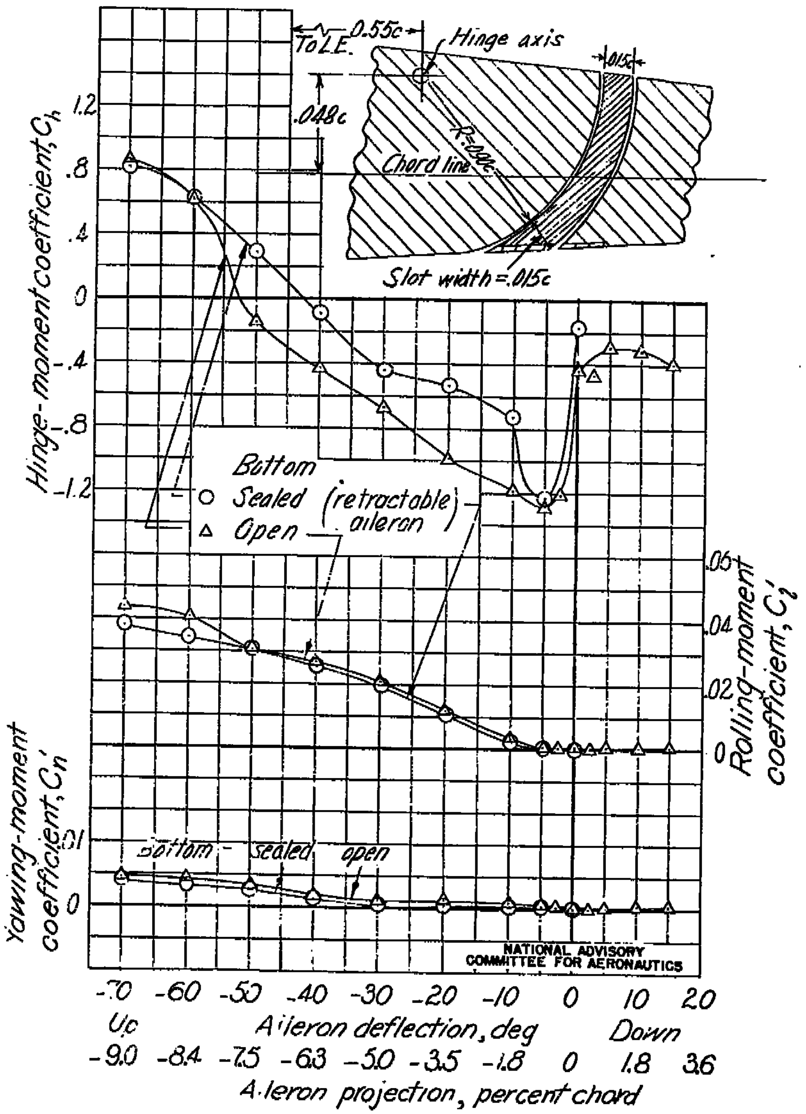

(a) Flap neutral; α, 9.70°; C_L, 0.77.

Figure B44.- Aileron characteristics of a 0.37 b/2 plug-type aileron on an NACA 23012 wing with a 0.2566c full-span slotted flap. Width of spoiler face 0.015c.

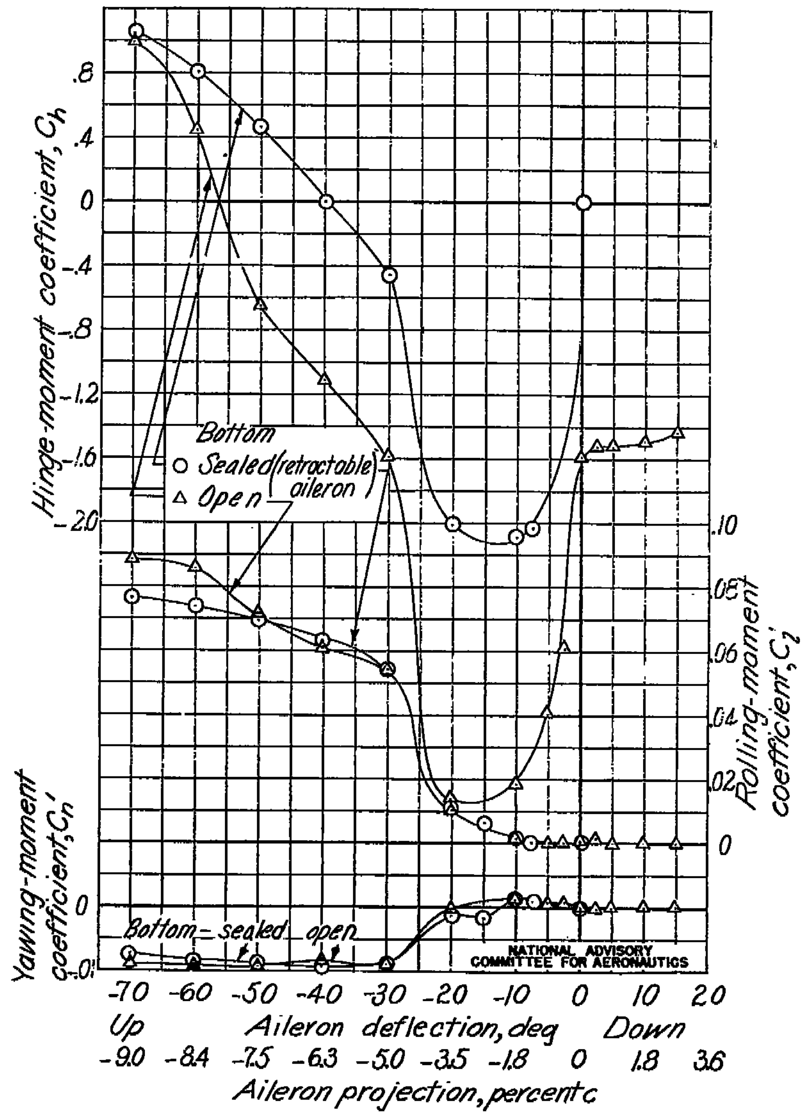

(b) Flap deflected 40°; α, 13.3°; C_L, 2.36.

Figure B44.- Concluded.

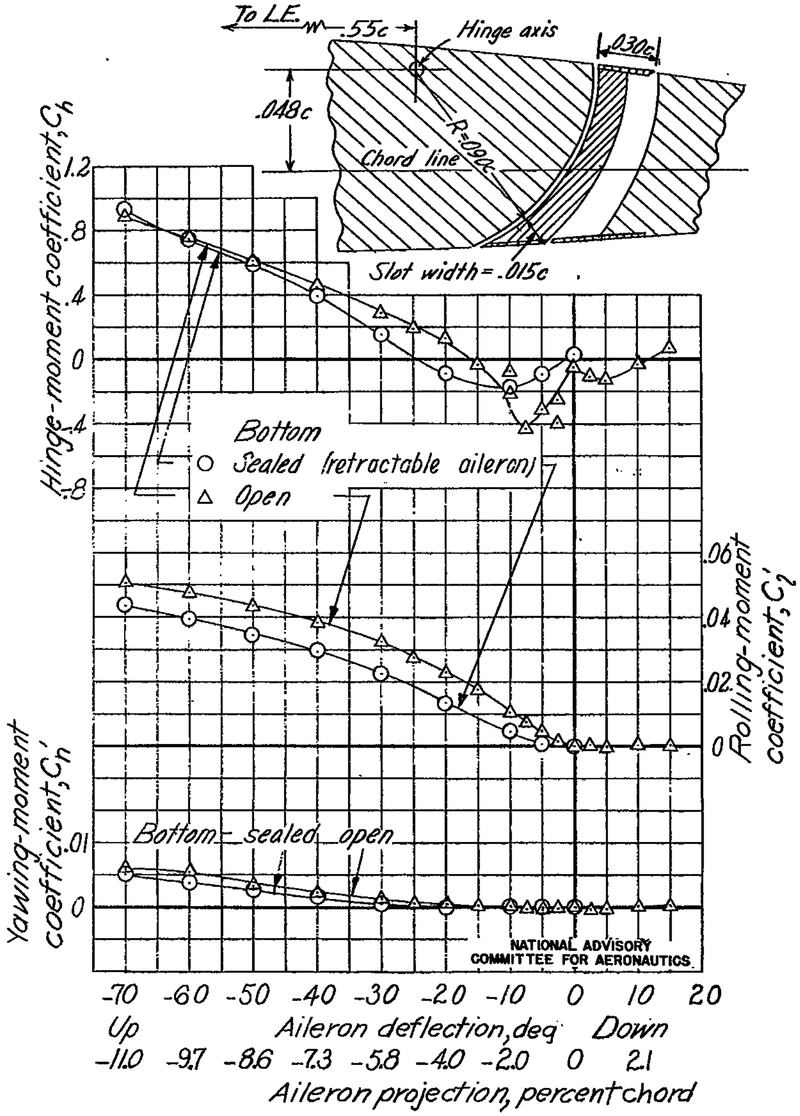

(a) Flap neutral; α, 9.7°; C_L, 0.77.

Figure B45.- Aileron characteristics of a 0.37 b/2 plug-type aileron on an NACA 23012 wing with a 0.2566c full-span slotted flap. Width of spoiler face, 0.030c.

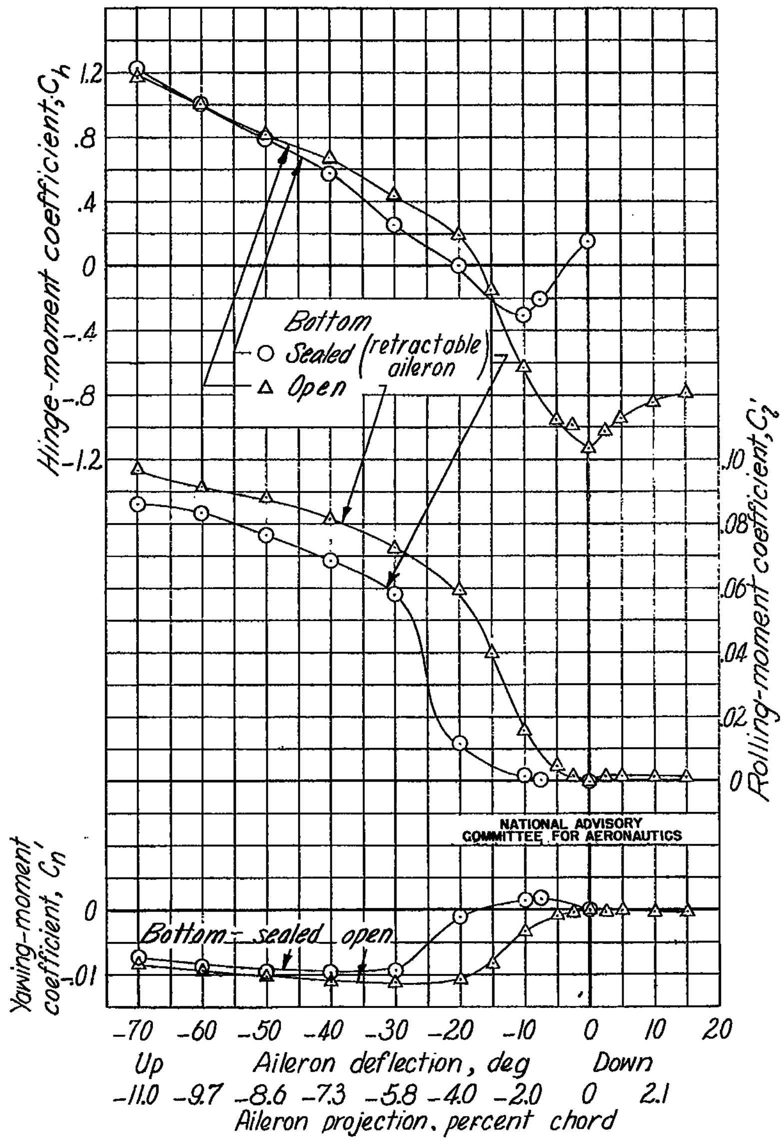

(b) Flap deflected 40°; α, 13.3°; C_L, 2.36.

Figure B45.- Concluded.

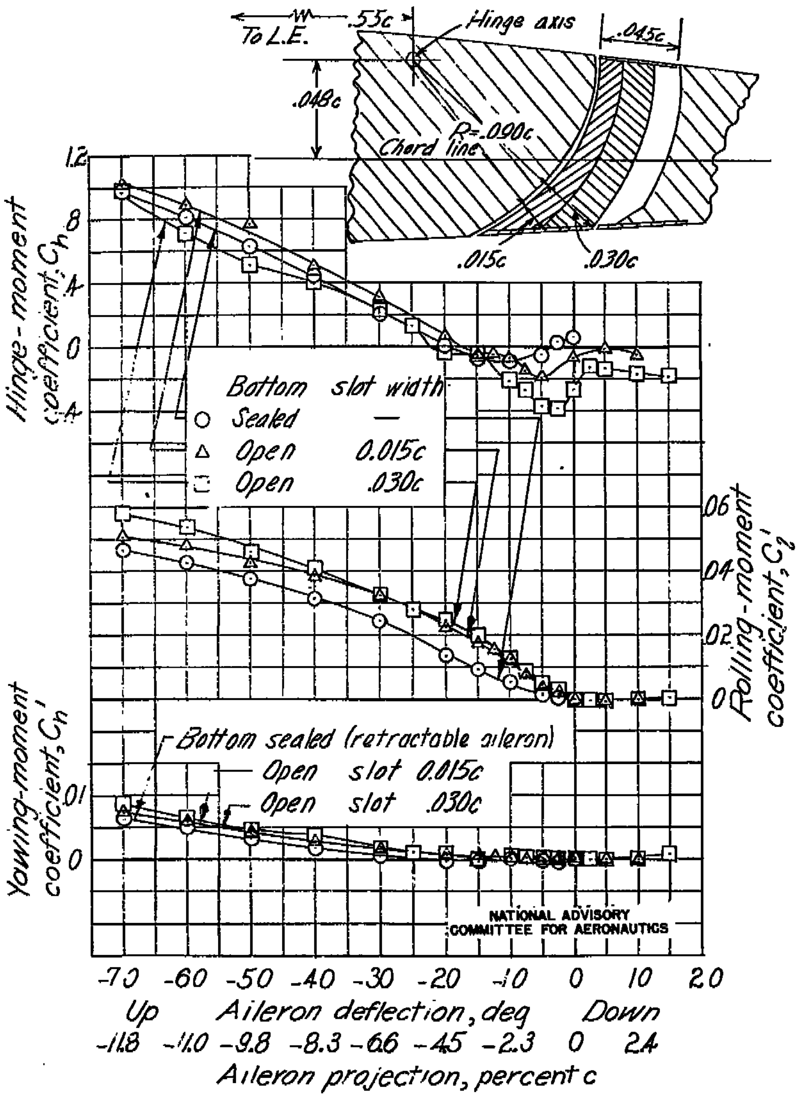

(a) Flap neutral; α, 9.7°; C_L, 0.77.

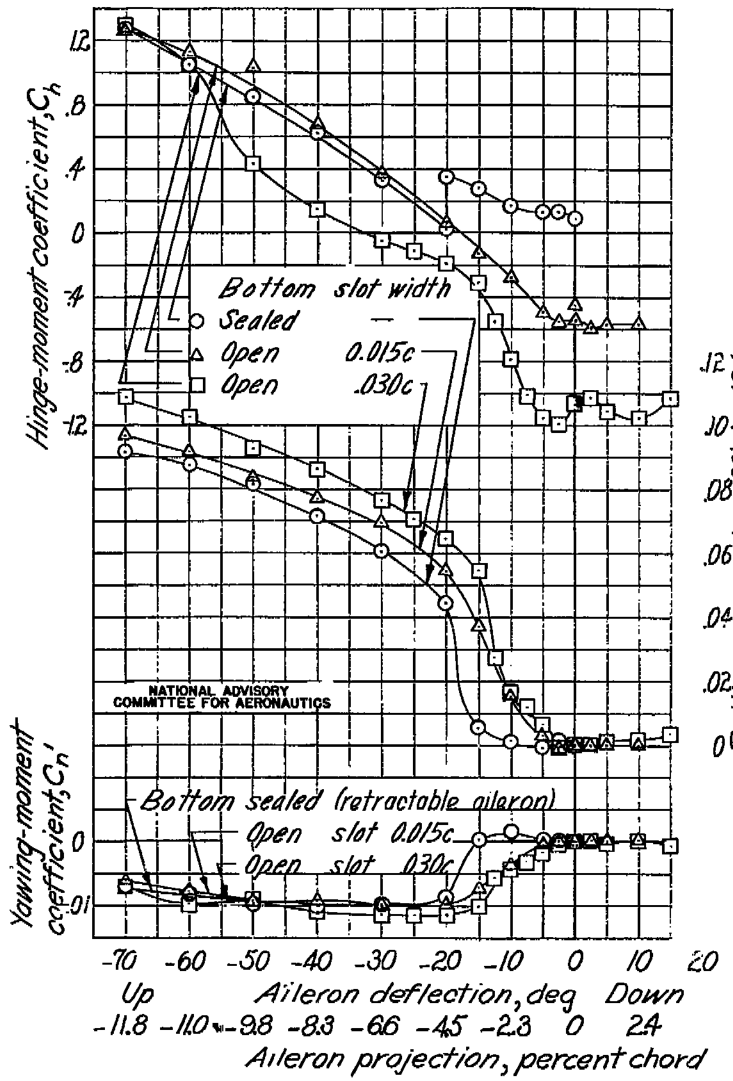

(b) Flap deflected 40°; α, 13.3°; C_L, 2.36.

Figure B46.- Aileron characteristics of a 0.37 b/2 plug-type aileron on an NACA 23012 wing with a 0.2566c full-span slotted flap. Width of spoiler face, 0.045c.

Figure B46.- Concluded.

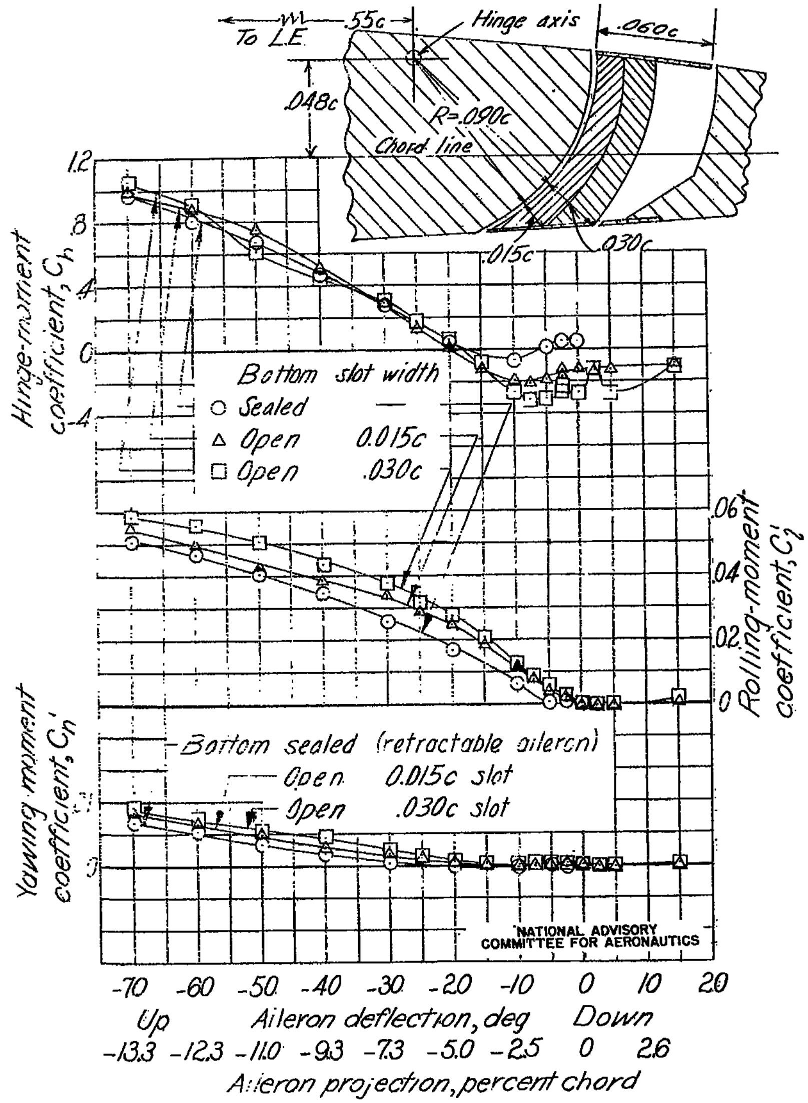

(a) Flap neutral; α, 9.7°; C_L, 0.77.

Figure B47.- Aileron characteristics of a 0.37 b/2 plug-type aileron on an NACA 23012 wing with a 0.2566c full-span slotted flap. Width of spoiler face, 0.060c.

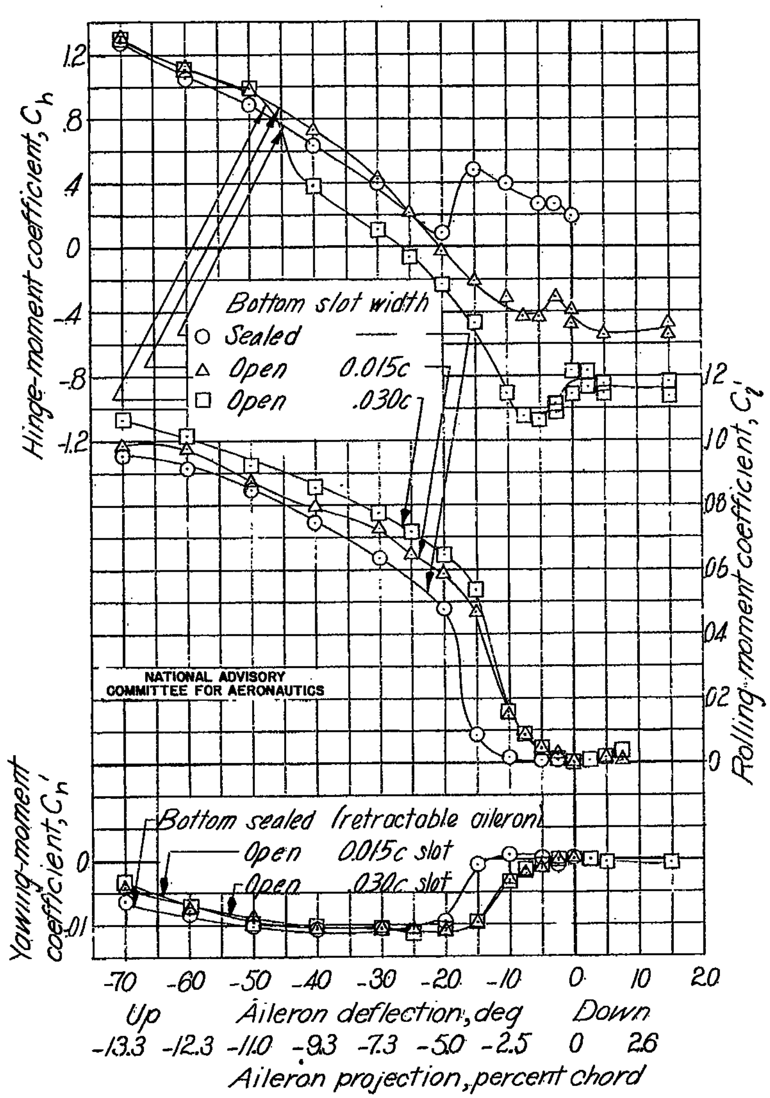

(b) Flap deflected 40°; α, 13.3°; C_L, 2.36.

Figure B47.- Concluded.

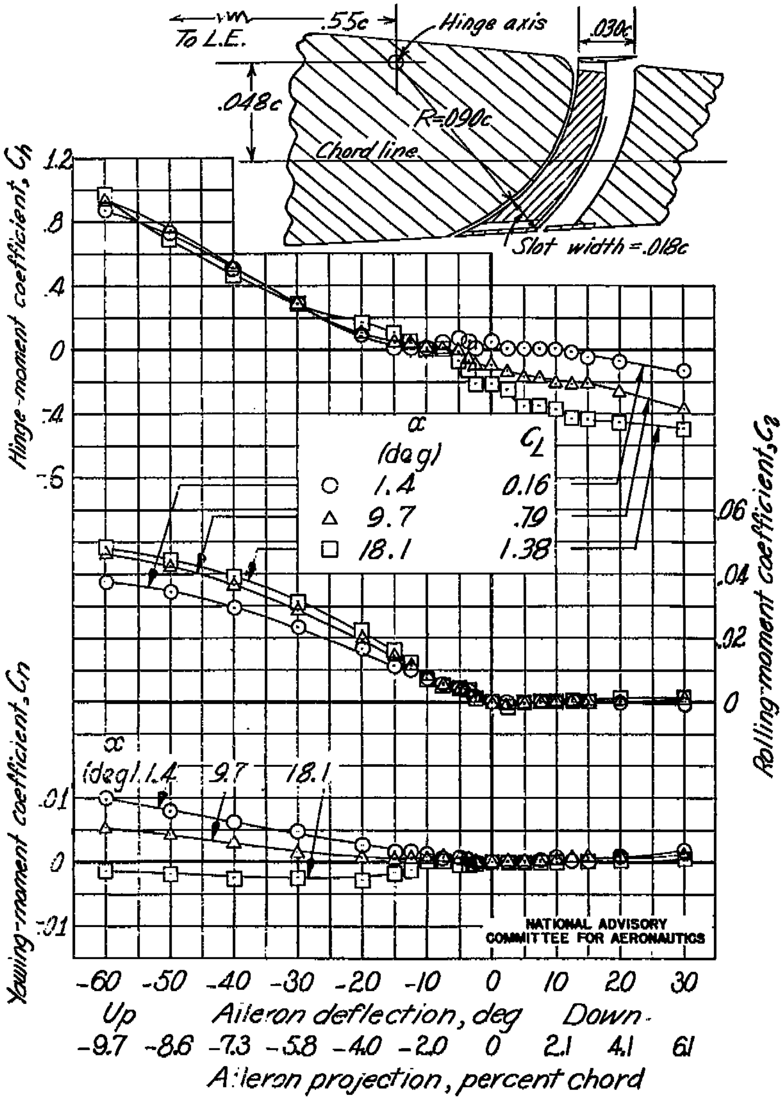

(a) Flap neutral.

Figure B49.- Aileron characteristics of a 0.37 b/2 plug-type aileron on an NACA 23012 wing with a 0.2566c full-span slotted flap, arrangement A.

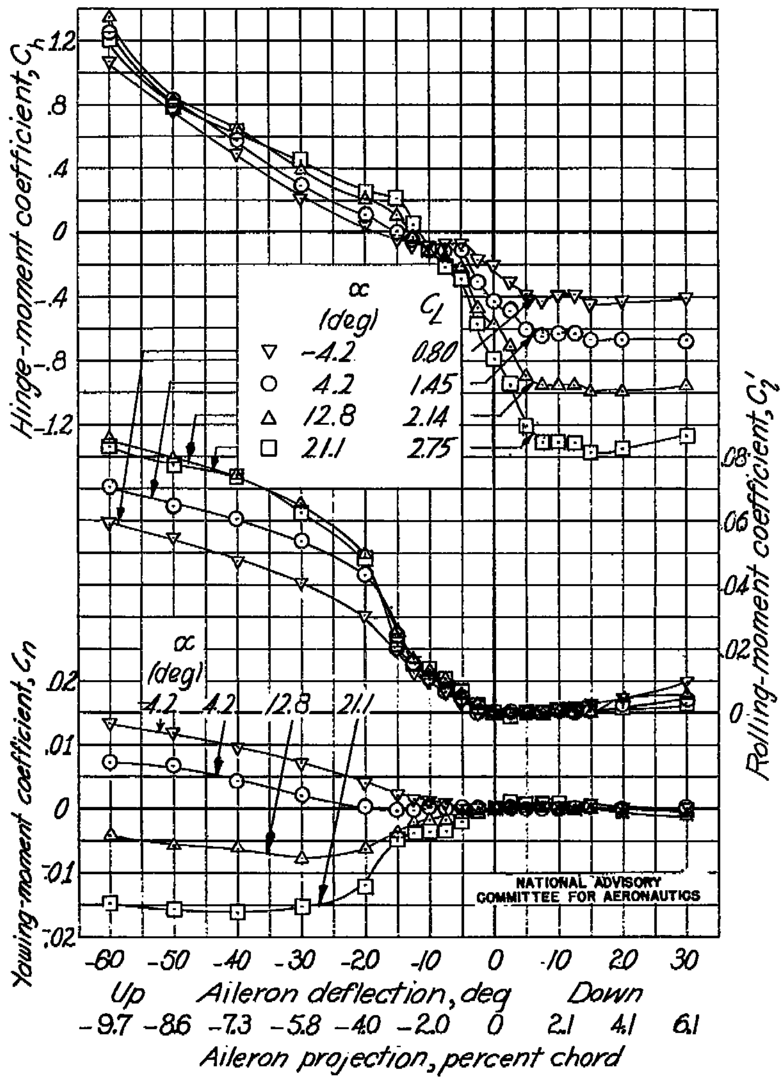

(b) Flap deflected 30°.

Figure B48.- Continued.

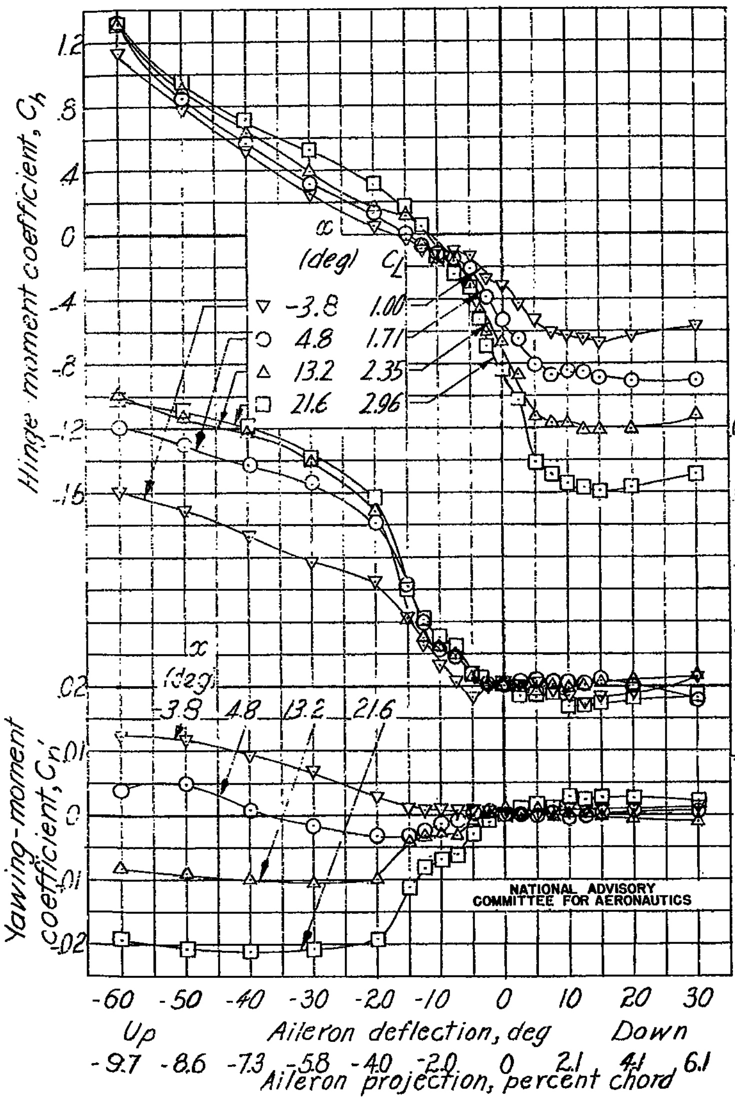

(c) Flap deflected 40°.

Figure B48.- Concluded.

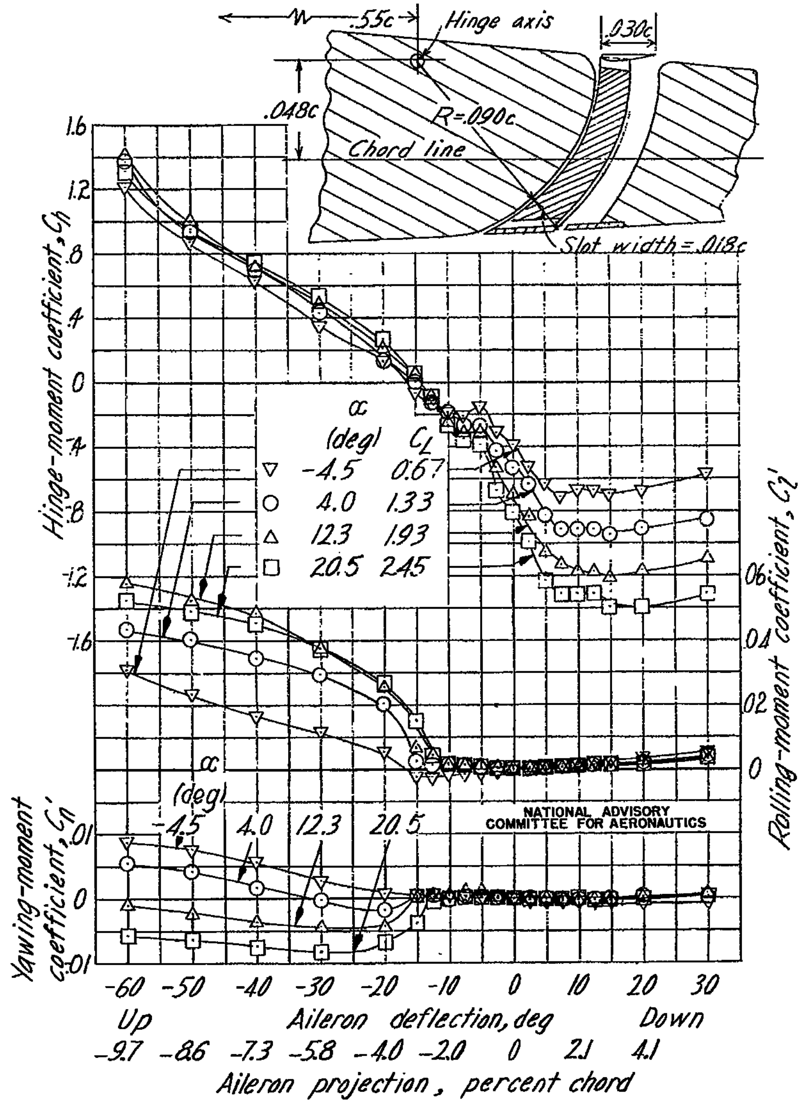

Figure B49.- Aileron characteristics of a 0.37 b/2 plug-type aileron on an NACA 23012 wing with a 0.20c full-span split flap deflected 60°. Arrangement A.

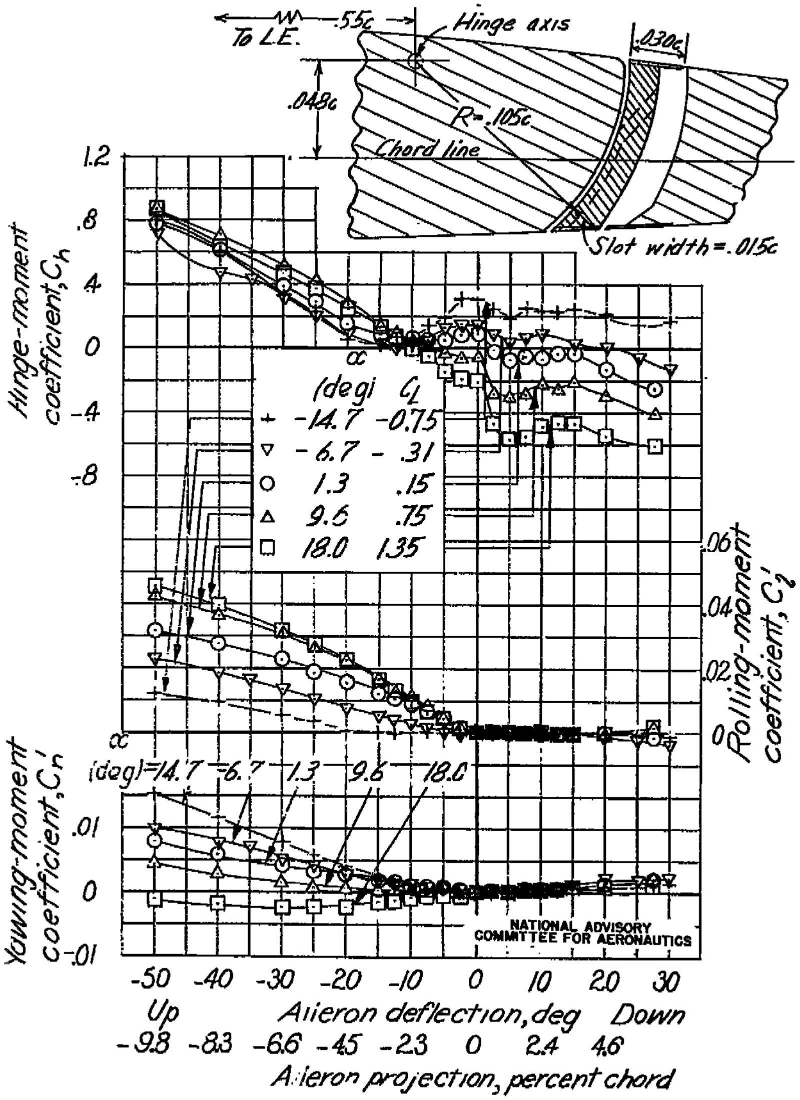

(a) Flap neutral.

Figure B50.- Aileron characteristics of a 0.37 b/2 plug-type aileron on an NACA 23012 wing with a 0.2566c full-span slotted flap. Arrangement B.

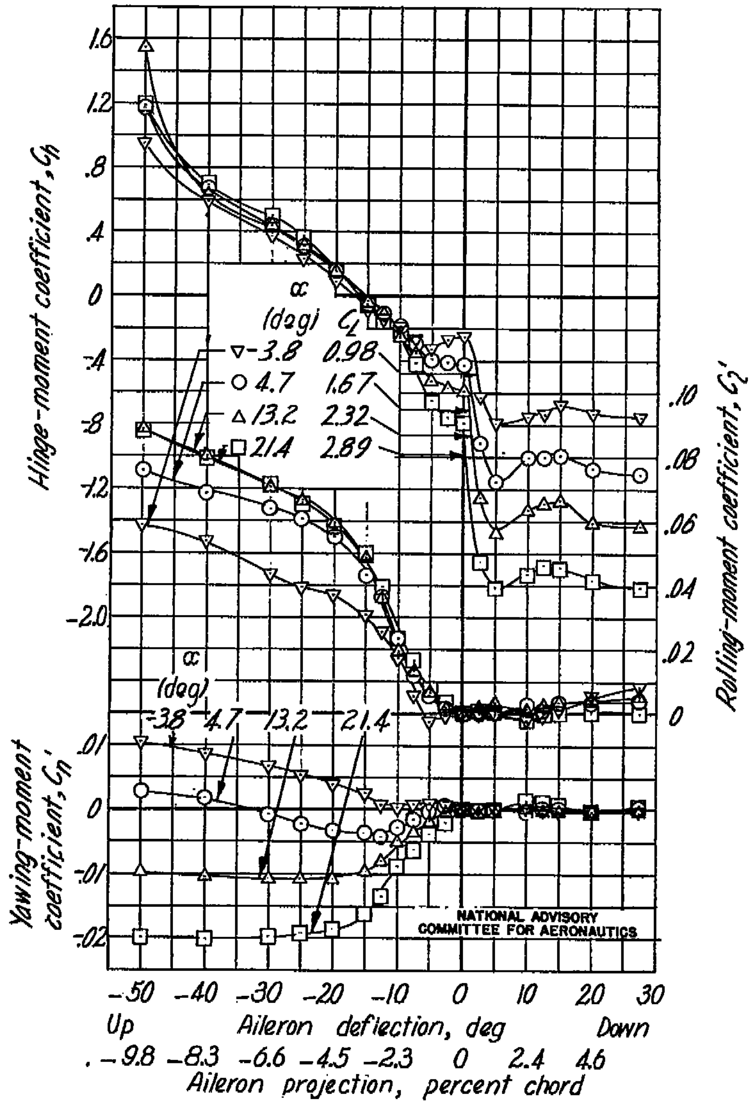

(b) Flap deflected 40°.

Figure B50.- Concluded.

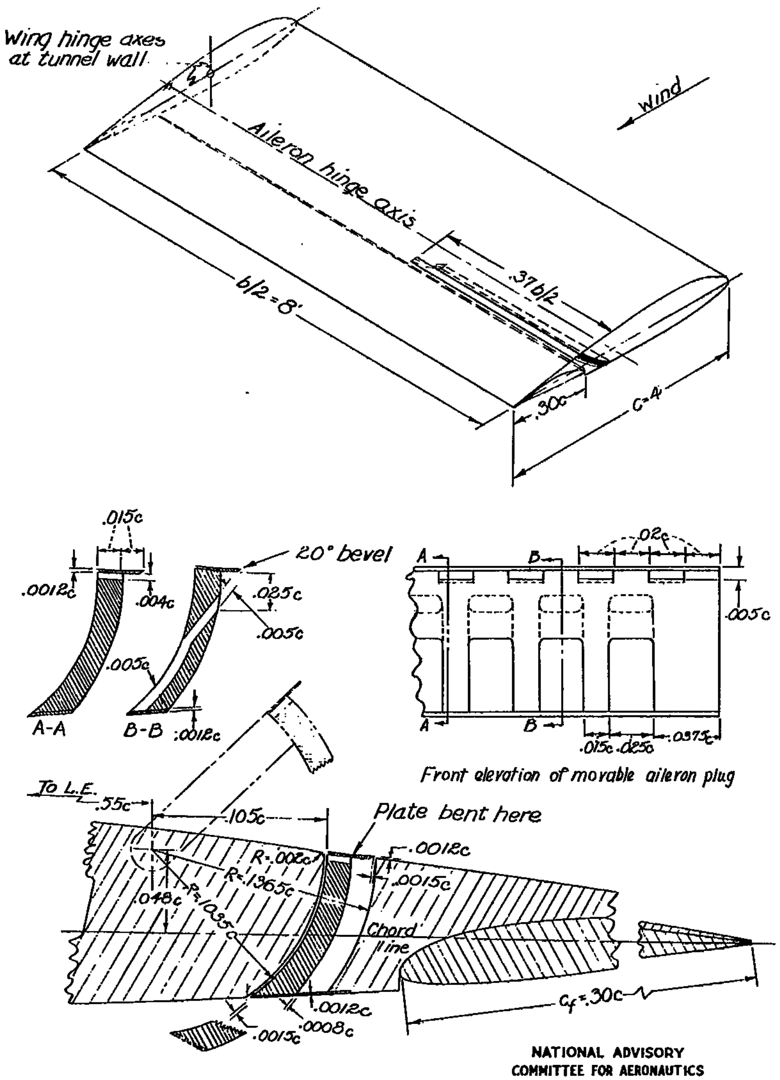

Figure B51.- Schematic diagram of model setup and details of the 0.37 b/2 plug-type aileron on a 4- by 8-foot semispan NACA 23012 wing with a 0.30c full-span Fowler flap.

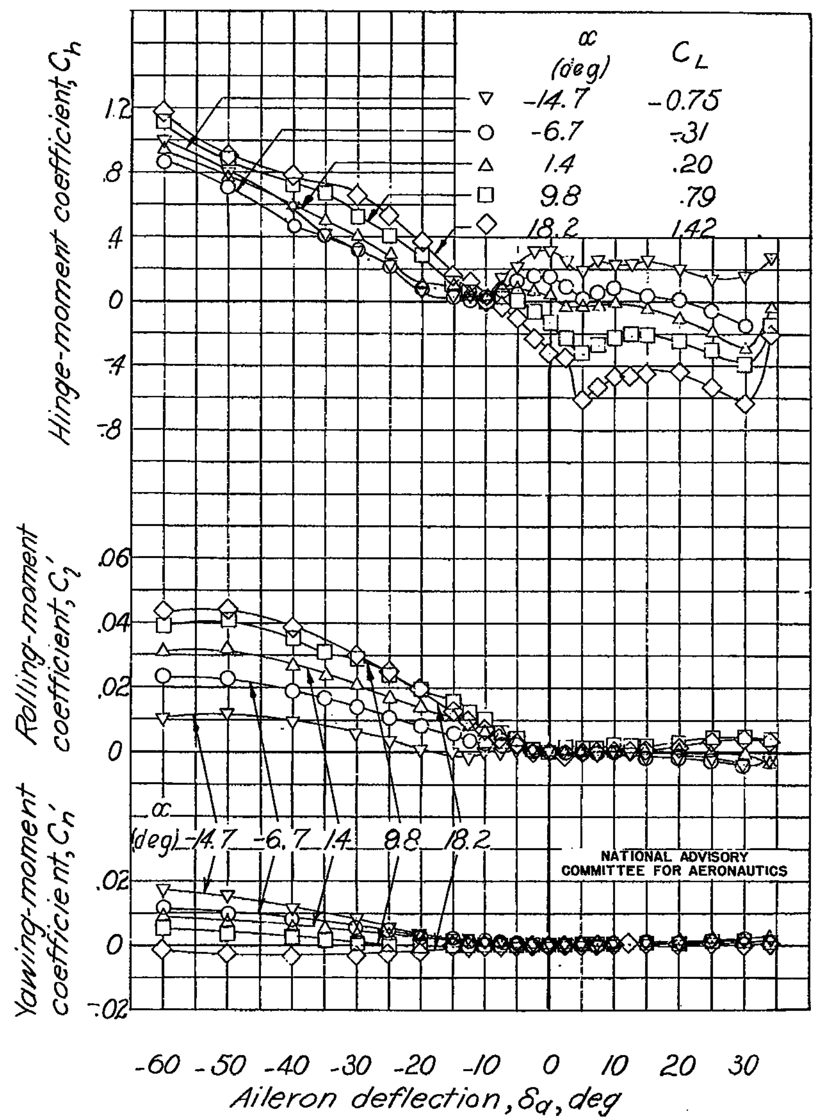

(a) Flap retracted.

Figure B52.- Aileron characteristics of a 0.37 b/2 plug-type aileron on an NACA 23012 wing with a 0.30c full-span Fowler flap.

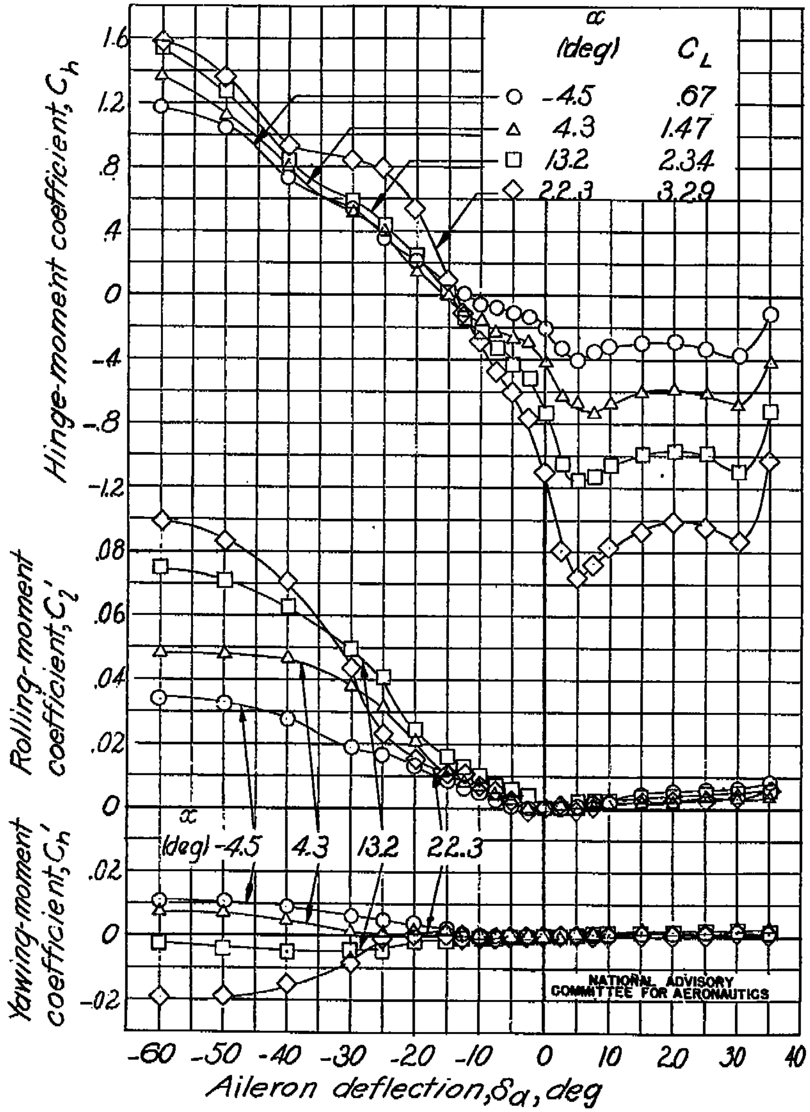

(b) Flap deflected 20°.

Figure B52.- Continued.

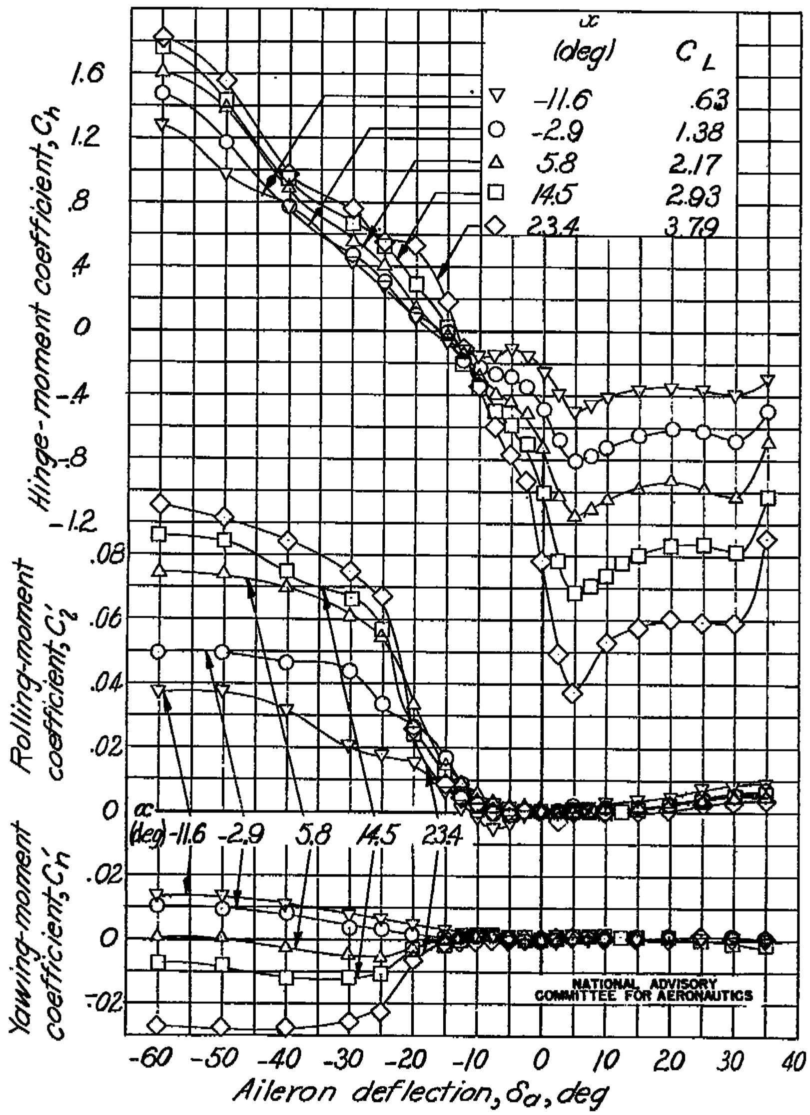

(c) Flap deflected 40°.

Figure B52.- Concluded.

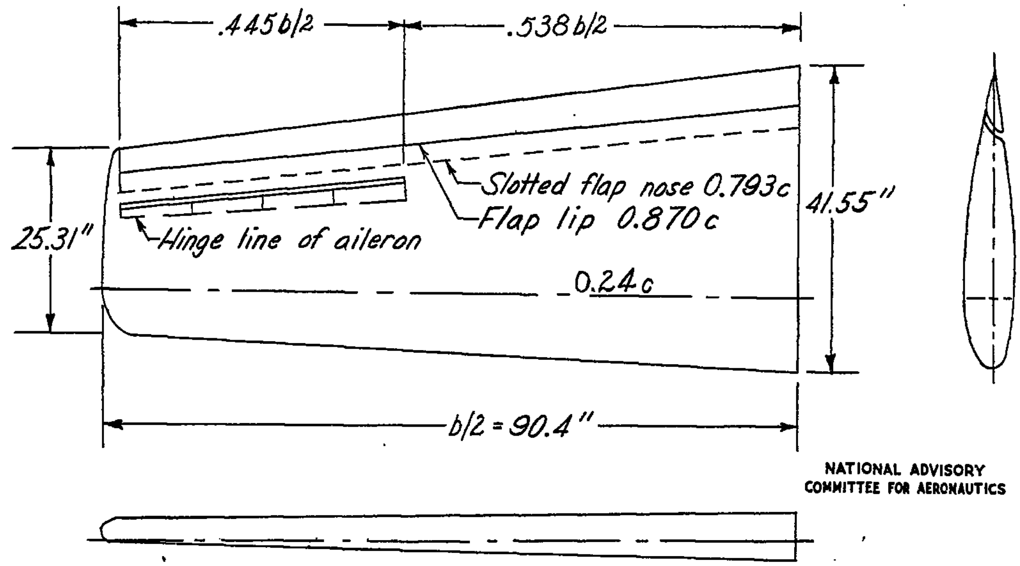

Figure B53.- The 0.4-scale model of a tapered semispan wing with a plug-type aileron and a full-span flap tested in the Langley 7- by 10-foot tunnel.

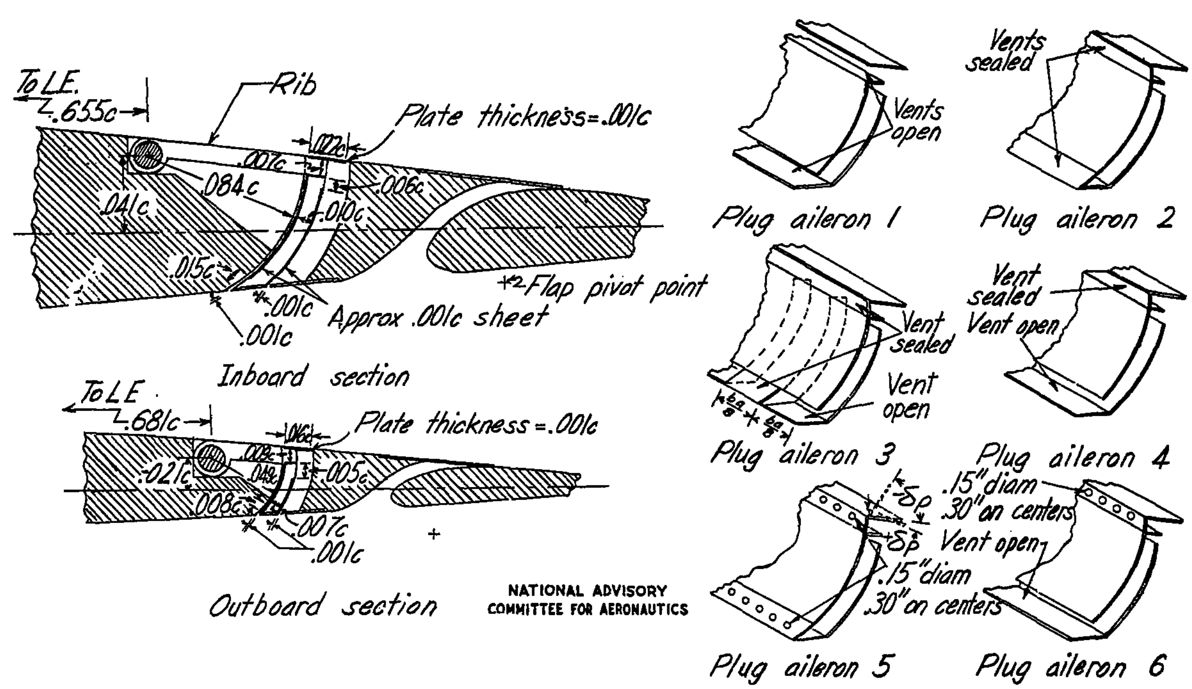

Figure B54.- Details of the plug aileron and various plug modifications on the tapered-wing model.

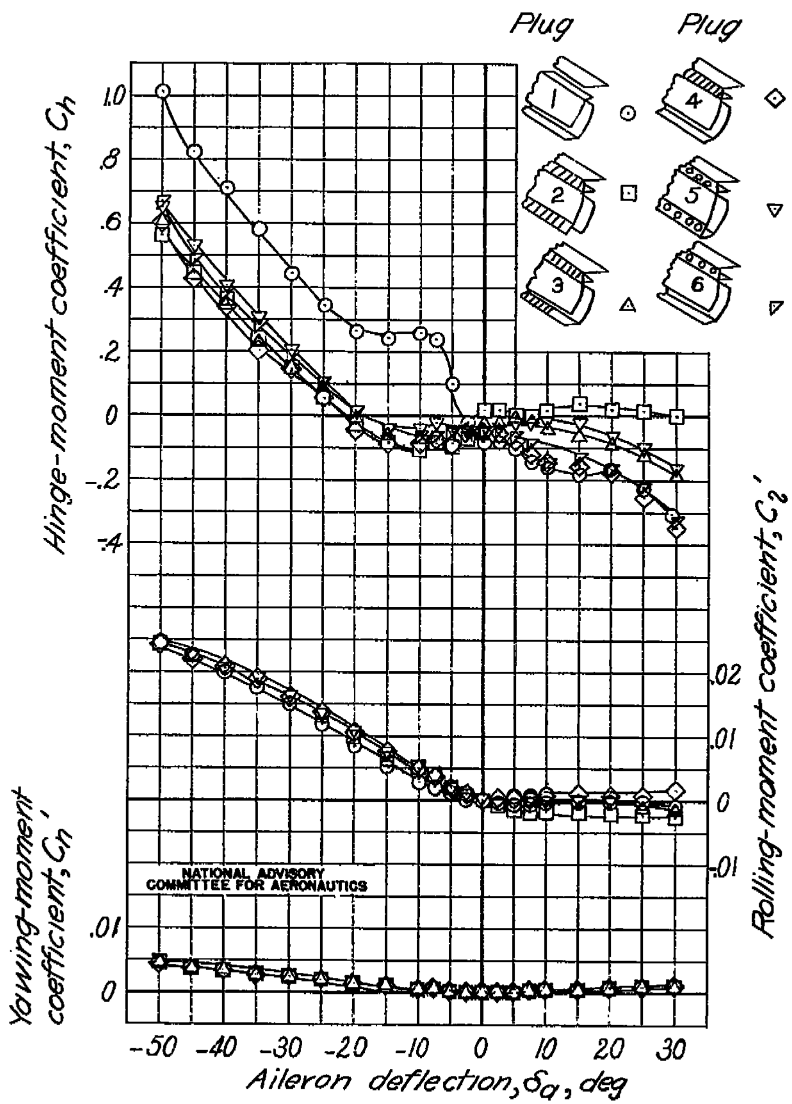

(a) α, 0.1°; C_L, 0.10.

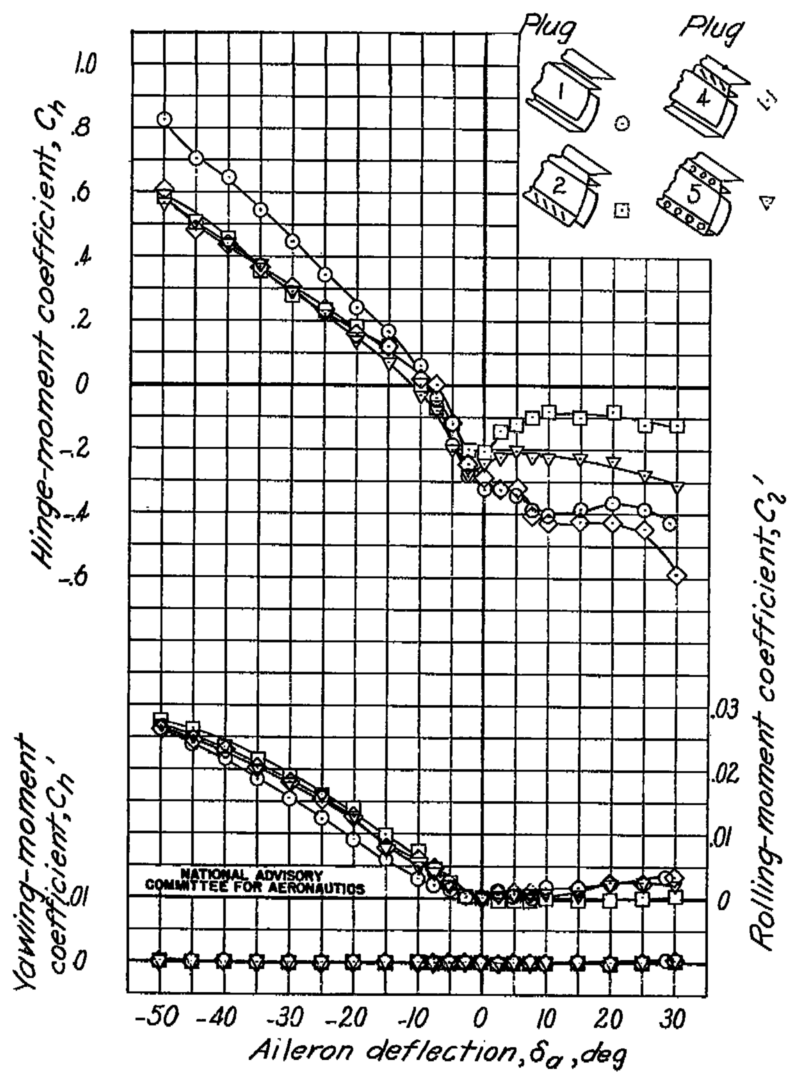

(b) α, 13.3°; C_L, 1.05.

Figure B55.- Rolling-, yawing-, and hinge-moment coefficients due to aileron deflection for various aileron modifications for the tapered wing model with a full-span flap and plug aileron; δ_p, 0°; δ_f, 0°.

Figure B55.- Concluded.

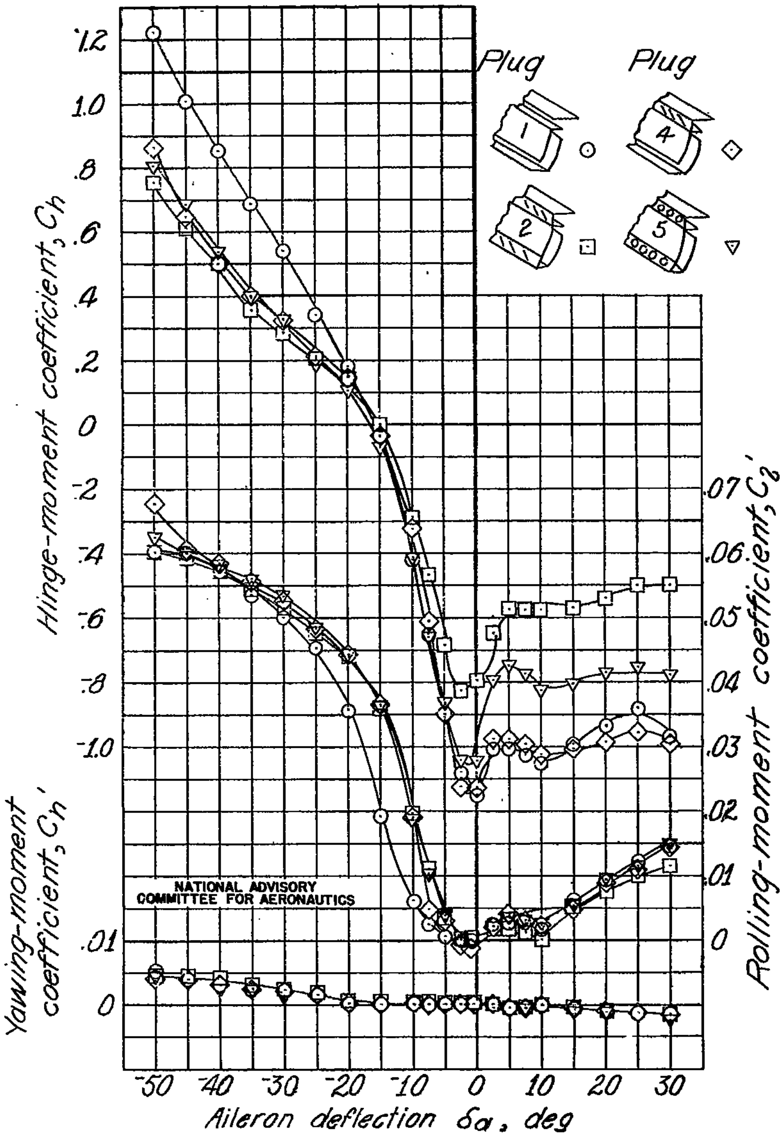

(a) α, 0.9°; C_L, 1.30.

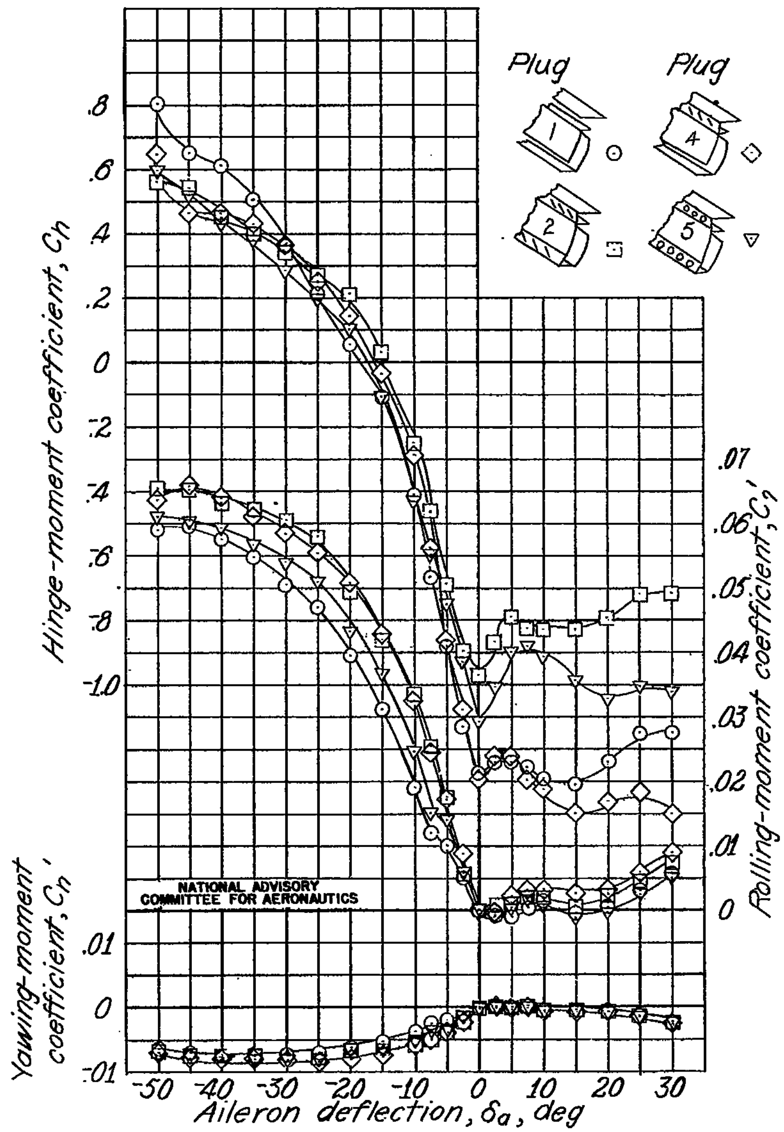

(b) α, 14.1°; C_L, 2.21.

Figure B56.- Rolling-, yawing-, and hinge-moment coefficients due to aileron deflection for various aileron modifications for the tapered-wing model with a full-span flap and plug aileron; δ_p, 0°; δ_f, 40°.

Figure B56.- Concluded.

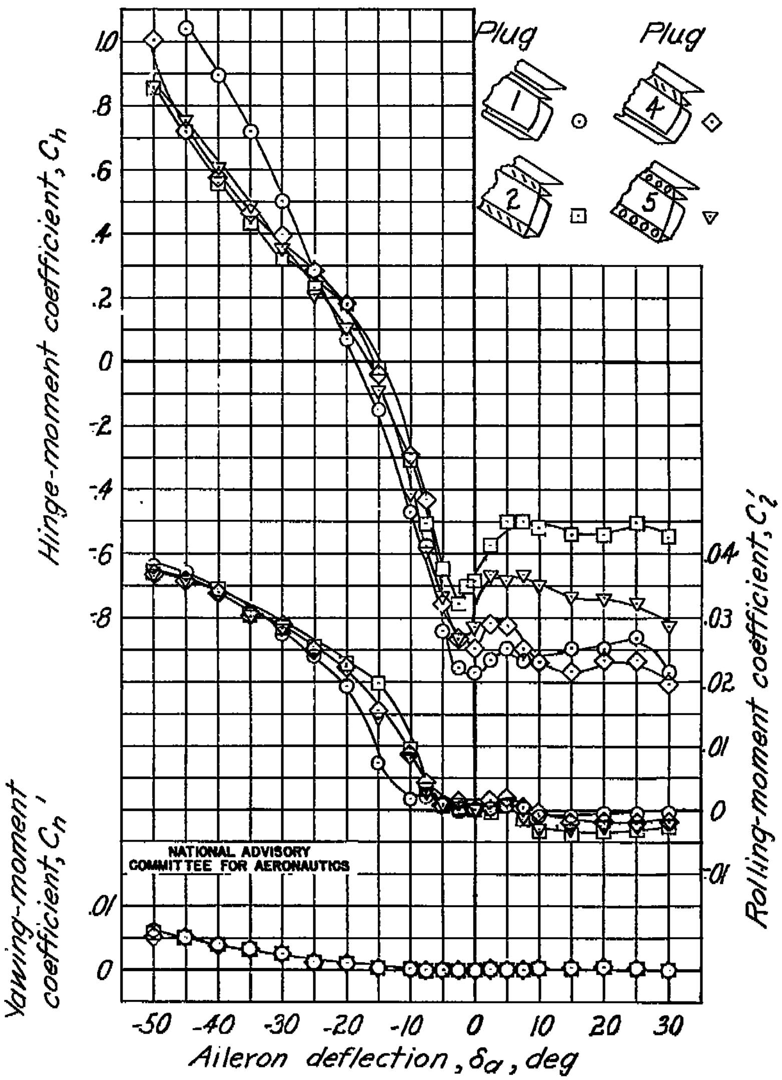

(a) α, 0.8°; C_L, 1.16.

Figure B57.- Rolling-, yawing-, and hinge-moment coefficients due to aileron deflection for various aileron modifications for the tapered-wing model with a full-span flap and plug aileron; δ_p, 0°; δ_f, 50°.

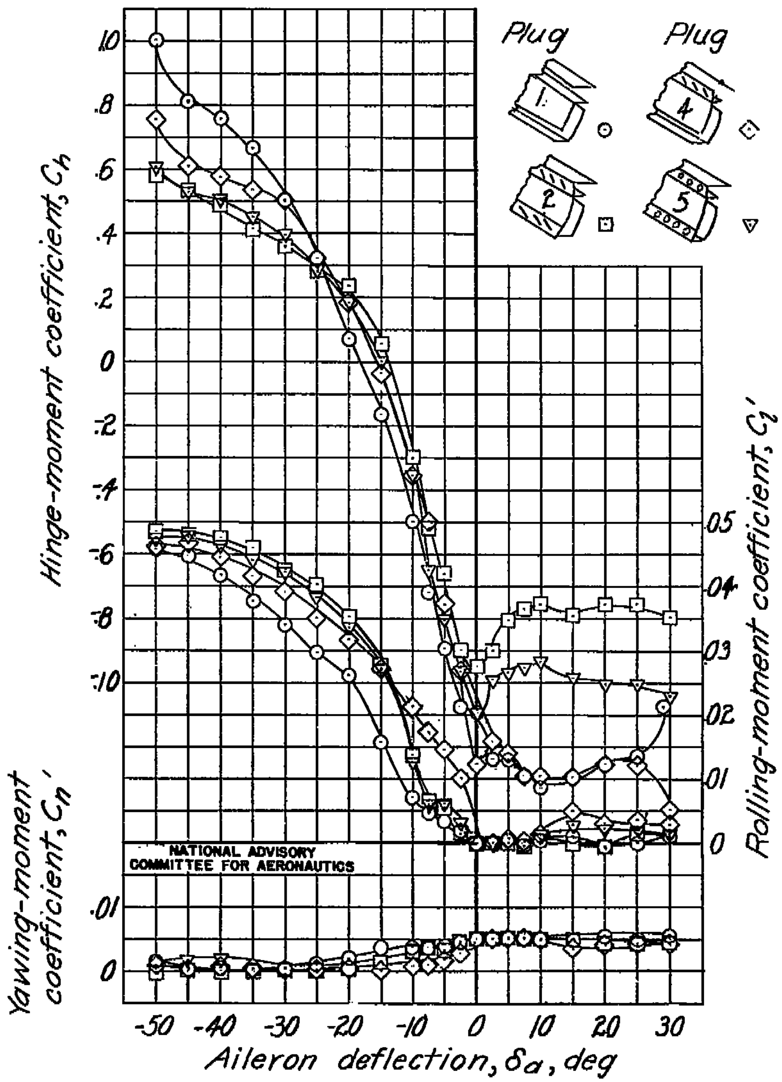

(b) α, 14.1°; C_L, 2.11.

Figure B57.- Concluded.

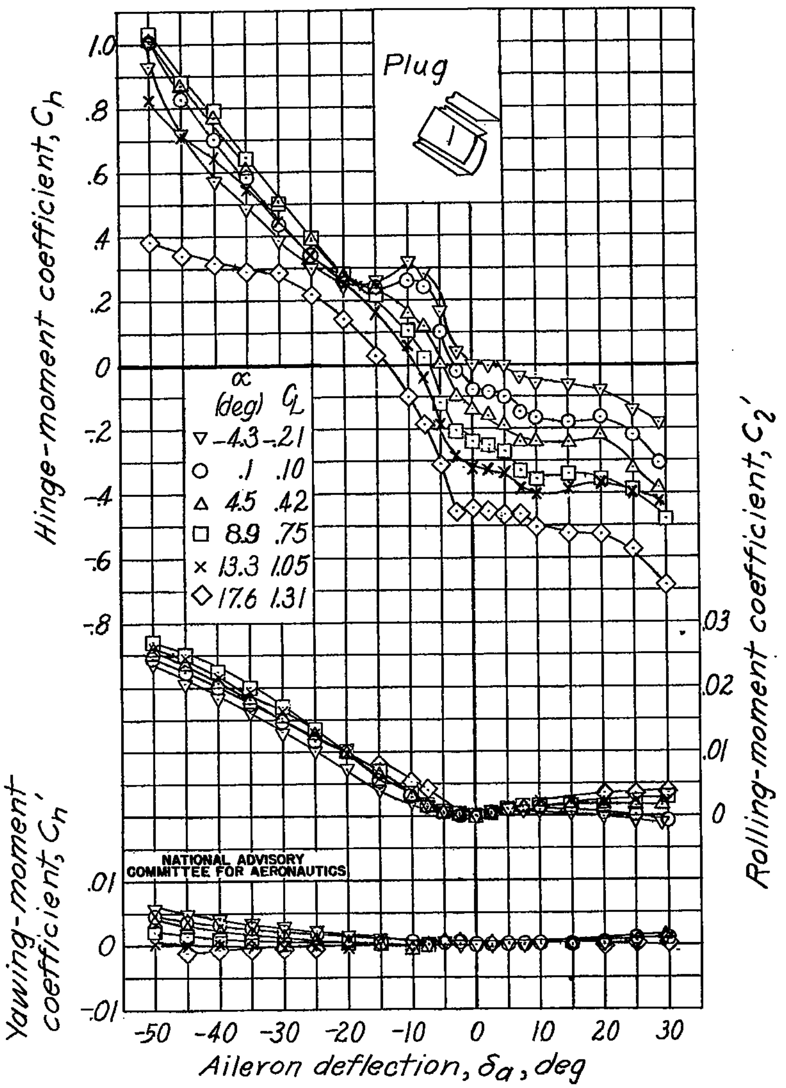

(a) δ_f, 0°.

Figure B58.- Rolling-, yawing-, and hinge-moment coefficients due to aileron deflection at various angles of attack for the tapered-wing model with a full-span flap and plug aileron 1; δ_p, 0°.

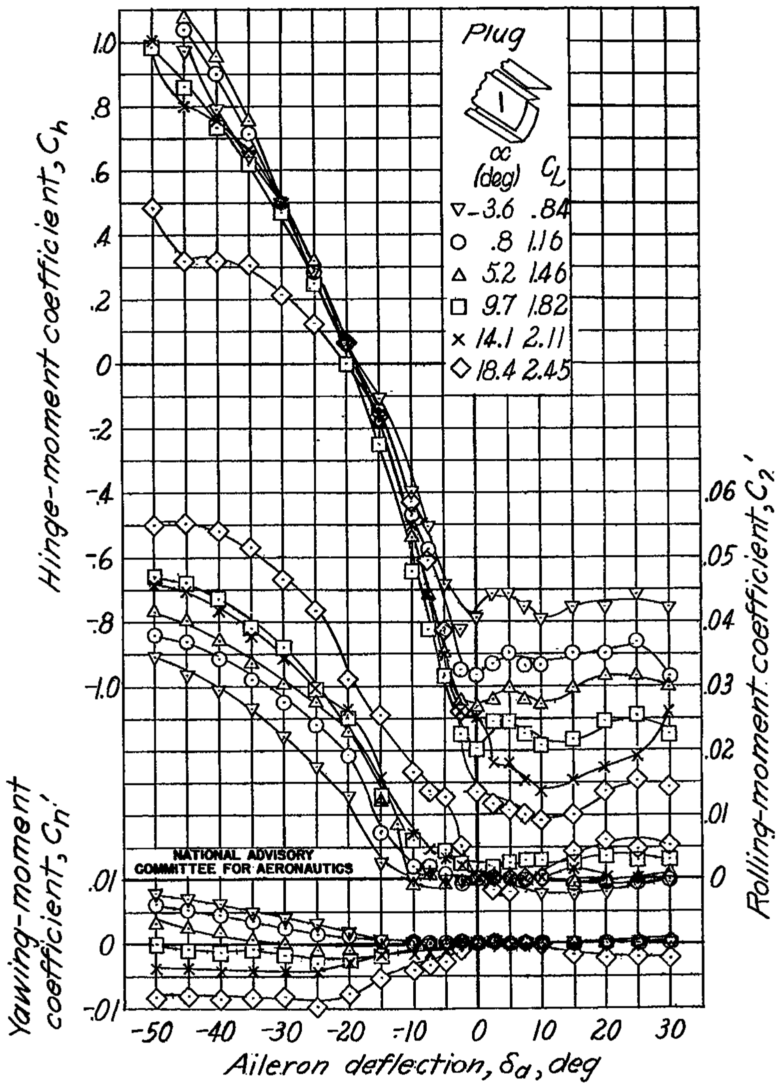

(b) δ_f, 50°.

Figure B58.- Concluded.

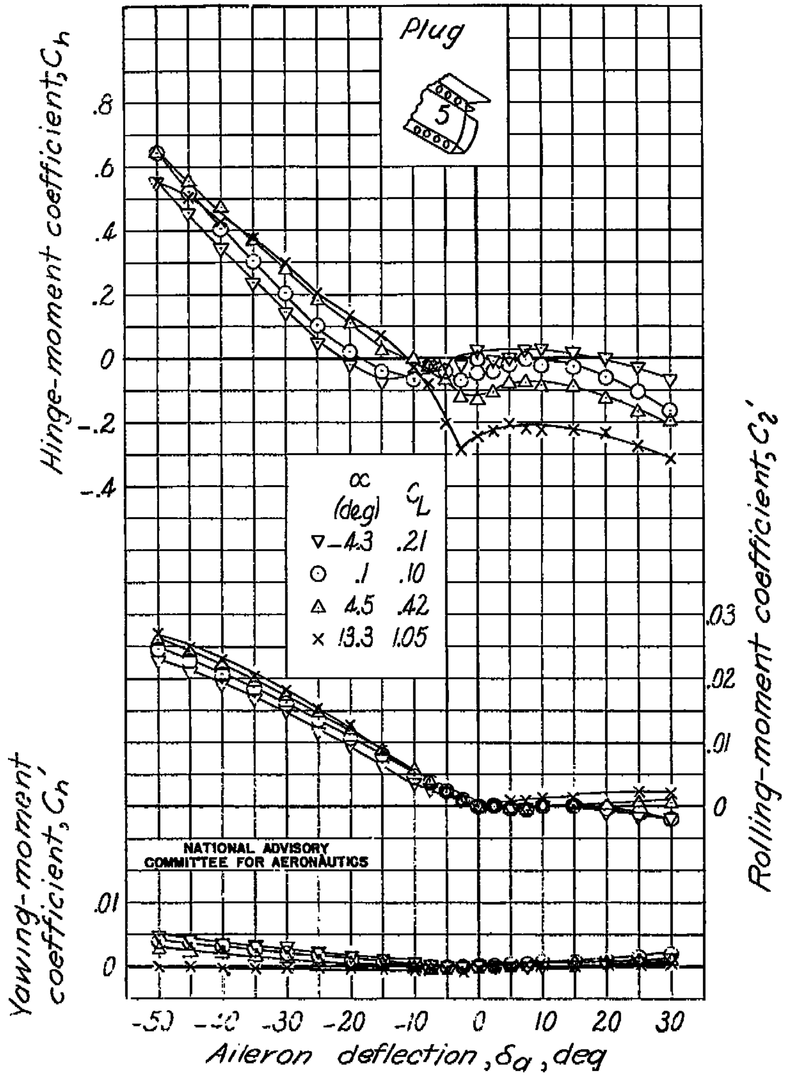

(a) δ_f, 0°.

Figure B59.- Rolling-, yawing-, and hinge-moment coefficients due to aileron deflection at various angles of attack for the tapered-wing model with a full-span flap and plug aileron 5; δ_p, 0°.

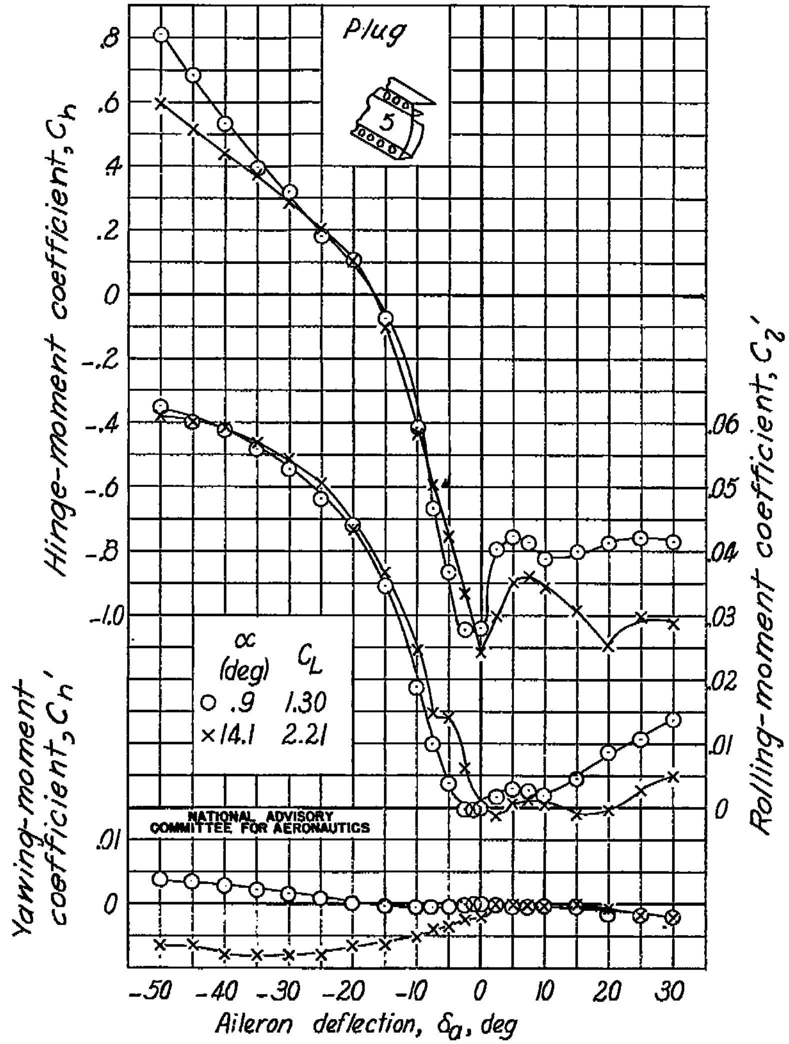

(b) δ_f, 40°.

Figure B59.- Concluded.

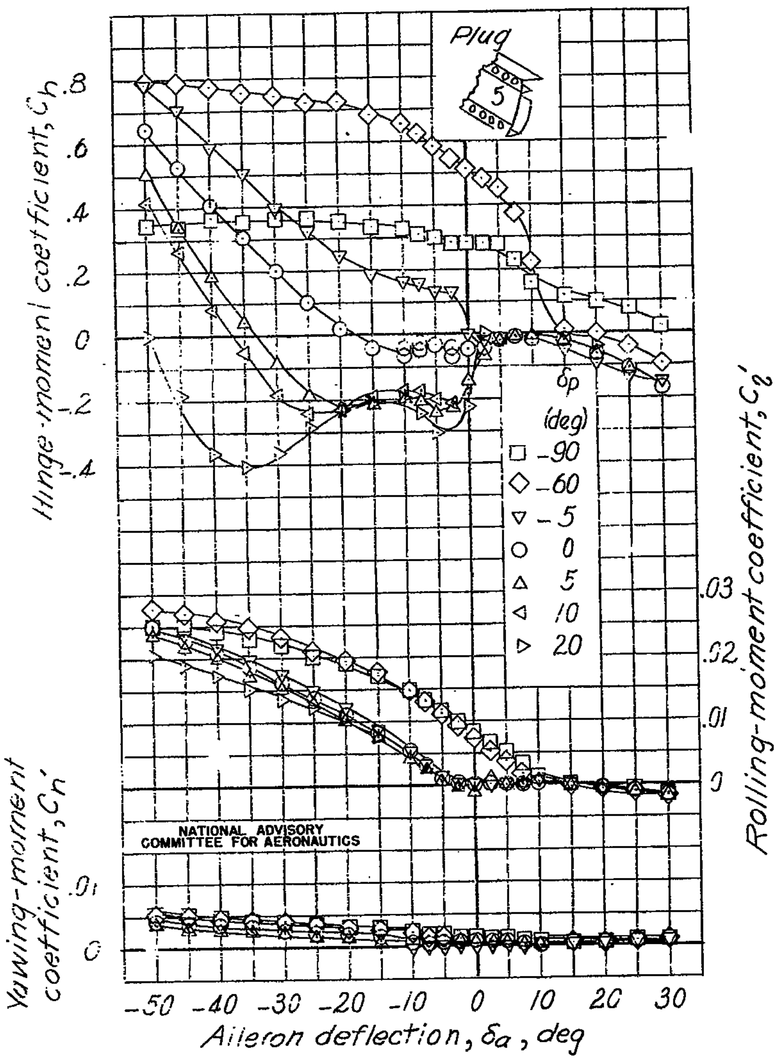

(a) α, 0.1°; C_L, 0.10.

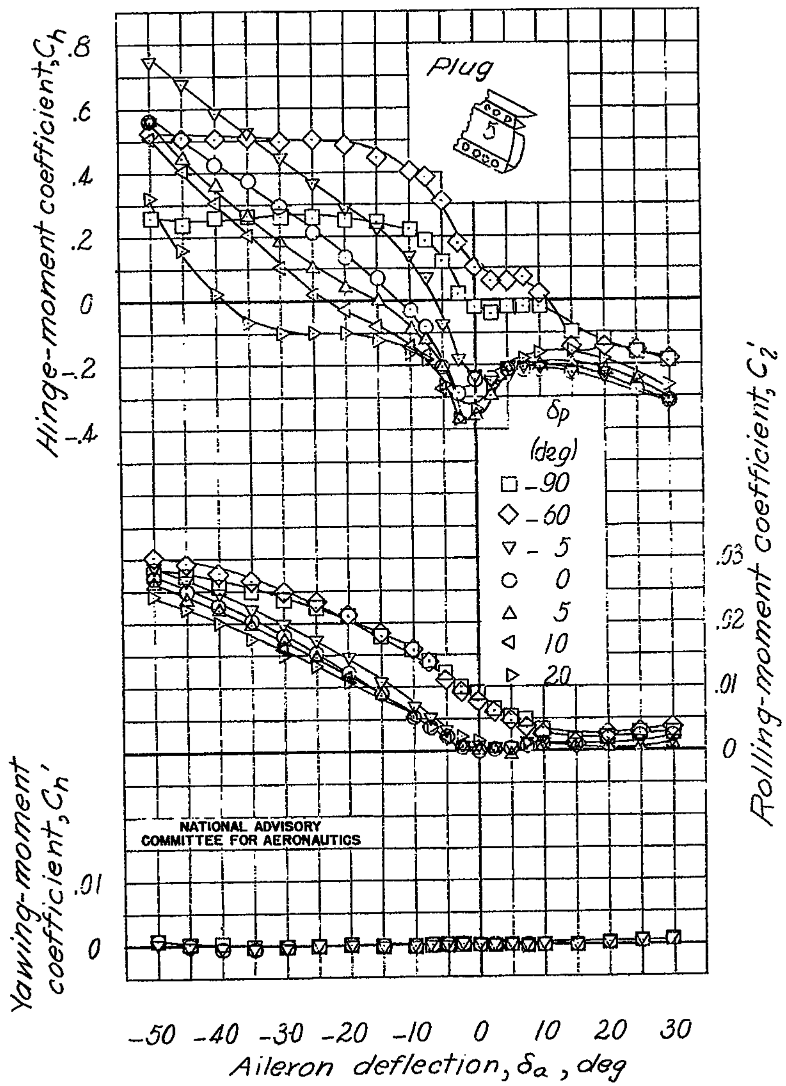

(b) α, 13.3°; C_L, 1.05.

Figure B6[illegible].- Rolling-, yawing-, and hinge-moment coefficients due to aileron deflection at various plate angles for the tapered-wing model with a full-span flap and plug aileron 5; δ_f, 0°.

Figure B60.- Concluded.

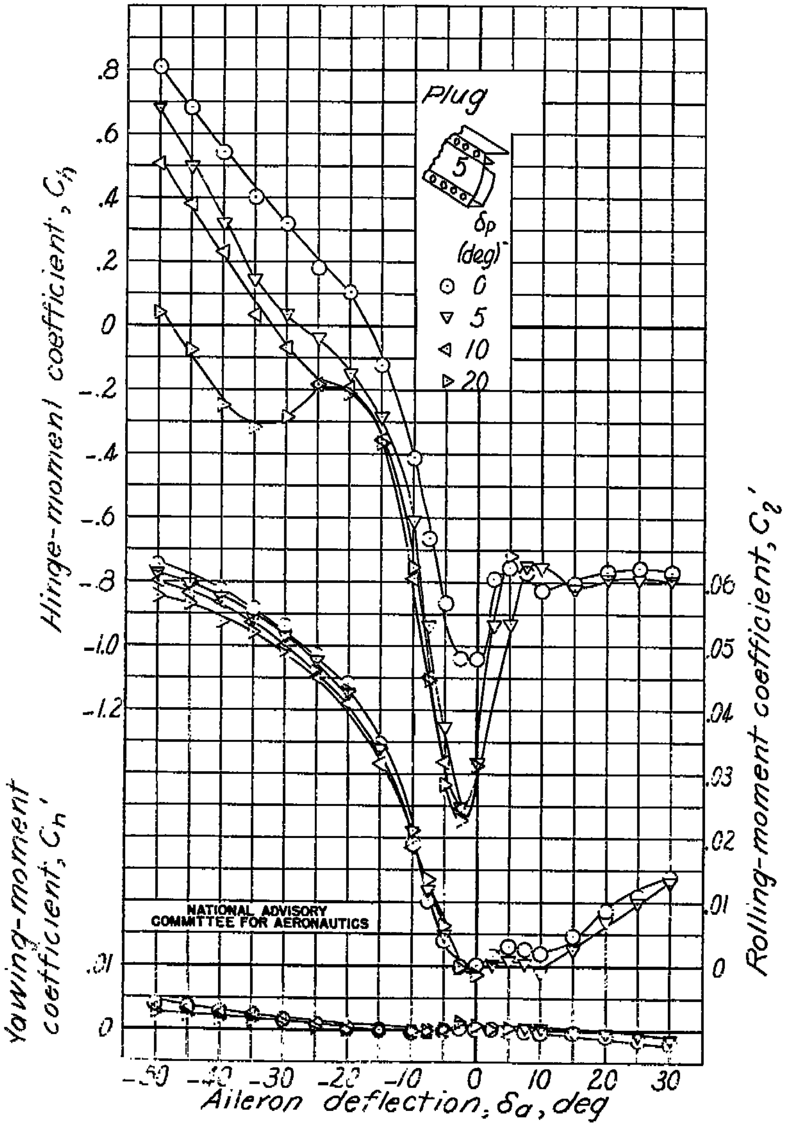

(a) α, [illegible]°; C_L, 1.30.

Figure B61.- Rolling-, yawing-, and hinge-moment coefficients due to aileron deflection at various plate angles for the tapered-wing model with a full-span flap and plug aileron 5; δ_f, 40°

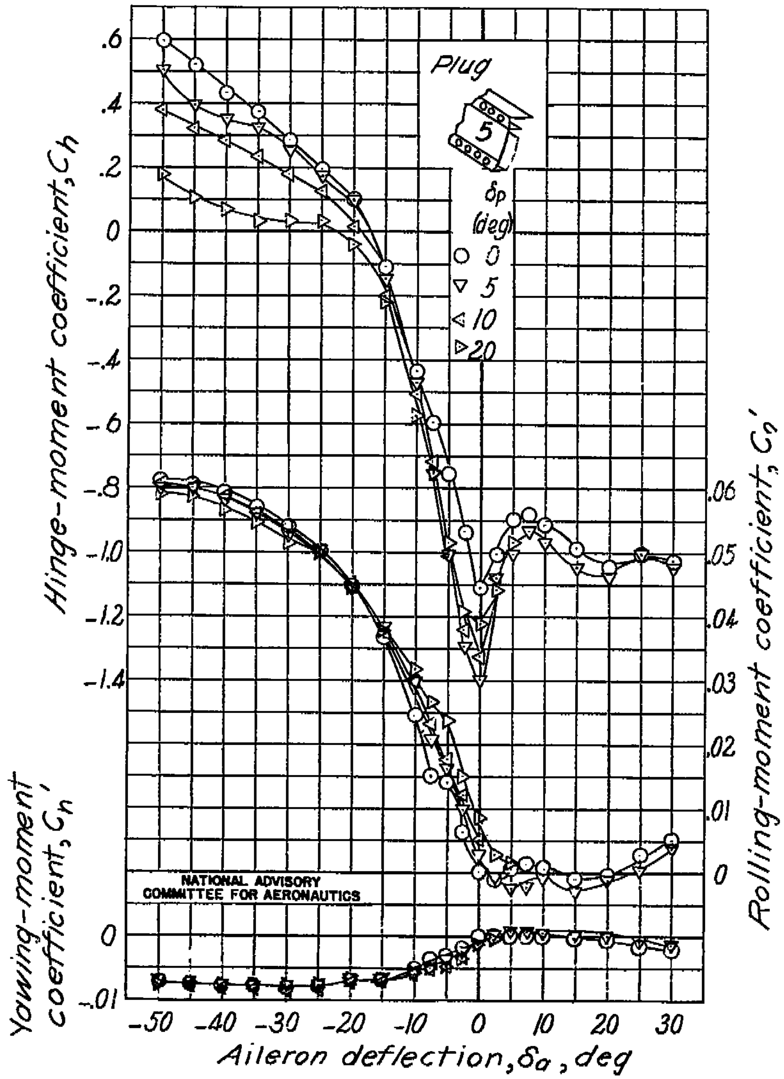

(b) α, 14.1°; C_L, 2.21.

Figure B61.- Concluded.

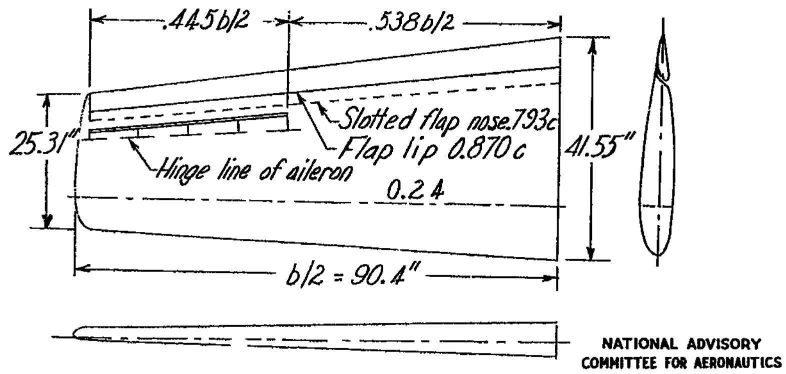

Figure B62.- The 0.4-scale model of a tapered semispan wing with a plug-type aileron and a full-span flap tested in the Langley 7- by 10-foot tunnel.

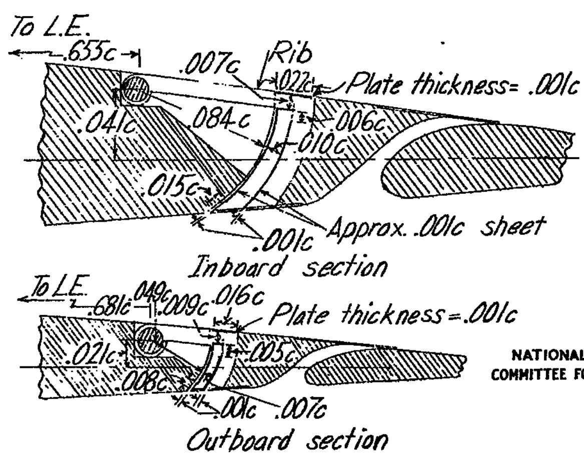

Figure B63.- Details of the plug aileron on the tapered-wing model.

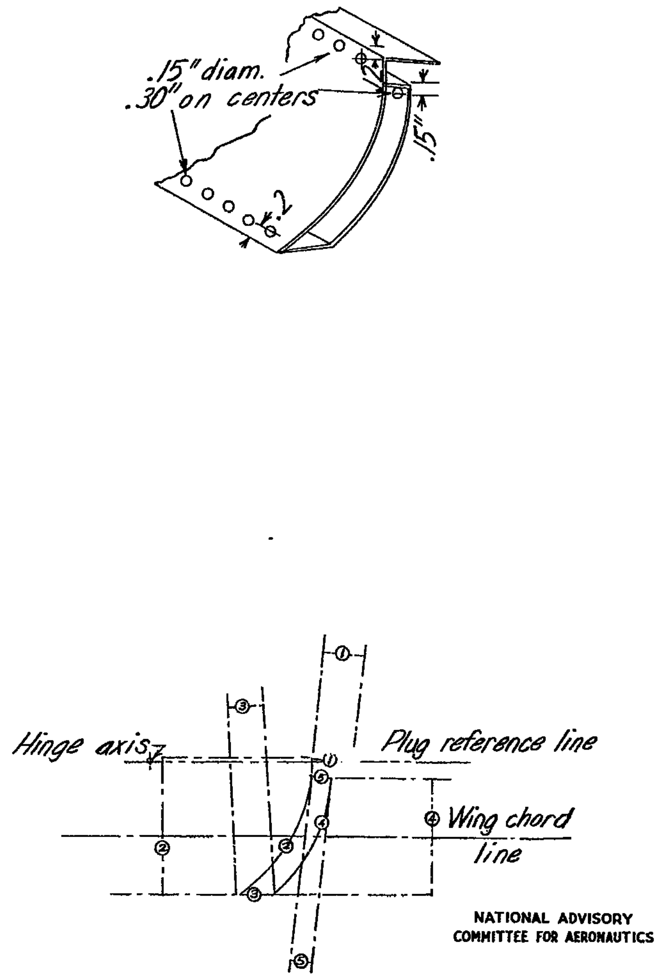

Figure B64.- Details of modified plug 5 of the plug aileron; and plate designation and pressure axes layout of plug aileron.

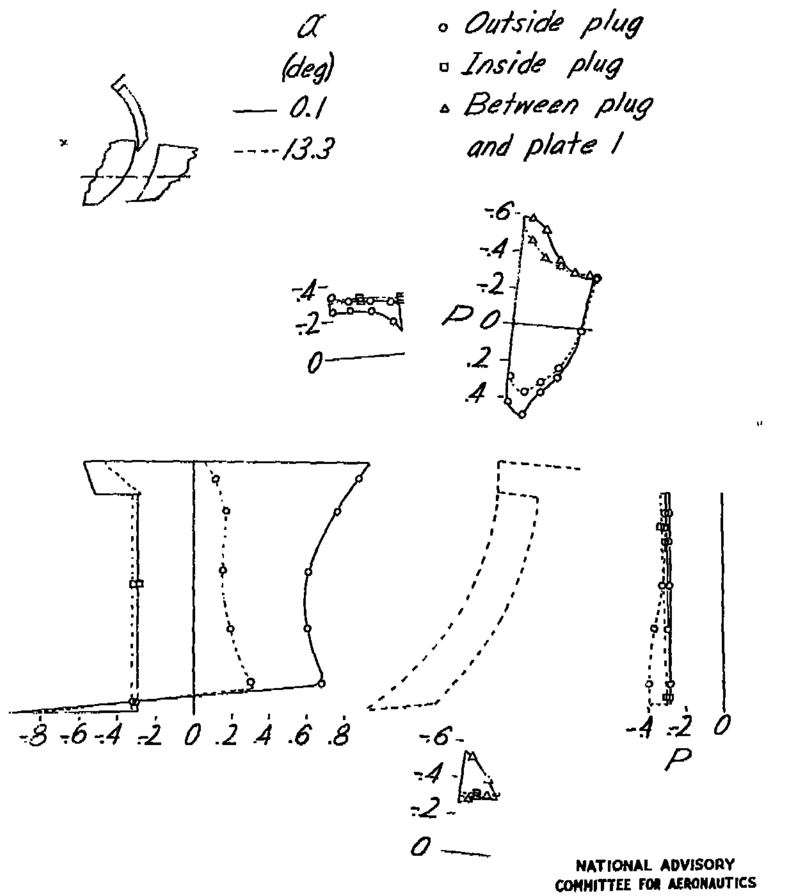

(a) δ_a, -50°.

Figure B65.- Pressure distribution on plug aileron 5 on the tapered-wing model with a full-span slotted flap; δ_f, 0°.

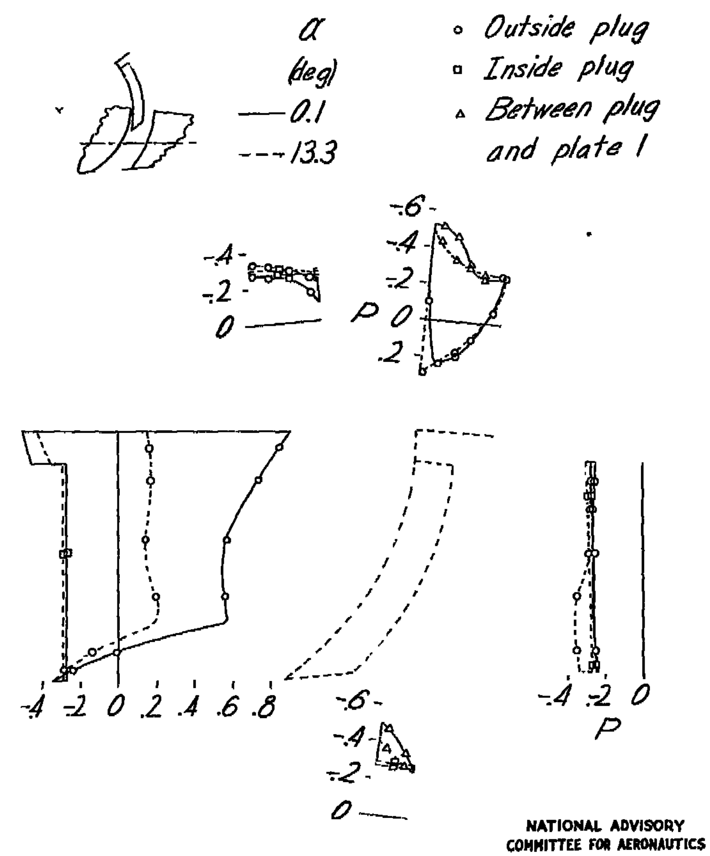

(b) δ_a, -40°.

Figure B65.- Continued.

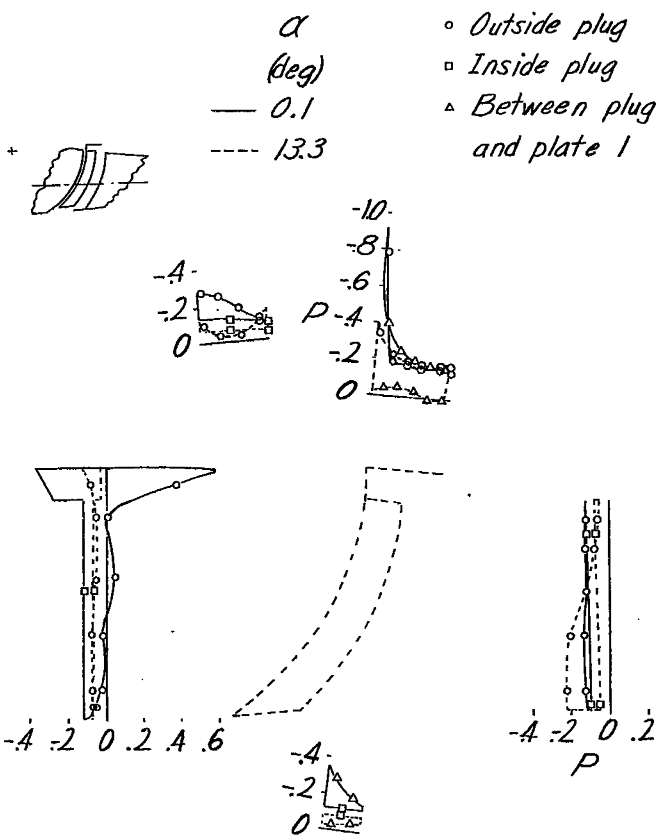

NATIONAL ADVISORY COMMITTEE FOR AERONAUTICS

(c) δ_a, -5°.

Figure B65.- Continued.

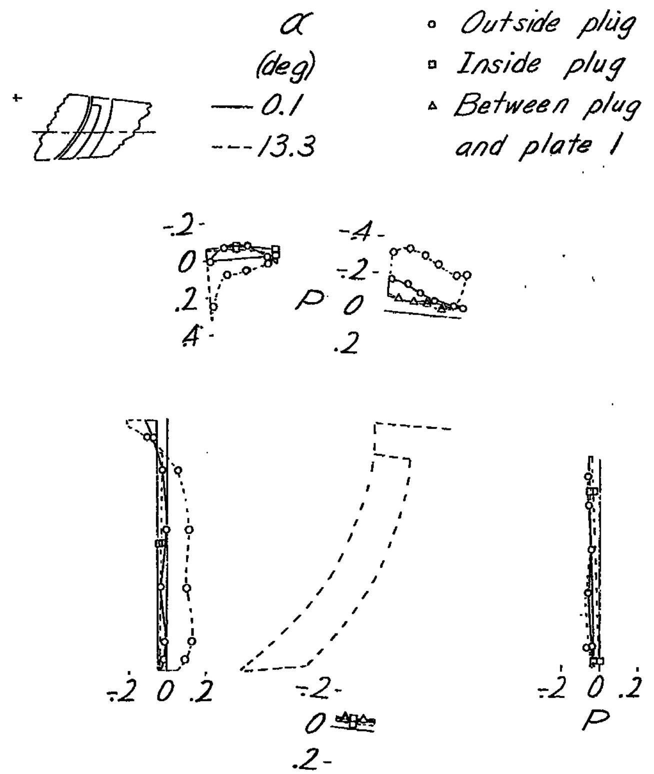

NATIONAL ADVISORY COMMITTEE FOR AERONAUTICS

(d) δ_a, 0°.

Figure B65.- Continued.

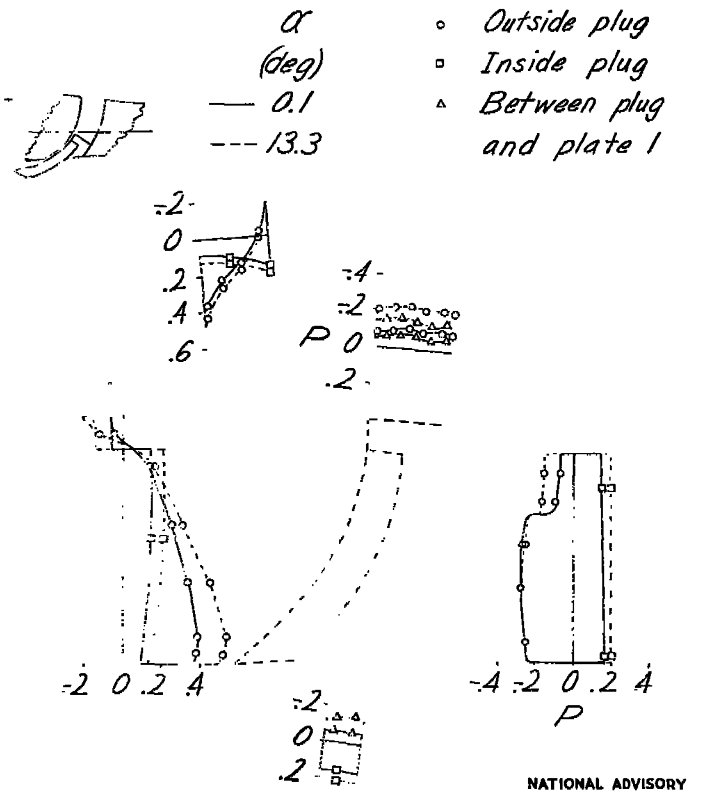

(e) δ_a, 30°.

Figure B65.- Concluded.

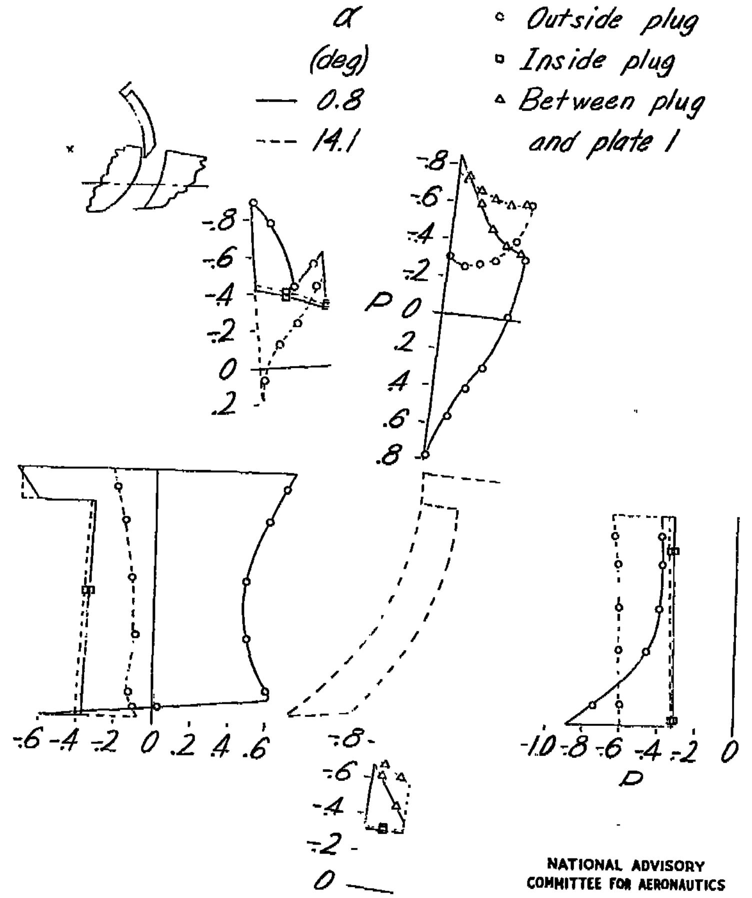

(a) δ_a, -50°.

Figure B66.- Pressure distribution on plug aileron 5 on the tapered-wing model with a full-span slotted flap; δ_f, 40°.

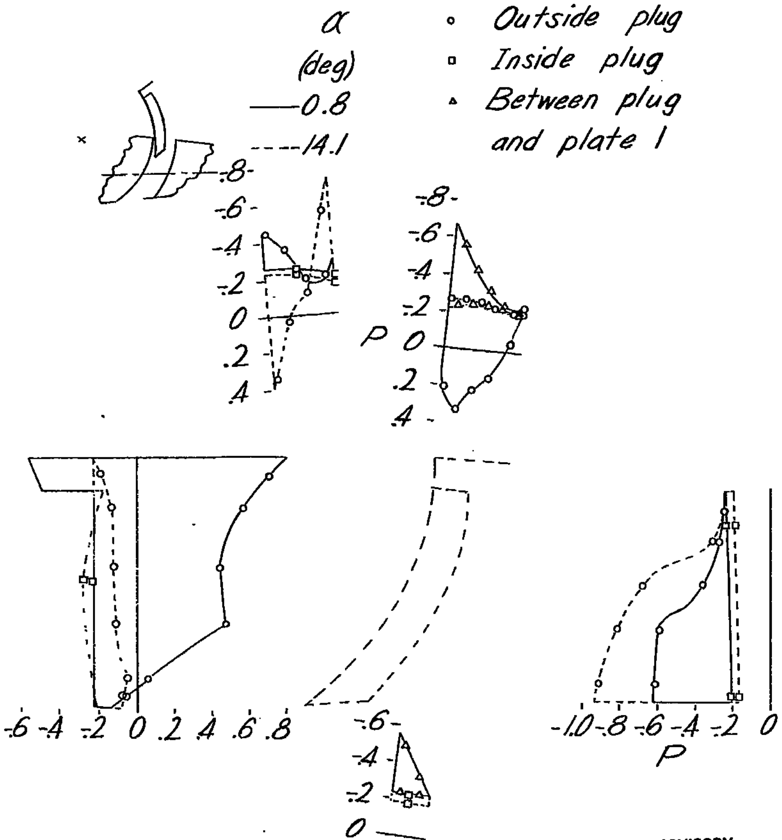

NATIONAL ADVISORY COMMITTEE FOR AERONAUTICS

(b) δ_a, -40°.

Figure B66.- Continued.

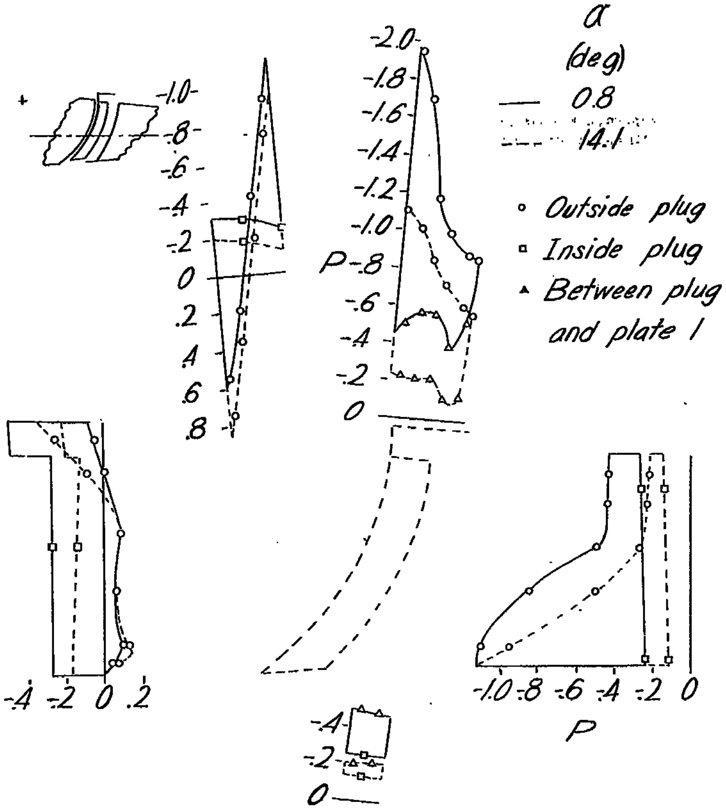

NATIONAL ADVISORY COMMITTEE FOR AERONAUTICS

(c) δ_a, -5°.

Figure B66.- Continued.

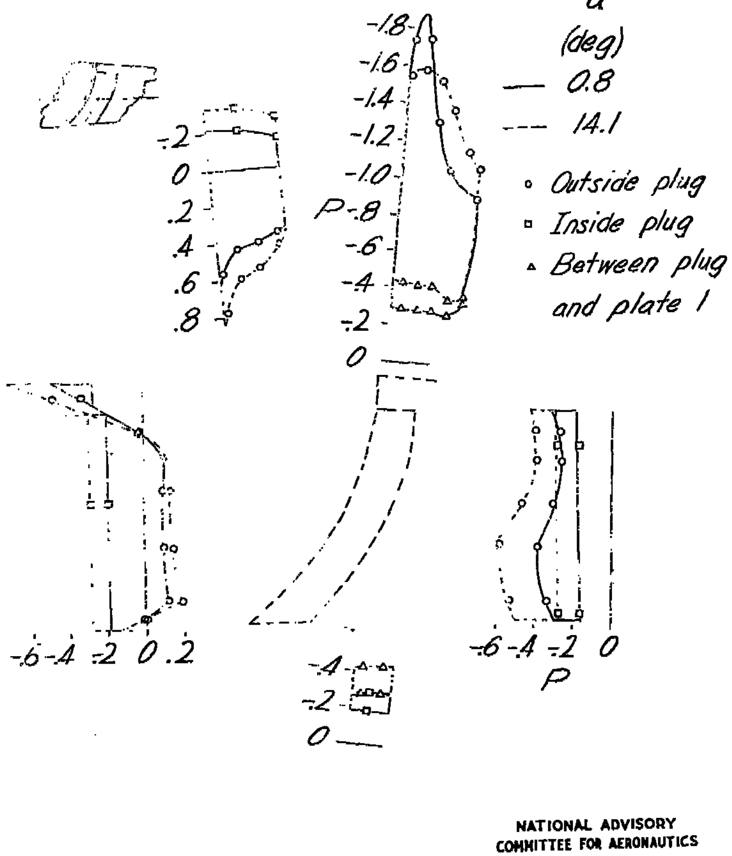

(d) δ_a, 0°.

Figure B66.- Continued.

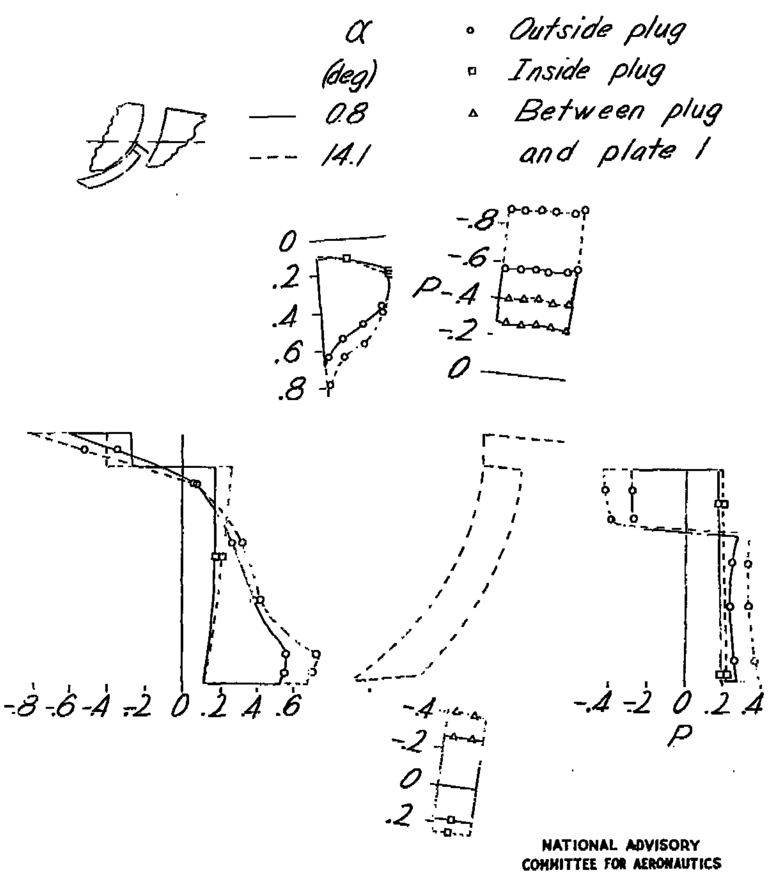

(e) δ_a, 30°.

Figure B66.- Concluded.

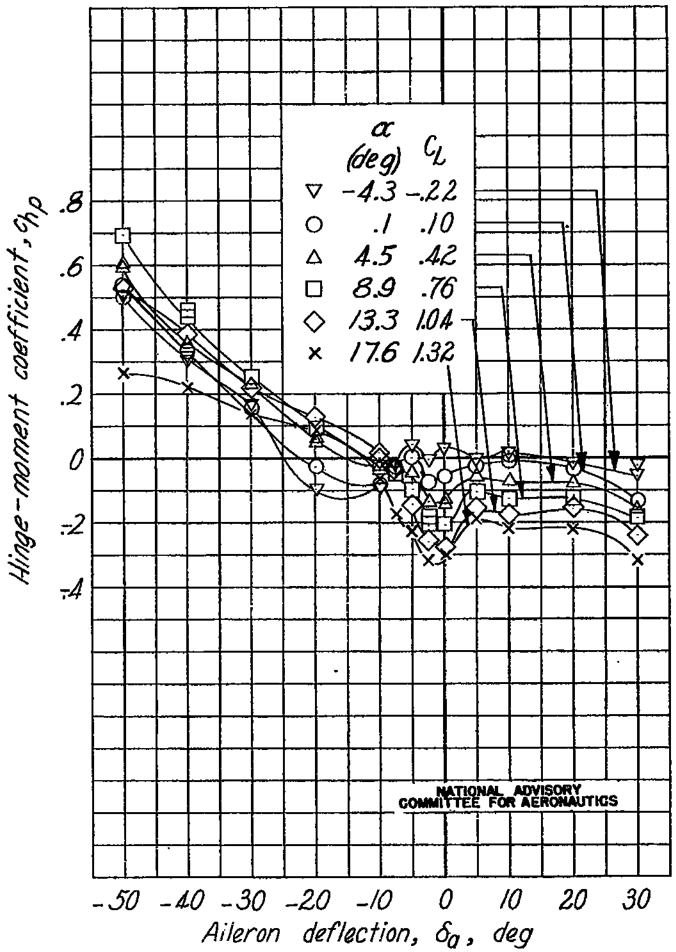

(a) δ_f, 0°.

Figure B67.- Plug aileron hinge-moment coefficient computed from pressure distribution data at a section 7.25 inches from inboard end of plug aileron 5; tapered-wing model with a full-span slotted flap.

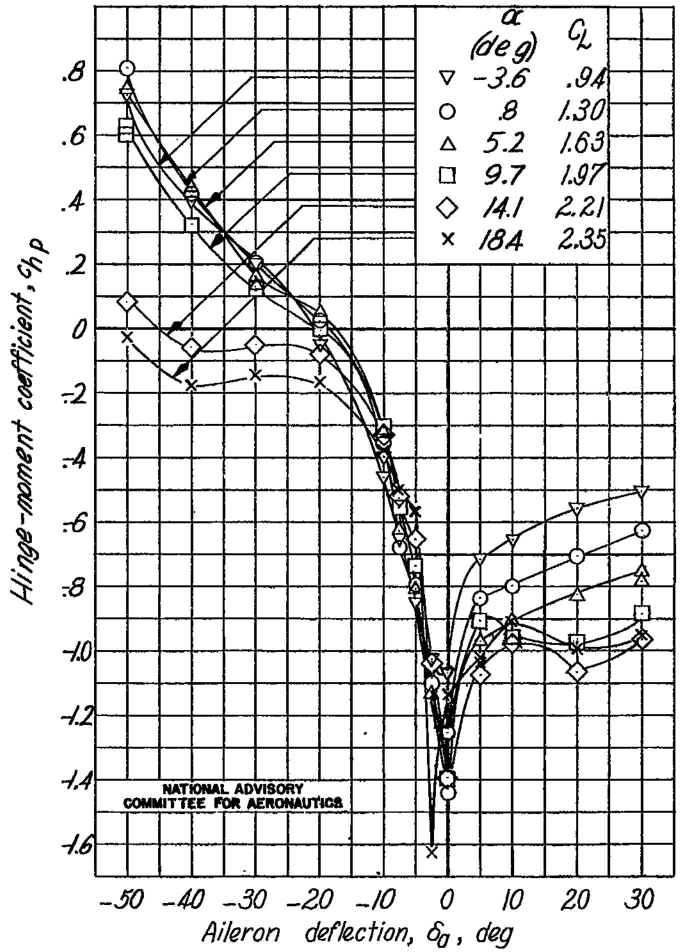

(b) δ_f, 40°.

Figure B67.- Concluded.

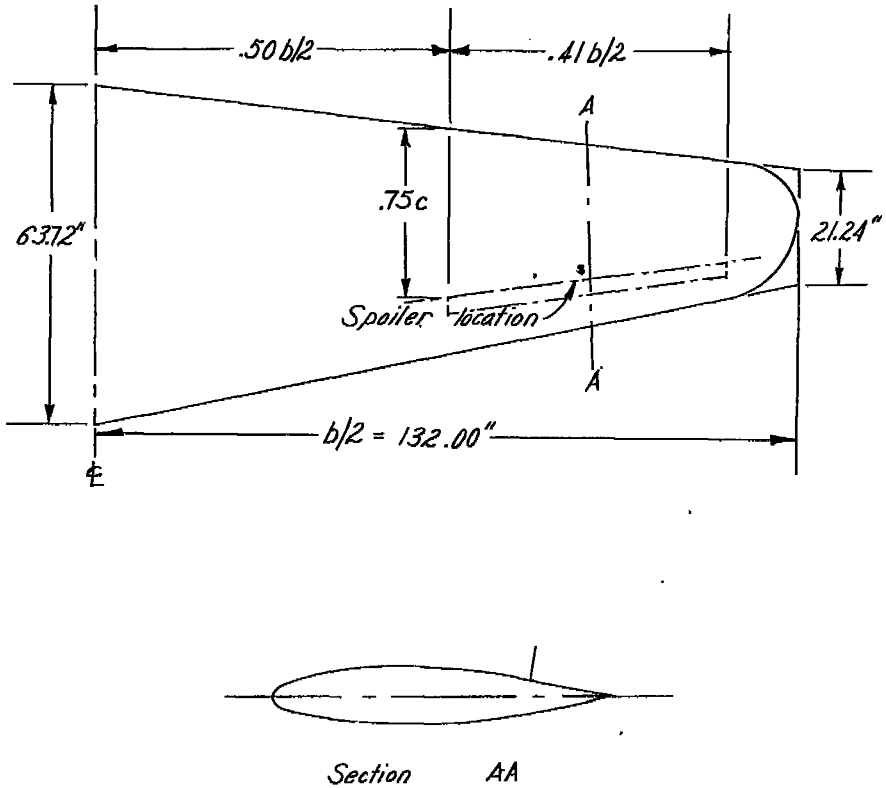

Figure B68.- Plan form and section of the 0.53-scale model of the semispan wing of a fighter-type airplane tested with spoiler ailerons in the Ames 16-foot high-speed tunnel.

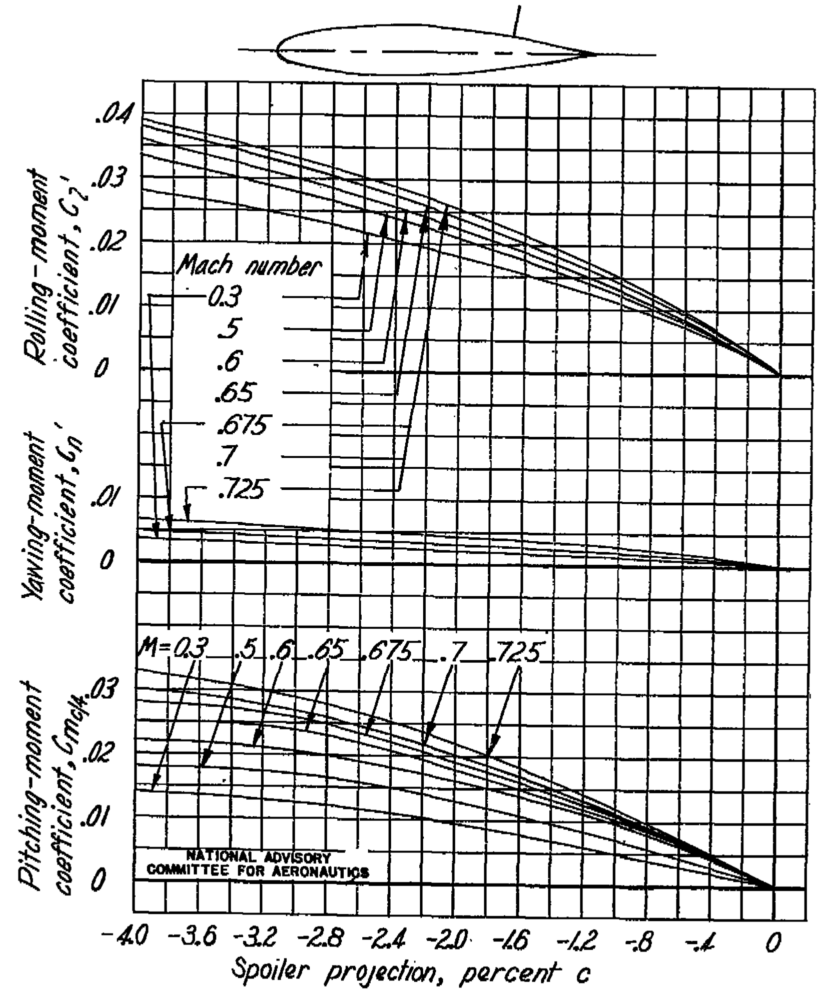

(a) C_L, -0.1.

Figure B69.- Variation of rolling-, yawing-, and pitching-moment characteristics with spoiler projection for the wing of a fighter-type airplane.

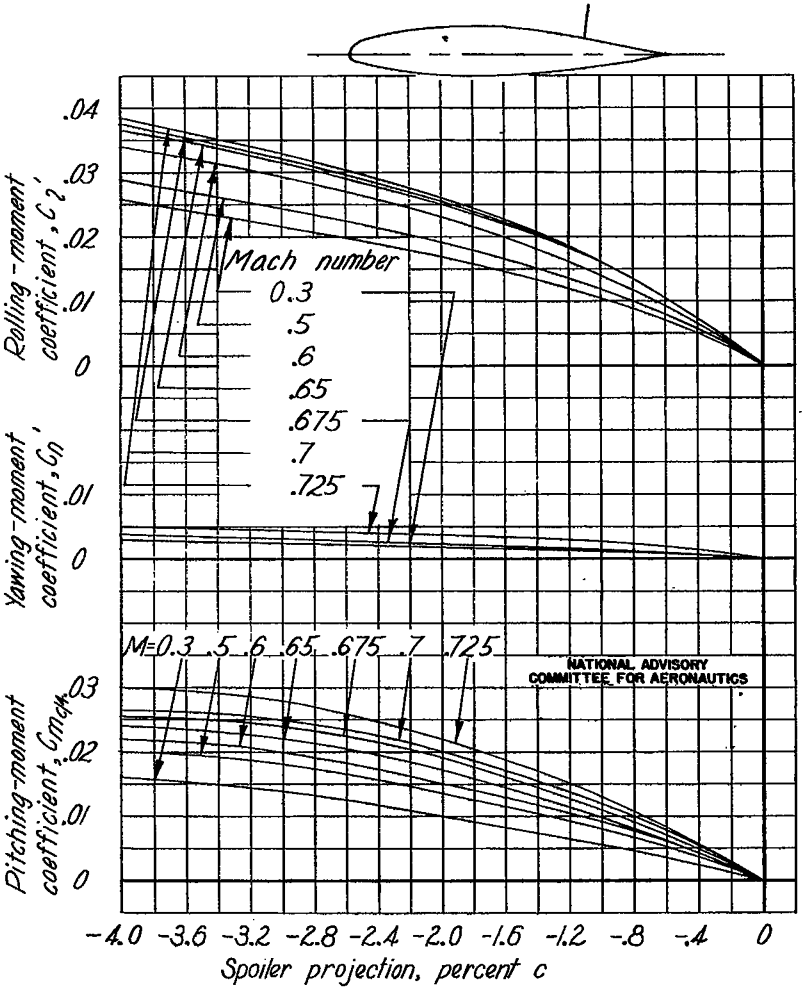

(b) C_L, 0.1.

Figure B69.- Continued.

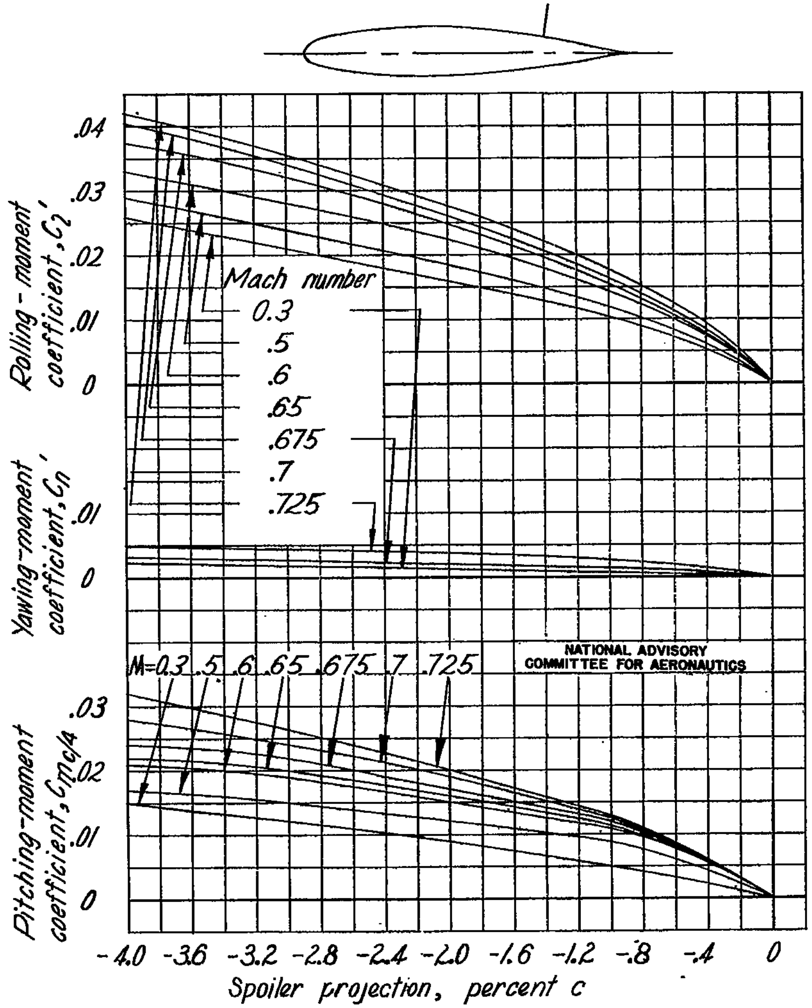

(c) C_L, 0.3.

Figure B69.- Concluded.

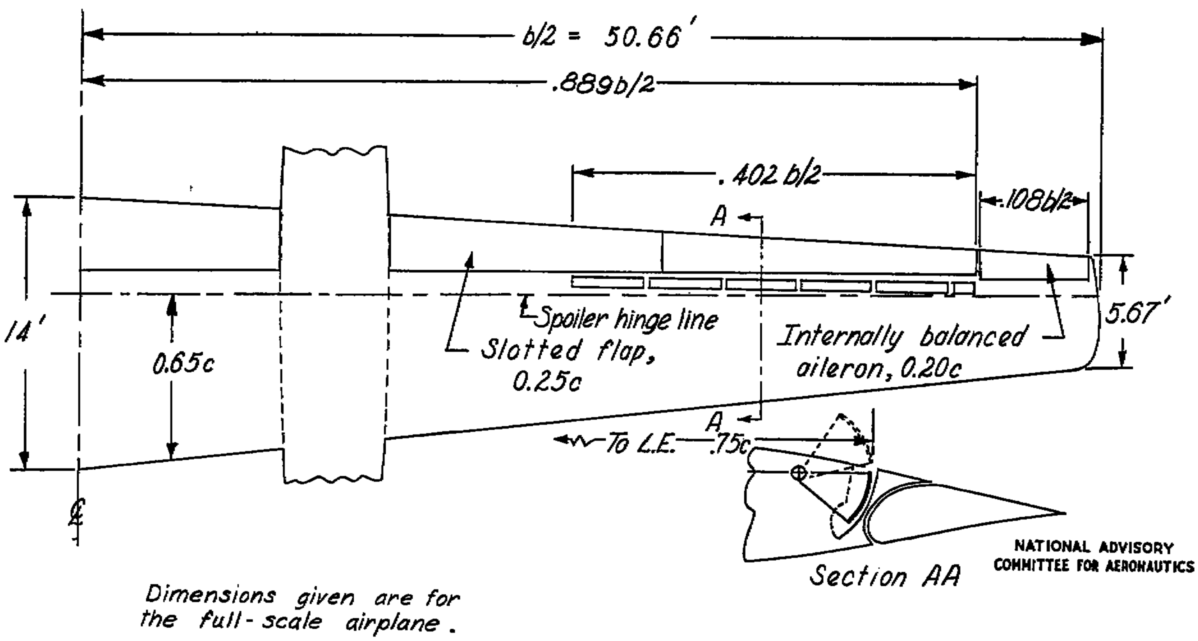

Figure B70.- Plan form and section of the wing of an 0.08-scale airplane model tested with spoiler and conventional ailerons and an almost full-span flap in the Ames 7- by 10-foot tunnel.

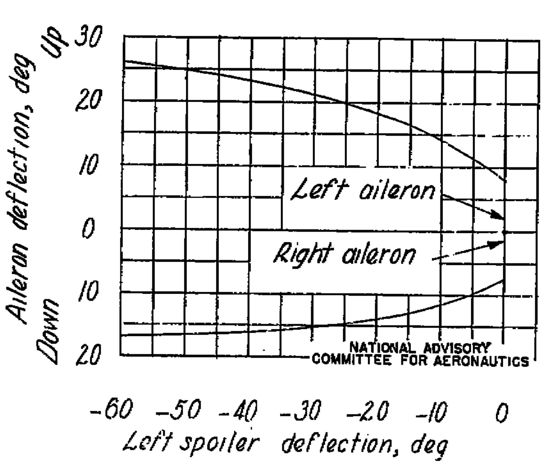

Figure B71.- Variation of aileron deflection with spoiler deflection on the 0.08-scale airplane model.

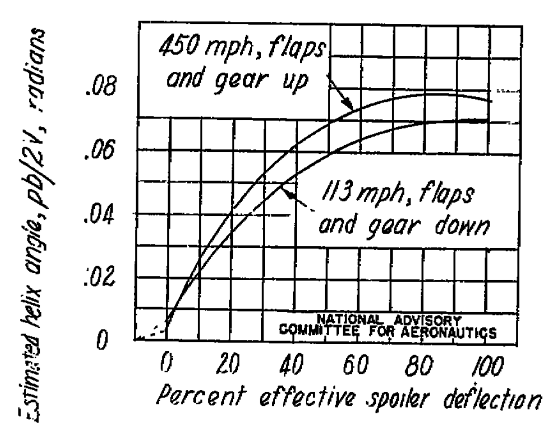

Figure B72.- Variation of helix angle with effective spoiler deflection, rudder locked, calculated for the 0.08-scale airplane model.

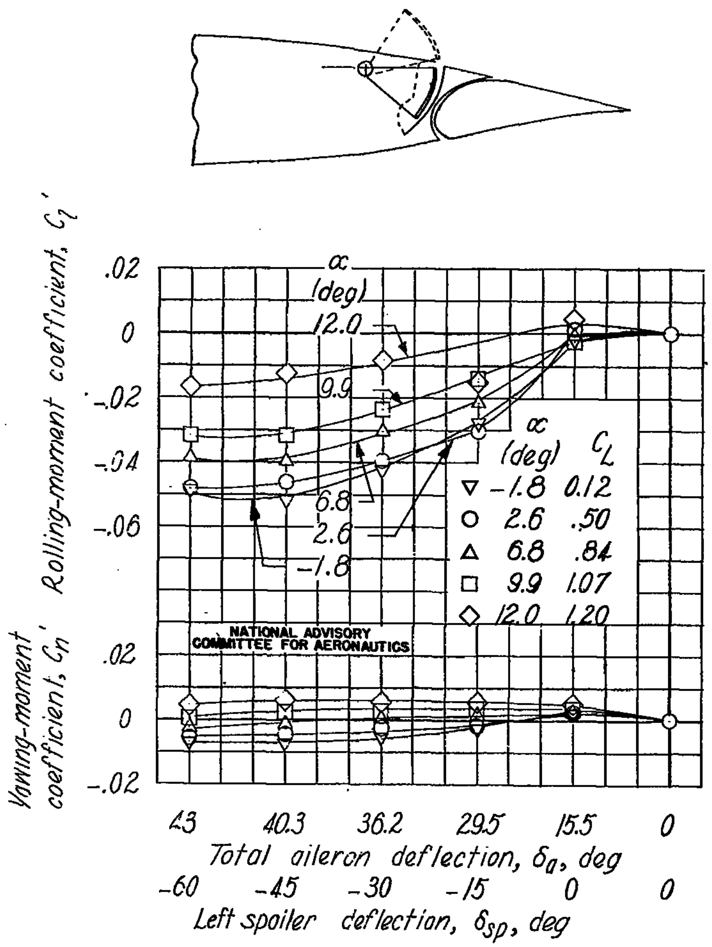

(a) δ_f, 0°.

Figure B73.- Effect of spoiler and aileron deflection on the rolling- and yawing-moment characteristics of the 0.08-scale airplane model.

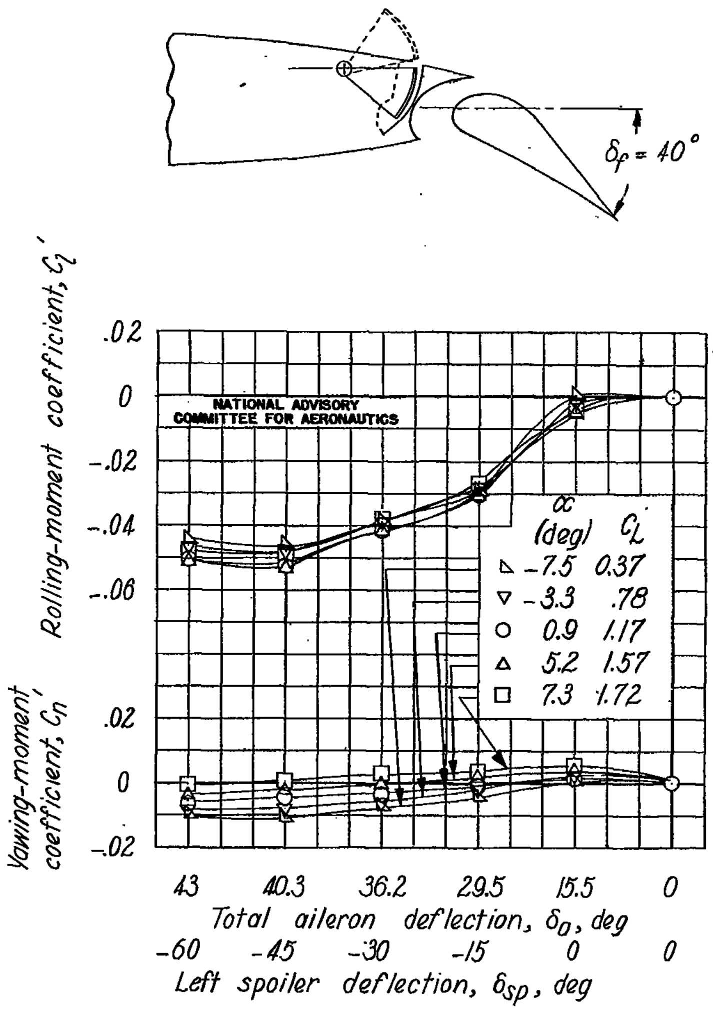

(b) δ_f, 40°.

Figure B73.- Concluded.

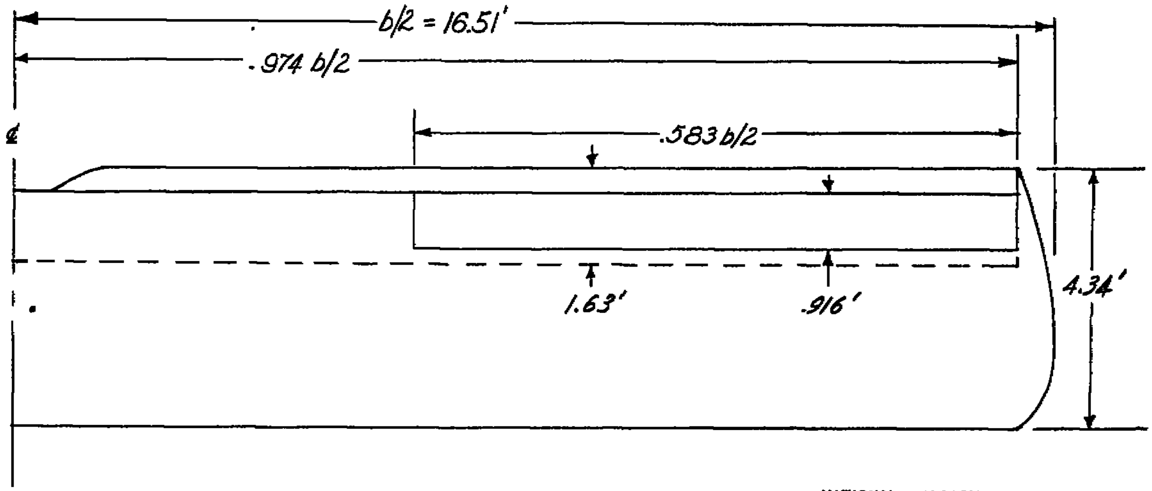

Figure B74.- Plan form of semispan wing of a personal-type airplane tested in Langley full-scale wind tunnel and in flight.

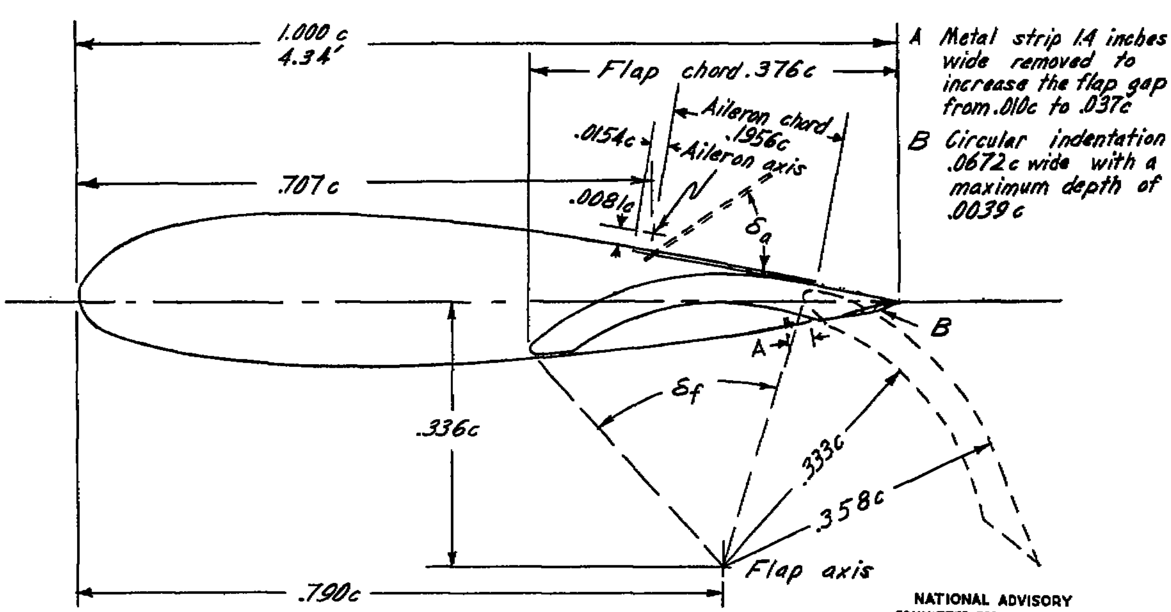

Figure B75.- Sectional view of wing showing Zap flap in retracted and fully deflected positions, upper-surface ailerons, and the trailing-edge and gap modifications.

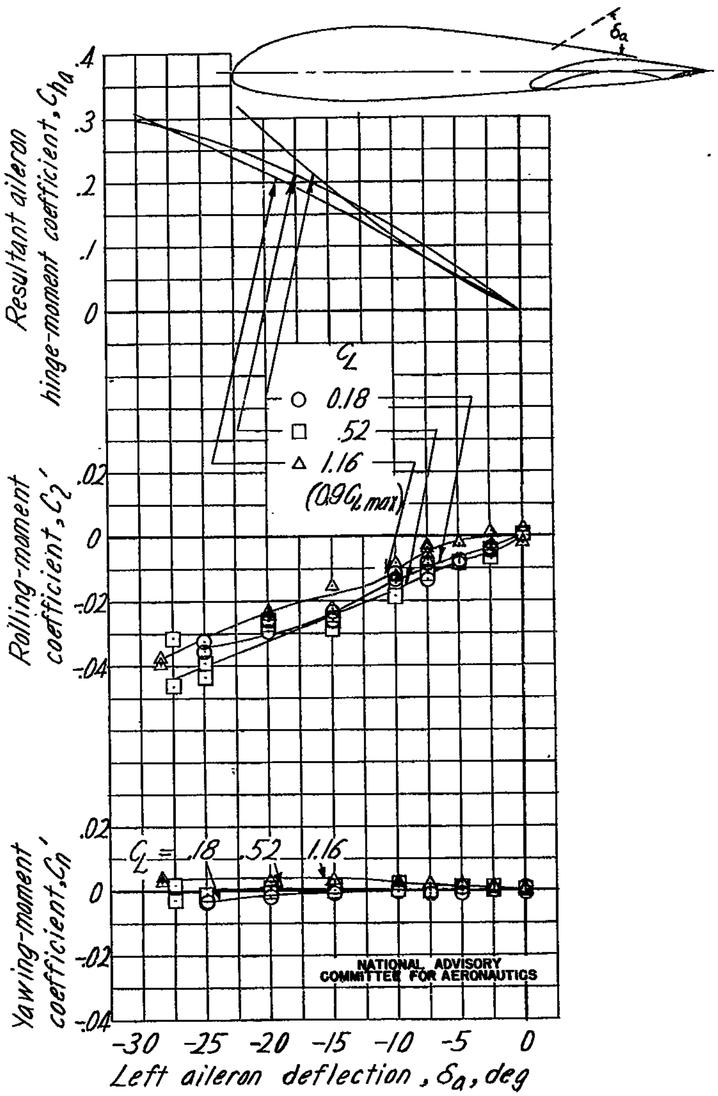

(a) δ_f, 0°.

Figure B76.- Aileron rolling- and yawing-moment coefficients about the wind axes and resultant aileron hinge-moment coefficients of a personal-type airplane with the Zap-flap wing installation. Approximate test speed, 58 miles per hour. Tested in Langley full-scale wind tunnel.

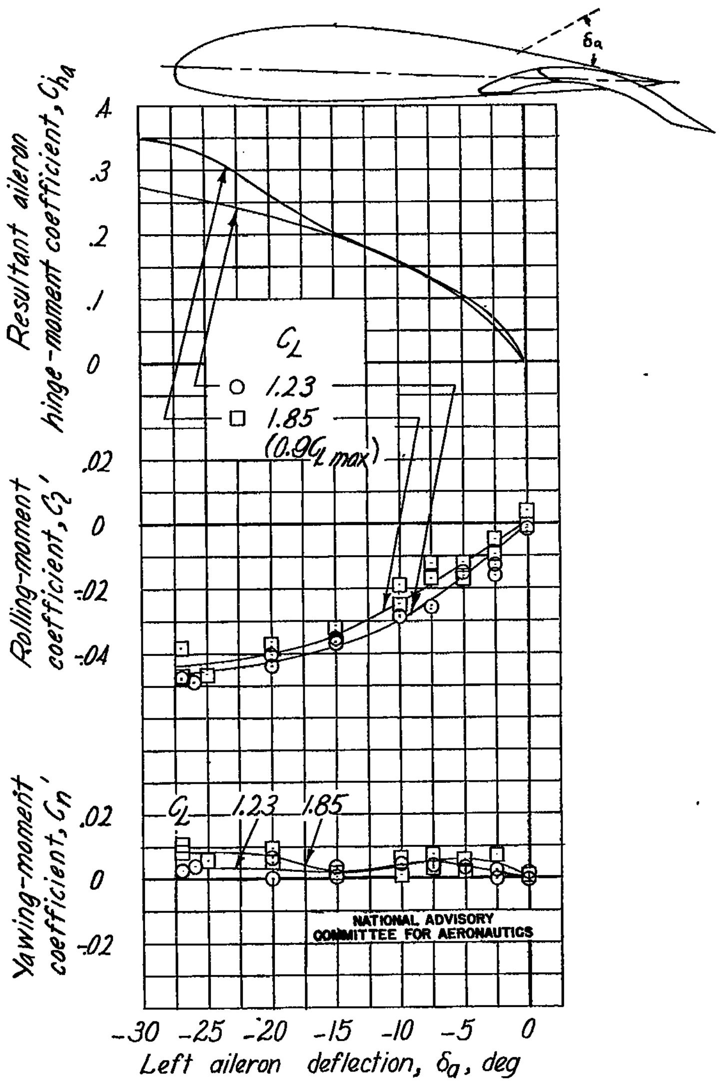

(b) δ_f, 26.3°.

Figure B76.- Continued.

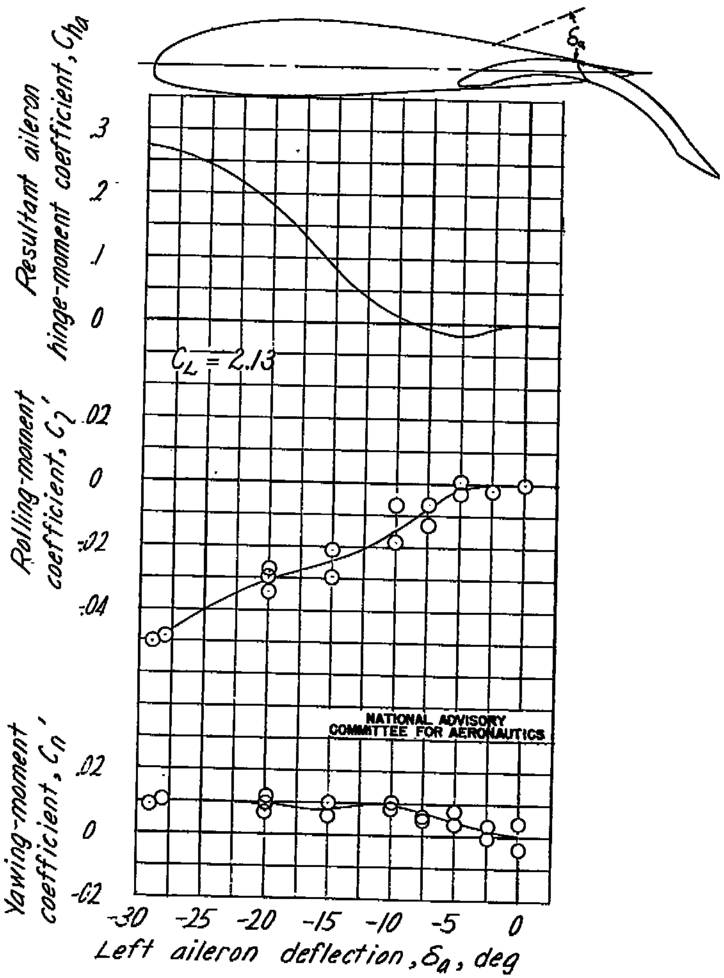

(c) δ_f, 43.0°.

Figure B76.- Concluded.

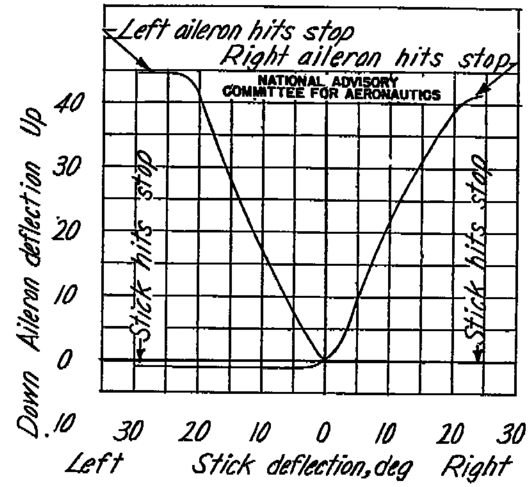

Figure B77.- Variation of aileron deflection with control-stick deflection.

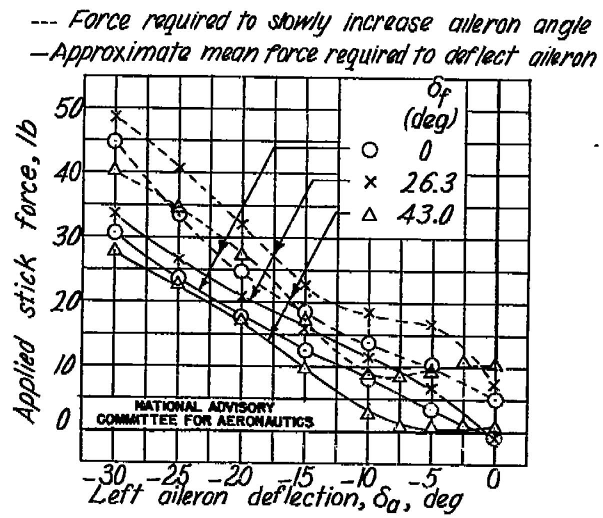

Figure B78.- Stick forces required to deflect the left aileron with the flap in various positions. Approximate test speed, 58 miles per hour. Langley full-scale wind tunnel.

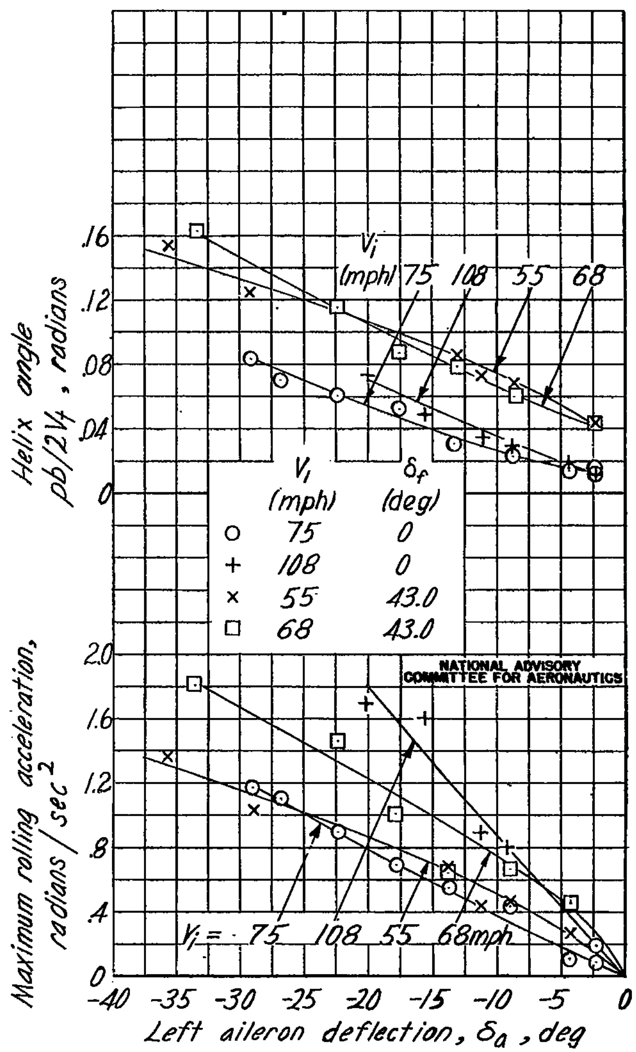

Figure B79.- Variation of the wing-tip helical angle and the maximum rolling acceleration with aileron deflection for several indicated airspeeds and flap settings in abrupt aileron rolls. Power-on, flight-test data.

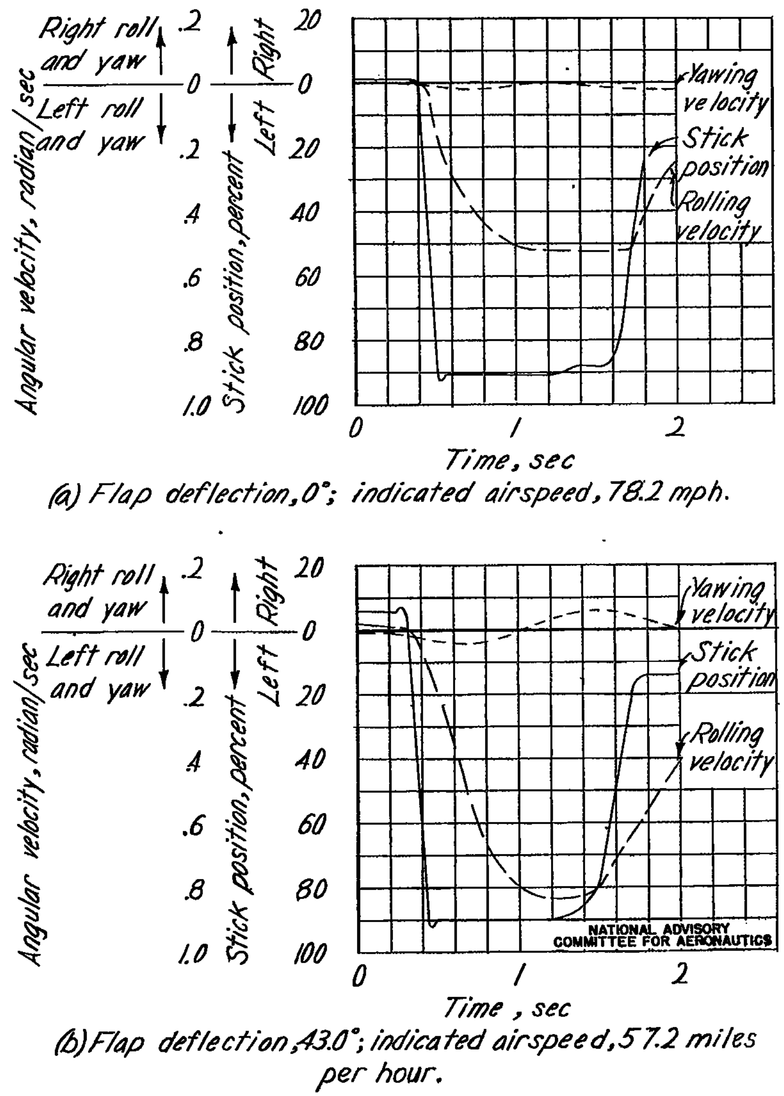

Figure B80.- Time histories of abrupt left aileron rolls. Rudder and elevator held fixed. Flight-test data.

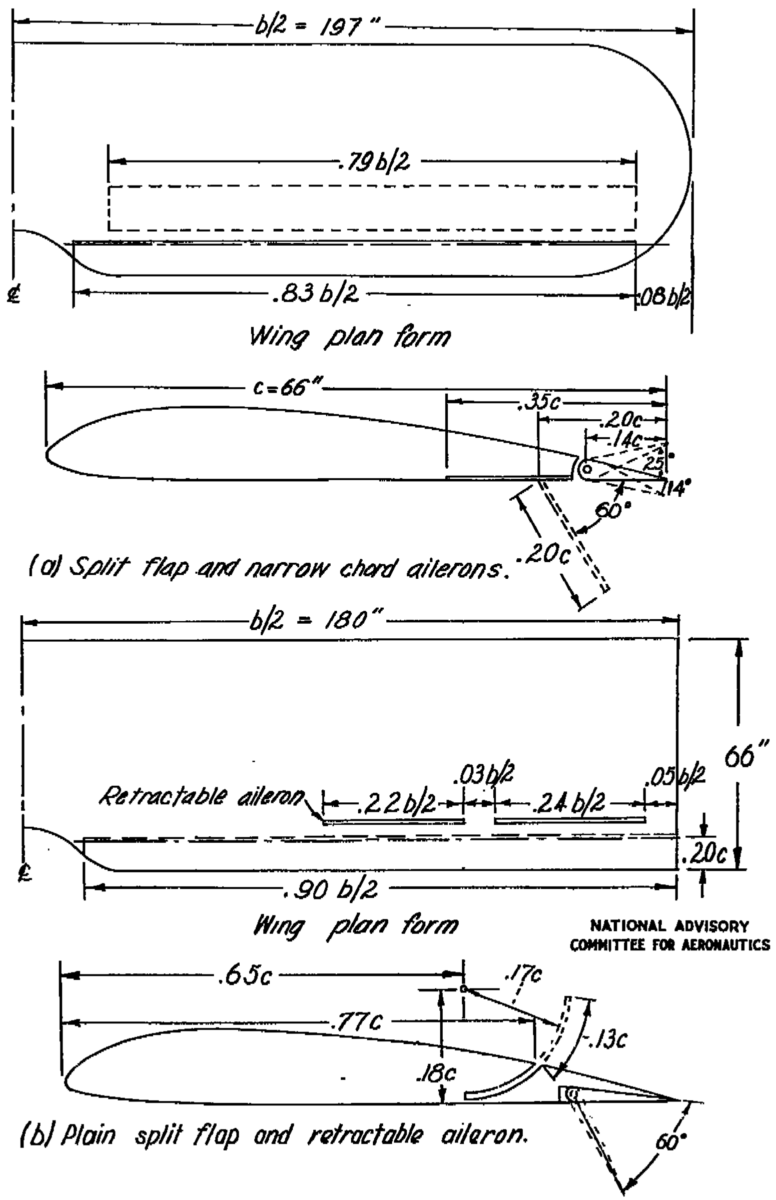

Figure B81.- Plan forms and sections of the wings with the two full-span flap lateral-control devices tested on the Fairchild 22 airplane. Langley flight tests.

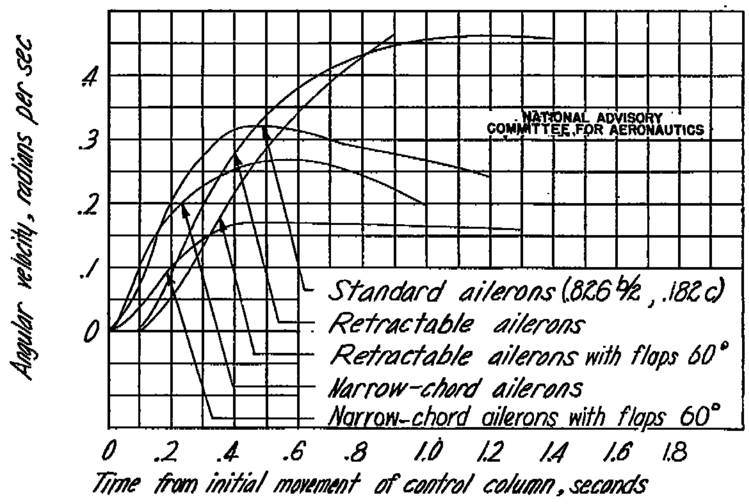

Figure B82.- Result of lag tests of various control devices on the Fairchild 22 airplane.

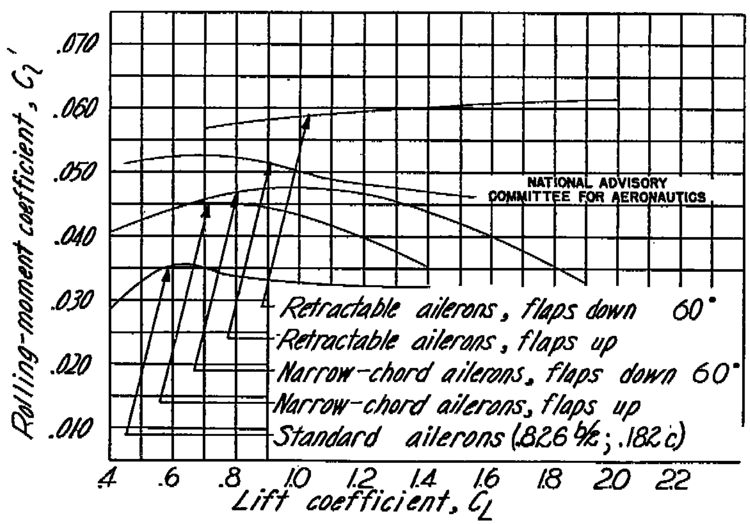

Figure B83.- Variation of rolling-moment coefficient with lift coefficient for standard, retractable, and narrow-chord ailerons.

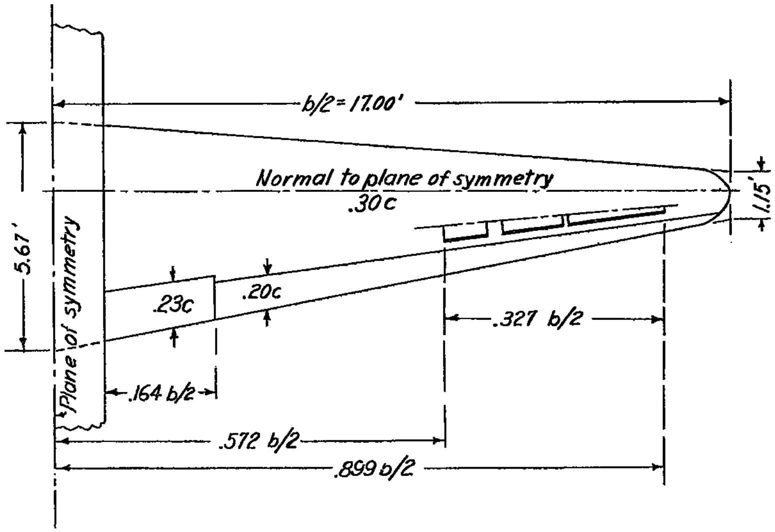

Wing area, S, sq ft	114
Aspect ratio, A	10
Taper ratio, λ	0.2
Wing section, root	NACA 23015
Wing section, tip	NACA 23009

NATIONAL ADVISORY
COMMITTEE FOR AERONAUTICS

Figure B84.- Plan form of semispan wing of modified Fairchild 22 airplane, tested in flight at Langley.

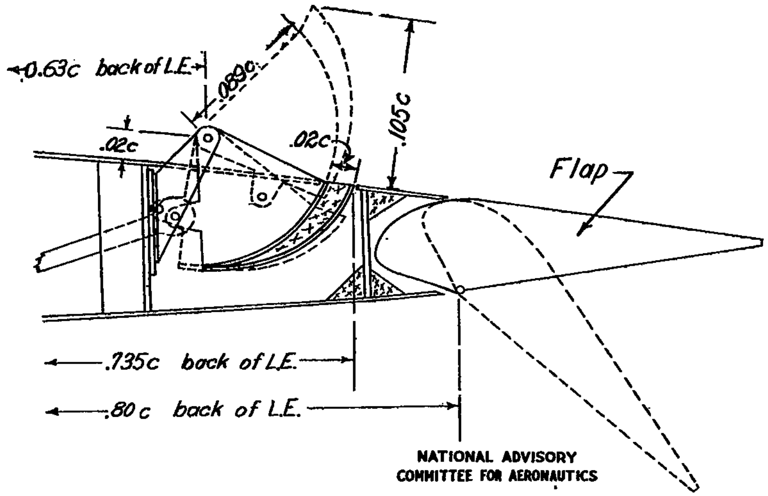

Figure B85.- Section of retractable ailerons and flaps installed on modified Fairchild 22 airplane.

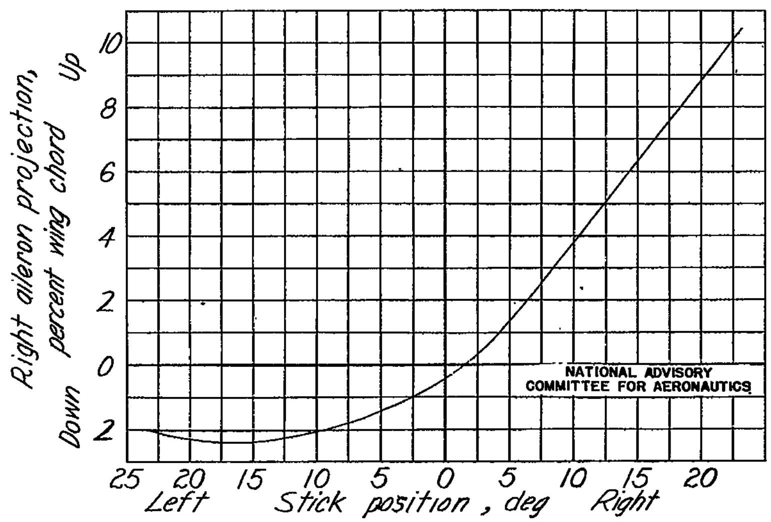

Figure B86.- Differential motion of retractable ailerons on modified Fairchild 22 airplane.

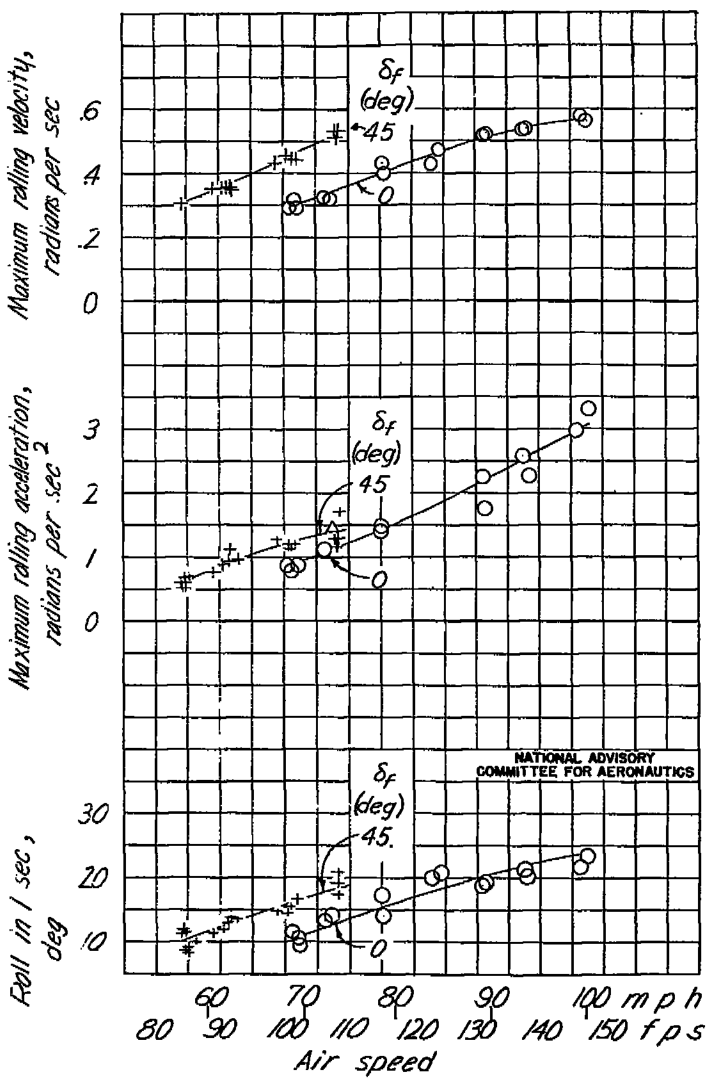

Figure B87.- Variation of maximum rolling acceleration, rolling velocity, and angle of roll attained in one second with airspeed; retractable ailerons fully deflected.

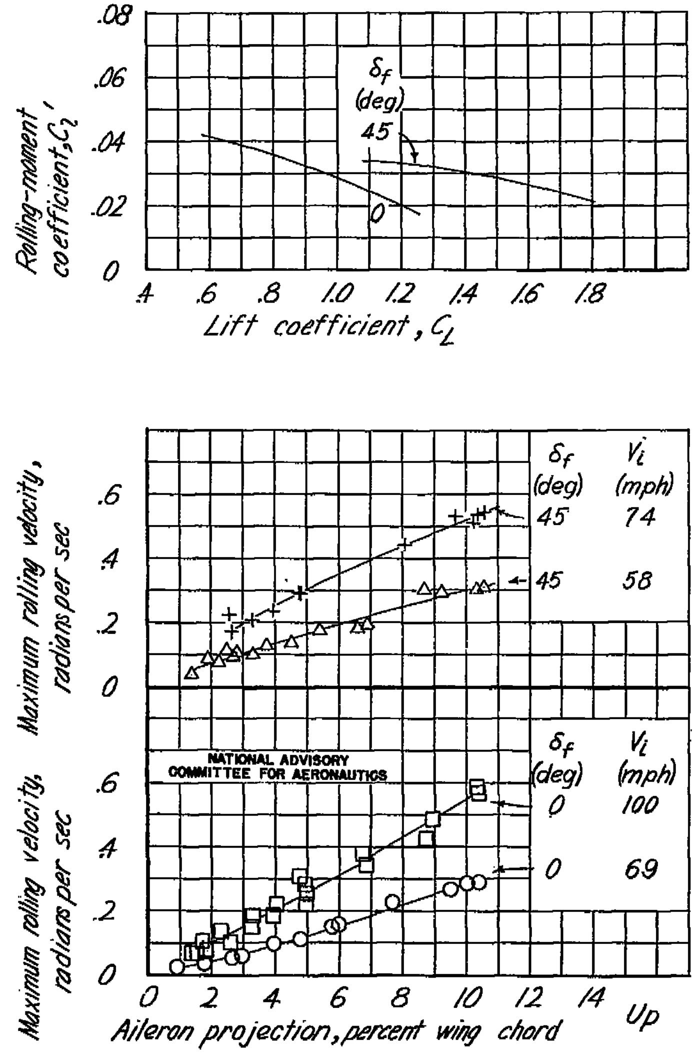

Figure B88.- Variation of maximum rolling-moment coefficient with lift coefficient, retractable ailerons fully deflected, and variation of maximum rolling velocity with aileron projection; modified Fairchild 22 airplane.

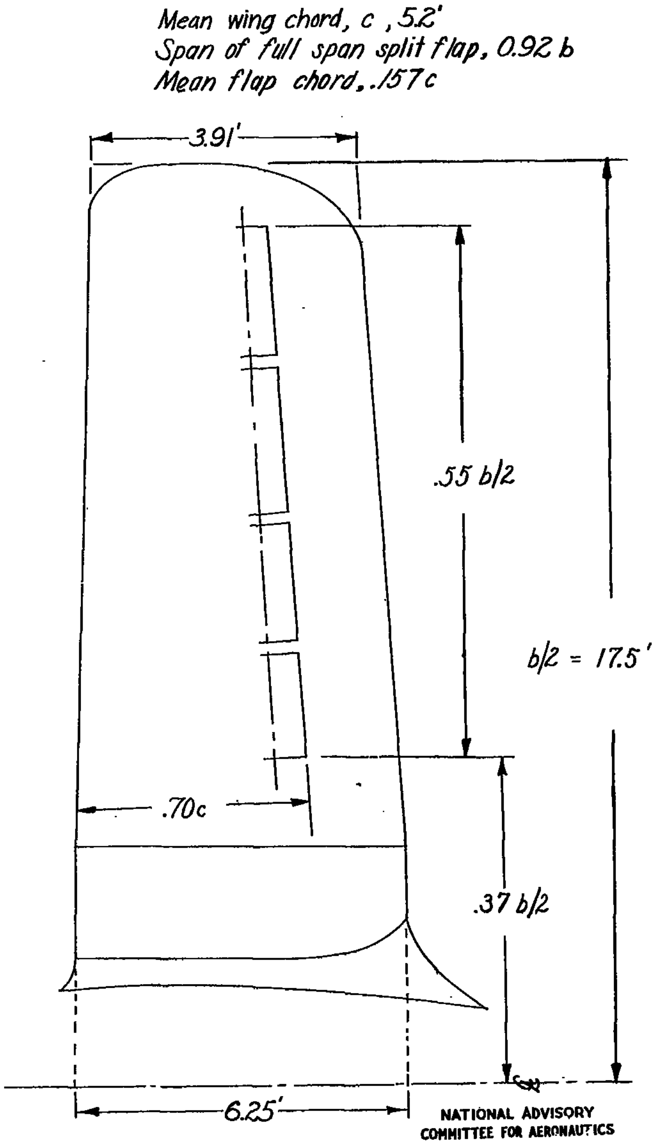

Figure B89.- Plan form of the semispan wing of a personal-type airplane, equipped with spoiler-type lateral controls, flight tested in England.

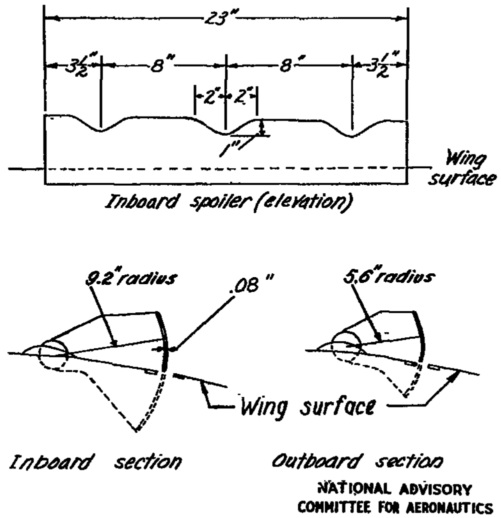

Figure B90.- Front elevation and sections of the spoiler tested on the airplane.

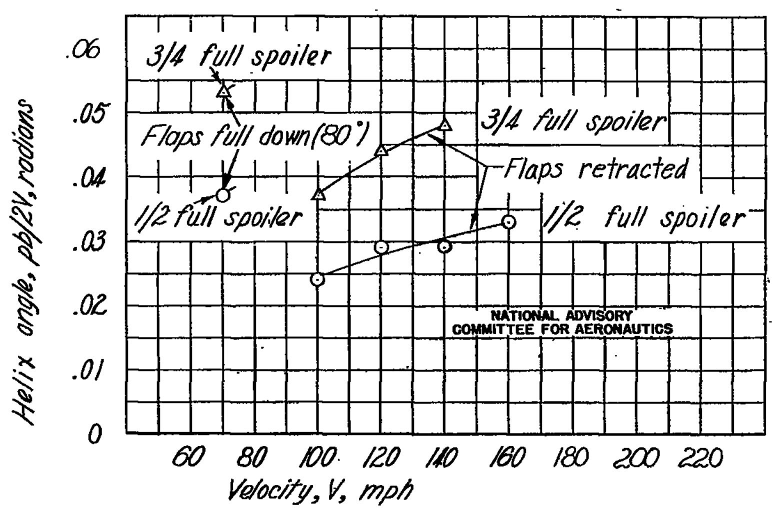

Figure B91.- Variation of the helix angle pb/2V due to spoiler deflection with velocity of the airplane.

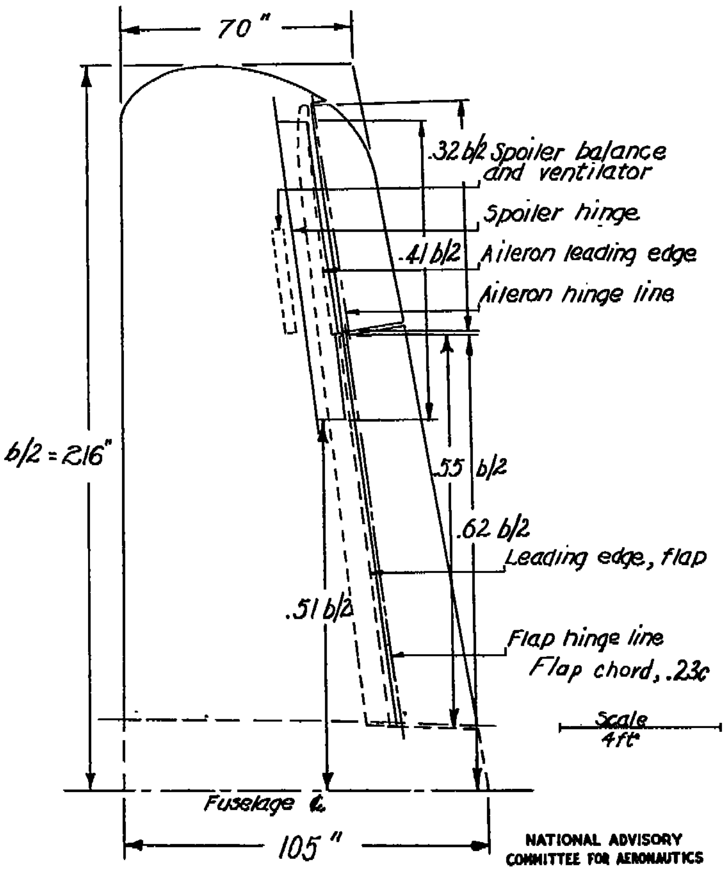

Figure B92.- Plan form of the semispan wing of a scout-observation-type airplane tested in flight by Vought-Sikorsky Aircraft.

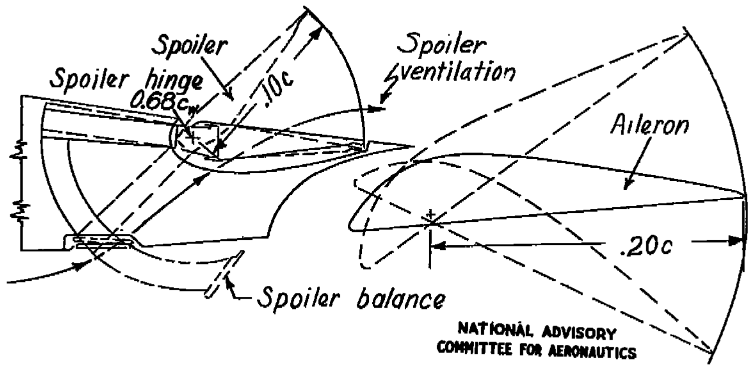

Figure B93.- Spoiler and aileron arrangement for an observation-scout-type airplane.

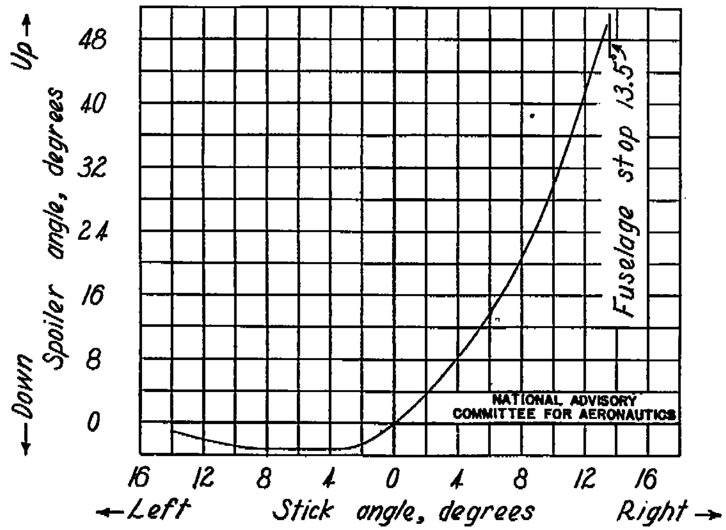

Figure B94.- Relation of stick and spoiler angles for the airplane.

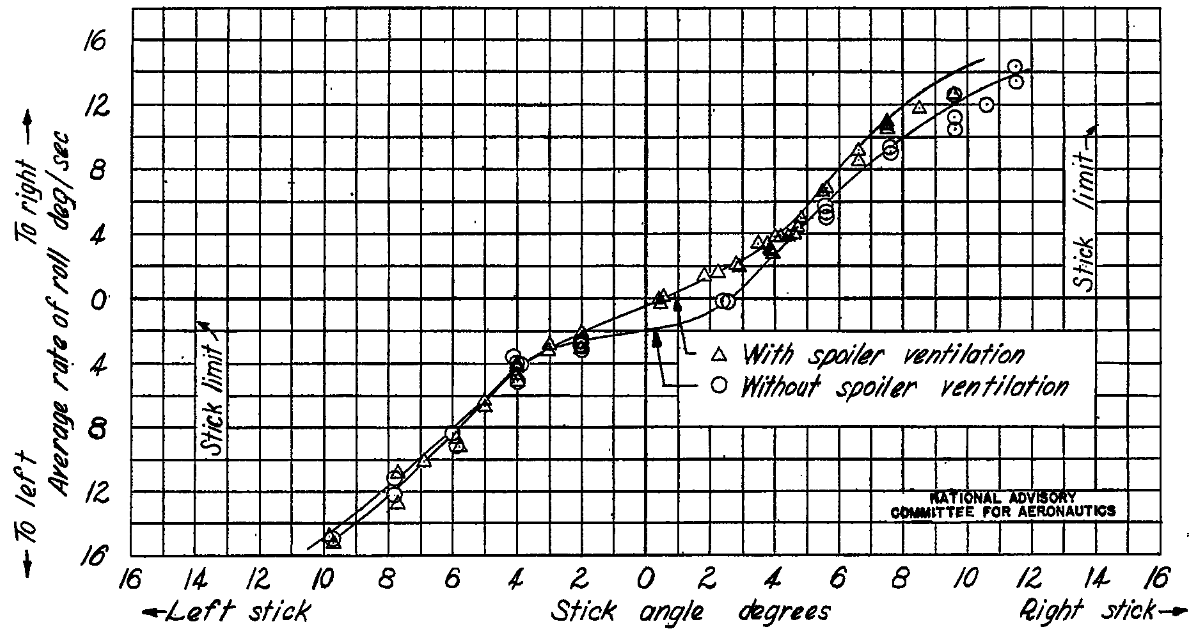

Figure B95.- Variation of average rate of roll due to spoiler deflection with stick angle for the airplane. Flaps full down and ailerons drooped 29°, 11.5 miles per hour above stall.

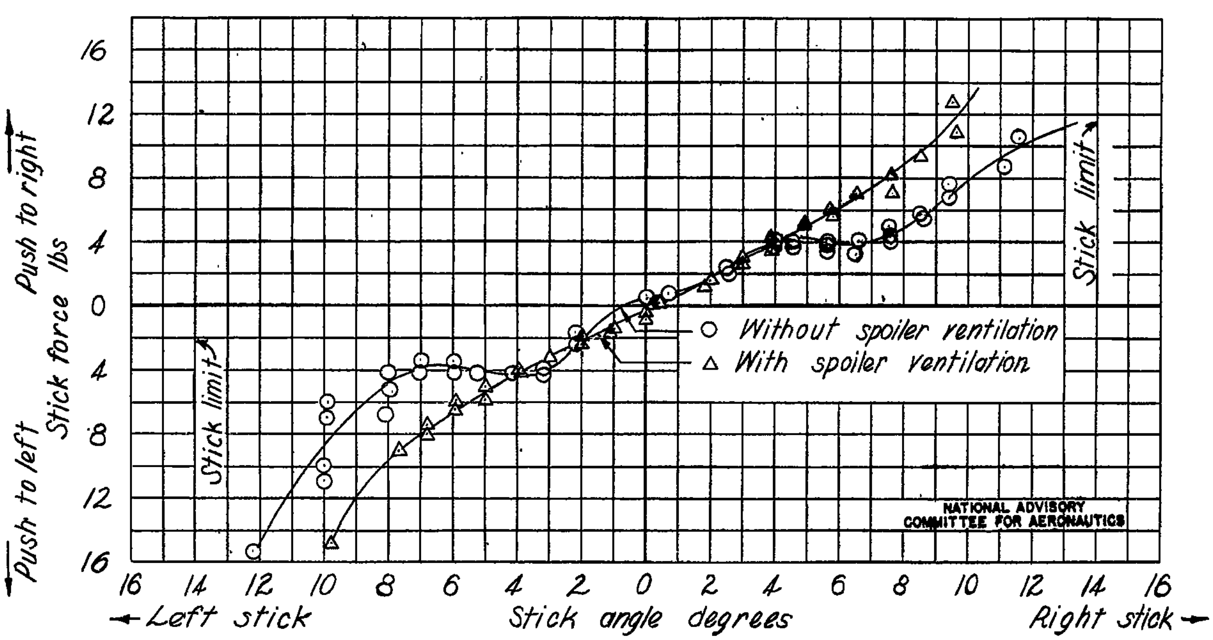

Figure B96.- Variation of stick force with stick angle for the airplane. Flaps full down and ailerons drooped 29°, 11.5 miles per hour above stall.

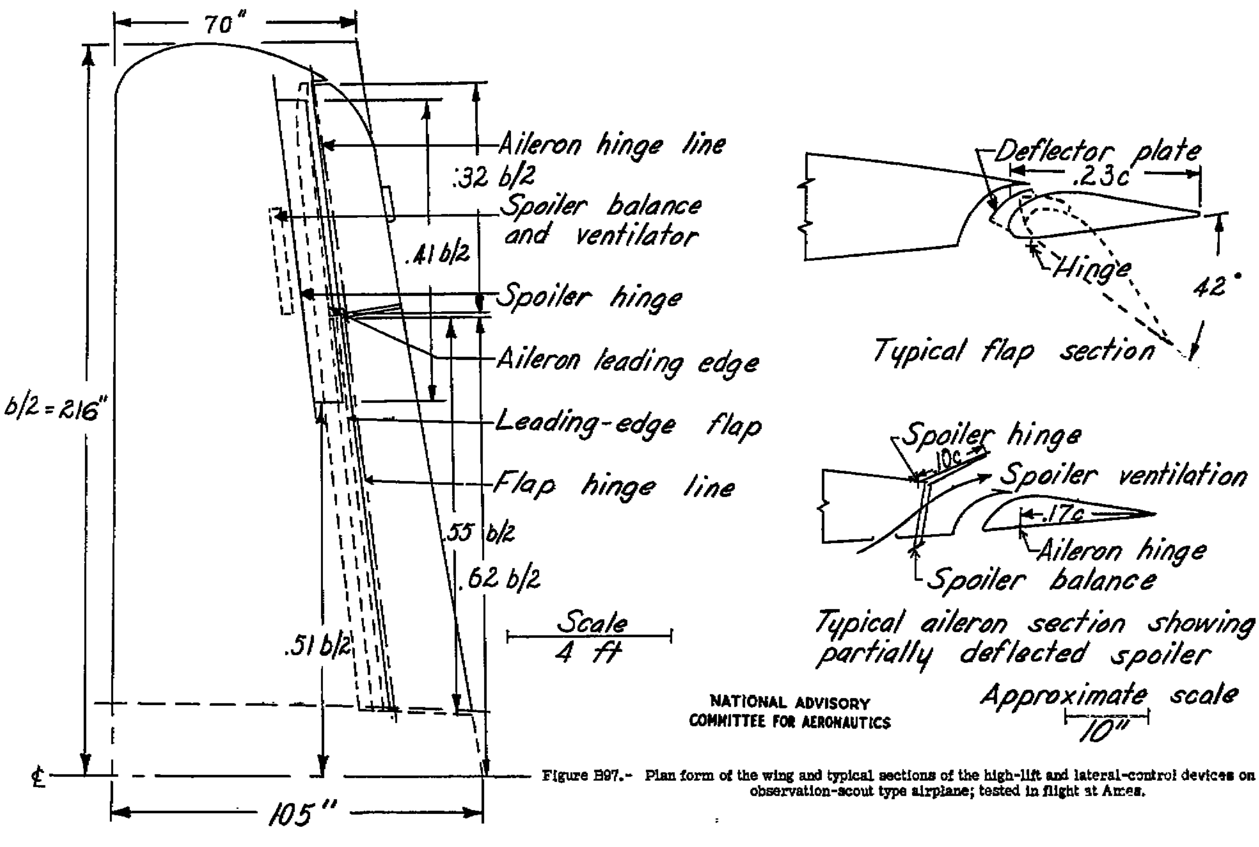

Figure B97.- Plan form of the wing and typical sections of the high-lift and lateral-control devices on an observation-scout type airplane; tested in flight at Ames.

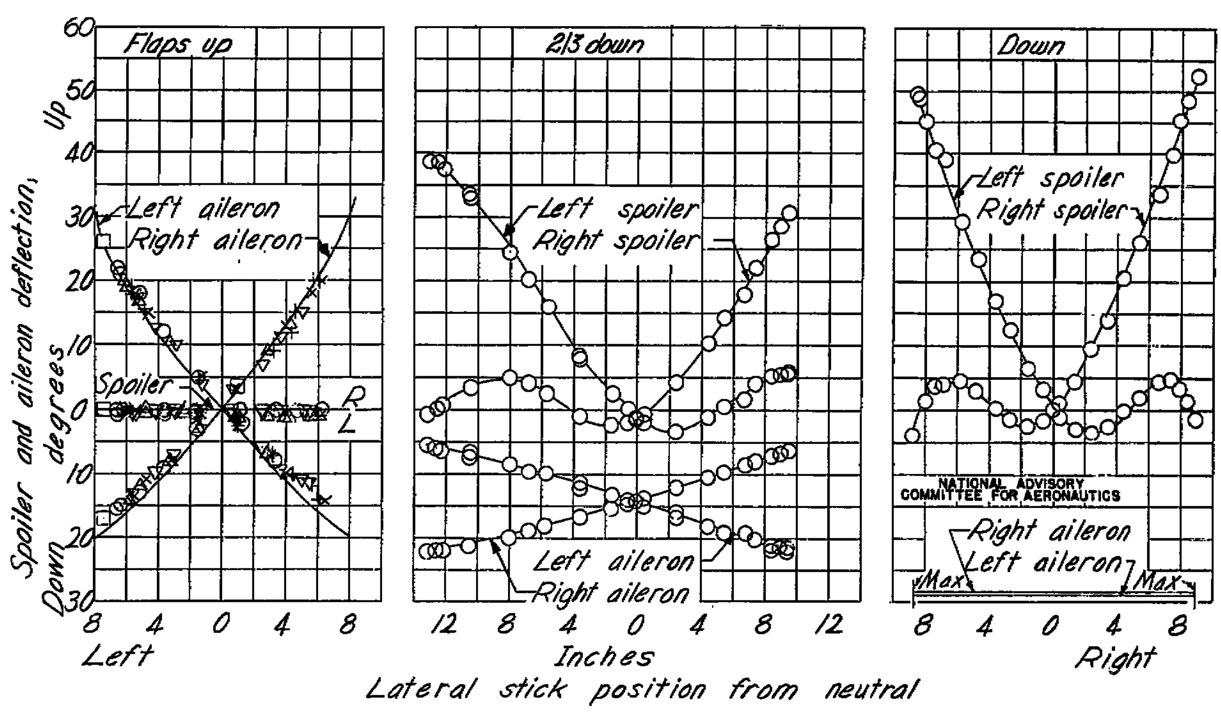

Figure B98.- Variation of aileron and spoiler angles with stick position as measured on the ground with no load on the surfaces.

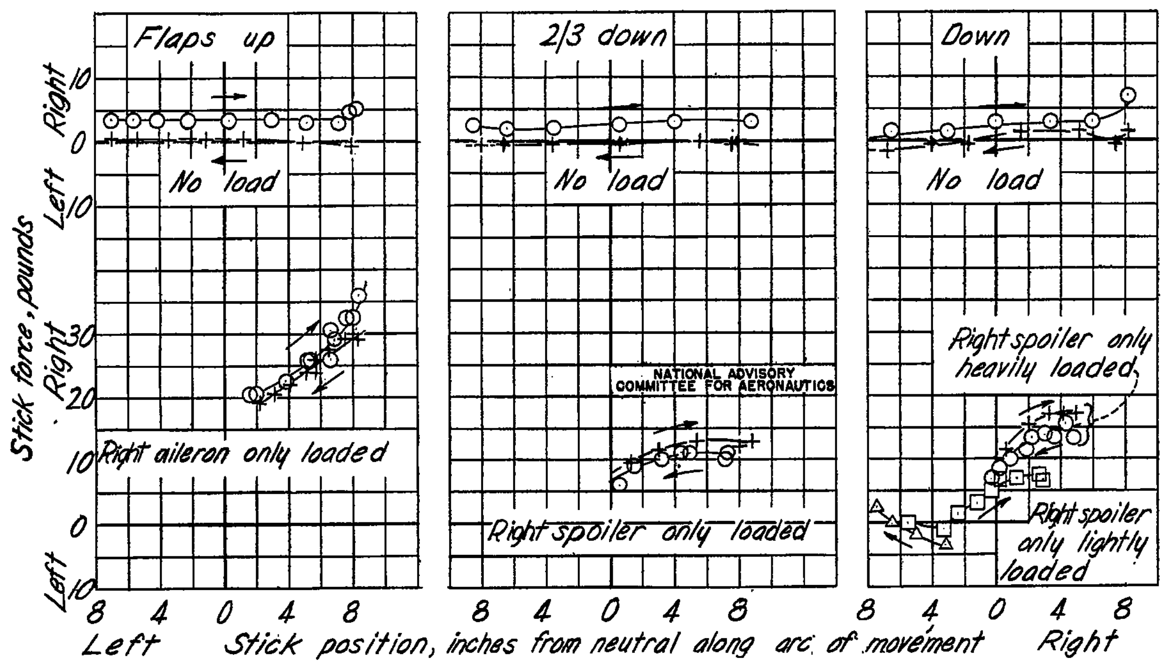

Figure B99.- Friction in the lateral-control system as indicated by the stick force required to move the controls on the ground.

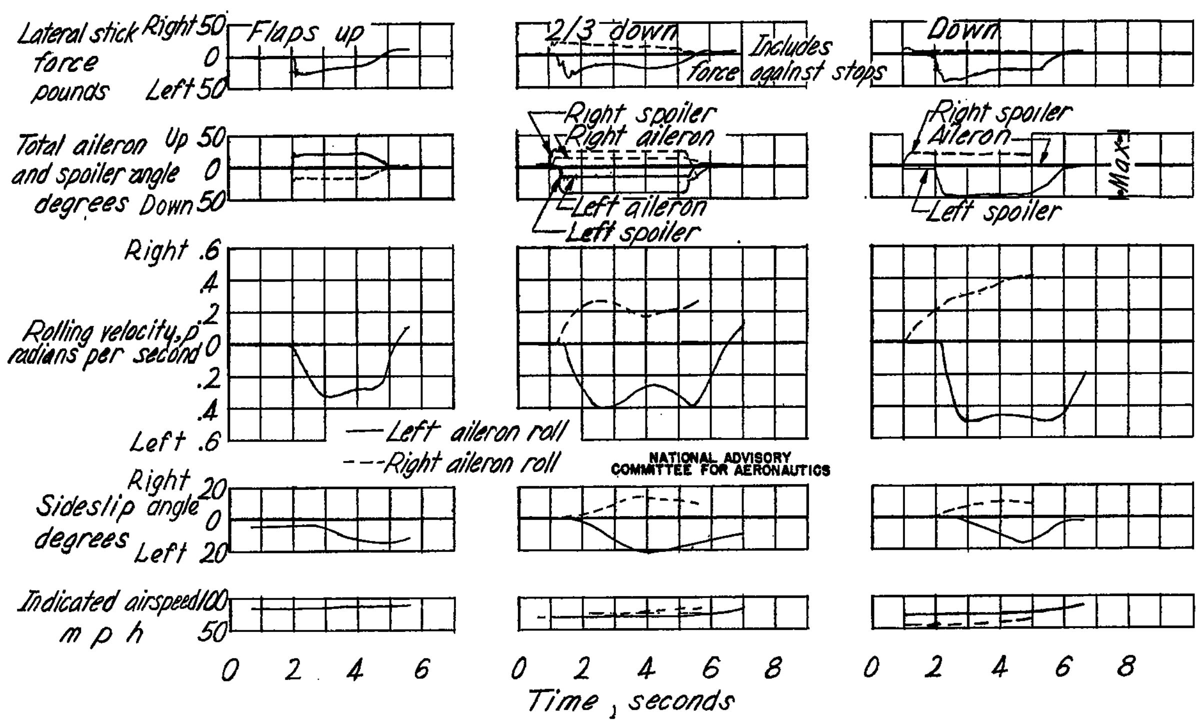

Figure B100.- Time history of a power-off aileron roll made with the rudder fixed in trim position.

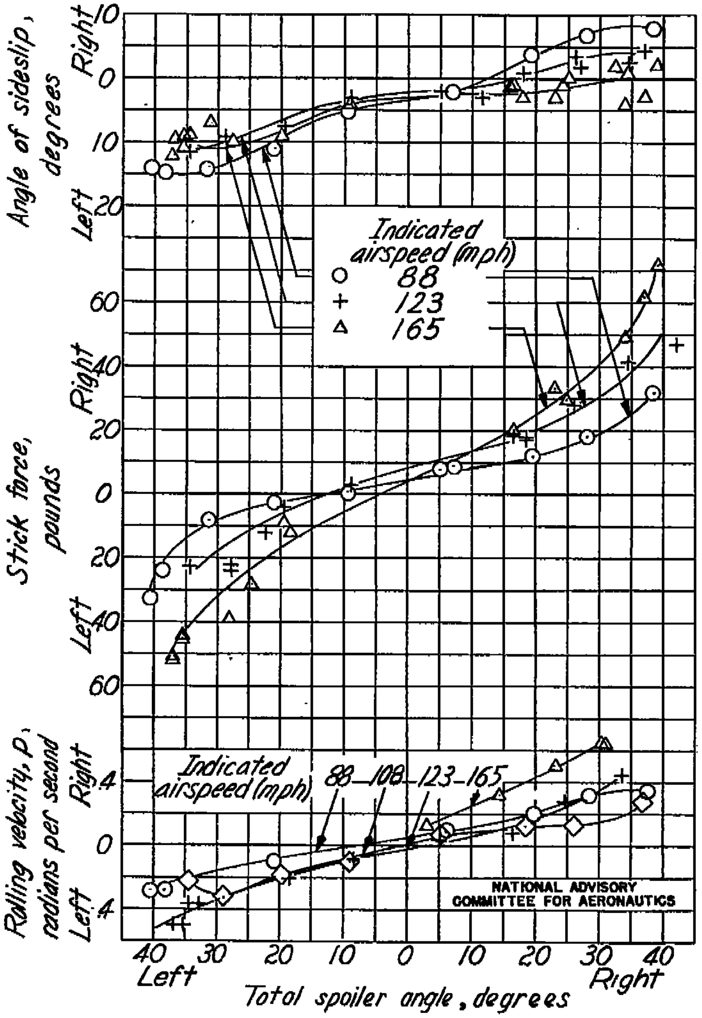

(a) Flaps up.

Figure B101.- Variation of rolling velocity, sideslip angle, and stick force with deflection of the lateral controls in abrupt aileron rolls with the rudder fixed in trim position.

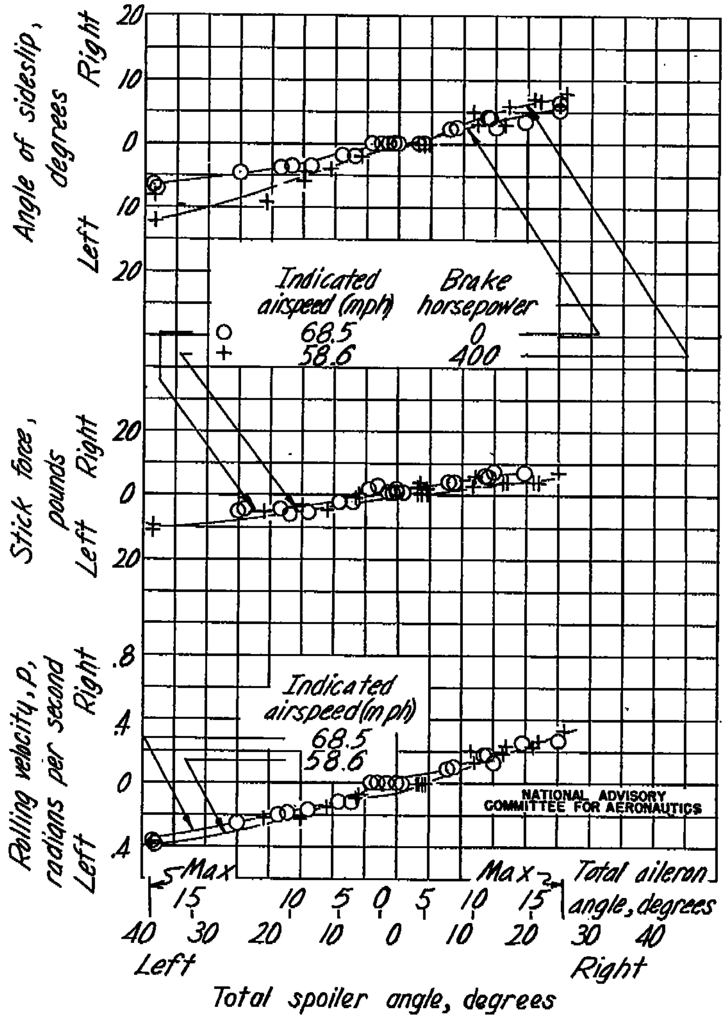

(b) Flaps two-thirds down.

Figure B101.- Continued.

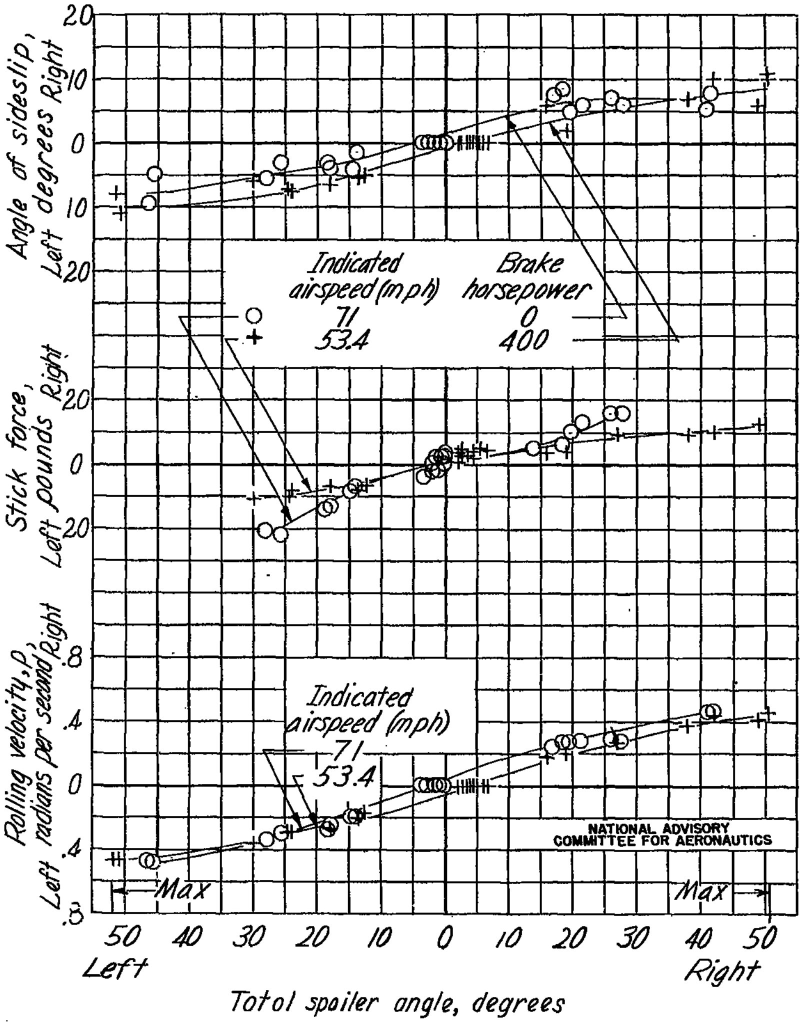

(c) Flaps down.

Figure B101.- Concluded.

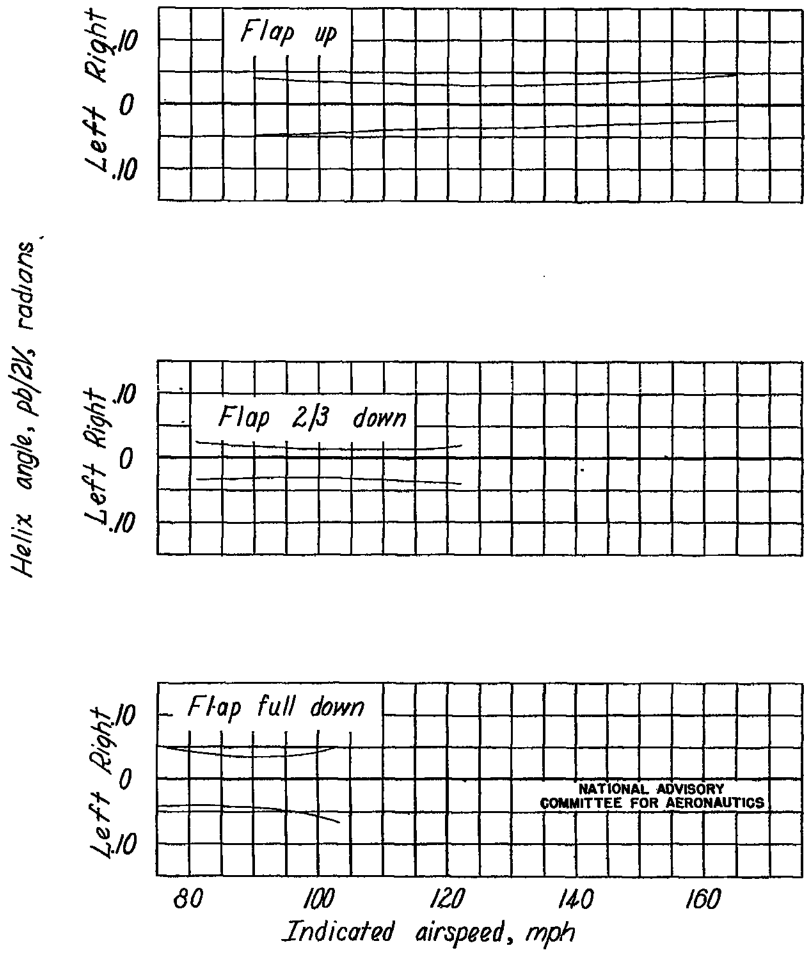

Figure B102.- Variation of the helix angle pb/2V with airspeed for a lateral stick force of 30 pounds or less, power-off conditions.

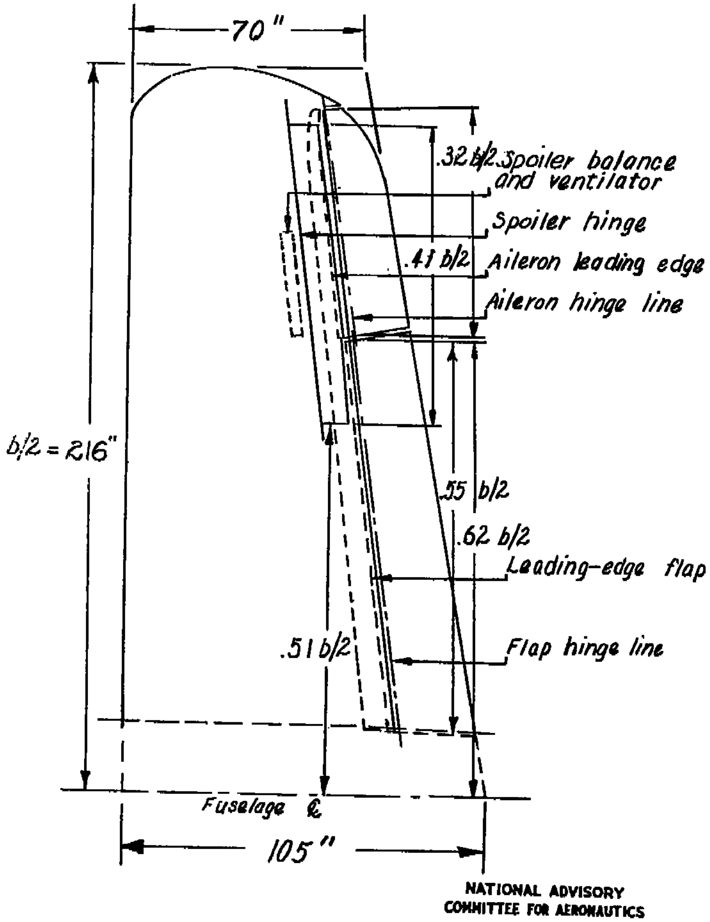

Figure B103.- Plan form of the semispan wing of an observation-scout-type airplane flight tested in England.

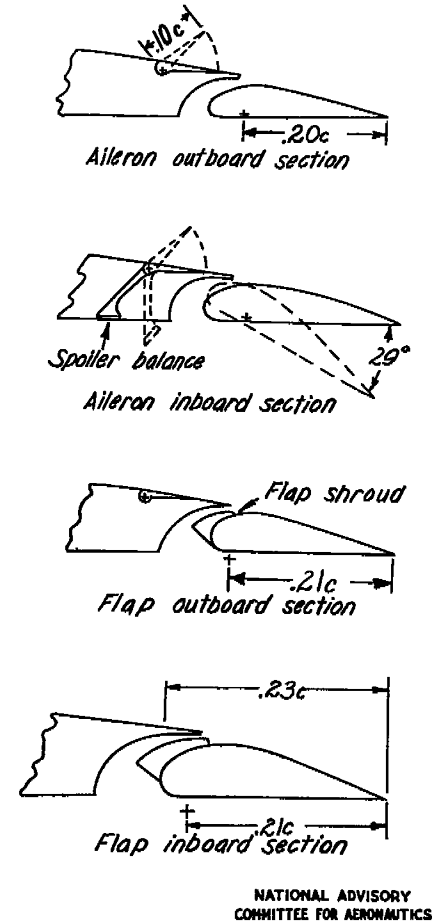

Figure B104.- Aileron, spoiler, and flap sections of the airplane wing.

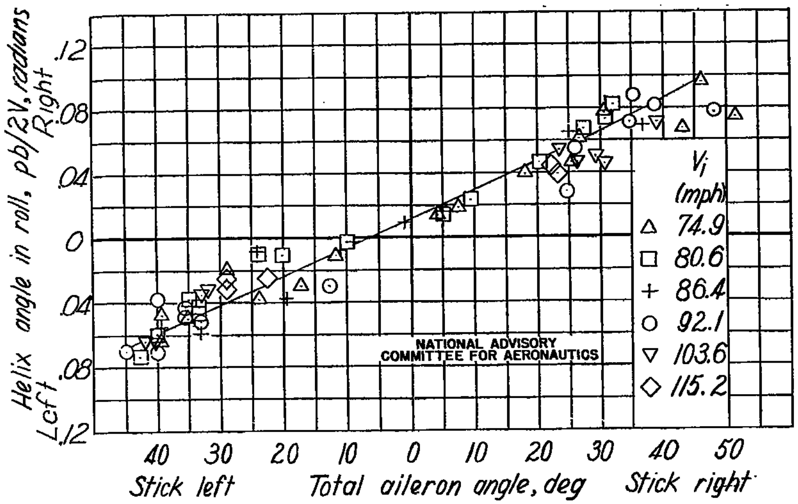

(a) Flaps up.

Figure B105.- Variation of helix angle in roll with control-surface angle.

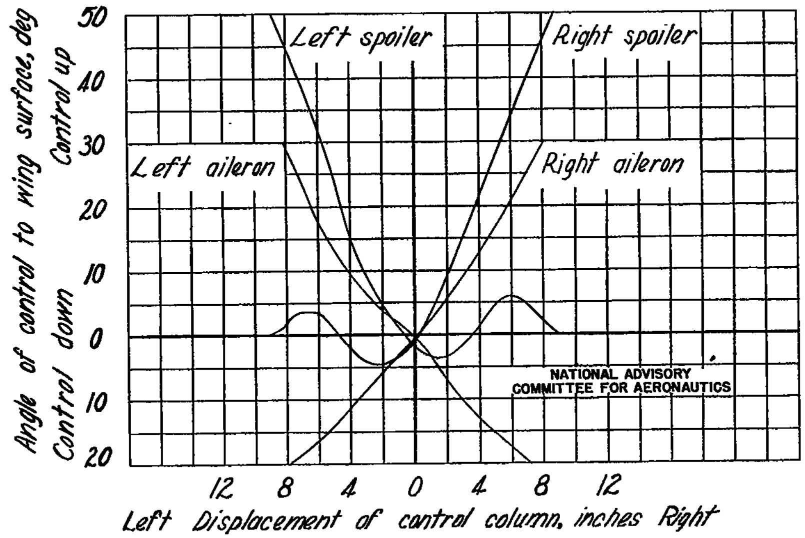

Figure B106.- Variation of spoiler (flaps down) and aileron (flaps up) angles with stick position.

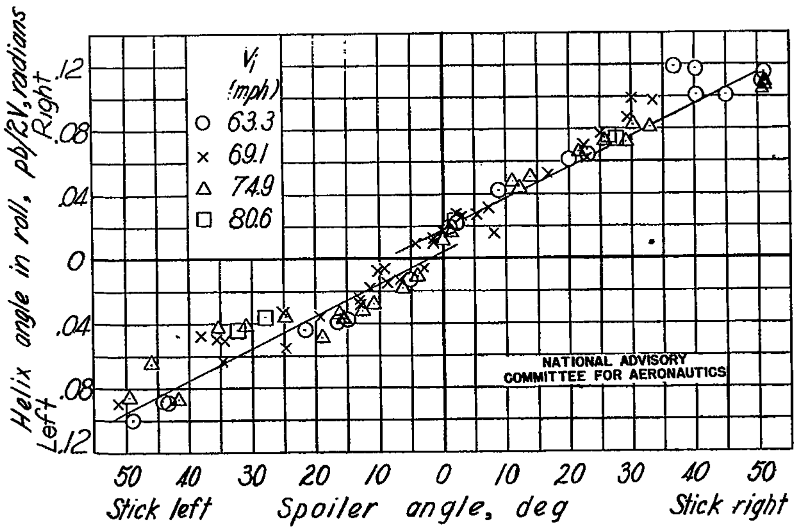

(b) Flaps down.

Figure B105.- Concluded.

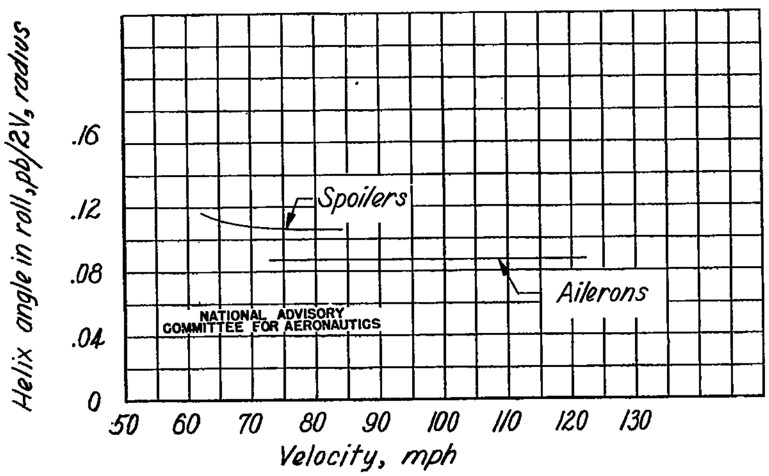

Figure B107.- Variation of helix angle in roll with velocity for a full stick displacement.

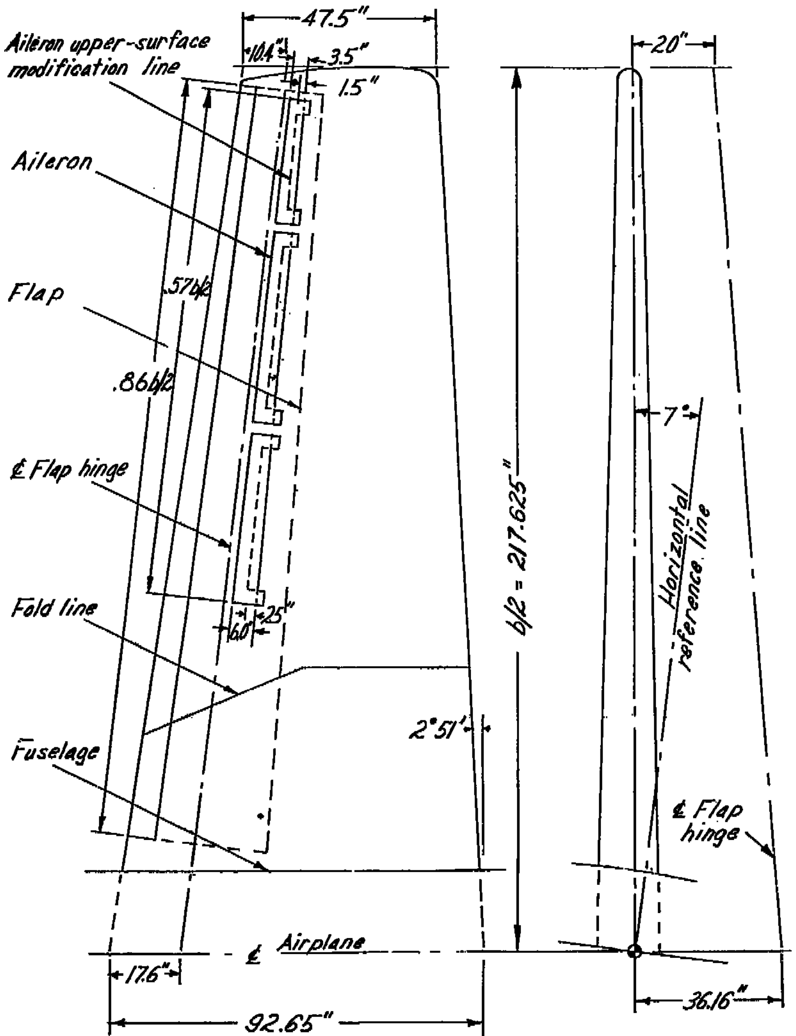

Figure B108.- Semispan wing of a modified observation-scout type airplane showing the aileron and Zap flap as tested in flight at Ames.

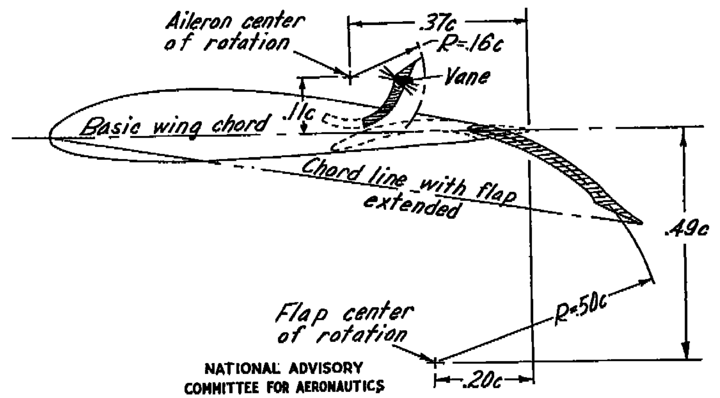

Figure B109.- Cross-sectional drawing of the wing showing the aileron and flap extended and retracte

Original condition - vane nose up
Modification 1 - vane nose down
Modification 2 - vane nose up, aileron upper-surface slots open, aileron upper-surface area reduced

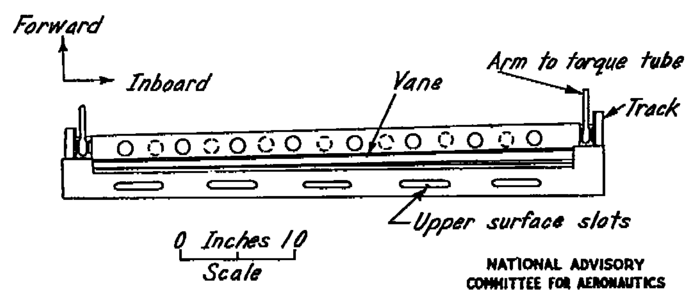

Figure B110.- Sketch of a typical aileron panel with modified upper surface.

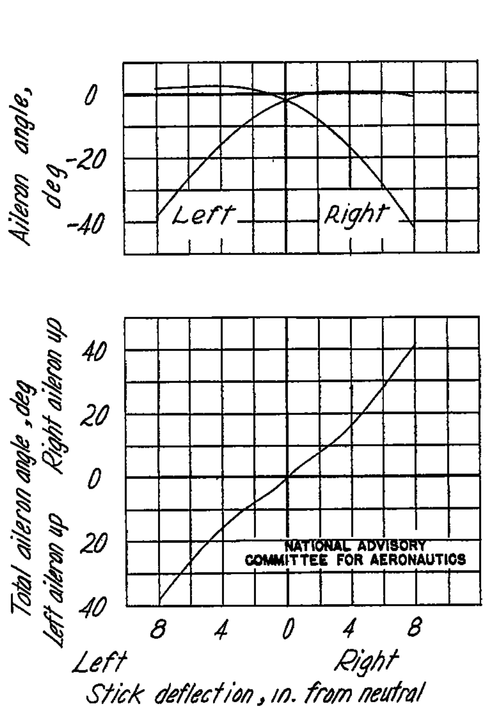

Figure B111.- Variation of aileron angle with stick deflection.

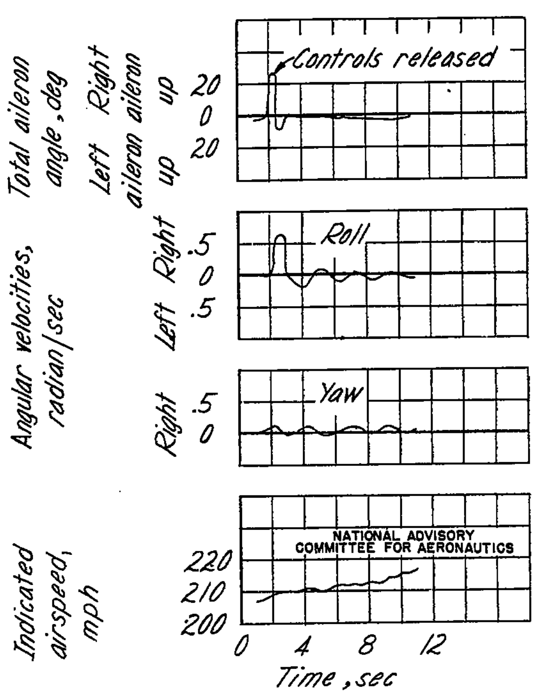

Figure B112.- Characteristics of uncontrolled lateral motion; rated power; flaps up; 207 miles per hour.

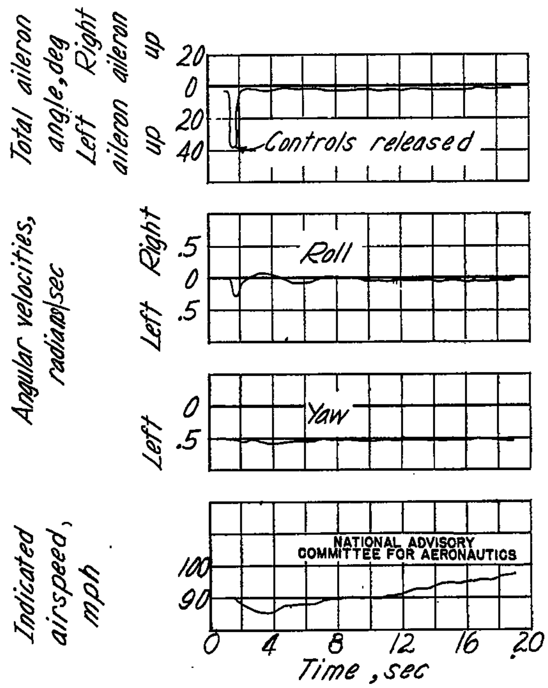

Figure B113.- Characteristics of uncontrolled lateral motion; power-off; flaps up; 92 miles per hour.

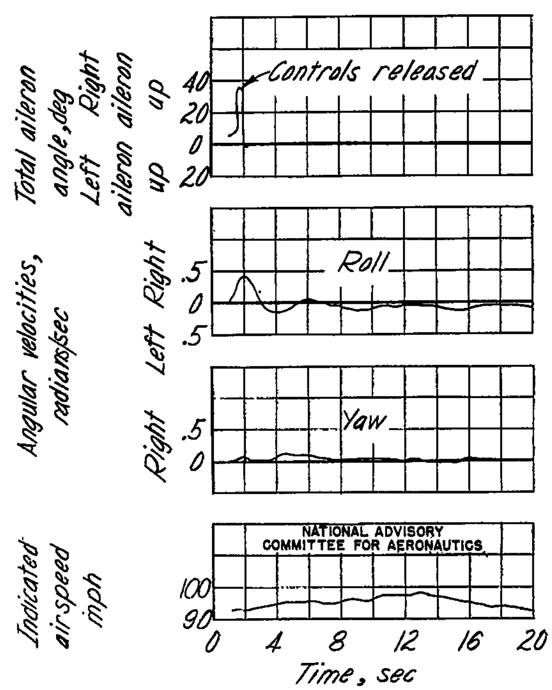

Figure B114.- Characteristics of uncontrolled lateral motion, power-off; flaps down; 92 miles per hour.

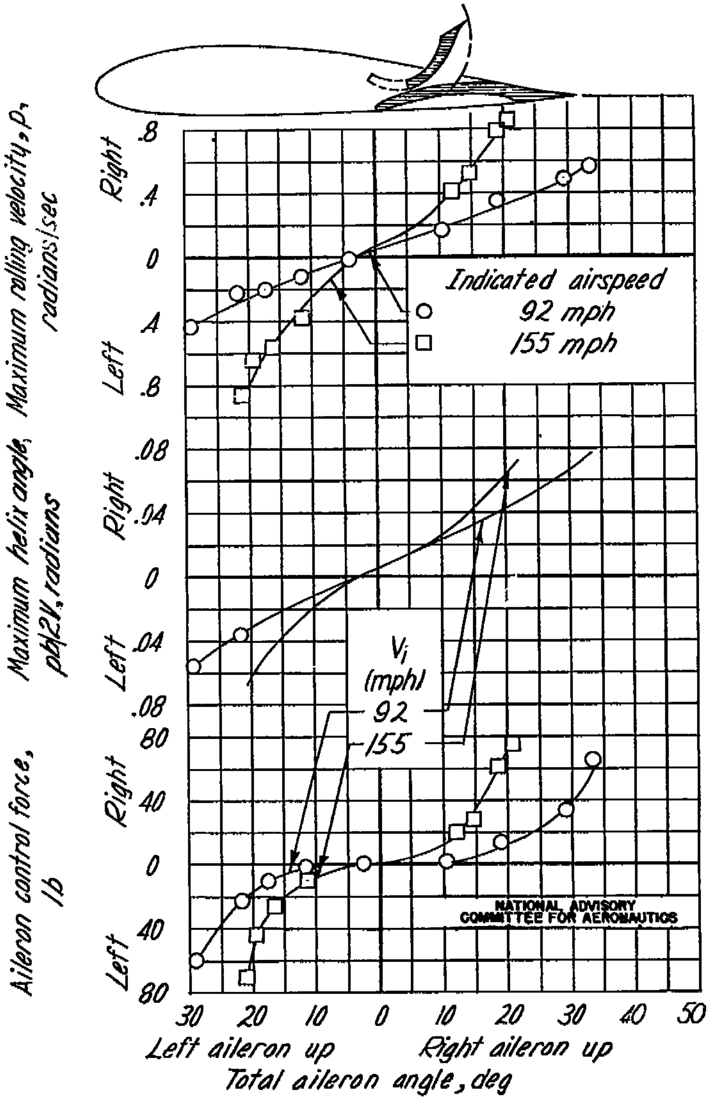

(a) Rated power.

Figure B115.- Aileron control characteristics of the modified observation-scout type airplane; flaps up; ailerons in original condition.

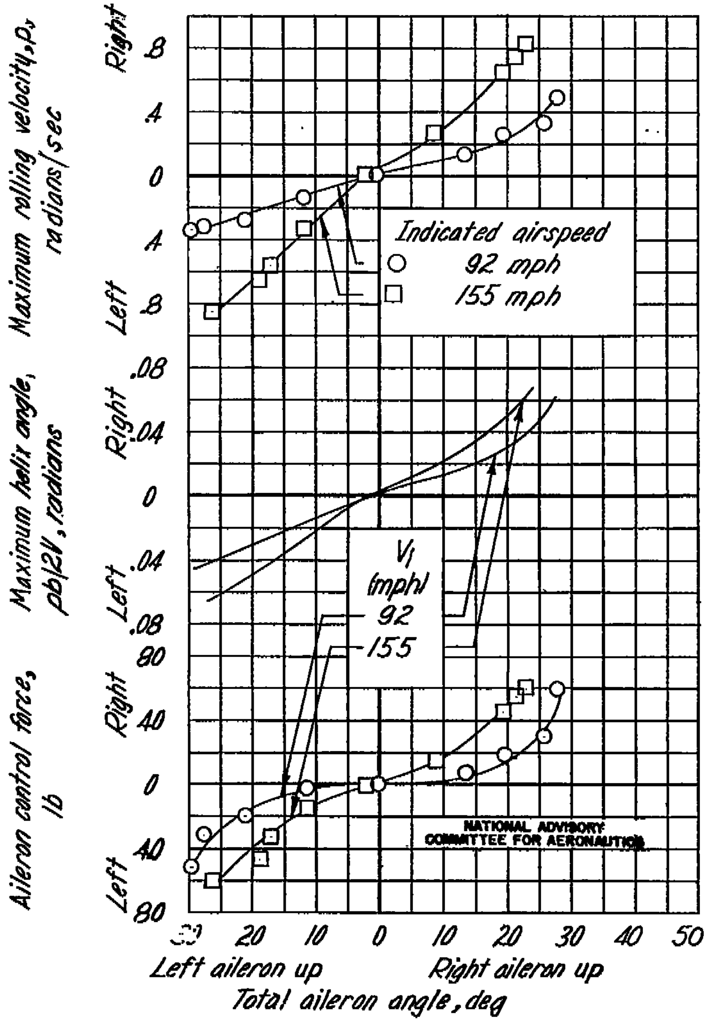

(b) Power off.

Figure B115.- Concluded.

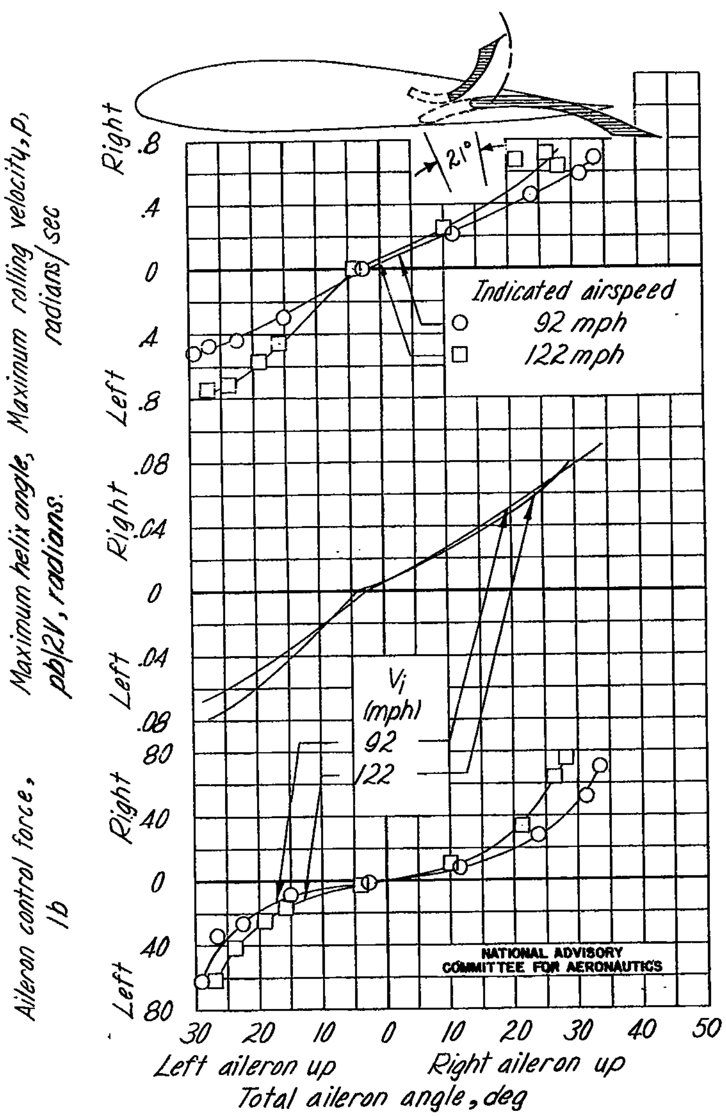

(a) Rated power.

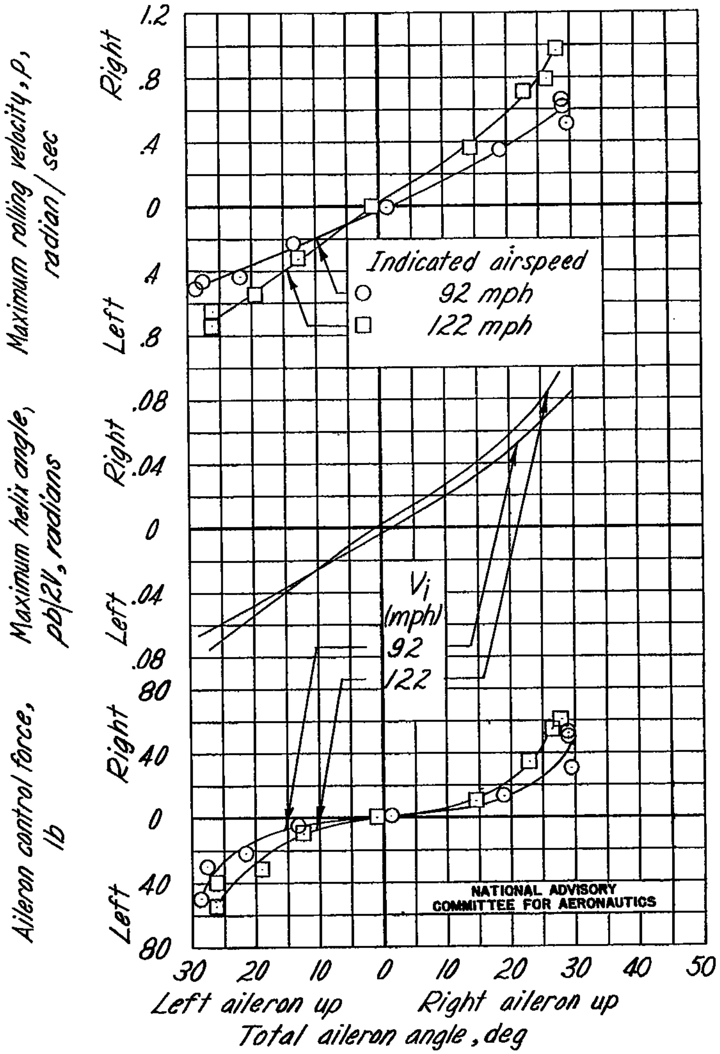

(b) Power off.

Figure B116.- Aileron control characteristics of the modified observation-scout type airplane; flaps half down; ailerons in original condition.

Figure B116.- Concluded.

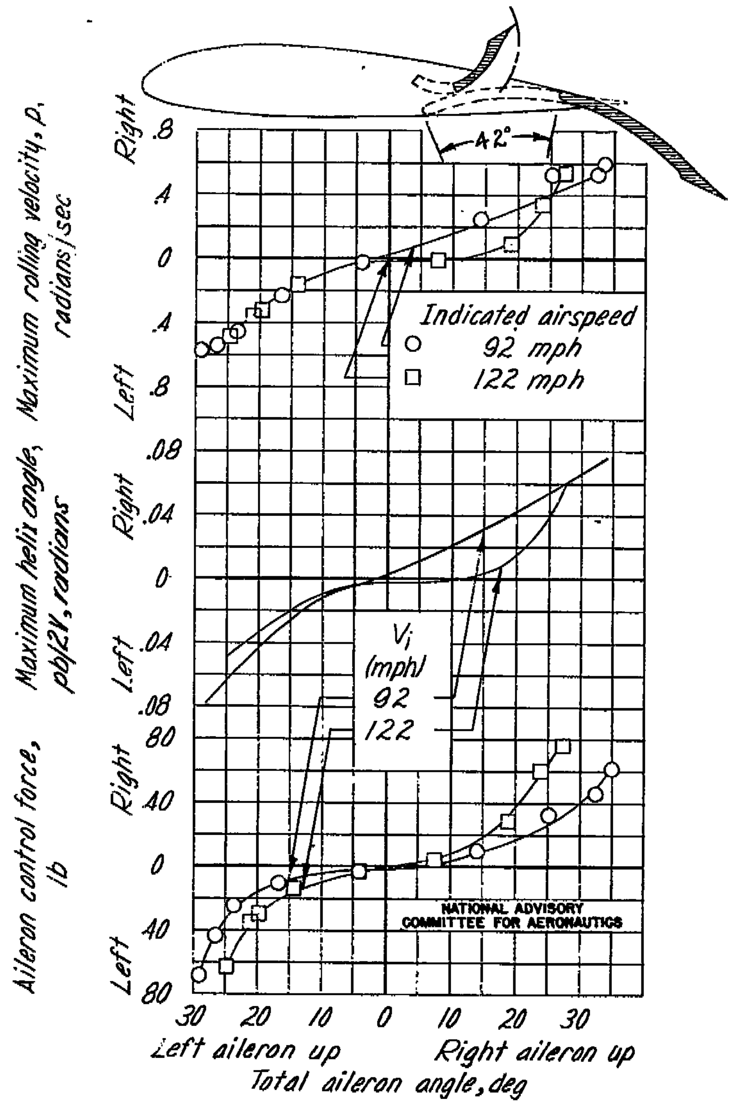

(a) Rated power.

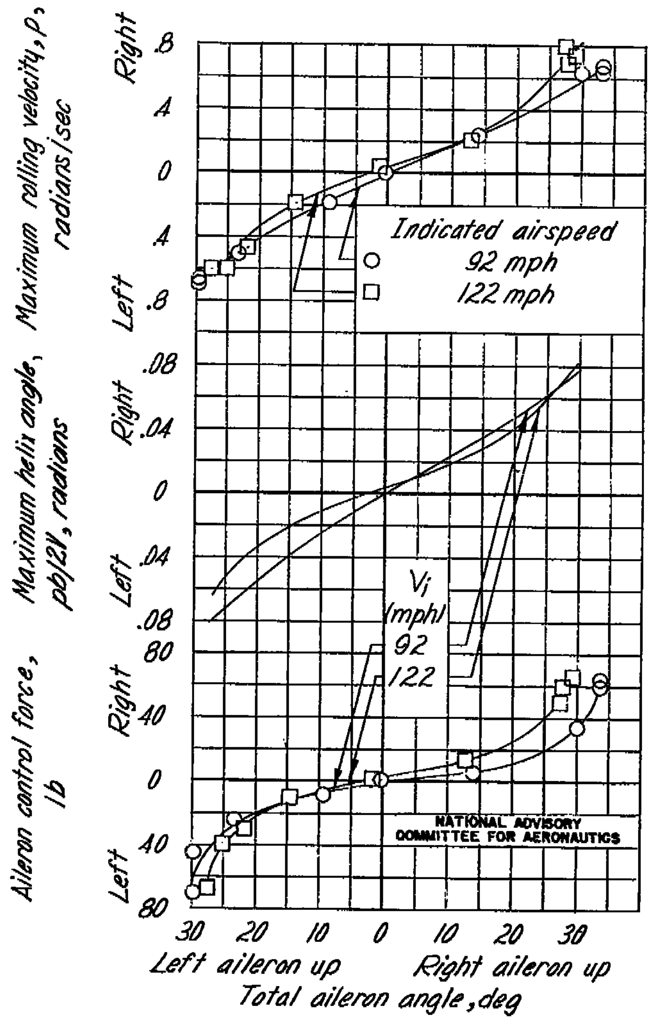

(b) Power off.

Figure B117.- Aileron control characteristics of the modified observation-scout type airplane; flaps down; ailerons in original condition.

Figure B117.- Concluded.

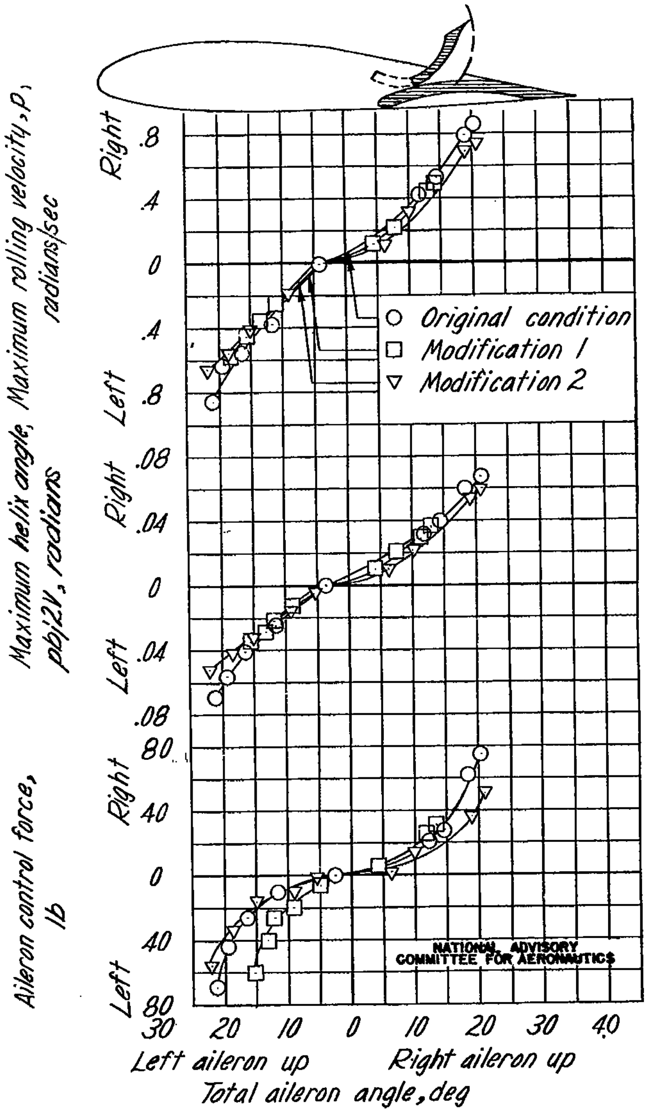

(a) Flaps up, 155 miles per hour.

Figure B118.- Aileron control characteristics of the modified observation-scout type airplane.

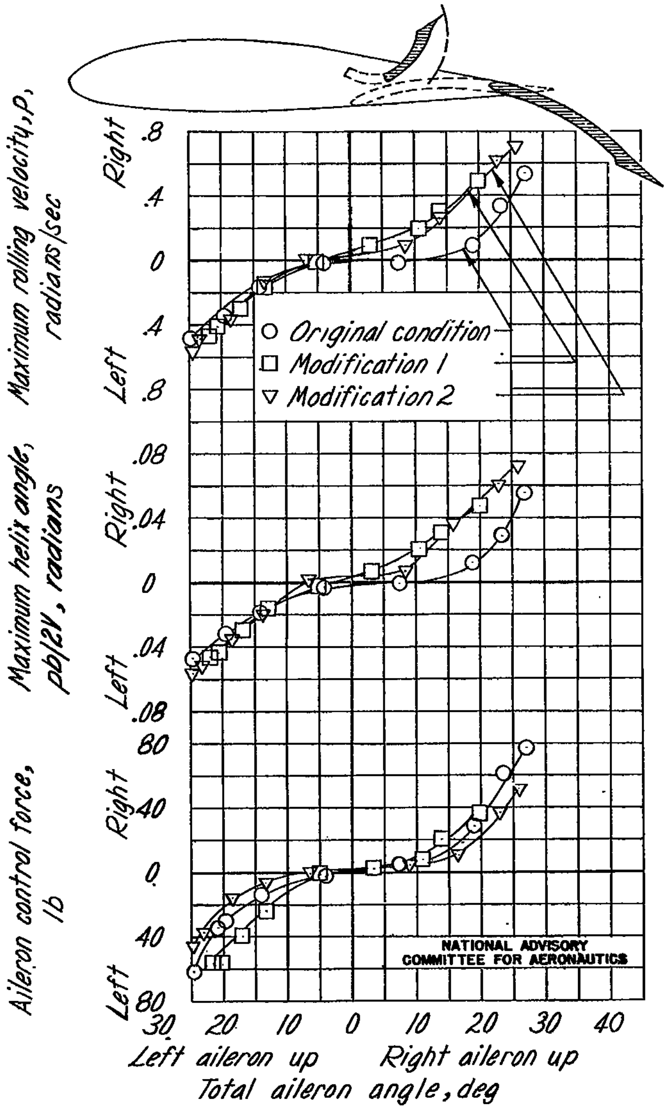

(b) Flaps down, 122 miles per hour.

Figure B118.- Concluded.

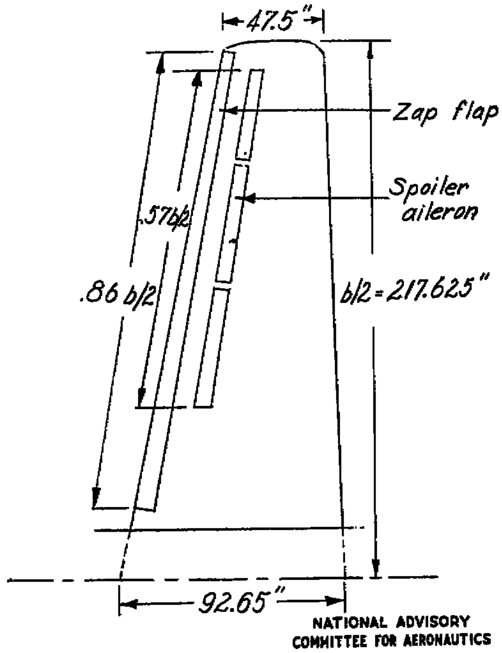

Figure B119.- Semispan wing of a modified observation-scout type airplane showing the Zap flap and spoiler ailerons as tested in flight at Ames.

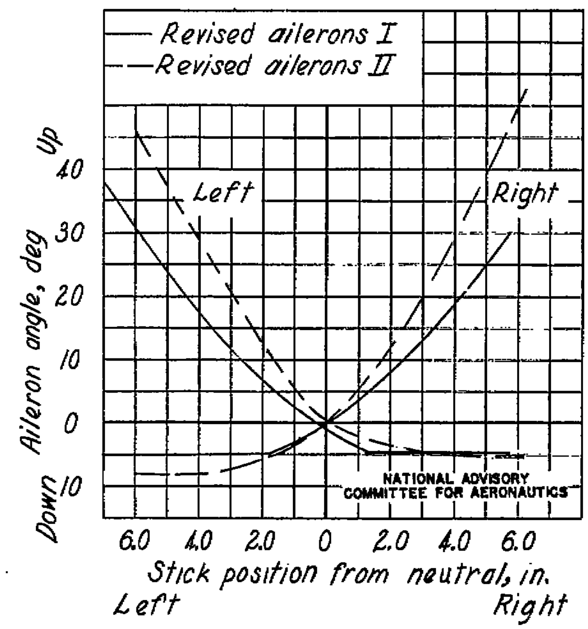

Figure B120.- Variation of stick position with aileron angle for the two sets of ailerons tested on the airplane.

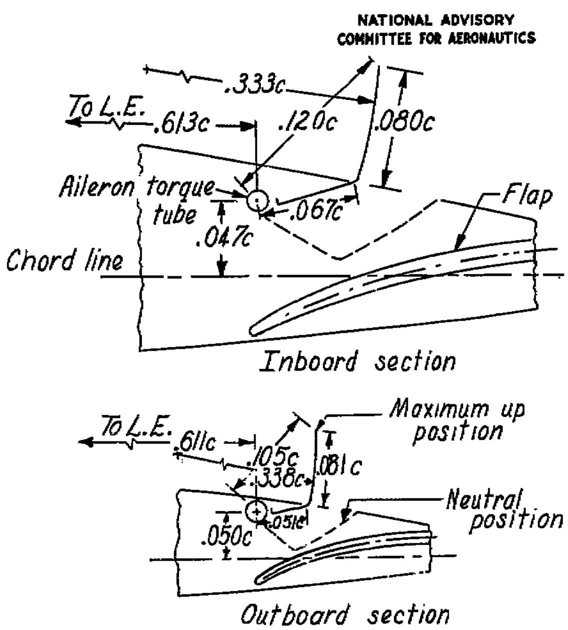

(a) Revised ailerons I.

Figure B121.- Section details of the spoiler ailerons tested on the airplane.

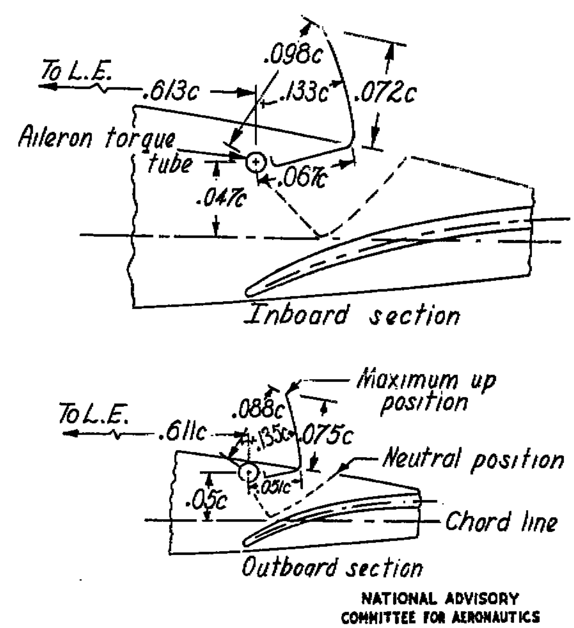

(b) Revised ailerons II.

Figure B121.- Concluded.

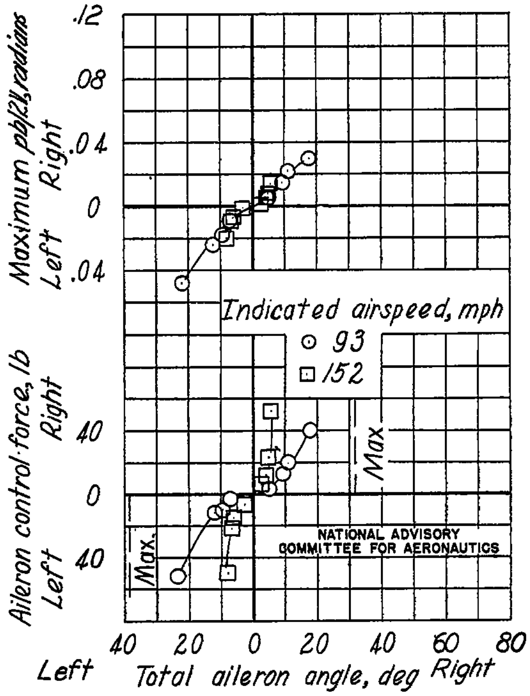

(a) Revised ailerons I.

Figure B122.- Aileron control characteristics of the modified observation-scout type airplane. Flaps up.

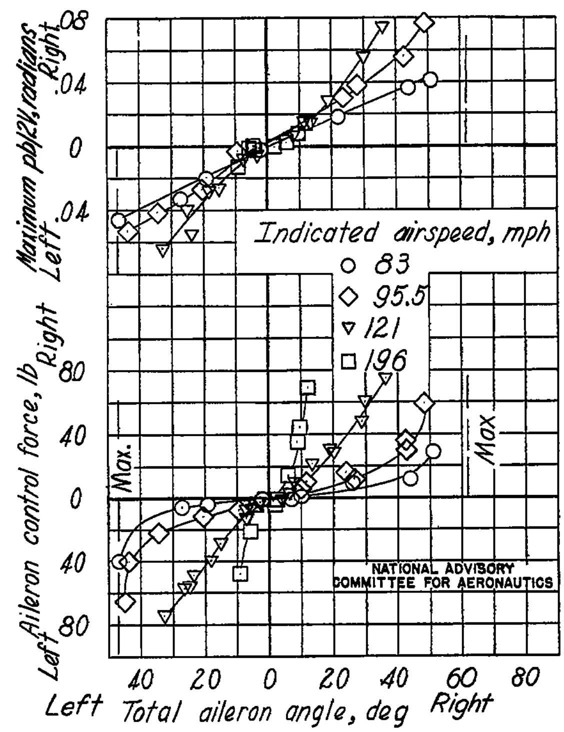

(b) Revised ailerons II.

Figure B122.- Concluded.

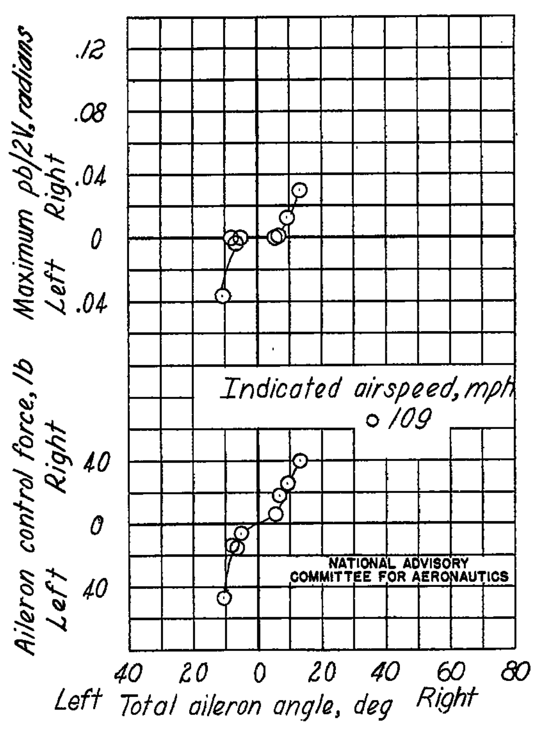

(a) Revised ailerons I.

Figure B123.- Aileron control characteristics of the modified observation-scout type airplane. Flaps down.

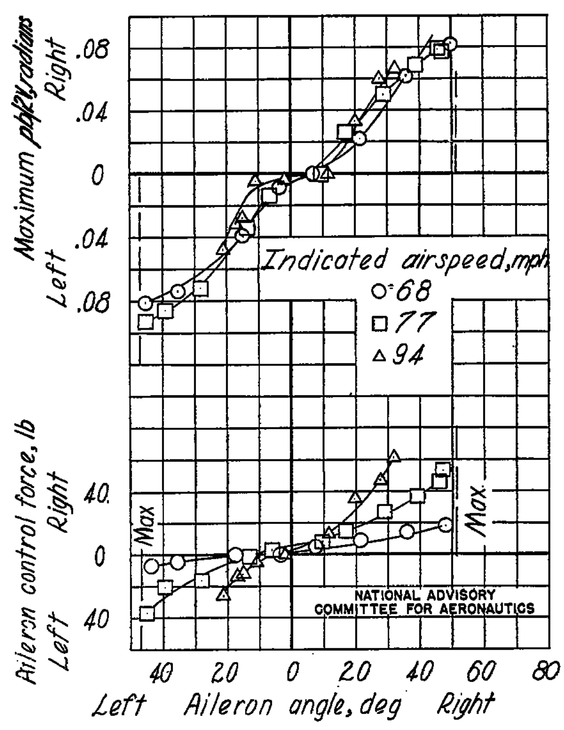

(b) Revised ailerons II.

Figure B123.- Concluded.

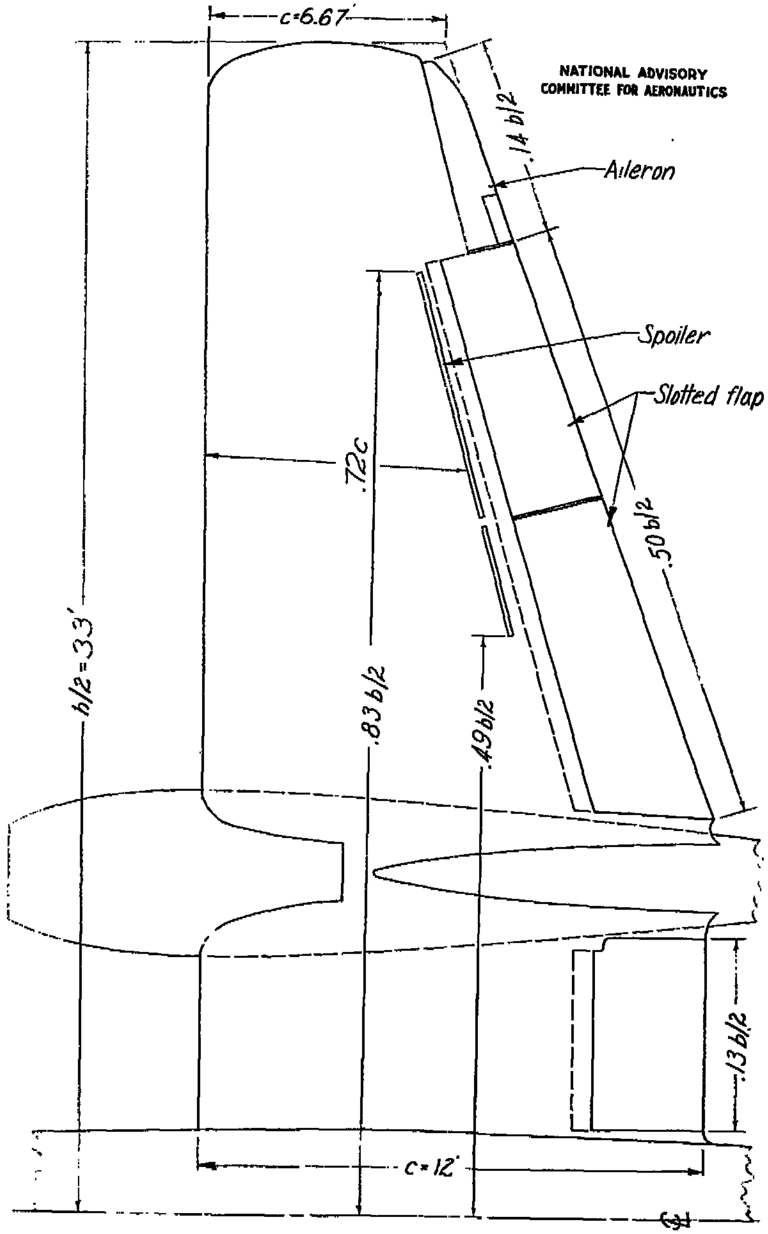

Figure B124.- Plan form of the semispan wing of a fighter-type airplane tested in flight at Ames.

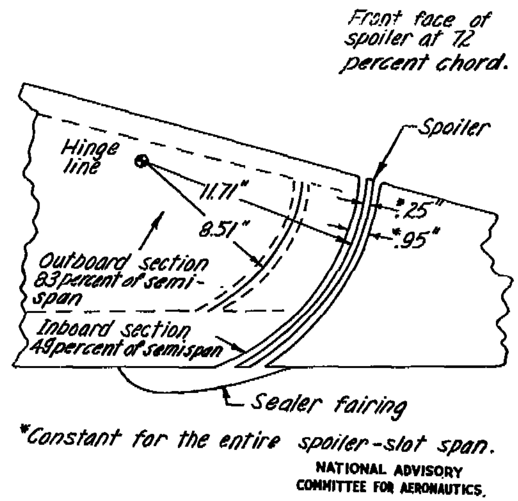

Figure B125.- Cut-away view of spoiler-slot arrangement on the wing of the fighter-type airplane.

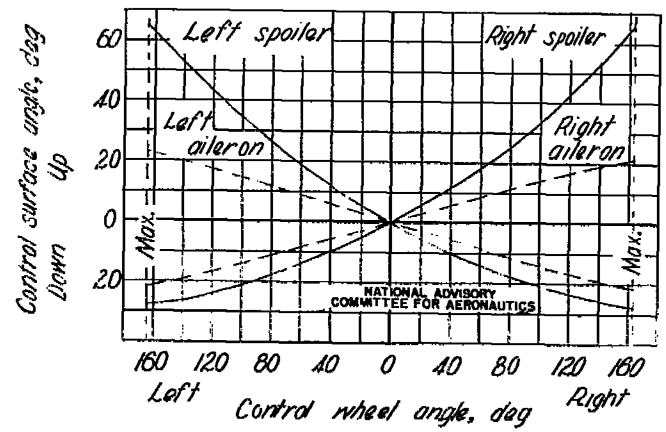

Figure B126.- Variation of lateral control-surface angle with control-wheel angle.

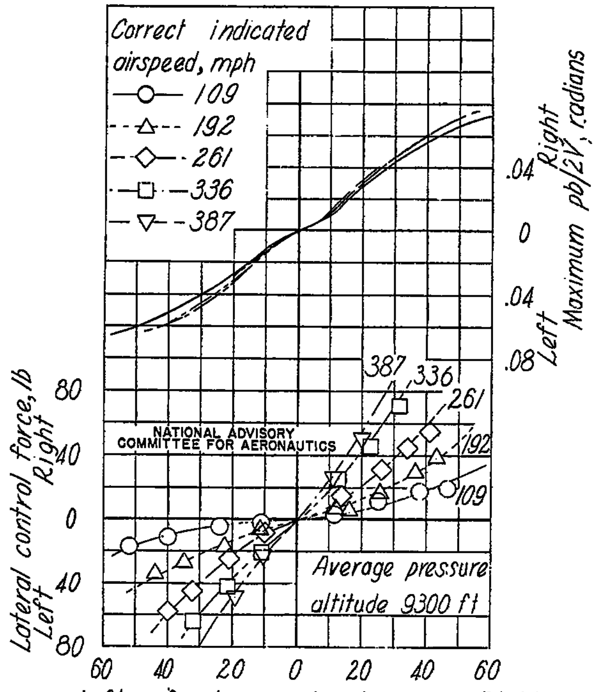

(a) Climb condition (power on, flaps up).

Figure B127.- Variation of the maximum helix angle pb/2V and control-wheel force with spoiler angle in abrupt rudder-fixed rolls. (Spoilers and ailerons deflected.)

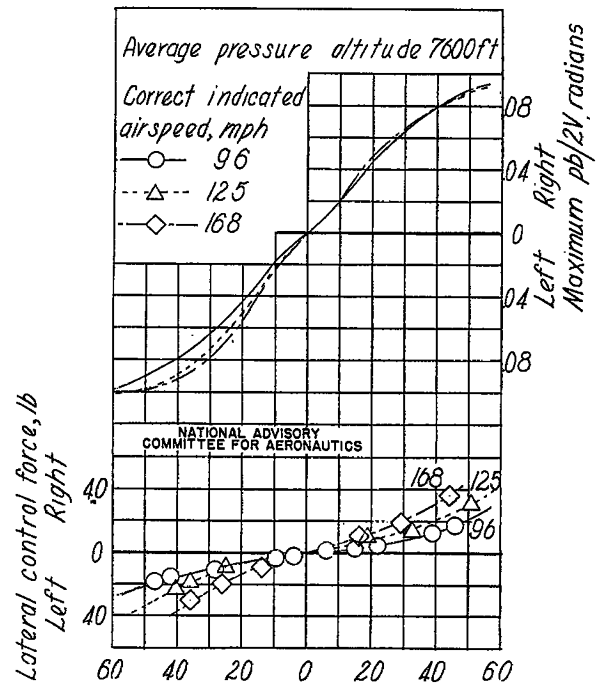

(c) Wave-off condition (power on, flaps down).

Figure B127.- Concluded.

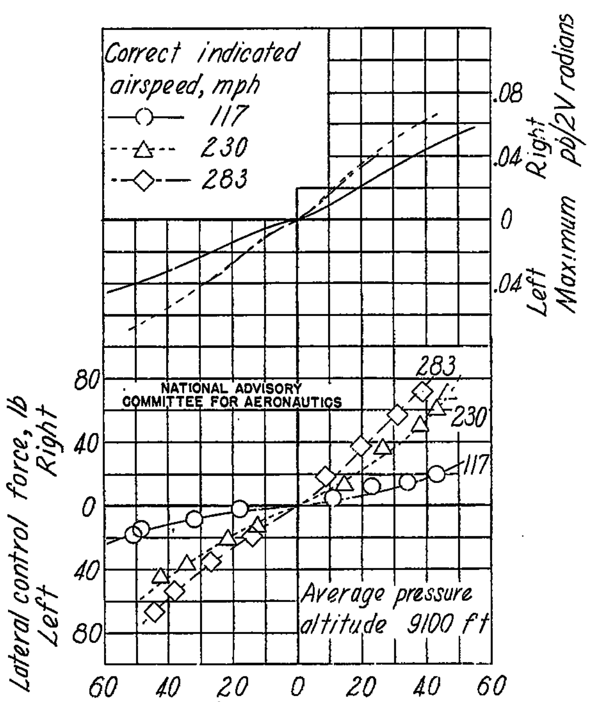

(b) Glide condition (power off, flaps up).

Figure B127.- Continued.

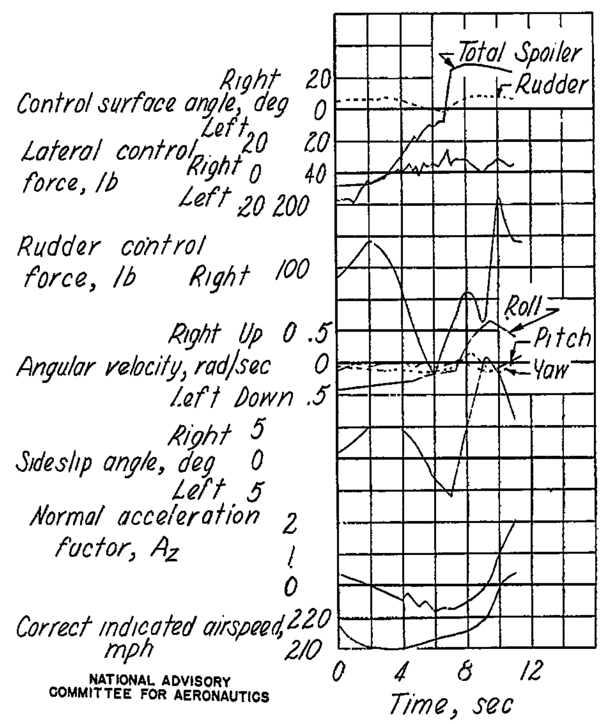

Figure B128.- Time history of a maneuver showing the spoiler effectiveness in approximately inverted flight. Ailerons fixed in neutral position, climb condition (power on, flaps up).

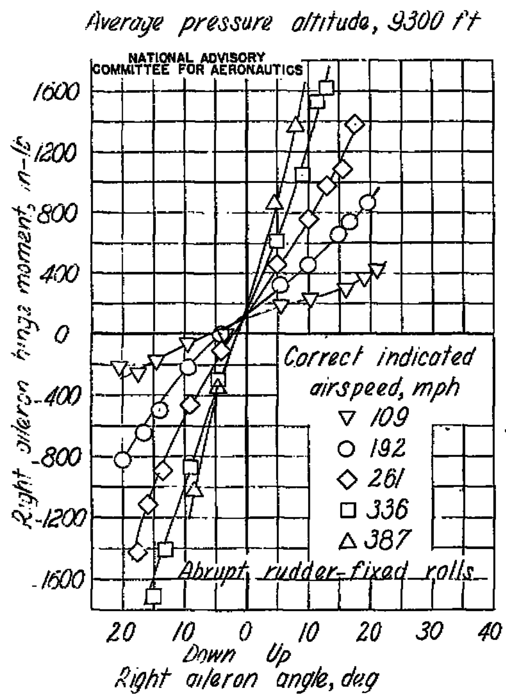

Figure B129.- Variation of right aileron hinge moment with aileron angle. Climb condition (power on, flaps up).

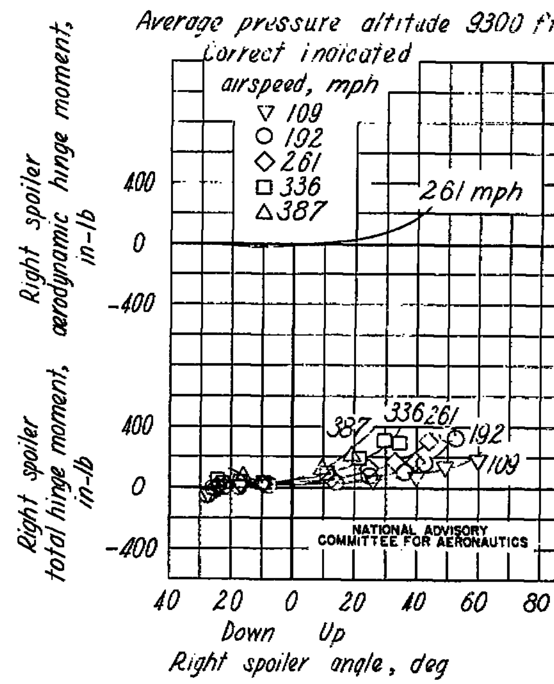

Figure B130.- Variation of right spoiler hinge moment with spoiler angle. Climb condition (power on, flaps up).

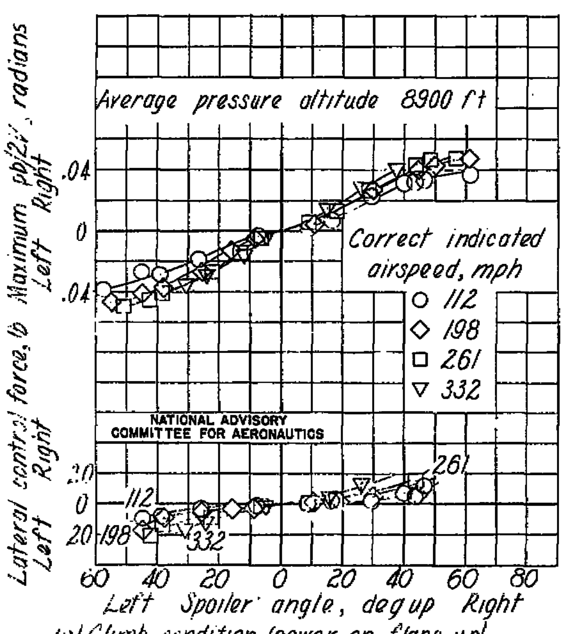

Figure B131.- Variation of the maximum helix angle pb/2V and control-wheel force with spoiler angle in abrupt rudder-fixed rolls. (Ailerons fixed in neutral position).

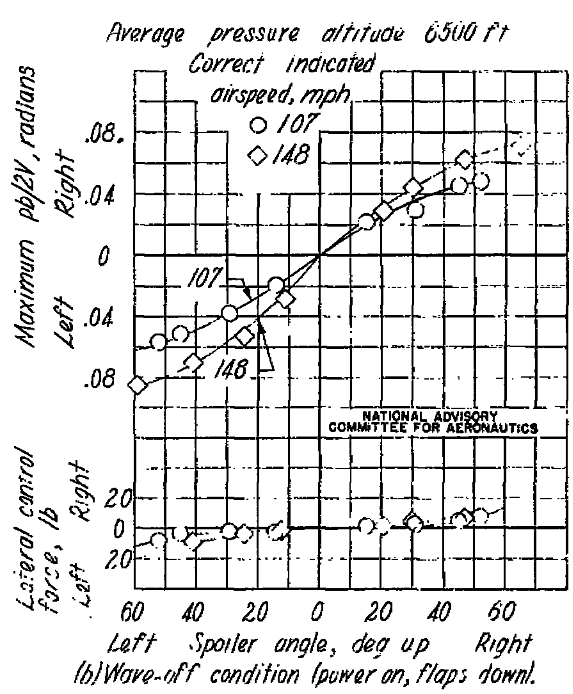

Figure 131.- Concluded.

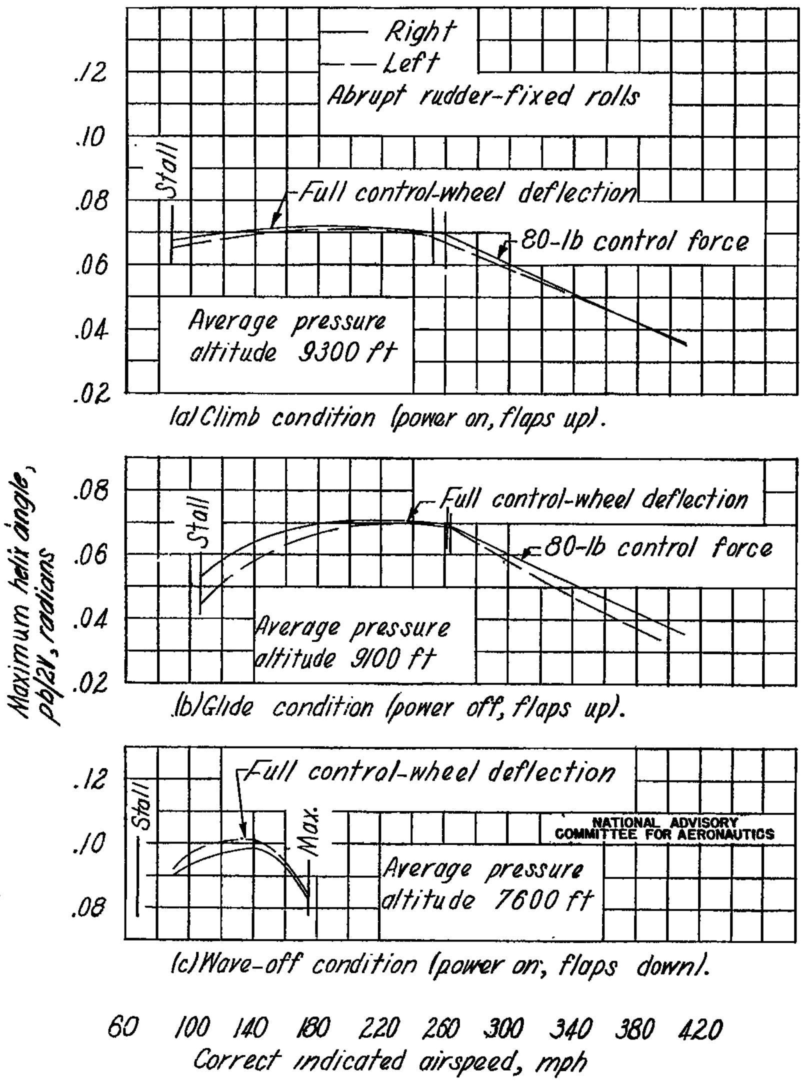

Figure B132.- Variation of maximum helix angle with airspeed in right and left rudder-fixed rolls. (Spoilers and ailerons deflected.)

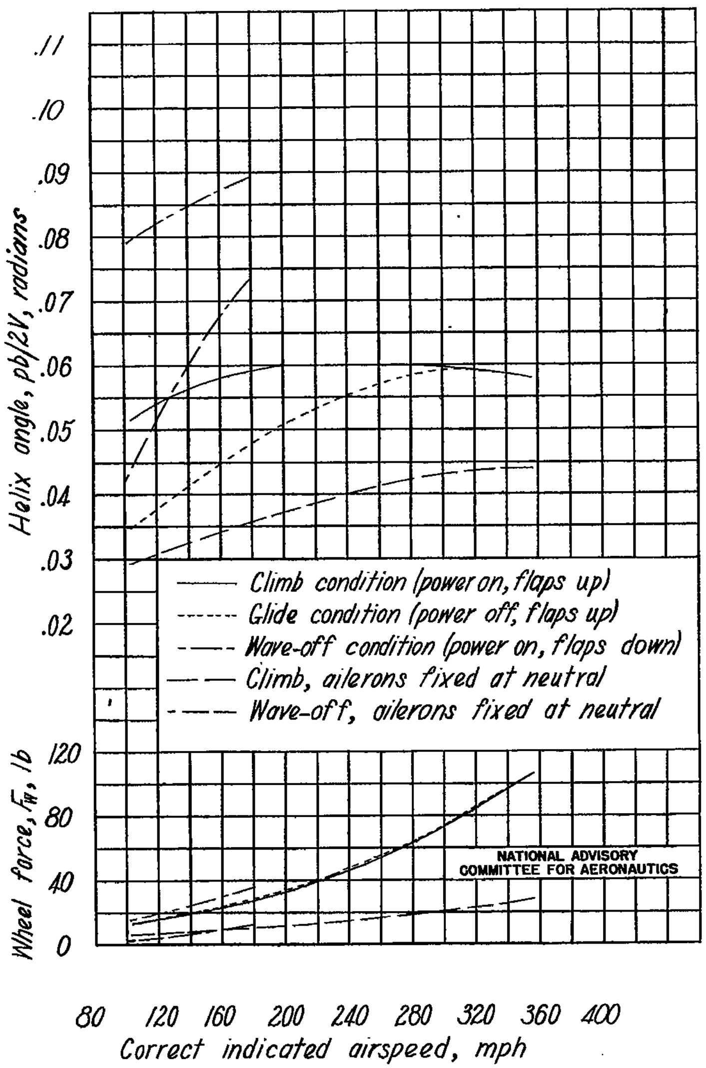

Figure B133.- Variation of maximum helix angle and wheel force with airspeed. Spoiler deflected 40° up. (Spoilers and ailerons deflected unless otherwise indicated.)

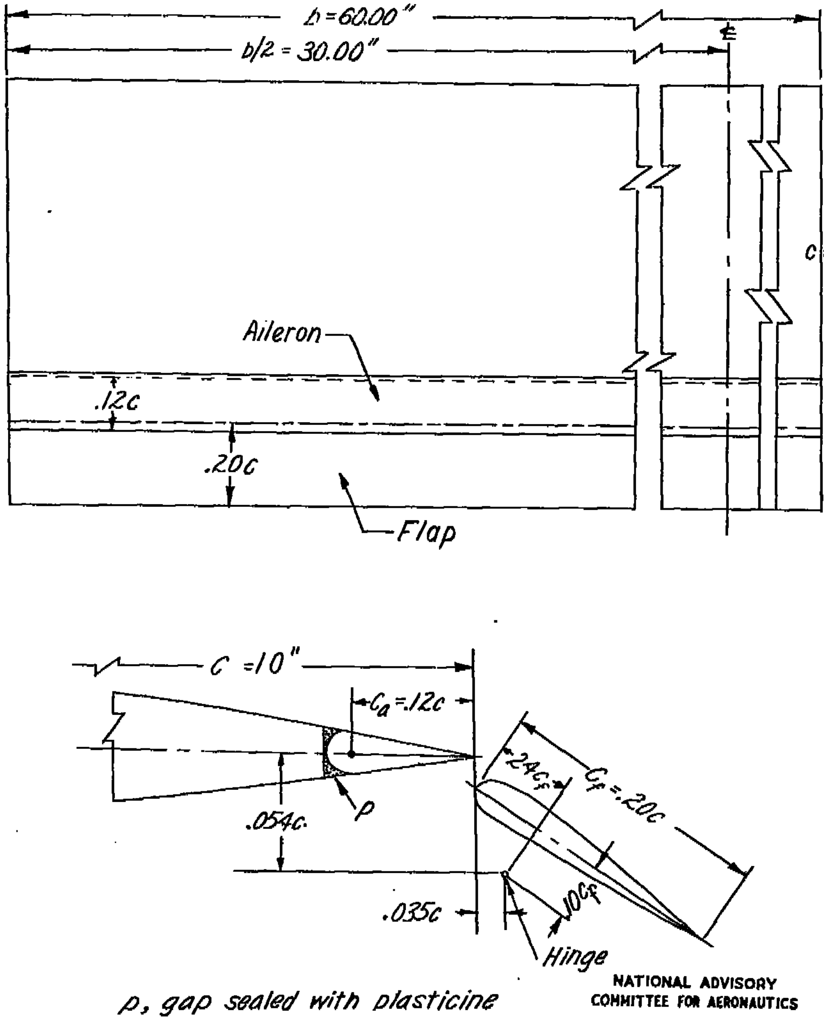

[illegible] C1 - Plan form and section of the 10- by 60-inch NACA [illegible] wing with 0.[illegible] NACA [illegible] external-airfoil flaps and full-span 0.[illegible] ordinary ailerons tested in the Langley [illegible] tunnel.

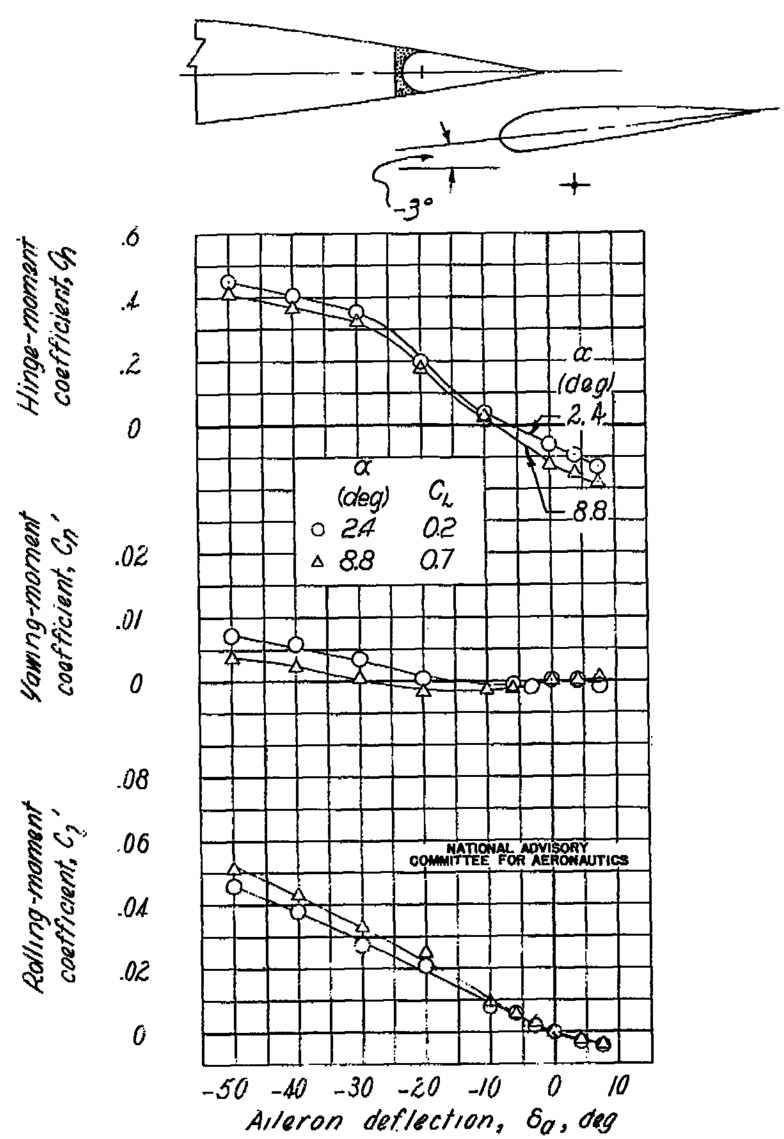

(a) δ_f, -3°.

[illegible] Aerodynamic characteristics of the full-span 0.12c ailerons on the NACA 23012 wing.

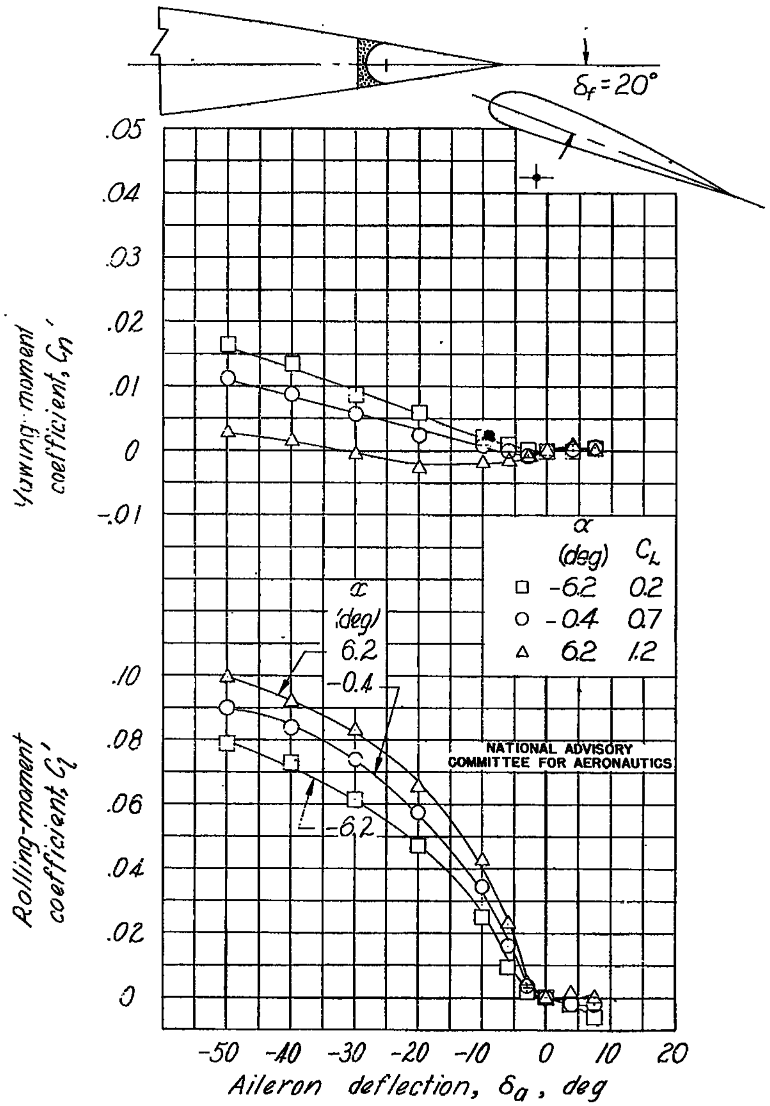

(b) δ_f, 20°.

Figure C2.- Continued.

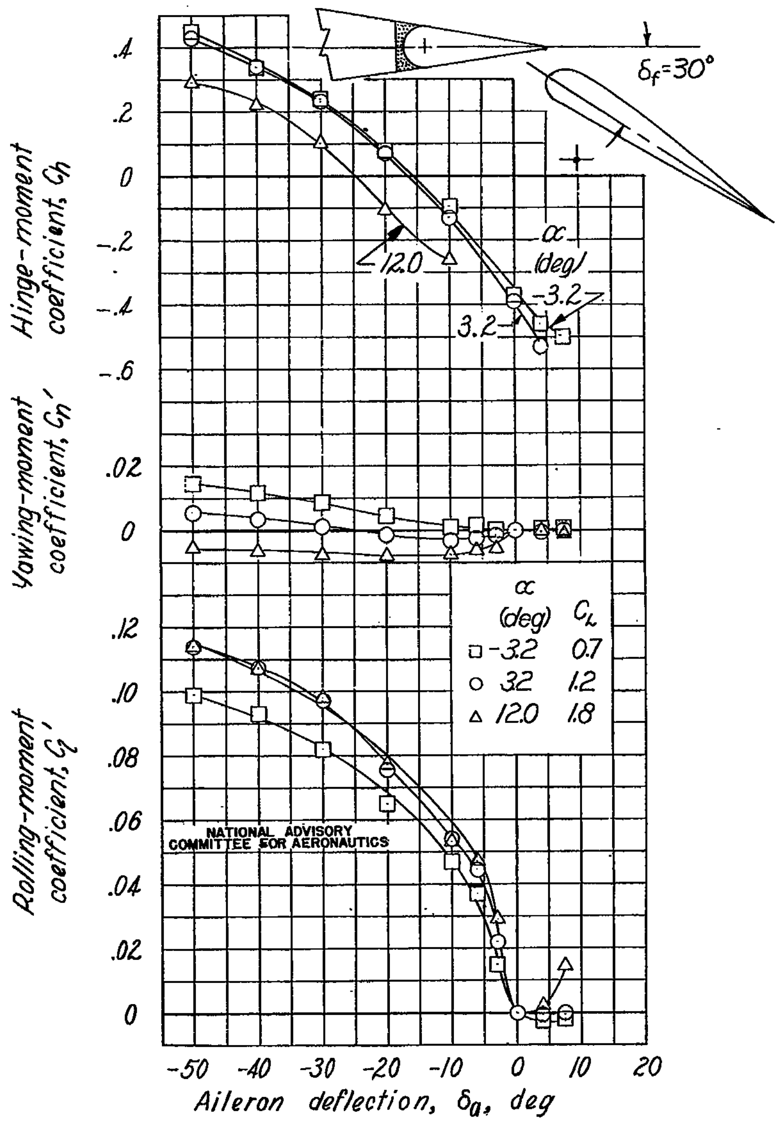

(c) δ_f, 30°.

Figure C2.- Concluded.

Model C-II

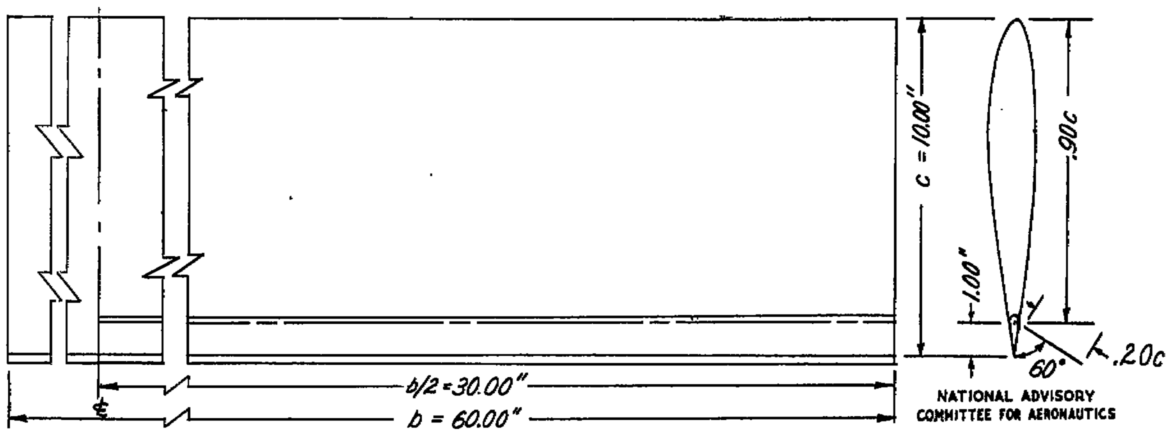

Figure C3.- The rectangular 10- by 60-inch NACA 23012 wing with a 0.10c by 1.00 b/2 plain aileron and full-span 0.20c split flaps at 0.90c. Tested in the Langley 7- by 10-foot tunnel.

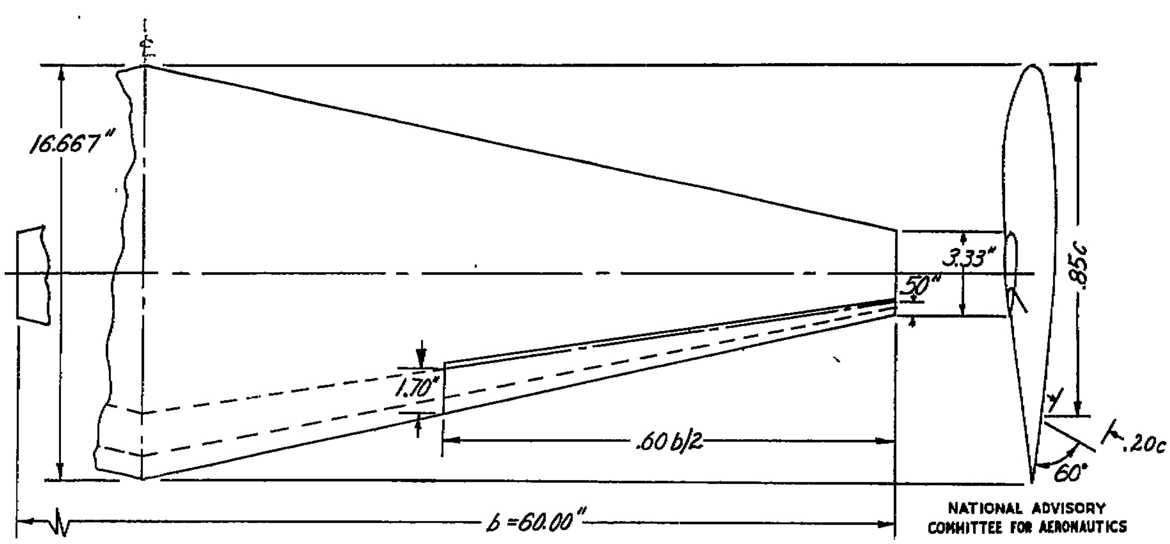

Figure C4.- The 5:1 tapered NACA 23012 wing with a 0.15c by 0.60 b/2 plain aileron and full-span 0.20c split flaps at 0.85c. Tested in the Langley 7- by 10-foot tunnel.

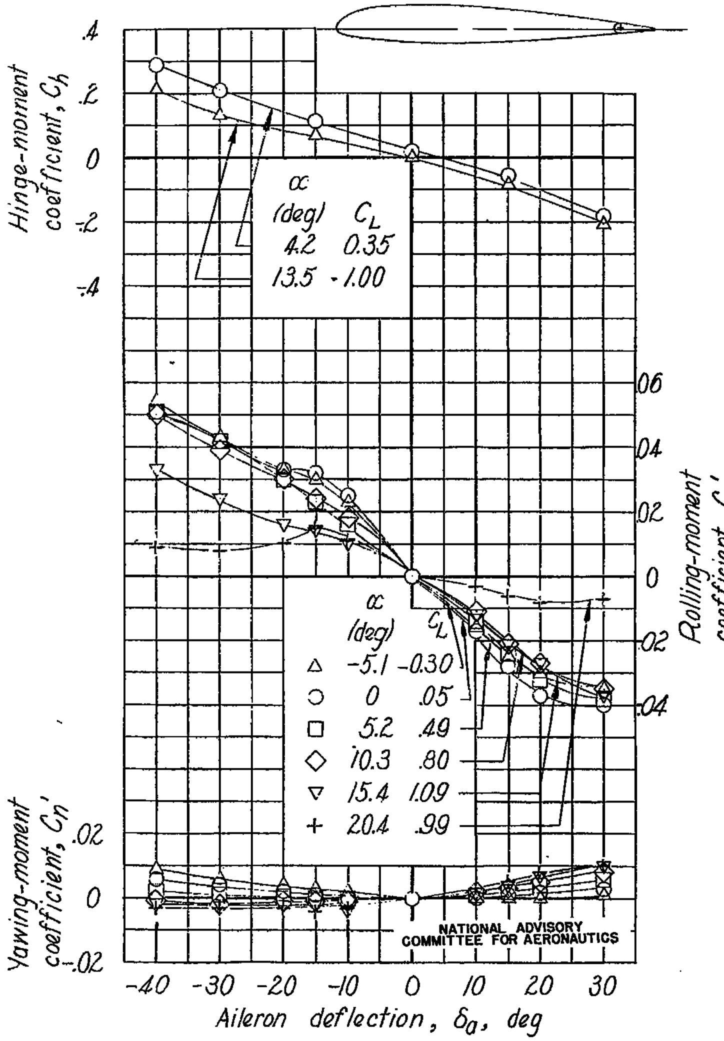

(a) Flap neutral.

Figure C5.- Aileron characteristics of a 0.10c by 1.00 b/2 plain aileron on a rectangular NACA 23012 wing with full-span 0.20c split flaps.

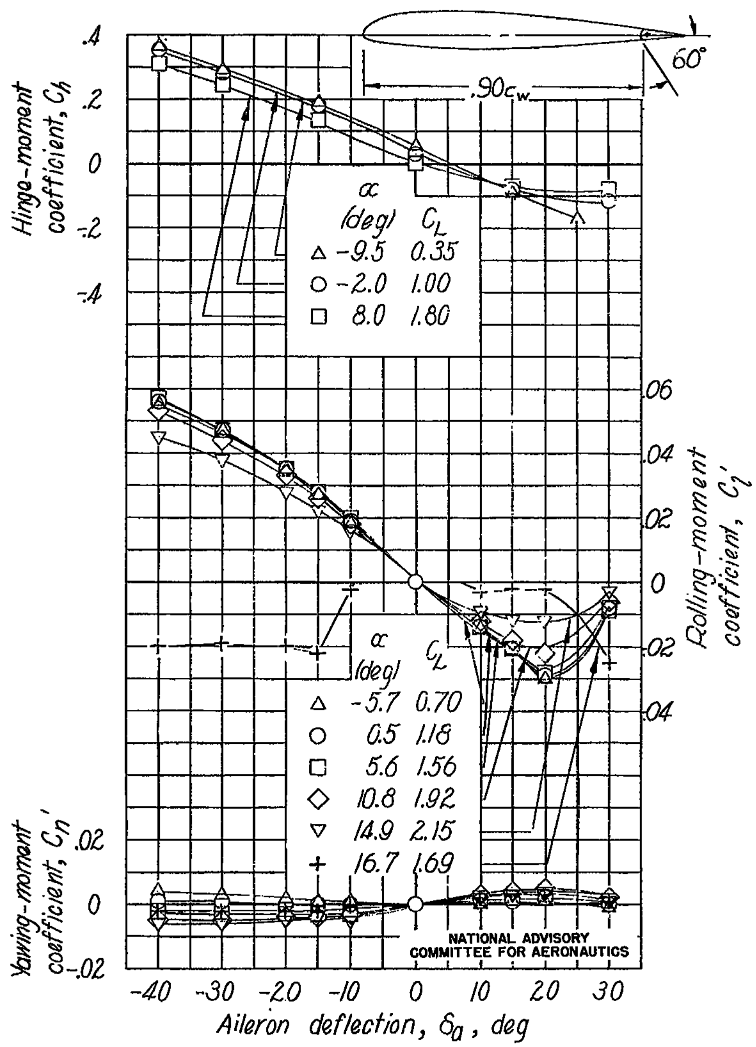

(b) Flap deflection, 60°.

Figure C5.- Concluded.

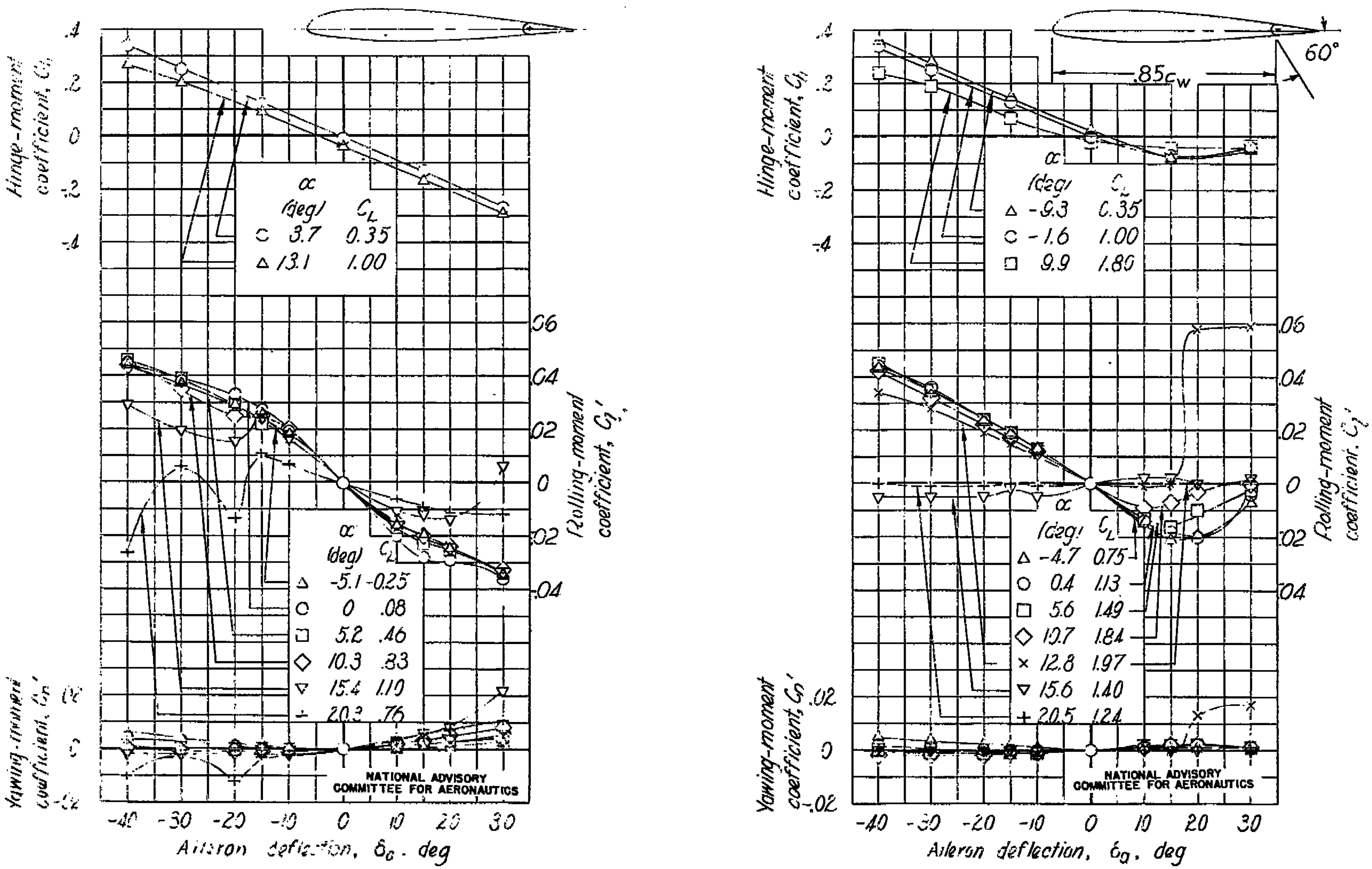

(a) Flap neutral.

(b) Flap 60°.

Figure C6.- Aileron characteristics of a 0.15c by 0.83 b/2 plain aileron on the 5:1 tapered NACA 23012 wing with full-span 0.20c split flaps.

Figure C6.- Concluded.

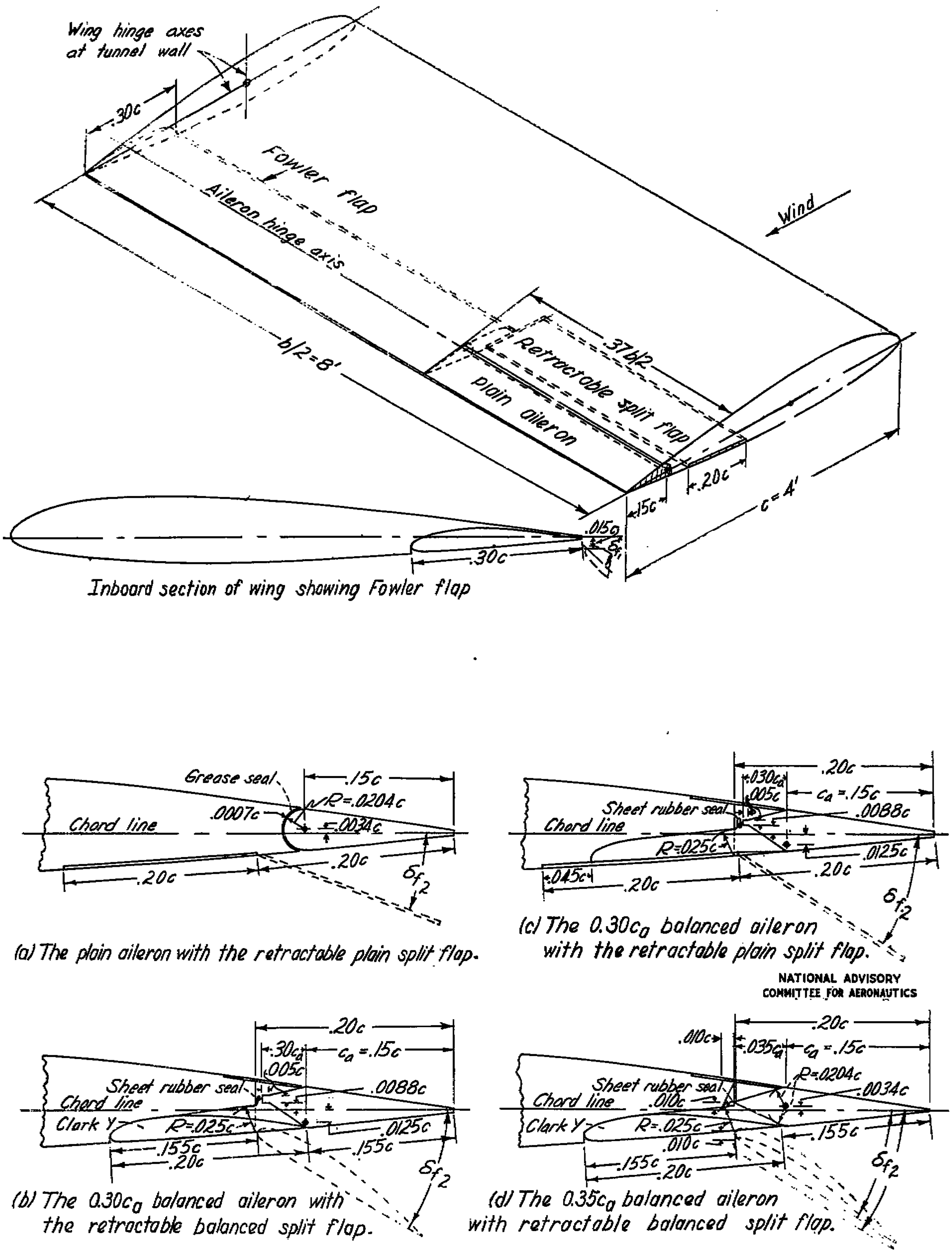

NATIONAL ADVISORY COMMITTEE FOR AERONAUTICS

Figure C7.- The NACA 23012 wing with a 0.30c by 0.63 b/2 inboard Fowler flap and four combinations of 0.15c by 0.37 b/2 sealed ailerons and 0.20c by 0.37 b/2 outboard retractable split flaps as tested in the Langley 7- by 10-foot tunnel.

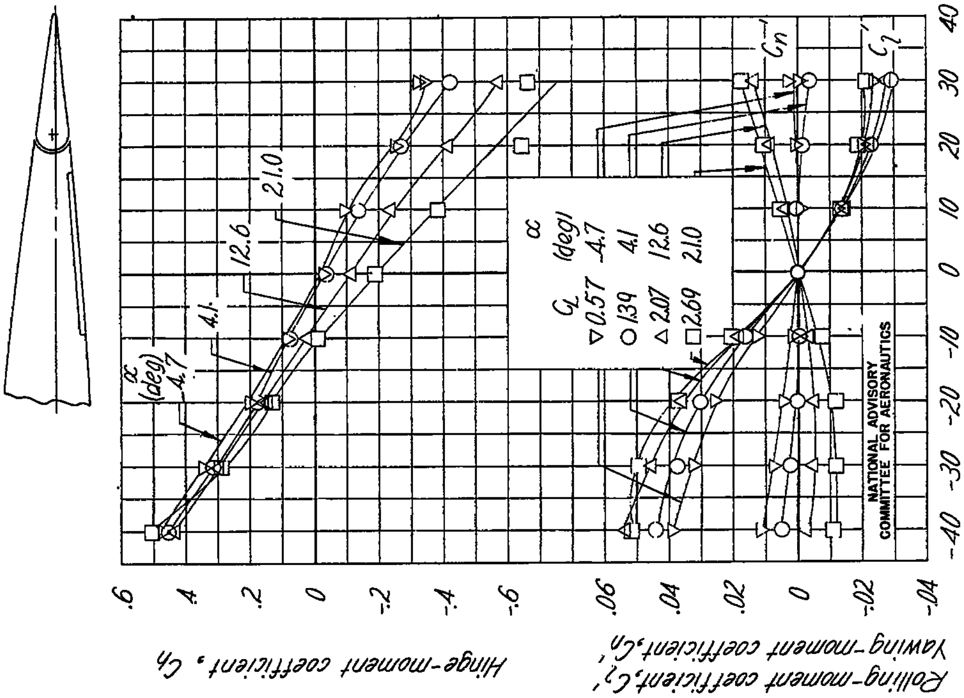

(b) δ_{f_1}, 40°; δ_{f_2}, 0°.

Figure C8.- Continued.

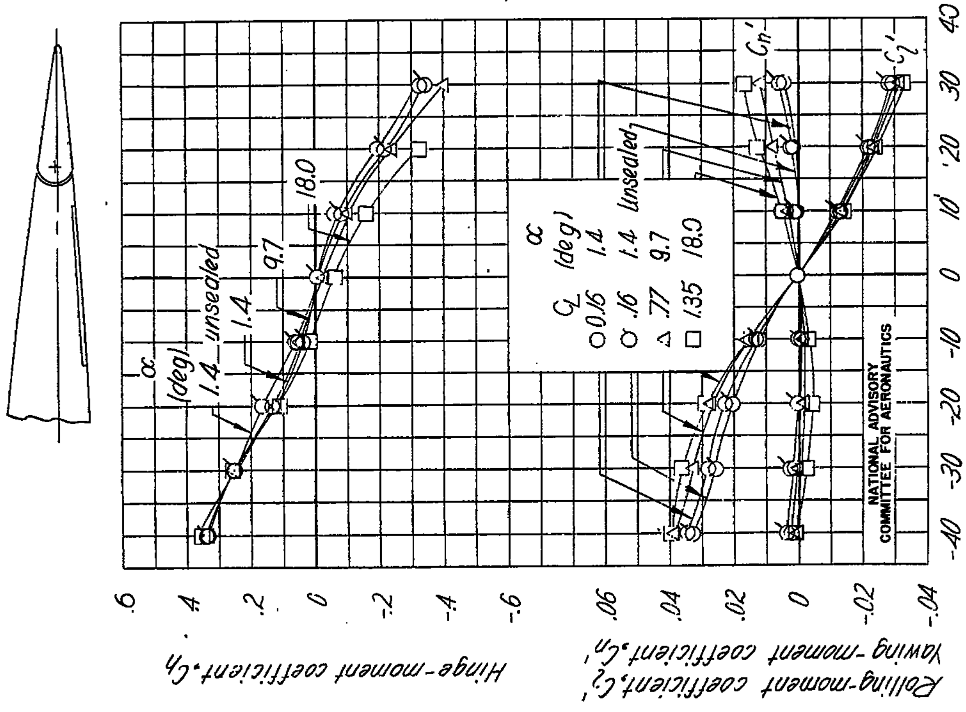

(a) δ_{f_1}, 0°; δ_{f_2}, 0°.

Figure C8.- Aerodynamic characteristics of a 0.15c by 0.37 b/2 plain sealed aileron on an NACA 23012 wing with a 0.30c by 0.63 b/2 inboard Fowler flap (f_1) and a 0.20c by 0.37 b/2 outboard retractable plain split flap (f_2).

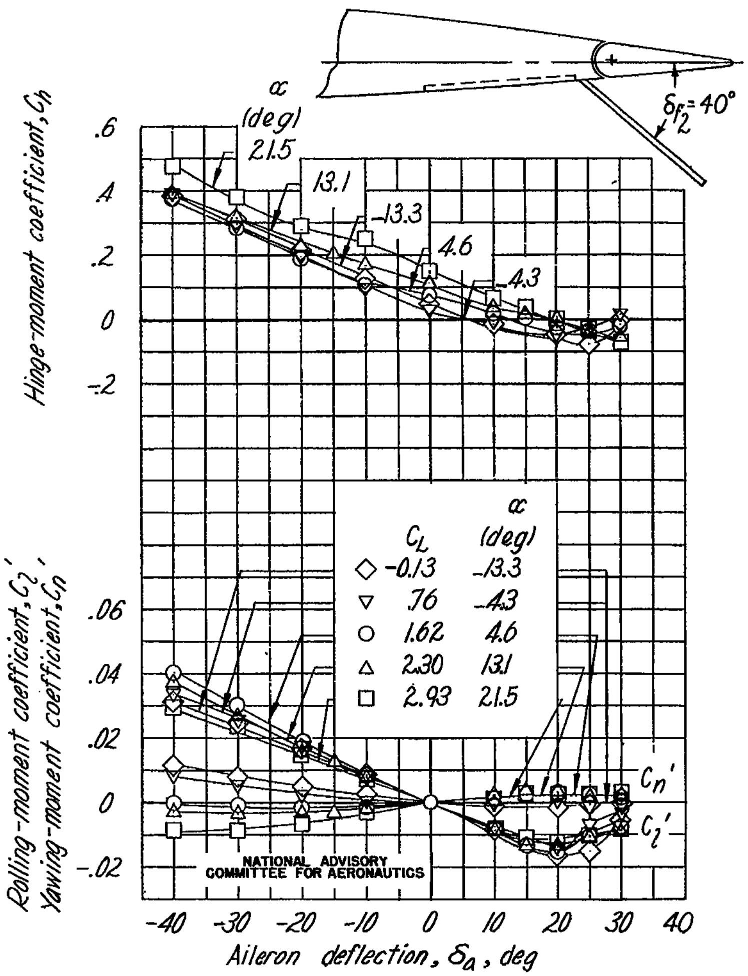

(c) δ_{f_1}, 40°; δ_{f_2}, 40°.

Figure C8.- Continued.

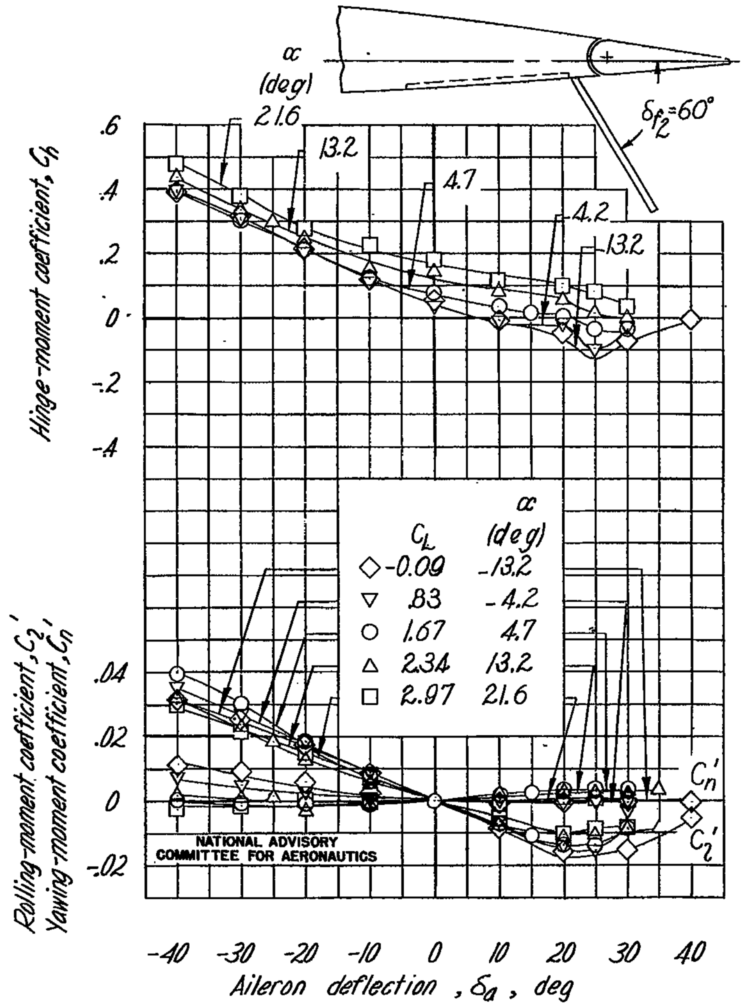

(d) δ_{f_1}, 40°; δ_{f_2}, 60°.

Figure C8.- Concluded.

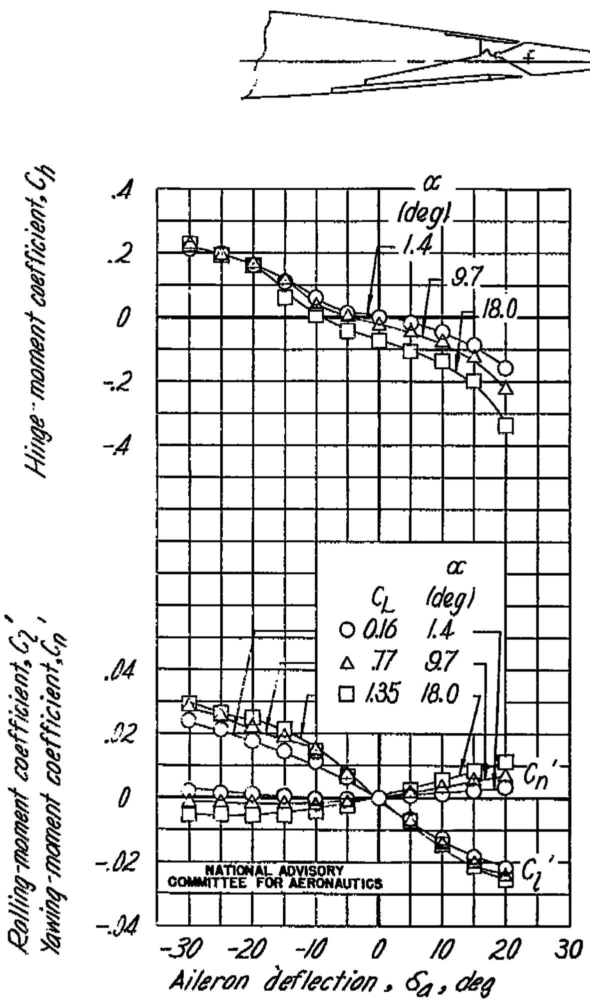

(a) δ_{f_1}, 0°; δ_{f_2}, 0°.

Figure C9.- Aerodynamic characteristics of a 0.15c by 0.37 b/2 sealed aileron with $0.30c_a$ balance on an NACA 23012 wing with a 0.30c by 0.63 b/2 inboard Fowler flap (f_1) and a 0.20c by 0.37 b/2 outboard retractable plain split flap (f_2).

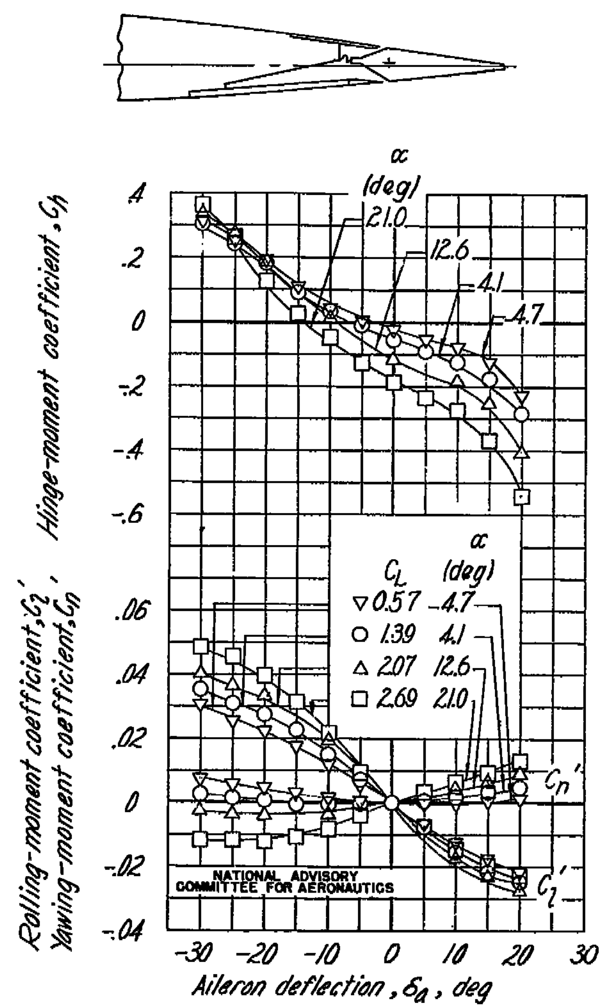

(b) δ_{f_1}, 40°; δ_{f_2}, 0°.

Figure C9.- Continued.

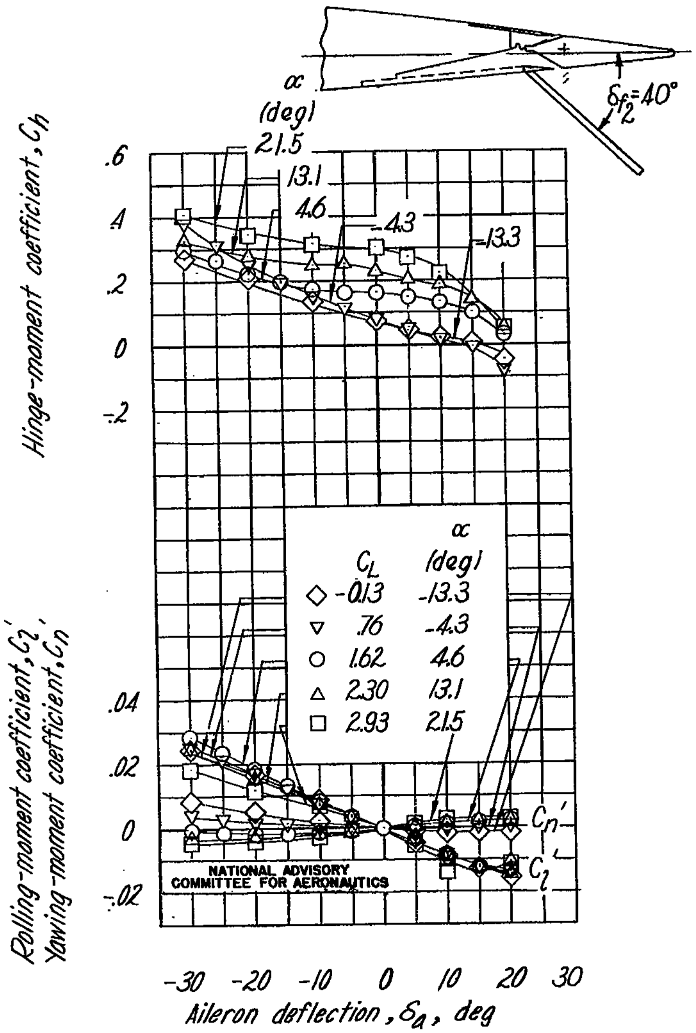

(c) δ_{f_1}, 40°; δ_{f_2}, 40°.

Figure C9.- Continued.

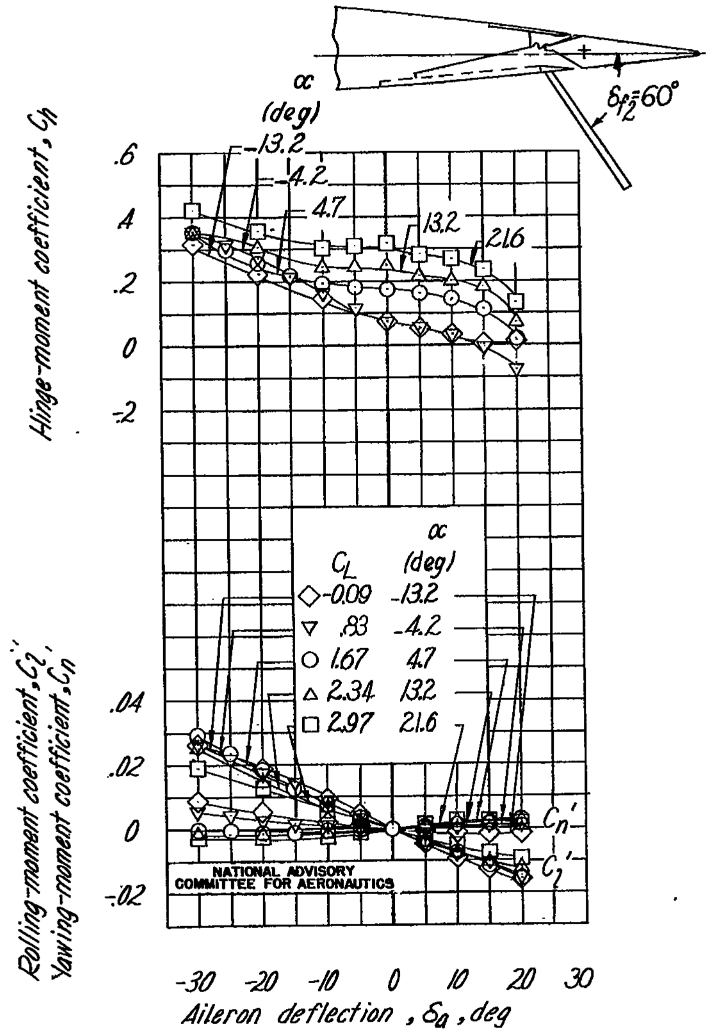

(d) δ_{f_1}, 40°; δ_{f_2}, 60°.

Figure C9.- Concluded.

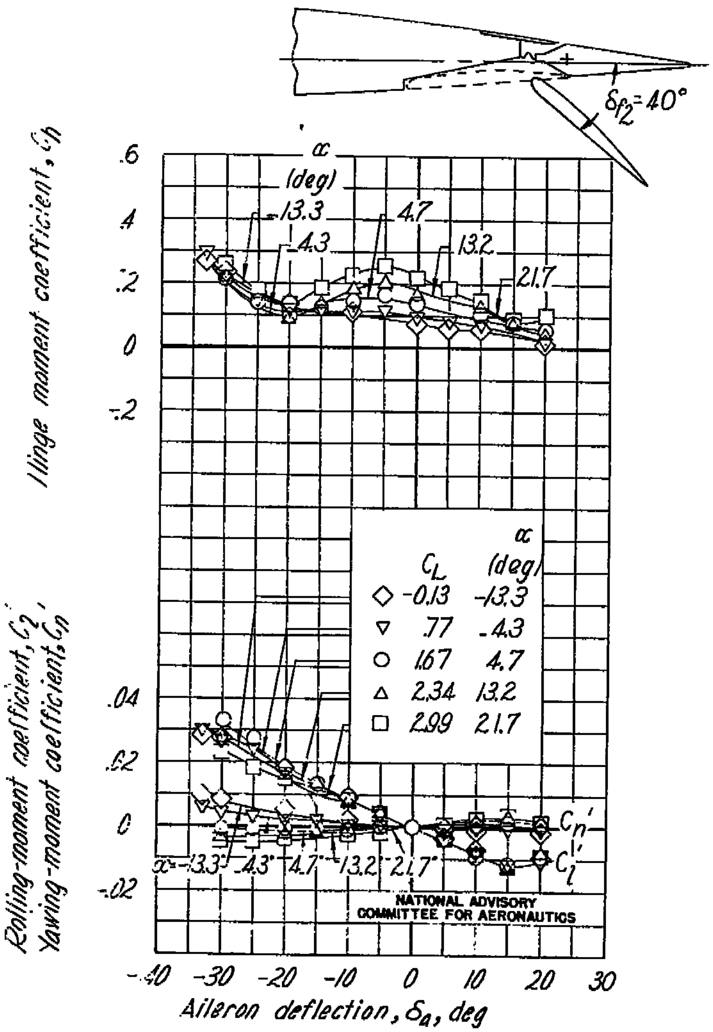

(a) δ_{f_1}, 40°; δ_{f_2}, 40°.

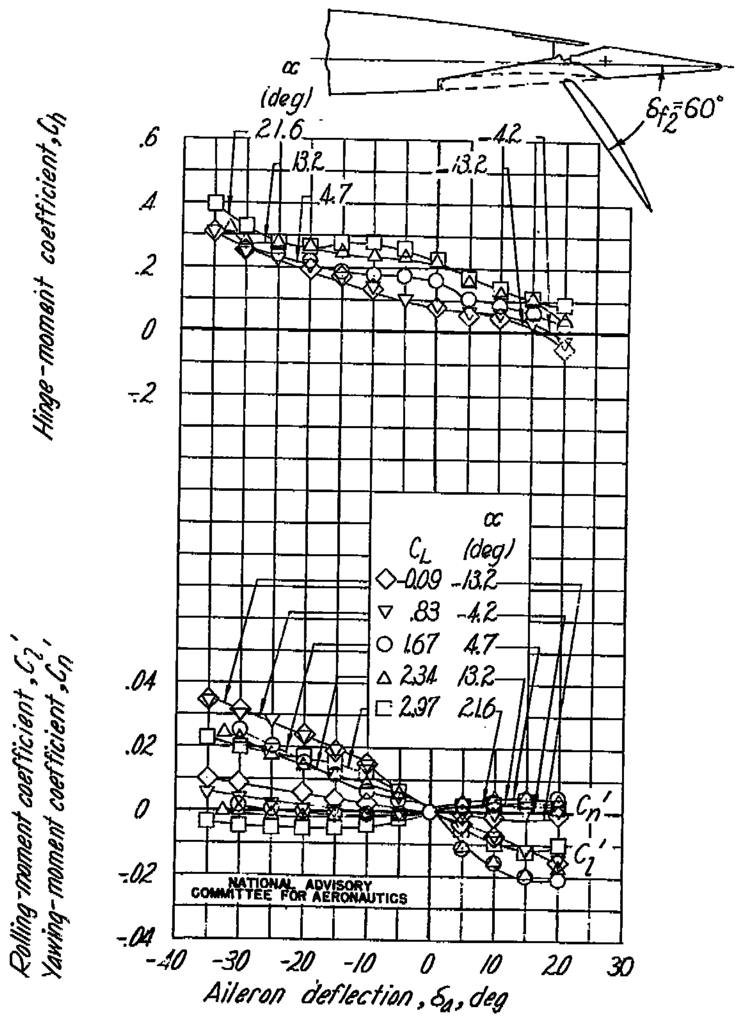

(b) δ_{f_1}, 40°; δ_{f_2}, 60°.

Figure C10.- Aerodynamic characteristics of a 0.15c by 0.37 b/2 sealed aileron with $0.30c_a$ balance on an NACA 23012 wing with a 0.30c by 0.63 b/2 inboard Fowler flap (f_1) and a 0.20c by 0.37 b/2 outboard retractable balanced split flap (f_2).

Figure C10.- Concluded.

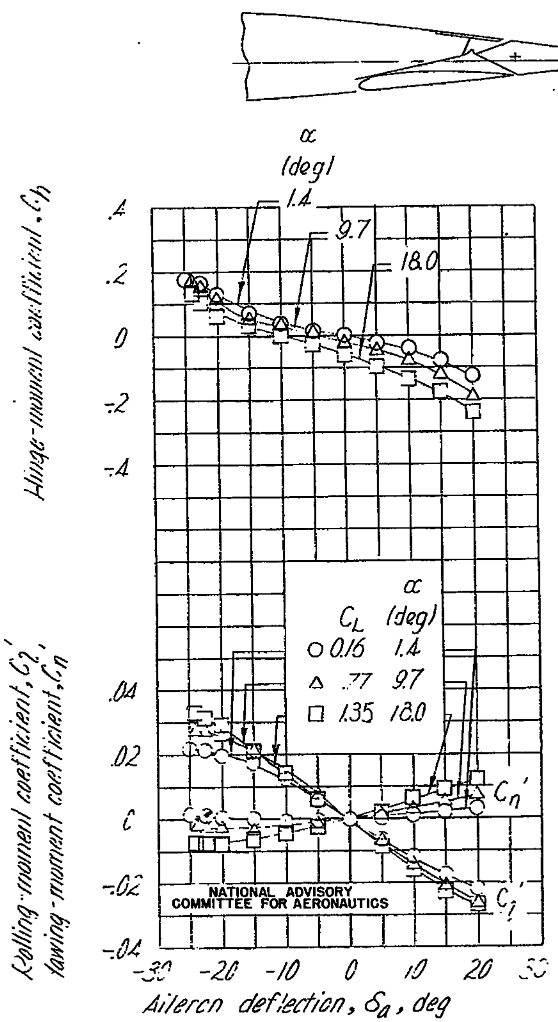

(a) δ_{f_1}, 0°; δ_{f_2}, 0°.

Figure C11.- Aerodynamic characteristics of a 0.15c by 0.37 b/2 sealed aileron with $0.35c_a$ balance on an NACA 23012 wing with a 0.30c by 0.63 b/2 inboard Fowler flap (f_1) and a 0.20c by 0.37 b/2 outboard retractable balanced split flap (f_2).

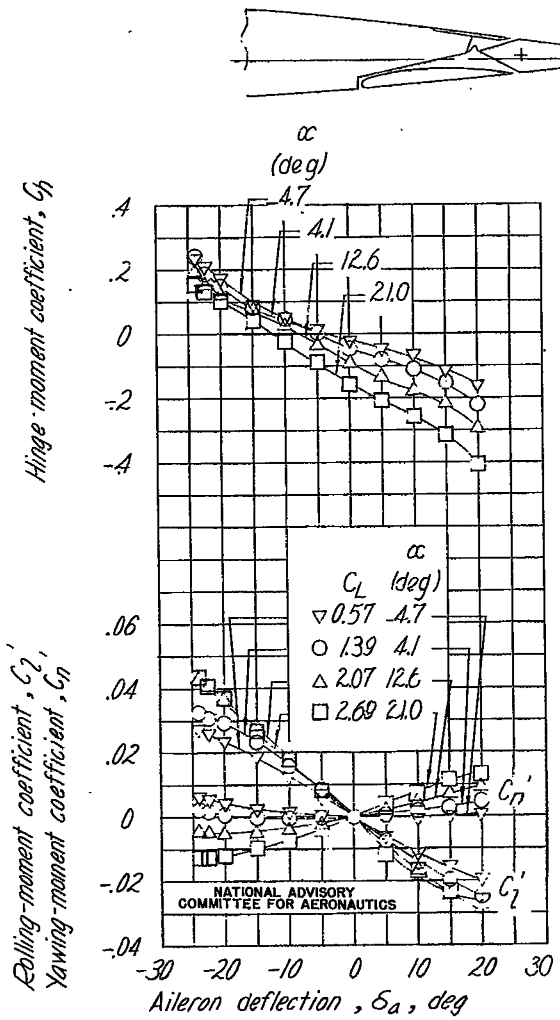

(b) δ_{f_1}, 40°; δ_{f_2}, 0°.

Figure C11.- Continued.

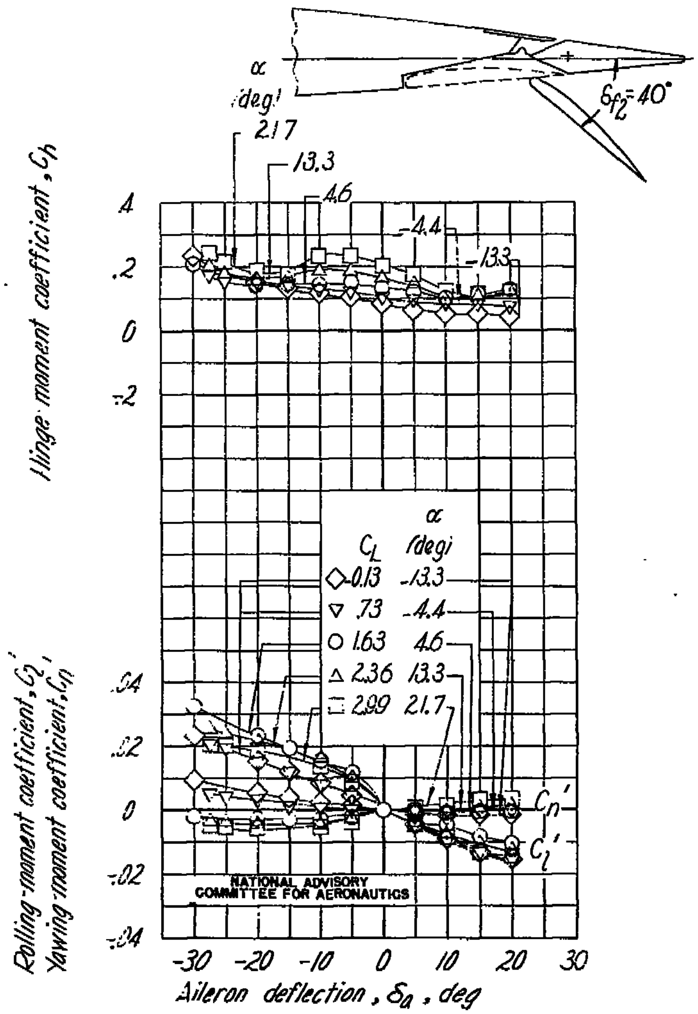

(c) δ_{f_1}, 40°; δ_{f_2}, 40°.

Figure C11.- Continued.

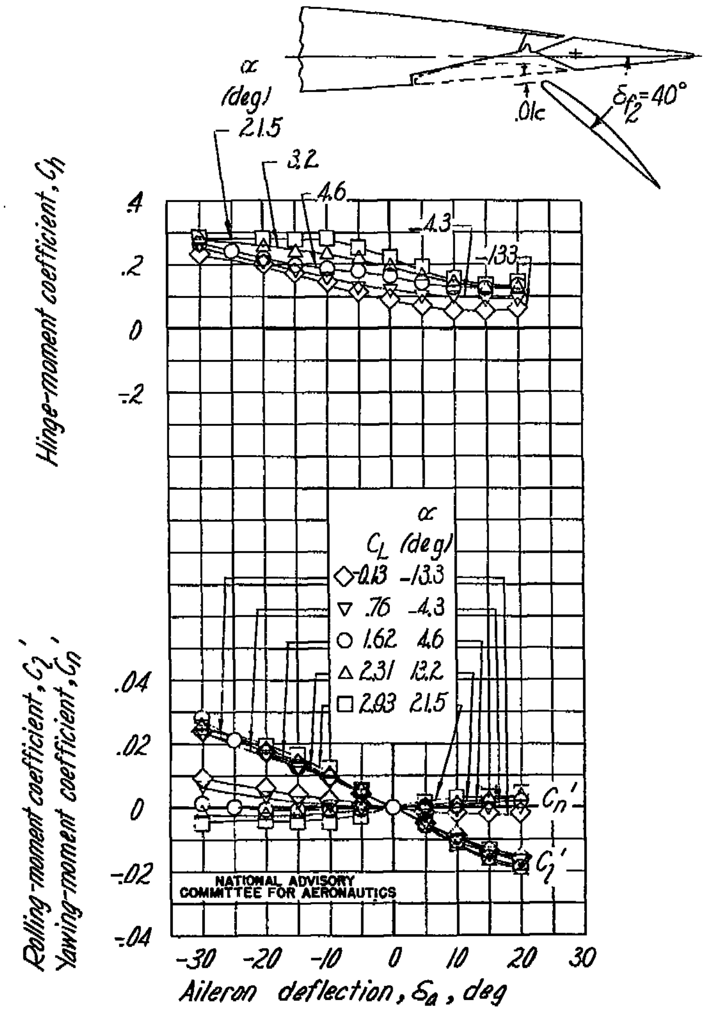

(d) δ_{f_1}, 40°; δ_{f_2}, 40°. Nose of f_2 is located 0.01c below lower surface of the wing.

Figure C11.- Concluded.

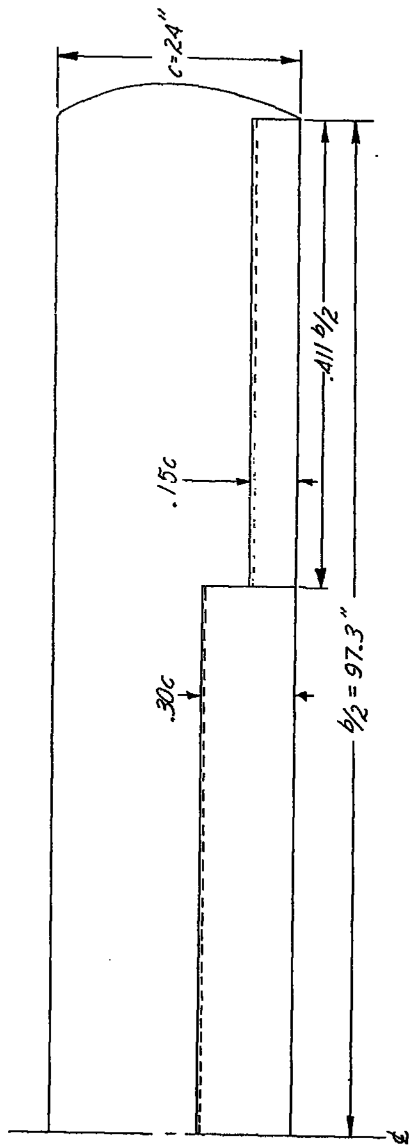

NATIONAL ADVISORY
COMMITTEE FOR AERONAUTICS

Figure C12.- Plan form of semispan rectangular wing model equipped with duplex flaps. Model tested in Ames 7- by 10-foot tunnel.

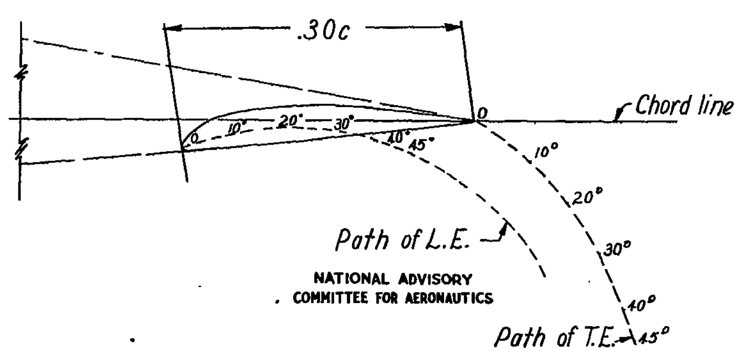

NATIONAL ADVISORY
COMMITTEE FOR AERONAUTICS

Figure C13.- Cut-away view of the 0.30c by 0.565 b/2 inboard Fowler flap on the rectangular wing model.

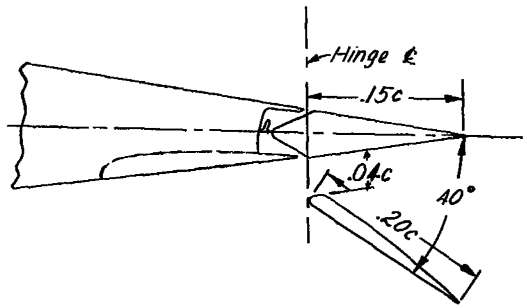

NATIONAL ADVISORY
COMMITTEE FOR AERONAUTICS

Figure C14.- Cut-away view of the 0.15c by 0.411 b/2 outboard sealed-gap aileron and retractable balanced split flap on the rectangular wing model.

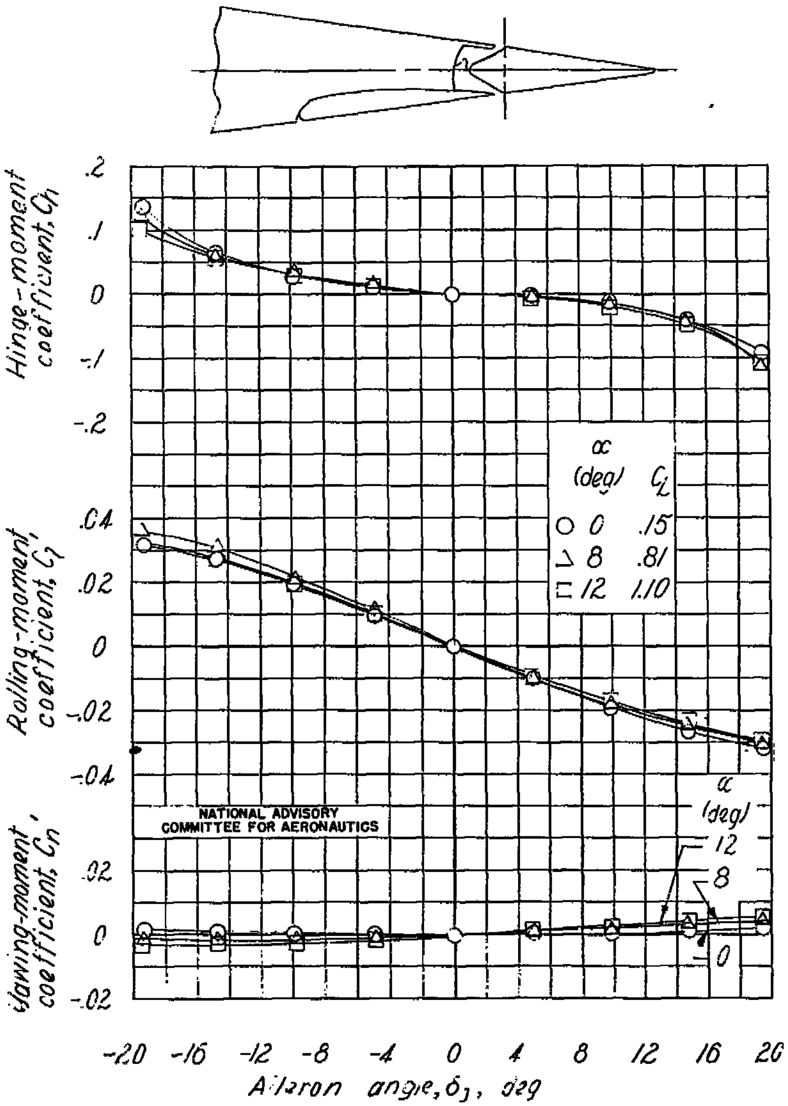

(a) Flaps retracted.

Figure C15.- Aerodynamic characteristics of the 0.15c sealed gap aileron on the rectangular wing model.

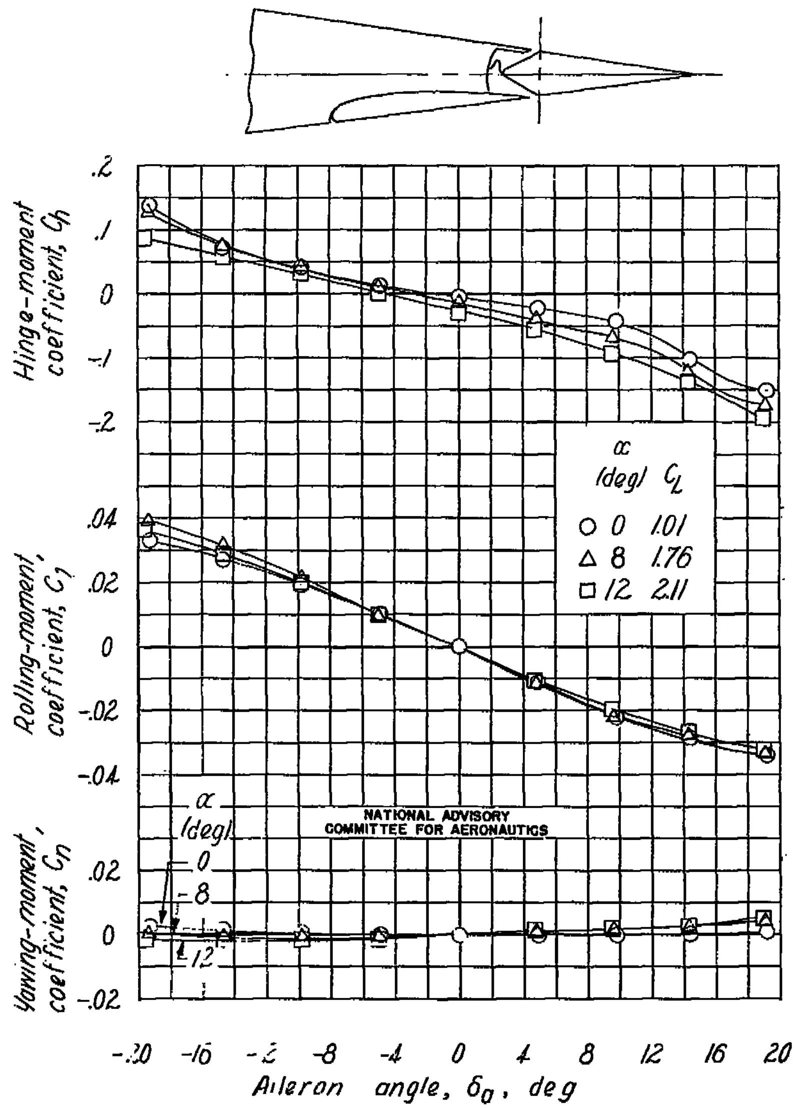

(b) Inboard Fowler flap 40°; outboard flap retracted.

Figure C15.- Continued.

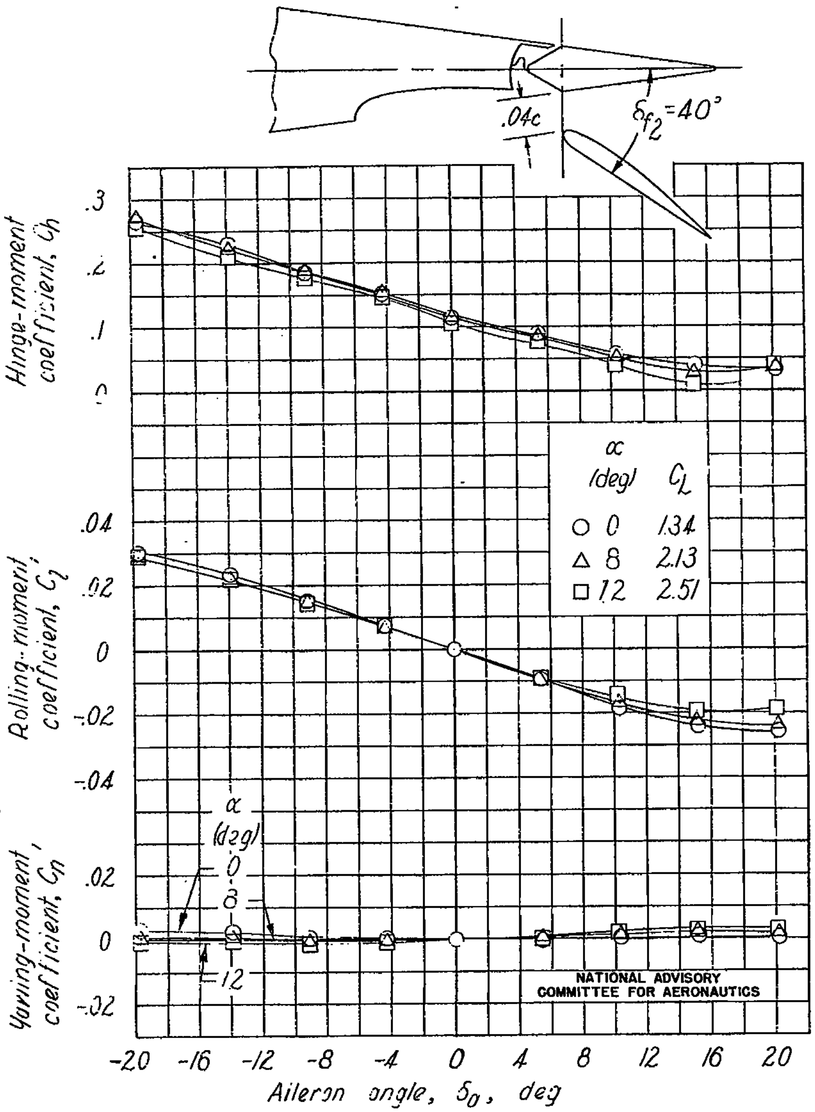

(c) Inboard Fowler flap 40°; outboard flap 40° with a gap of 0.04c at hinge line.

Figure C15.- Continued.

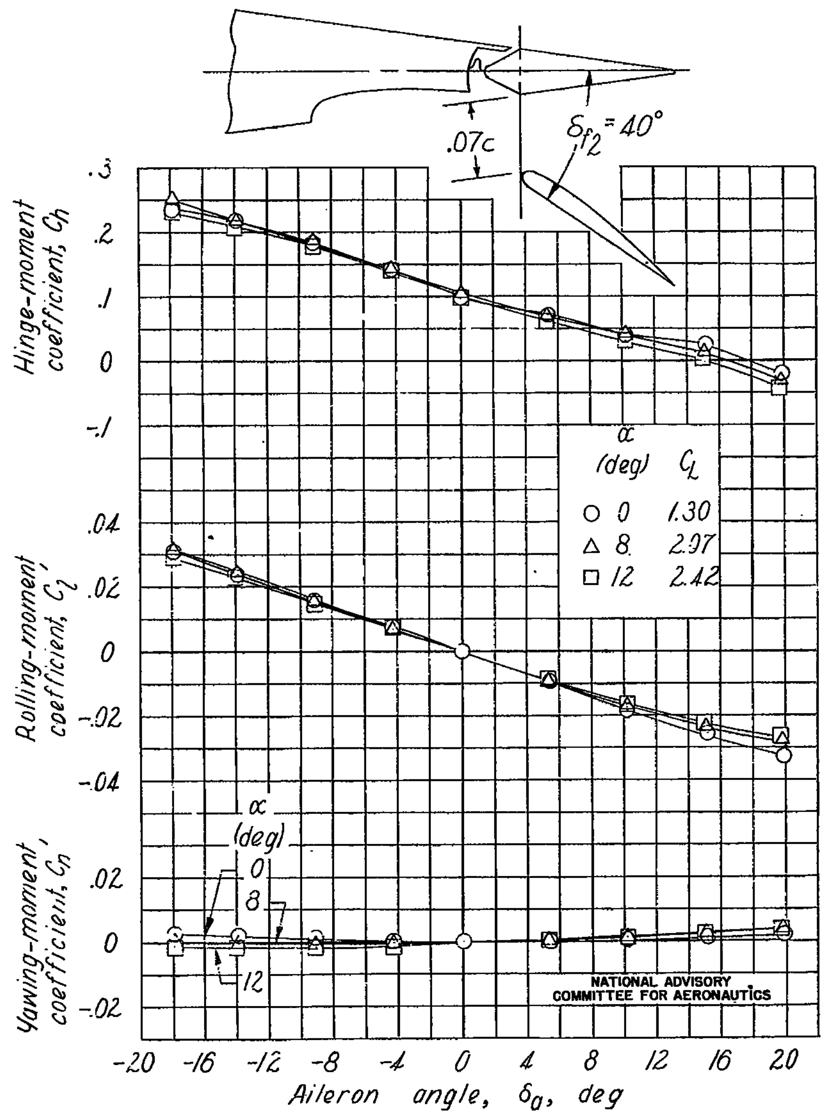

(d) Inboard Fowler flap 40°; outboard flap 40° with a gap of 0.07c at hinge line.

Figure C15.- Concluded.

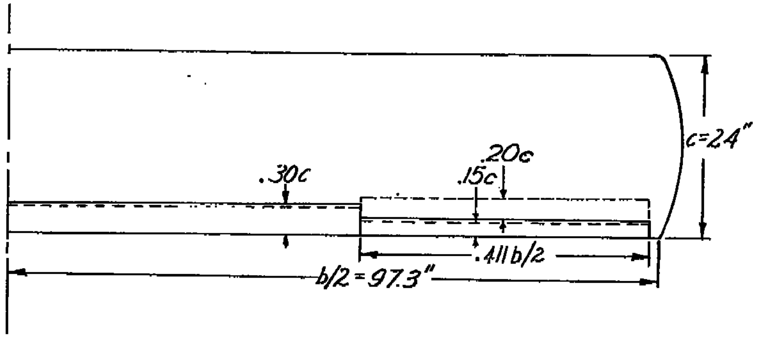

Figure C16.- Plan form of semispan rectangular wing model equipped with duplex flaps. Model tested in Ames 7- by 10-foot tunnel.

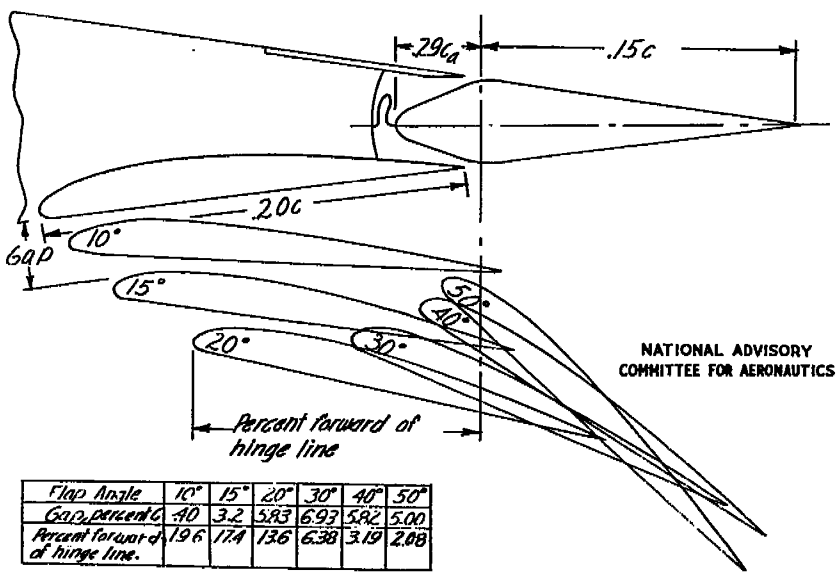

Flap Angle	10°	15°	20°	30°	40°	50°
Gap, percent c	.40	3.2	5.83	6.93	5.82	5.00
Percent forward of hinge line.	19.6	17.4	13.6	6.38	3.19	2.08

Figure C17.- Cut-away view of the sealed-gap aileron, outboard balanced split flap and flap path on the rectangular wing model.

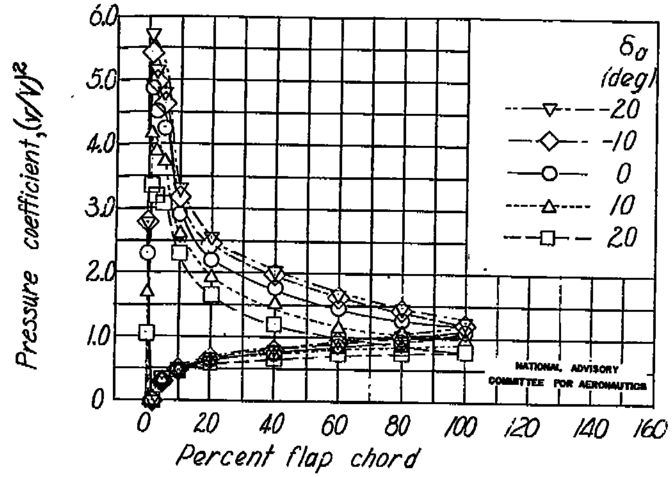

(a) δ_{f_2}, 10°.

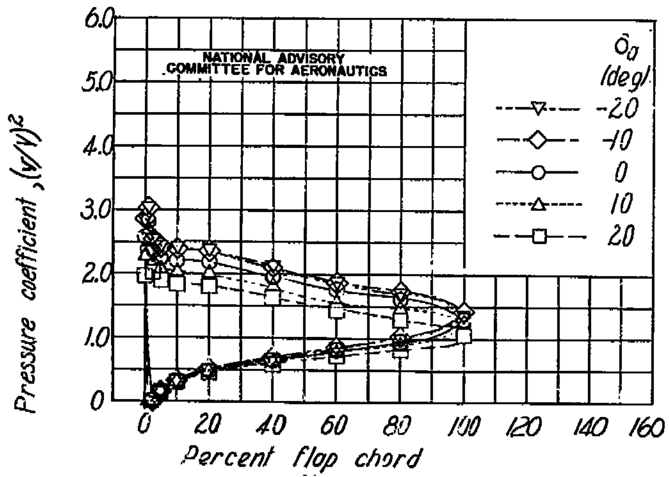

(b) δ_{f_2}, 15°.

Figure C18.- Variation of chordwise pressure coefficient with percent flap chord over the outboard balanced split flap on the rectangular wing model. $\alpha = 12°$.

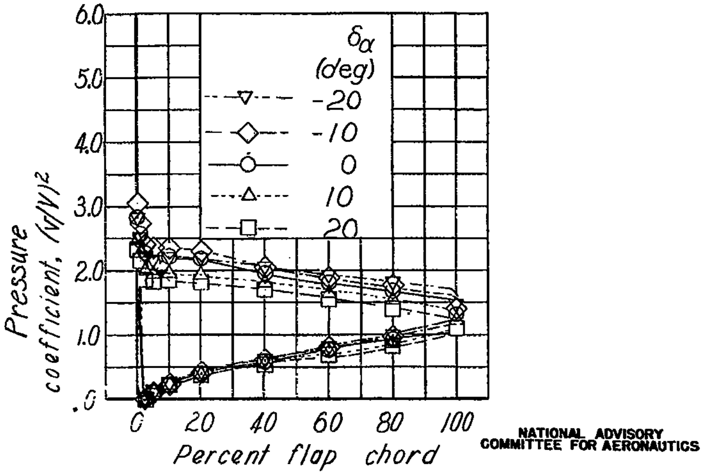

(c) δ_{f_2}, 20°.

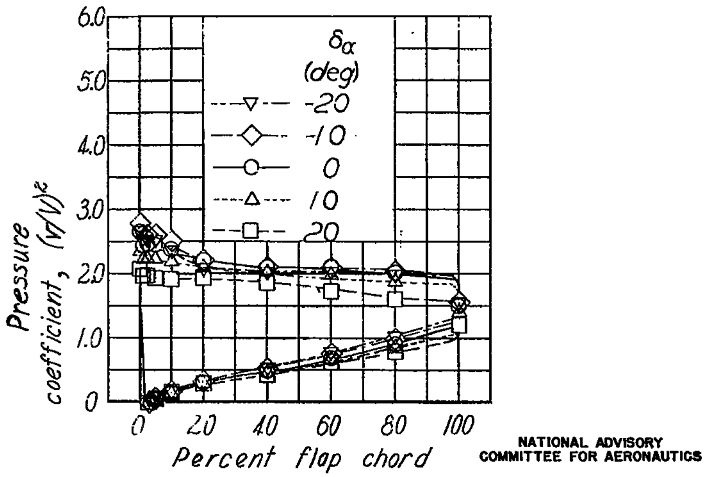

(d) δ_{f_2}, 30°.

Figure C18.- Continued.

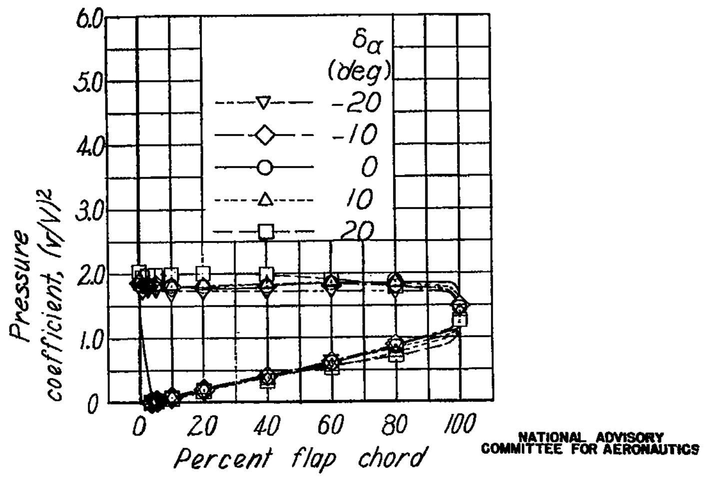

(e) δ_{f_2}, 40°.

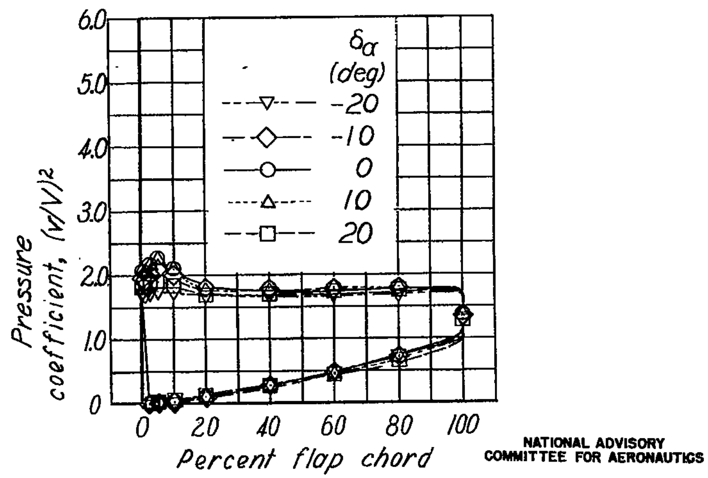

(f) δ_{f_2}, 50°.

Figure C18.- Concluded.

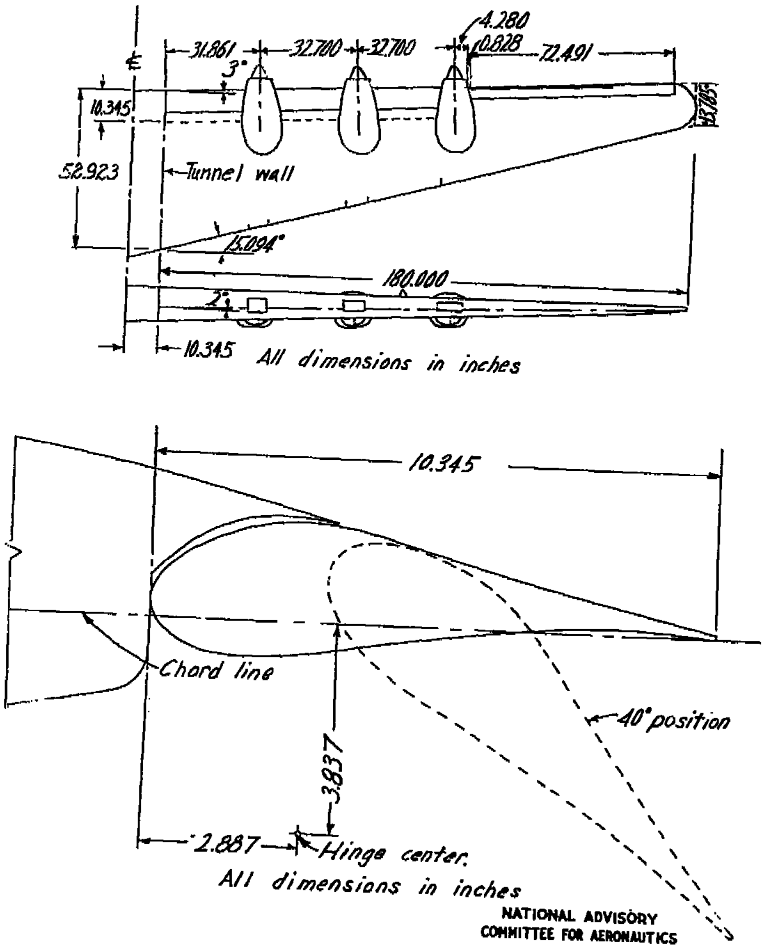

Figure C19.- The $\frac{4}{20}$-scale partial-span wing model tested in the Langley 19-foot pressure tunnel and the inboard slotted flap positions at a typical section of the model wing.

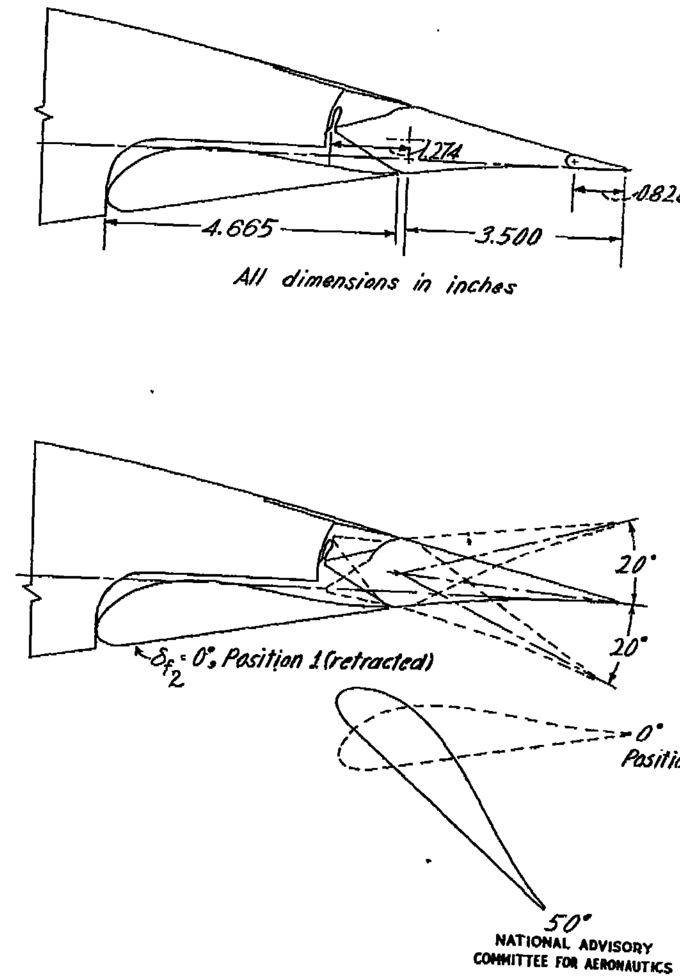

Figure C20.- Sections of the aileron and balanced split flap on the model wing, showing the path of the flap to the extended position.

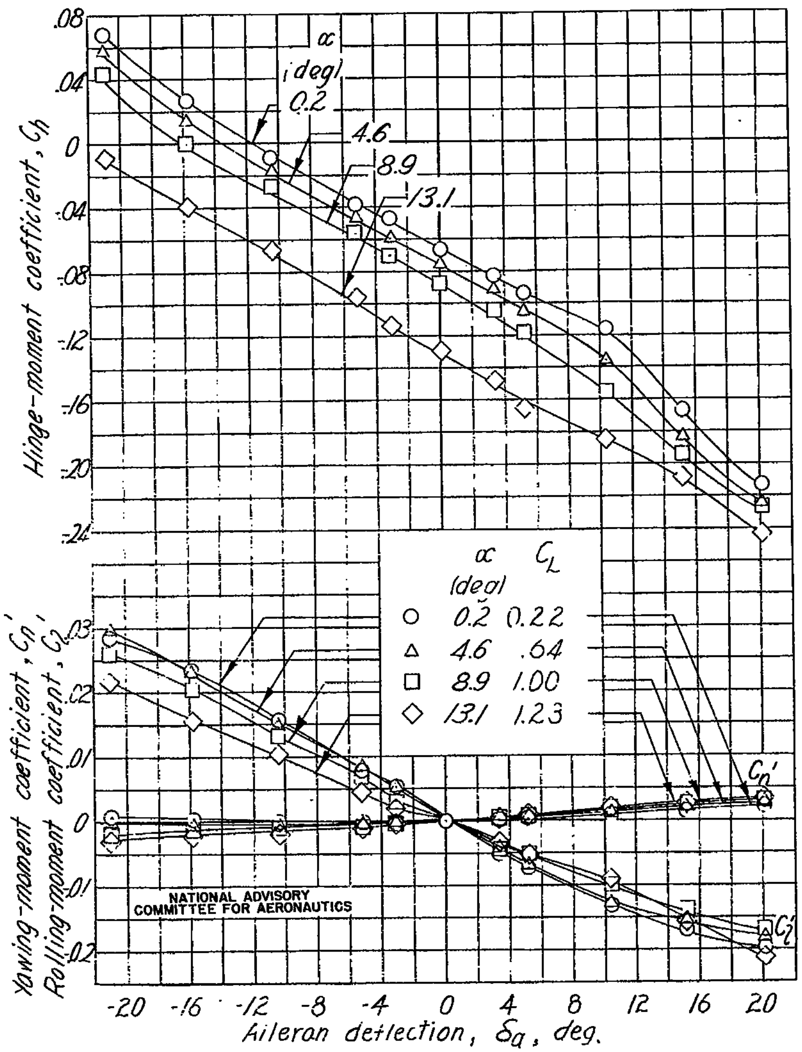

(a) Flaps neutral.

Figure C21.- Effect of right aileron deflection on the aileron characteristics of the semispan wing model equipped with full-span duplex flaps.

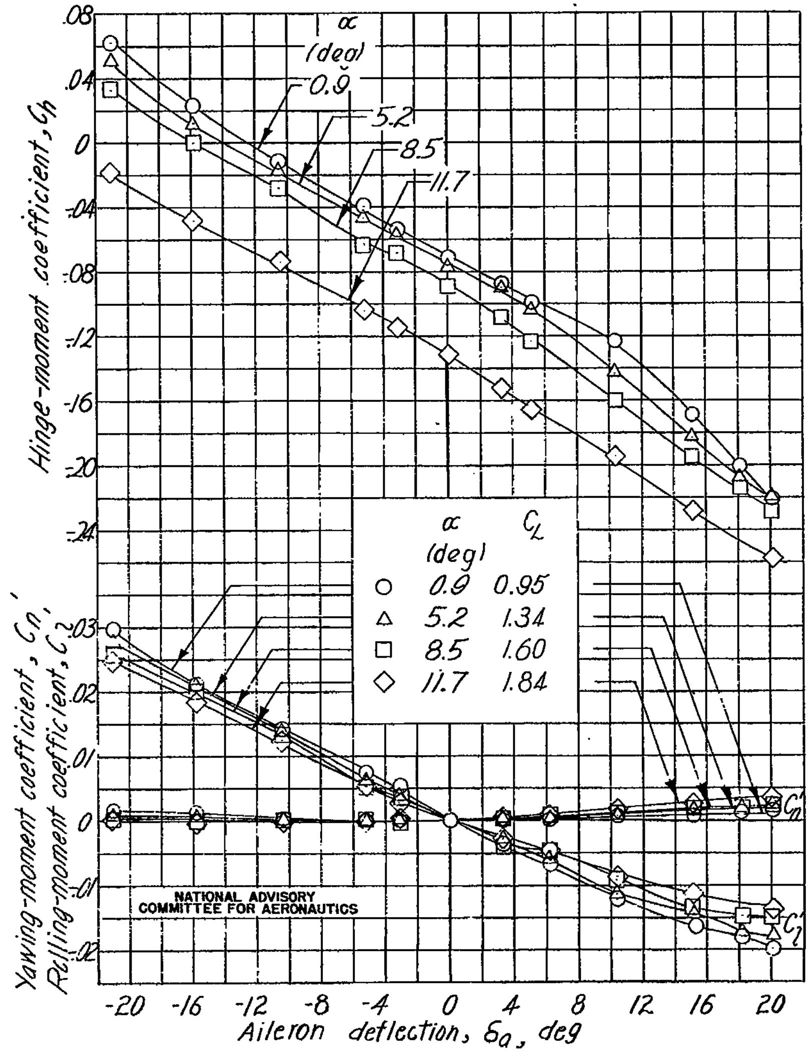

(b) δ_{f_1}, 40°; δ_{f_2}, 0°, No. 1 position.

Figure C21.- Continued.

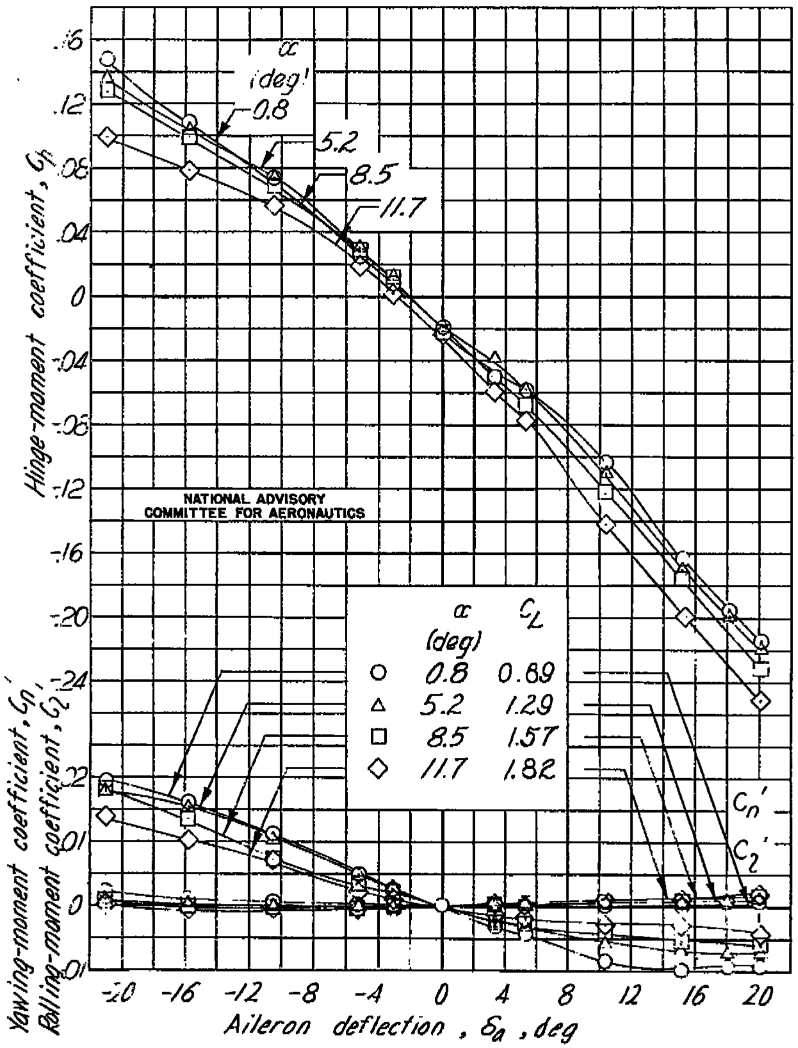

(c) δ_{f_1}, 40°; δ_{f_2}, 0°, No. 2 position.

Figure 221.- Continued.

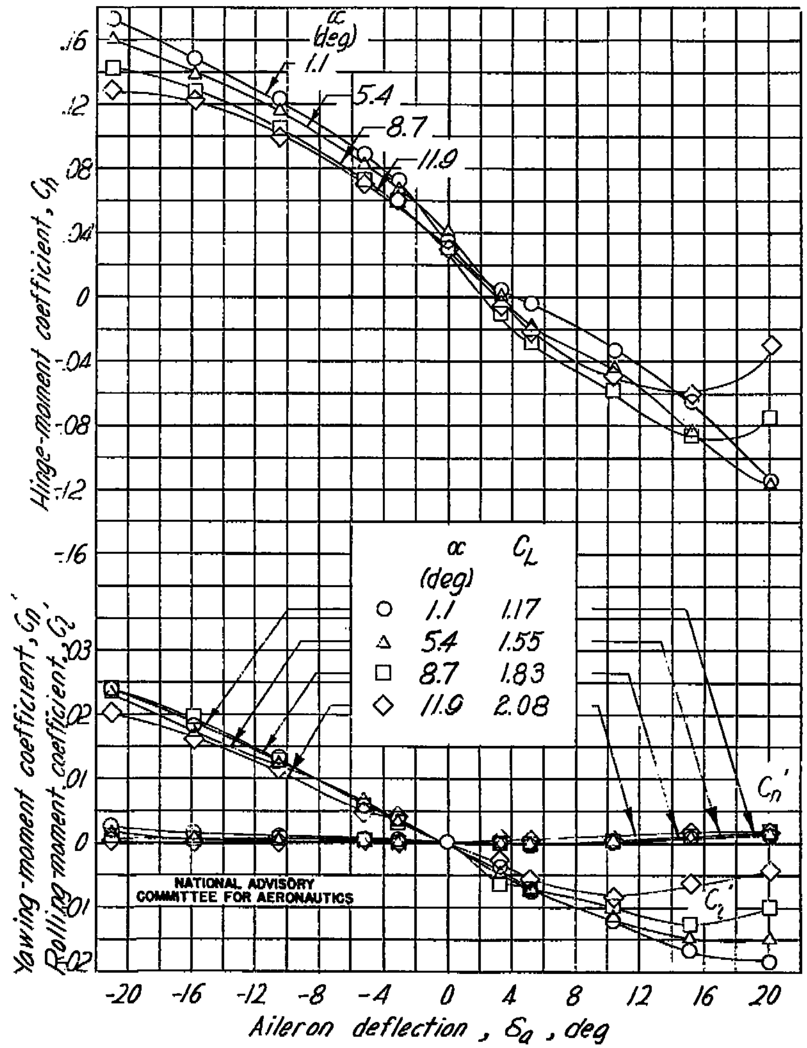

(d) δ_{f_1}, 40°; δ_{f_2}, 50°.

Figure 221.- Concluded.

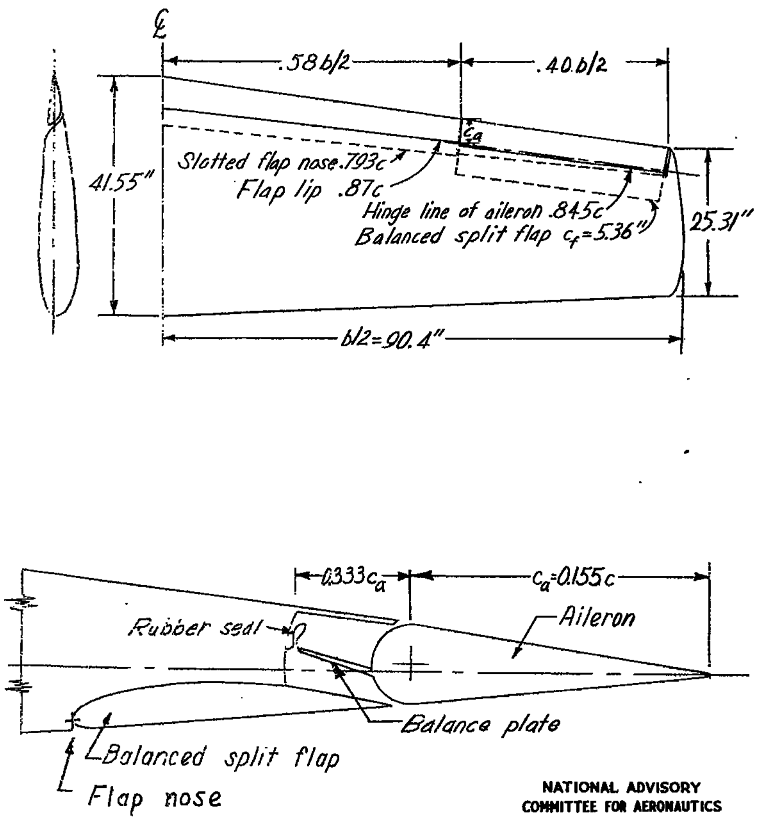

Figure C22.- Plan form and an aileron section of the 0.4-scale model of a tapered semispan wing tested with duplex flaps in the Langley 7- by 10-foot tunnel.

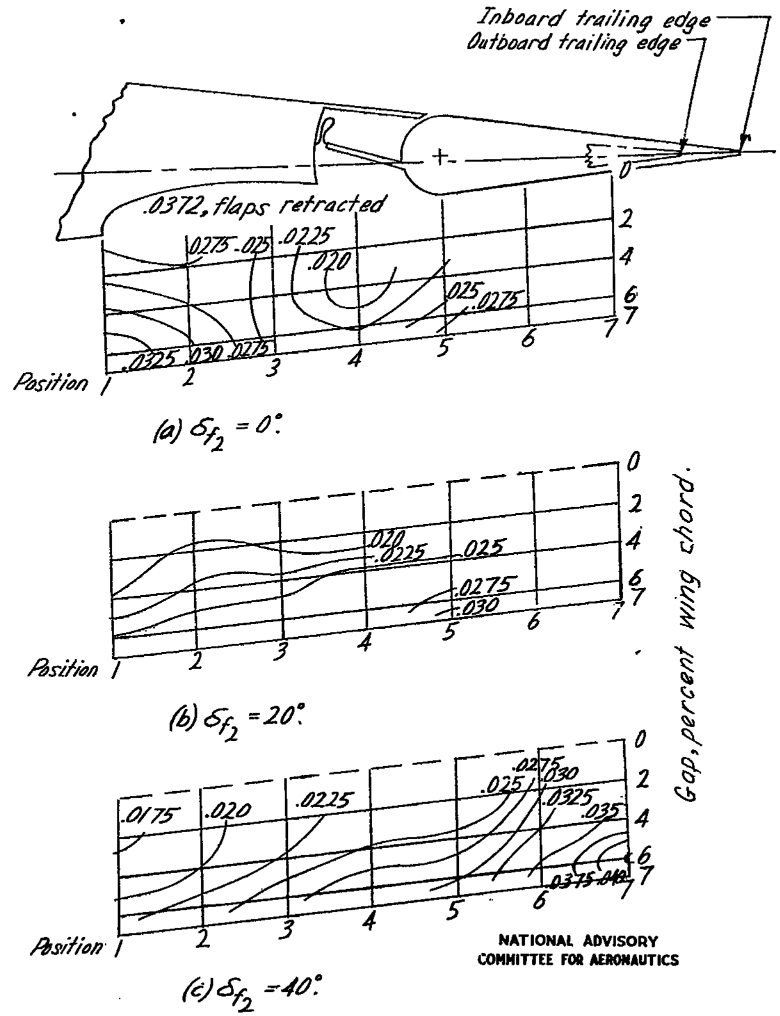

Figure C23.- Contours of outboard flap-nose location for rolling-moment coefficient due to aileron deflection of ±14°. Tapered-wing model with duplex flaps. δ_{f_1}, 50°; α, 14°.

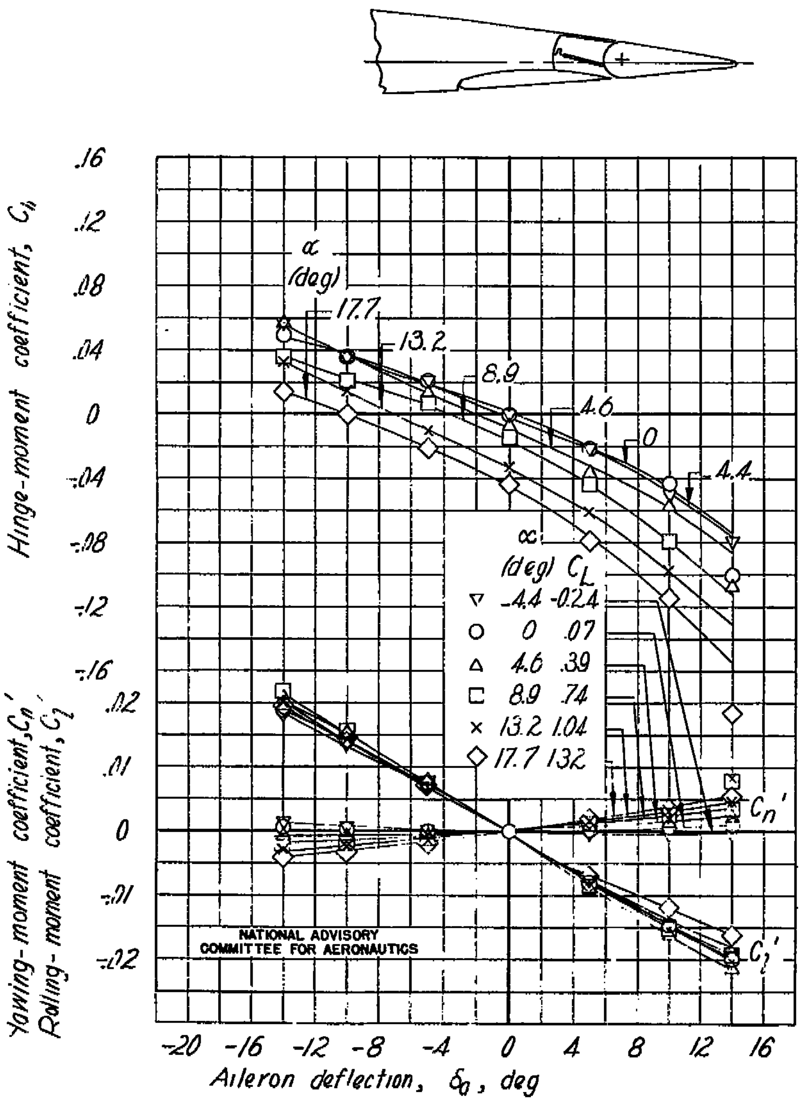

(a) Flaps retracted.

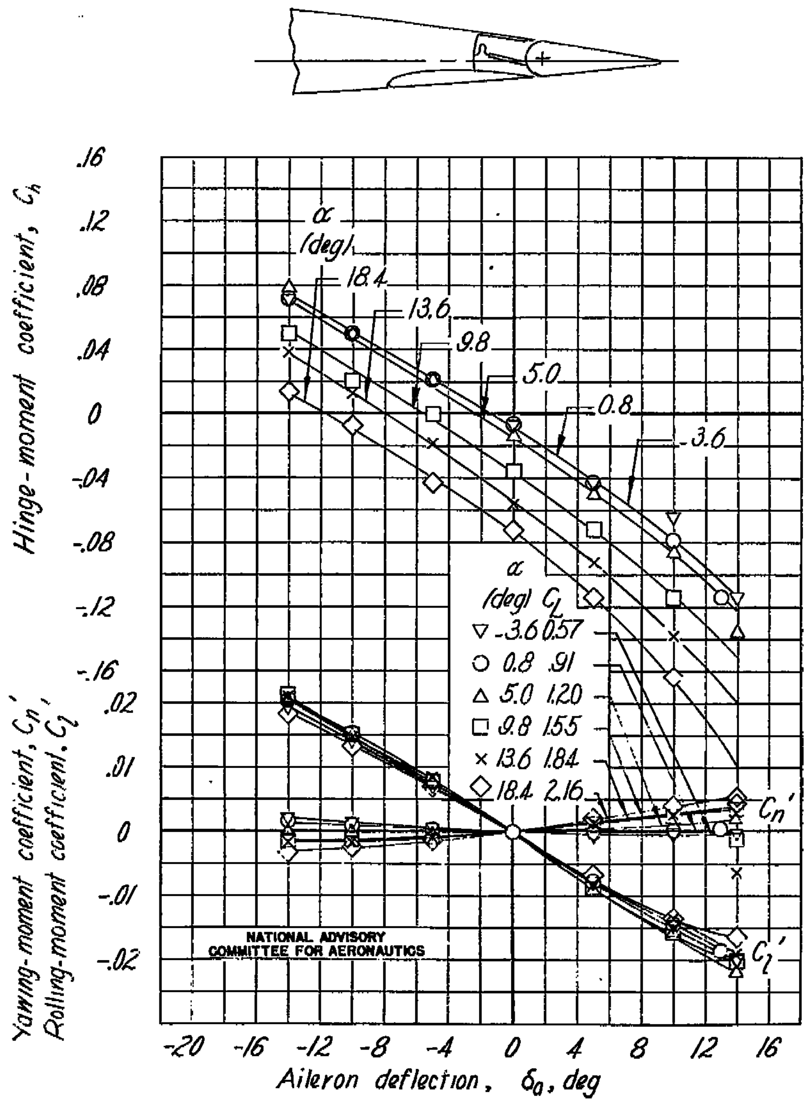

(b) δ_{f_1}, 50°; δ_{f_2}, retracted.

Figure C24.- Rolling-, yawing-, and hinge-moment coefficients of the tapered-wing model with duplex flaps and 0.333c_a balanced aileron. Right aileron deflected. (See fig. C23 for flap-nose location.)

Figure C24.- Continued.

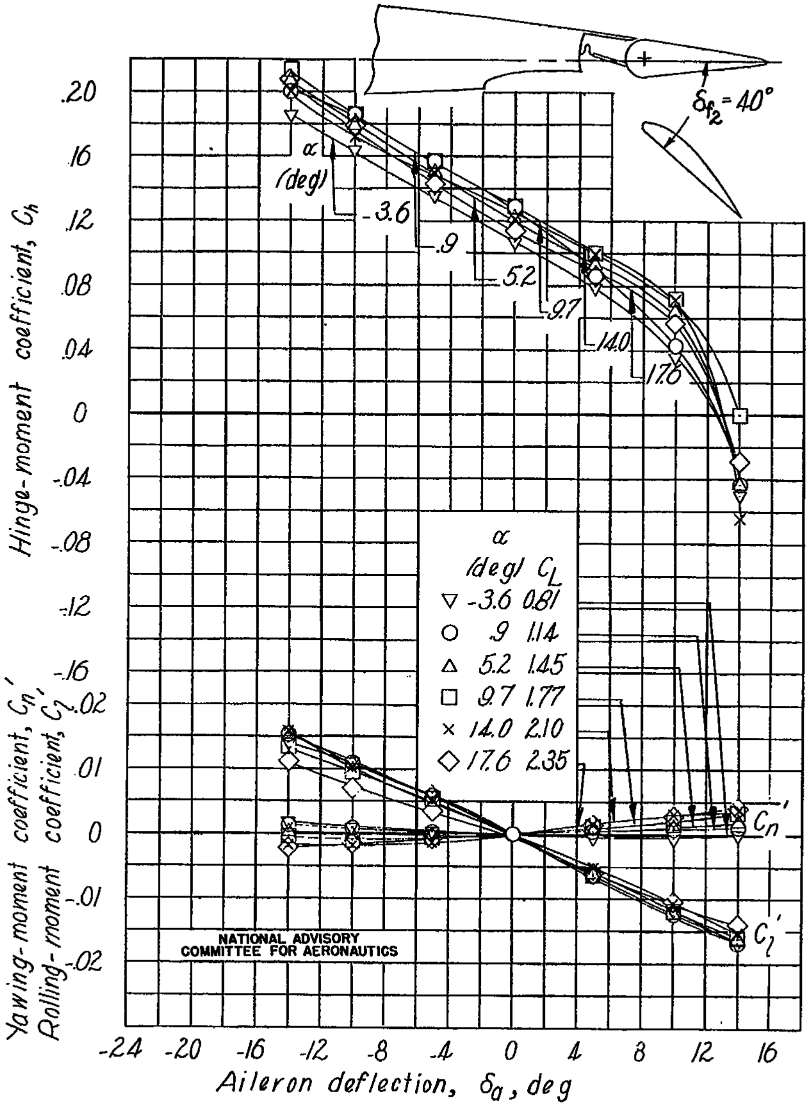

(c) δ_{f_1}, 50°; δ_{f_2}, 40° at position 5 with 0.06c gap.

Figure C24.- Continued.

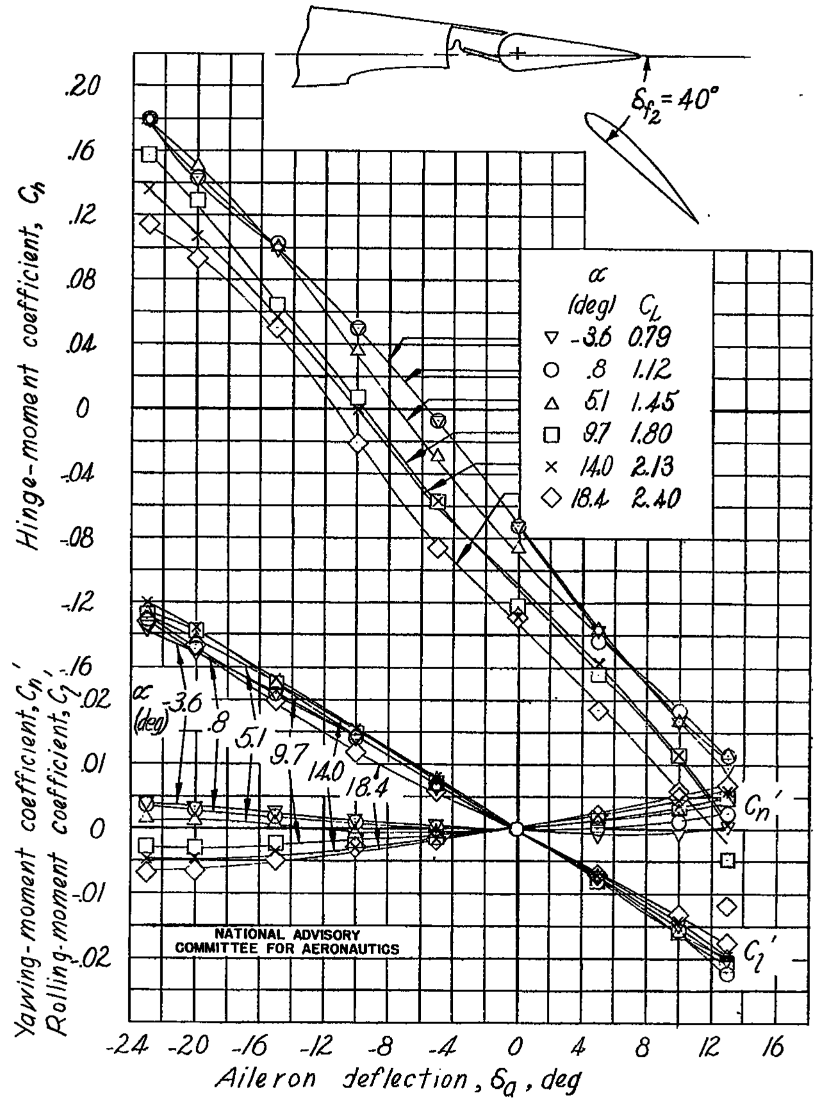

(d) δ_{f_1}, 50°; δ_{f_2}, 40° at position 7 with 0.06c gap.

Figure C24.- Concluded.

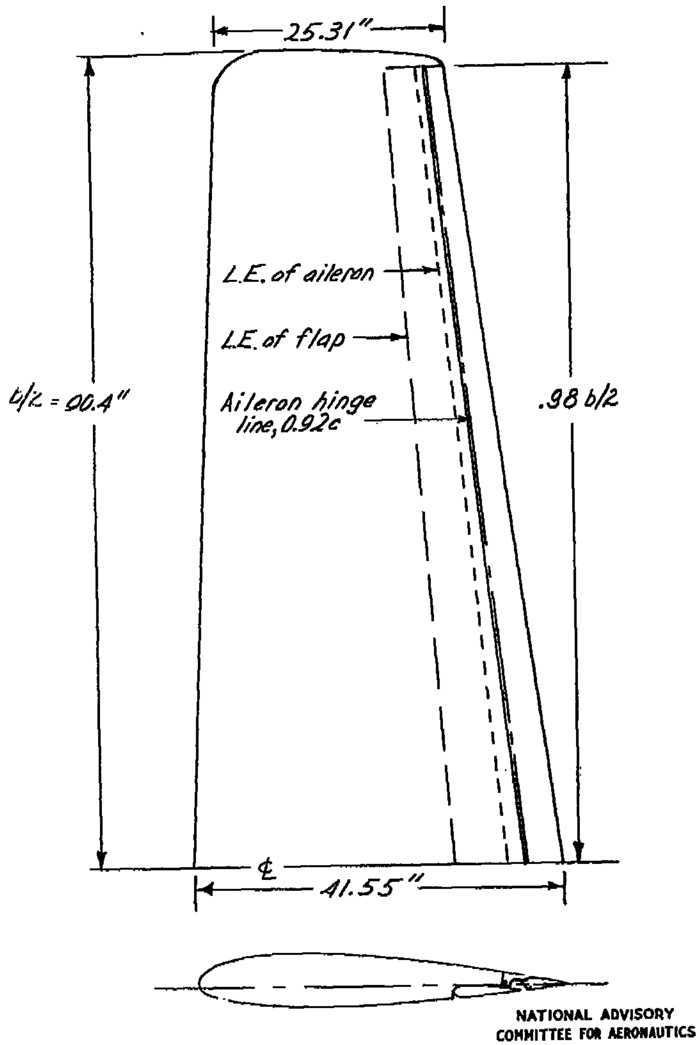

[illegible] Plan form of the 0.4-scale model of a tapered semispan wing tested with a full-span flap and a full-span aileron in the Langley 7- by 10-foot tunnel.

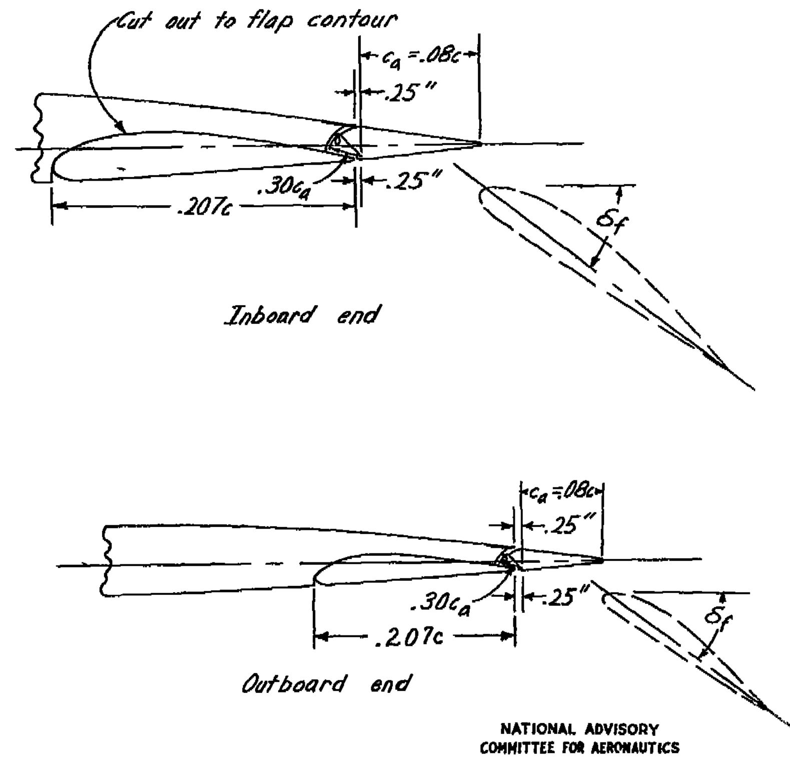

Figure C26.- Sections of the wing showing the 0.08c aileron with $0.30c_a$ internal balance and the retractable flap.

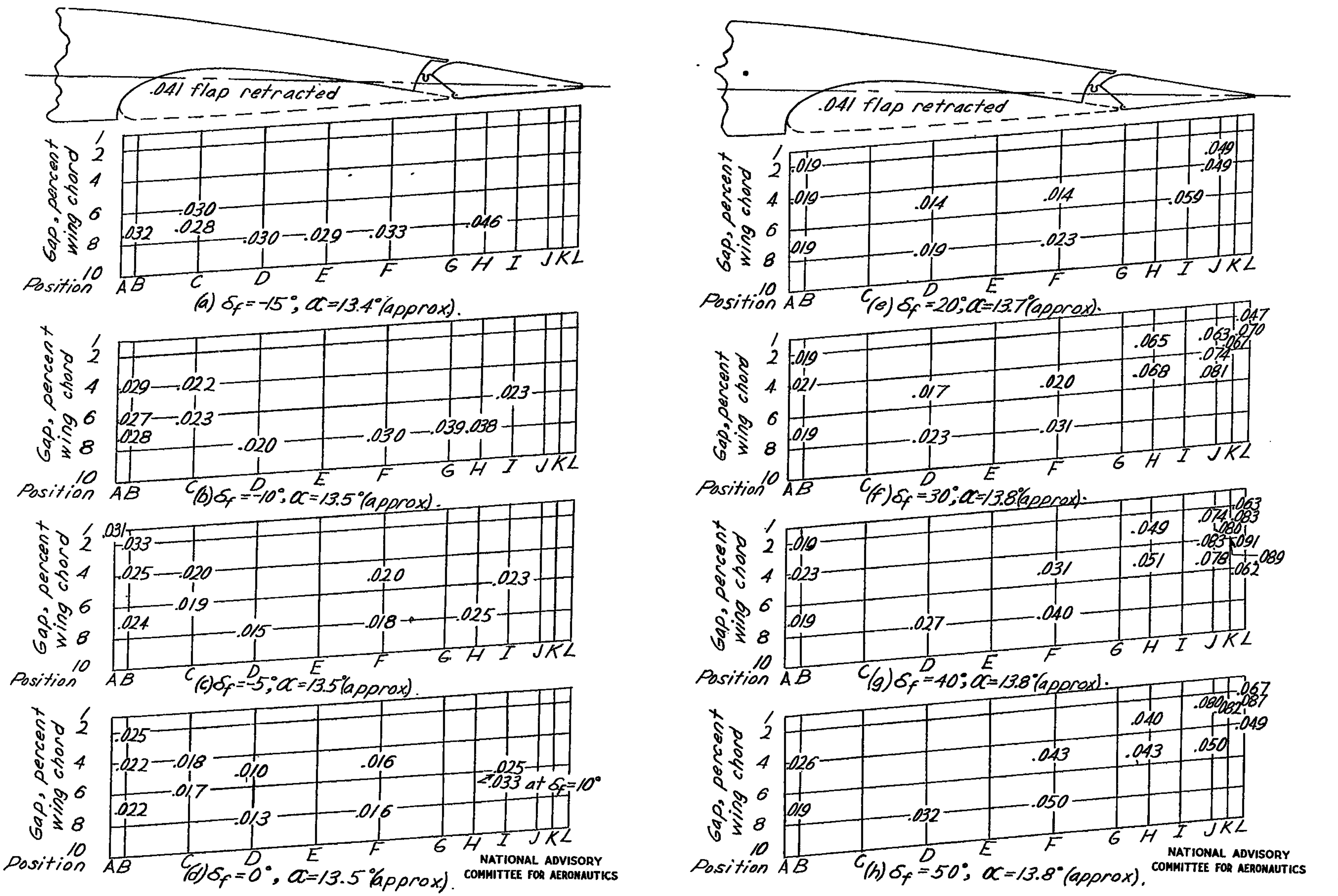

Figure C27.- Values of rolling-moment coefficient due to aileron deflections of ±15° at various flap-nose positions and flap deflections. Tapered wing model with a full-span flap and a full-span aileron with $0.30c_a$ internal balance.

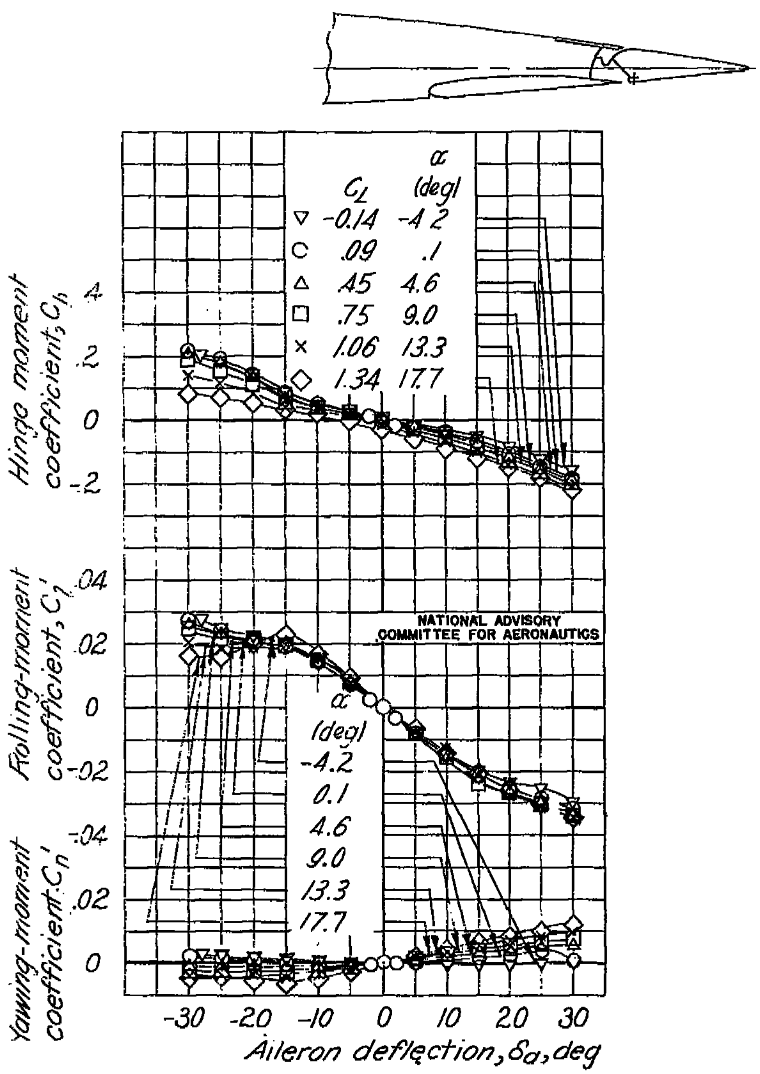

(a) Flap retracted.

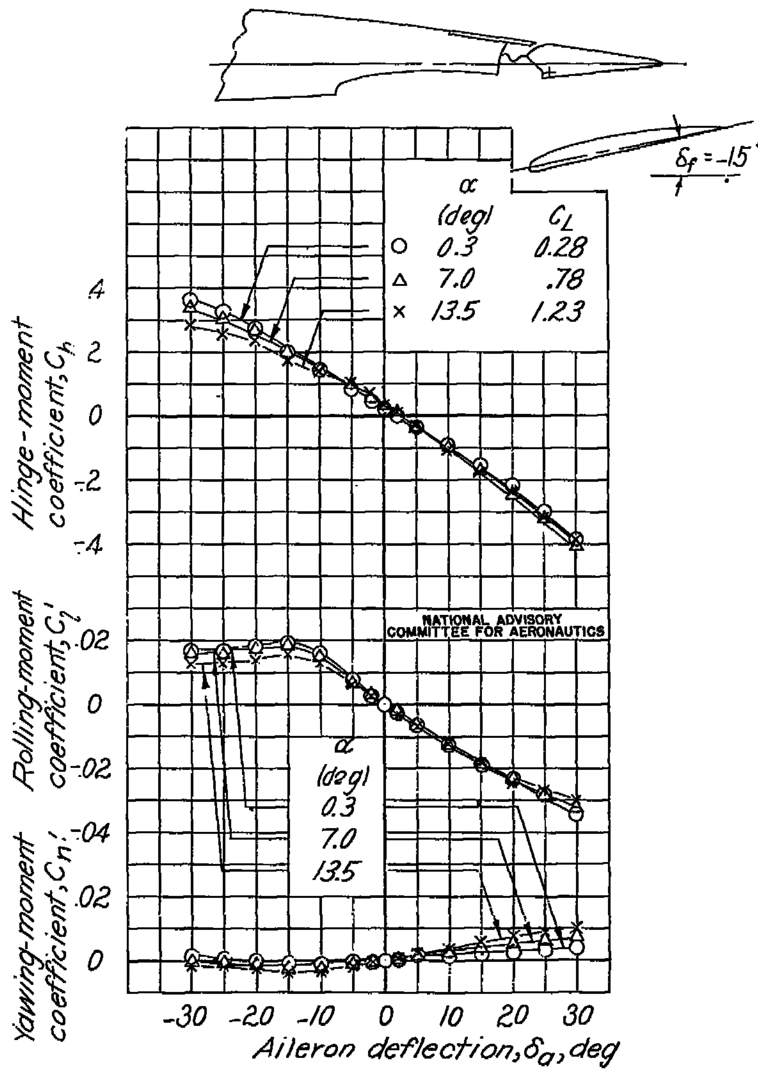

(b) Flap-nose position, F - 8; δ_f, -15°.

Figure C28.- Rolling-, yawing-, and hinge-moment coefficients of the tapered wing model with a full-span flap and a full-span aileron with $0.30c_a$ internal balance. (See fig. C27 for flap-nose position.)

Figure C28.- Continued.

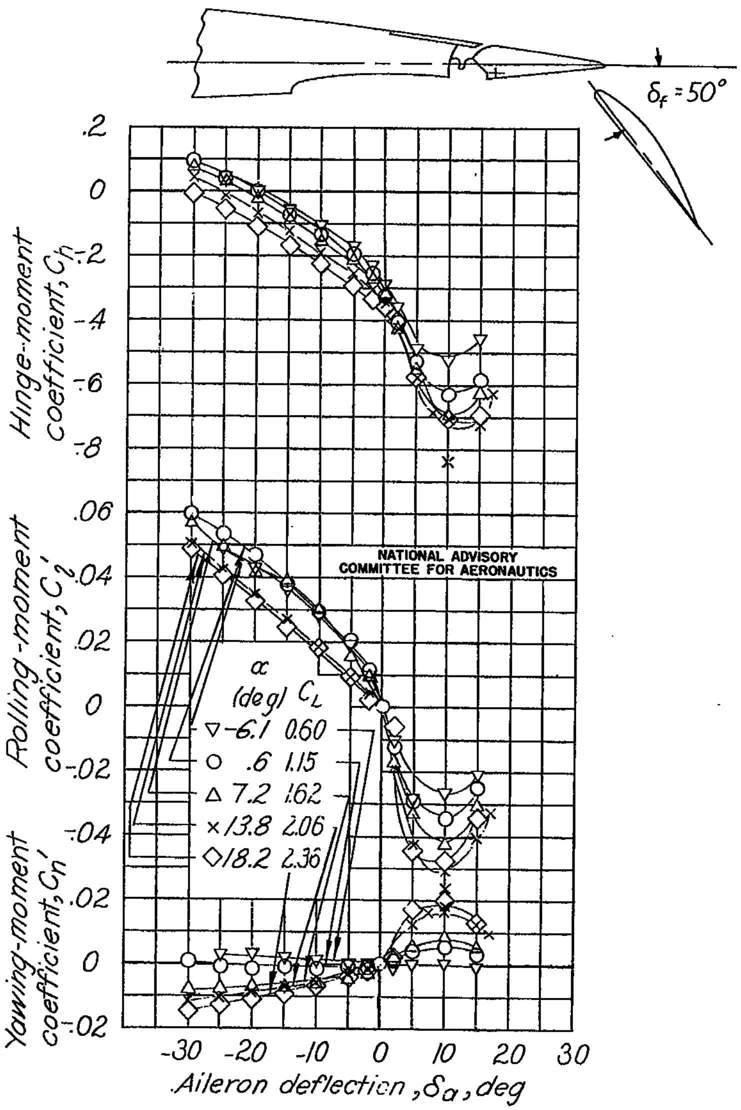

(c) Flap-nose position, L - 2; δ_f, 50°.

Figure C28.- Concluded.

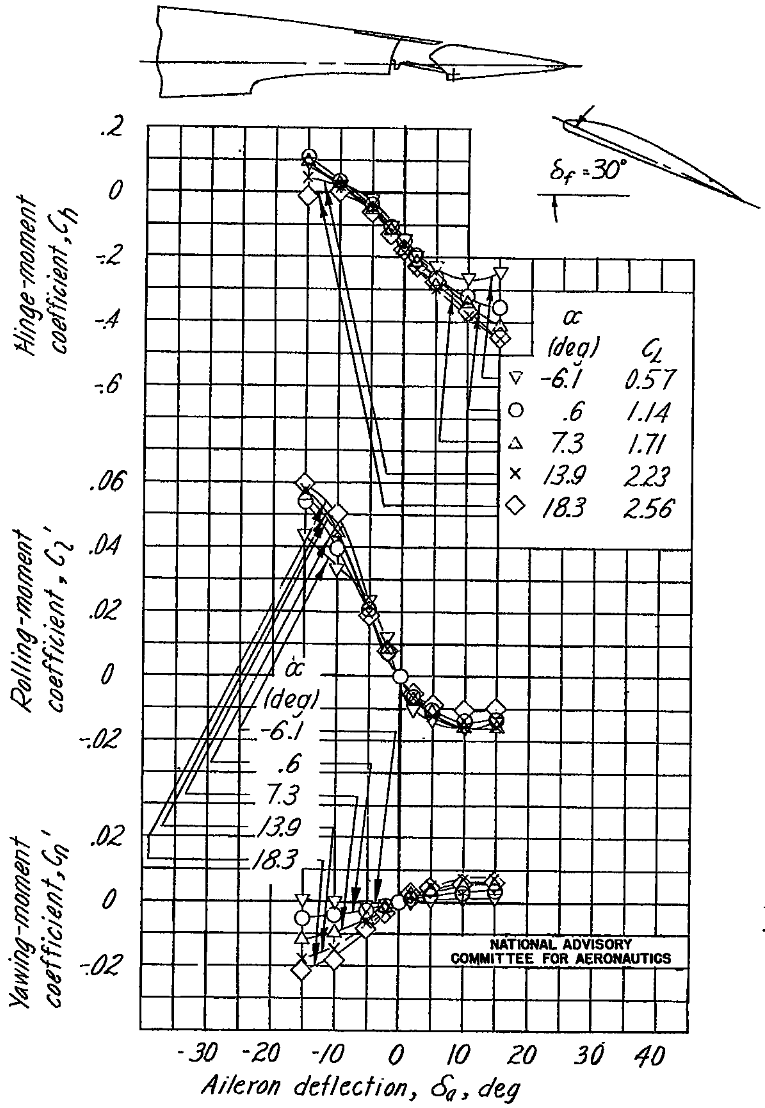

Figure C29.- Rolling-, yawing-, and hinge-moment coefficients of the tapered wing model with a full-span flap and a full-span aileron with $0.56c_a$ internal balance. Flap-nose position L - 3; δ_f, 30°. (See fig. C27 for flap-nose position.)

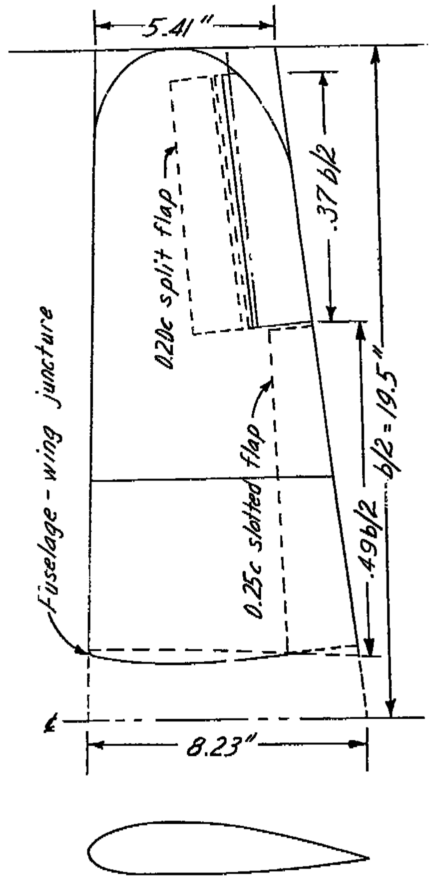

Inboard flap deflection δ_{f_1} (deg)	Outboard flap deflection δ_{f_2} (deg)	pb/2V Level flight	pb/2V Recovery	Rolling-moment coefficient, C_l
0	0	0.060	0.076	0.0407
60	0	.075	.066	.0430
60	60	.040	.028	.0145

NATIONAL ADVISORY
COMMITTEE FOR AERONAUTICS

Figure C30.- Semispan wing of the $\frac{1}{12}$-scale model of a dive-bomber-type airplane tested with full-span duplex flaps in the NACA free-flight tunnel.

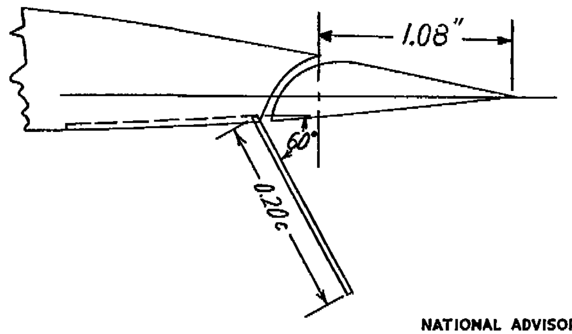

Figure C31.- Section of the wing of a dive-bomber-type airplane showing the aileron and the outboard split flap.

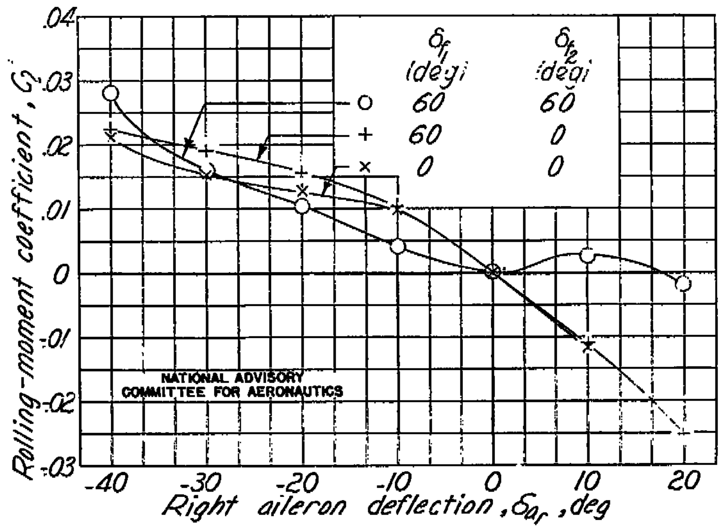

Figure C32.- Effect of flap deflection on the lateral control of the full-span flap model, α = 10°.

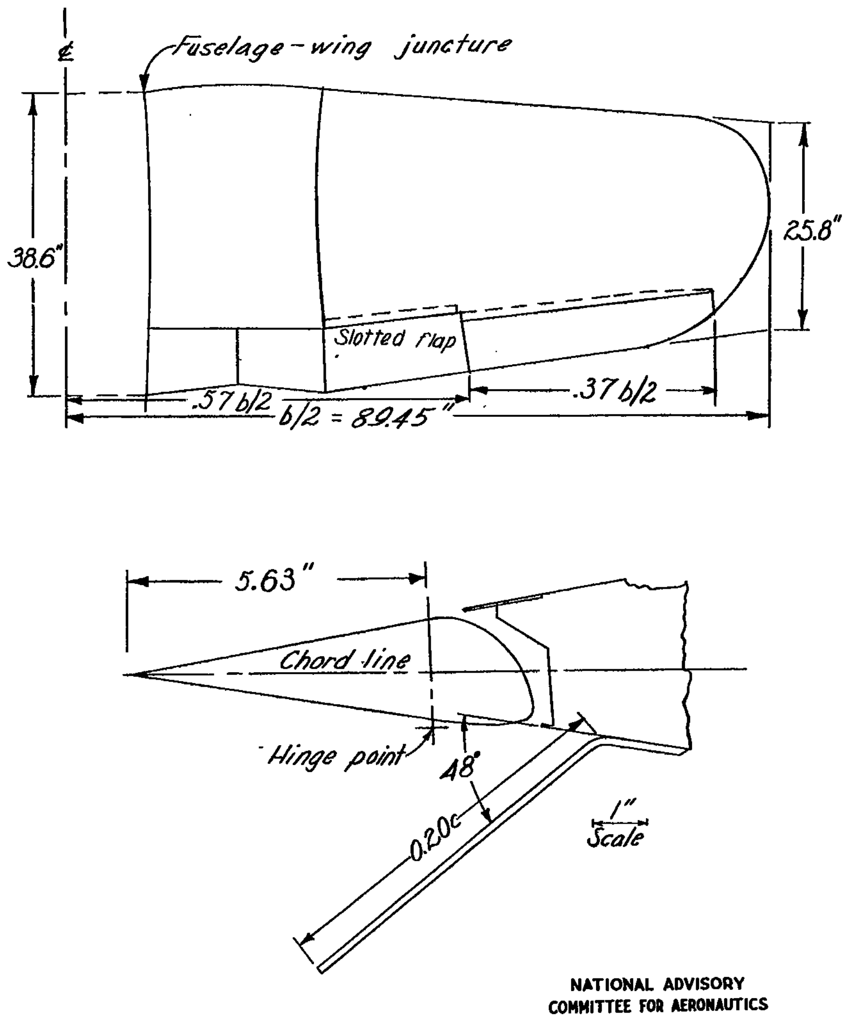

Figure C33.- Plan form and an aileron section of the wing of the $\frac{1}{2.75}$ -scale model of a fighter-type airplane tested with full-span duplex flaps in the Langley 19-foot pressure tunnel.

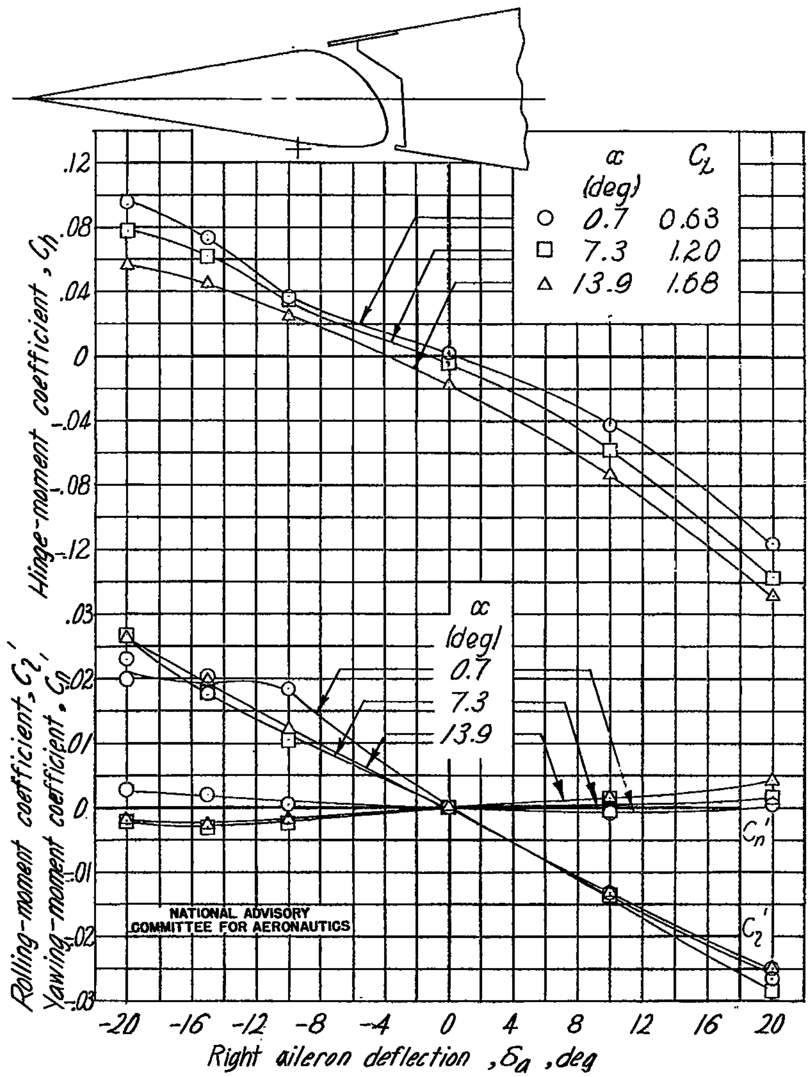

(a) δ_{f_1}, 30°; δ_{f_2}, 0°; δ_{a_l} = 7.85°.

Figure C34.- Variation of rolling-, yawing-, and hinge-moment coefficients with right aileron deflection on the model of a fighter-type airplane.

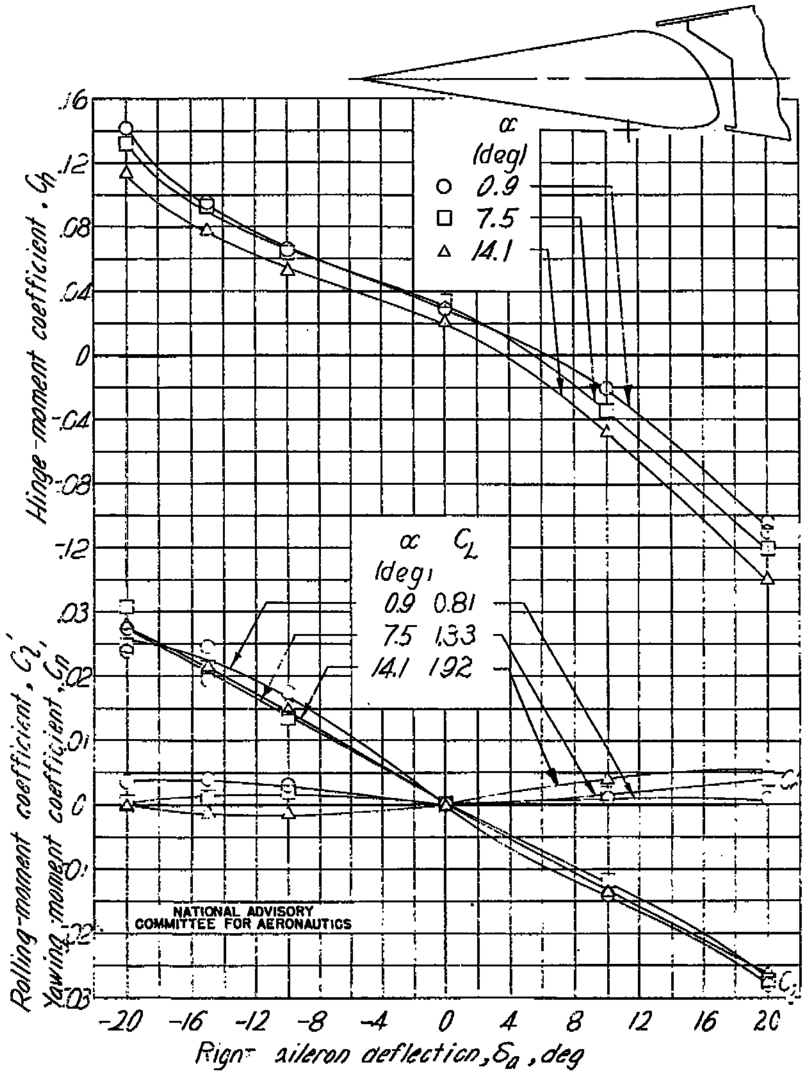

(b) δ_{f_1}, 50°; δ_{f_2}, 0°; δ_{a_l} = [illegible].

Figure C34.- Continued.

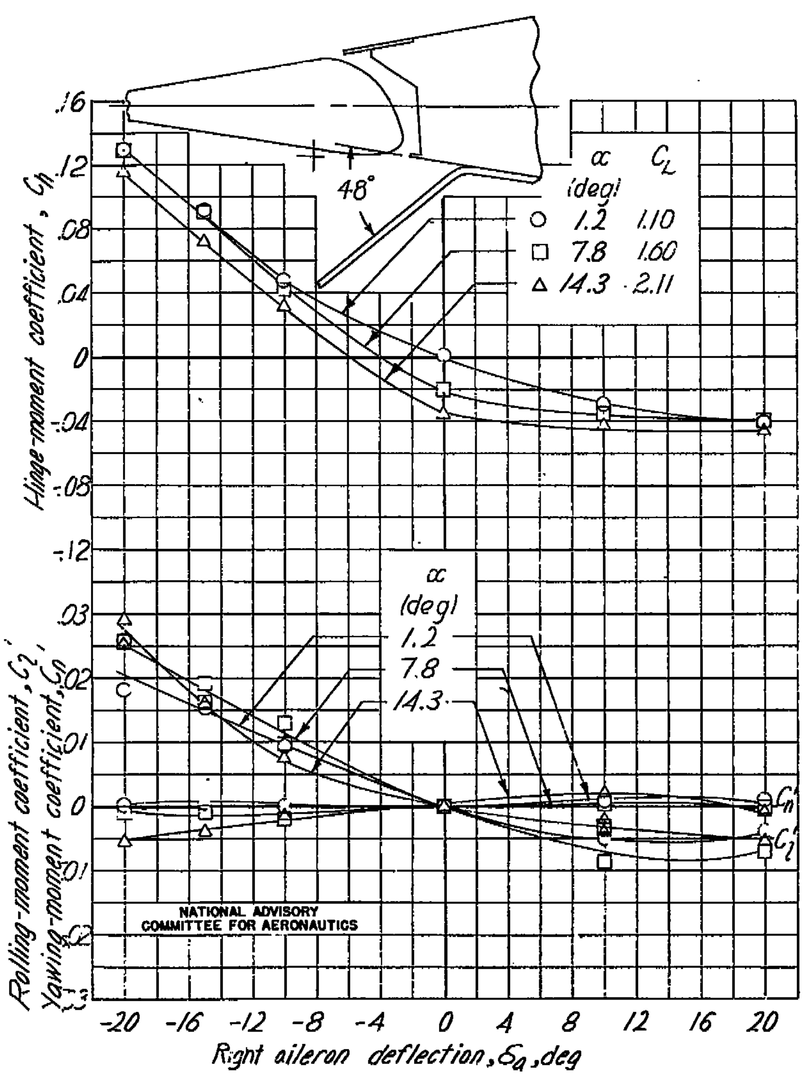

(c) δ_{f_1}, 50°; δ_{f_2}, 48°; δ_{a_l} = 0°.

Figure C34.- Concluded.

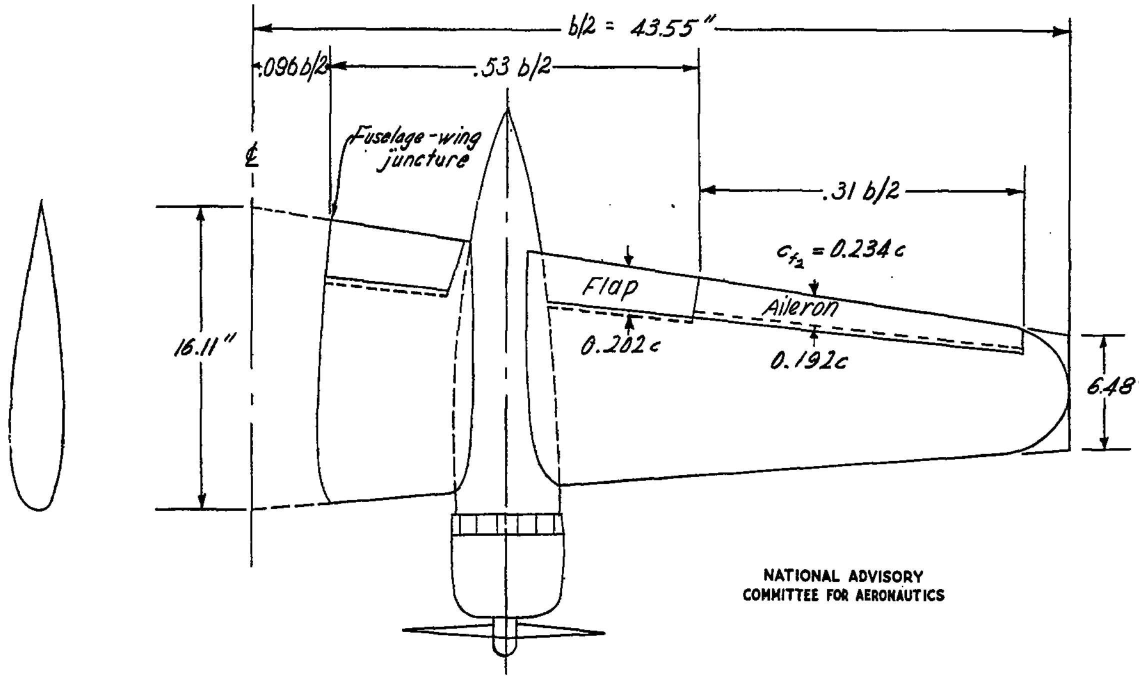

Figure C35.- Plan form of the semispan wing of the $\frac{1}{10}$-scale model of a bomber-type airplane with full-span duplex flaps as tested in the Langley 7- by 10-foot tunnel.

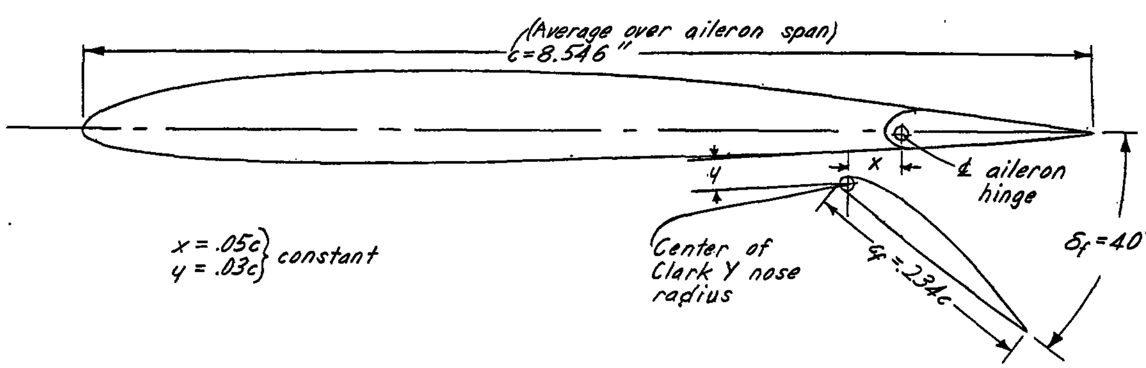

Figure C36.- Typical section through the outboard flap and aileron on the wing of the model of a bomber-type airplane.

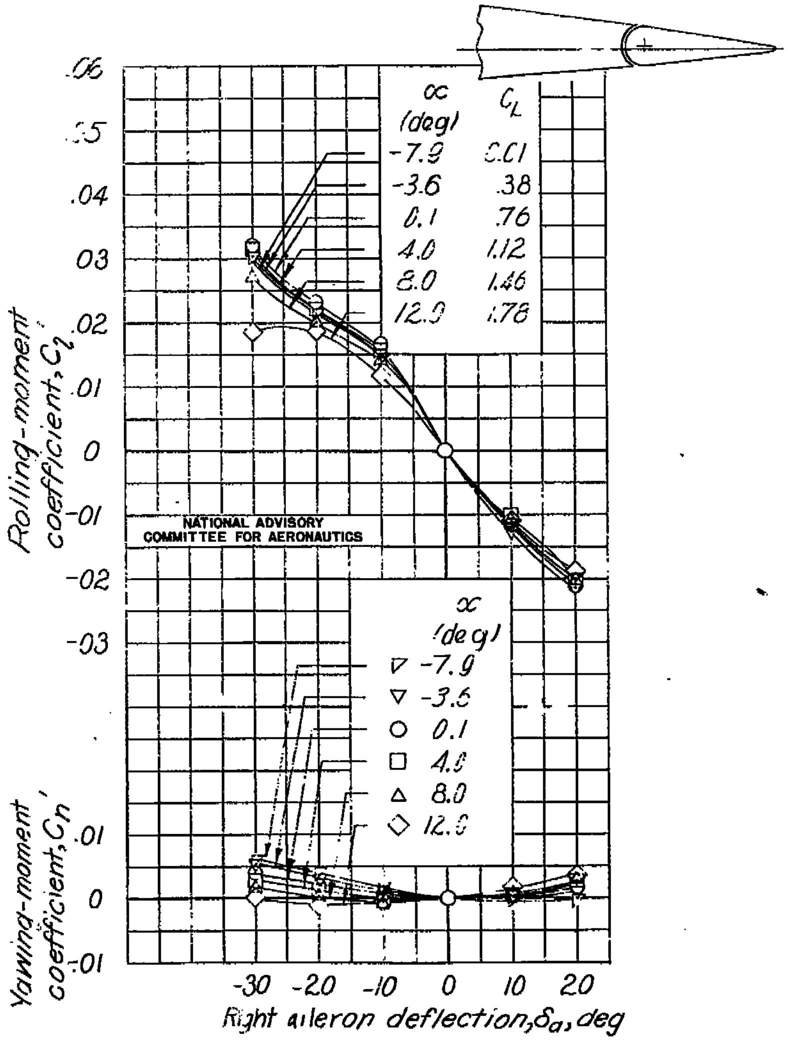

(a) δ_{f_1}, 45°.

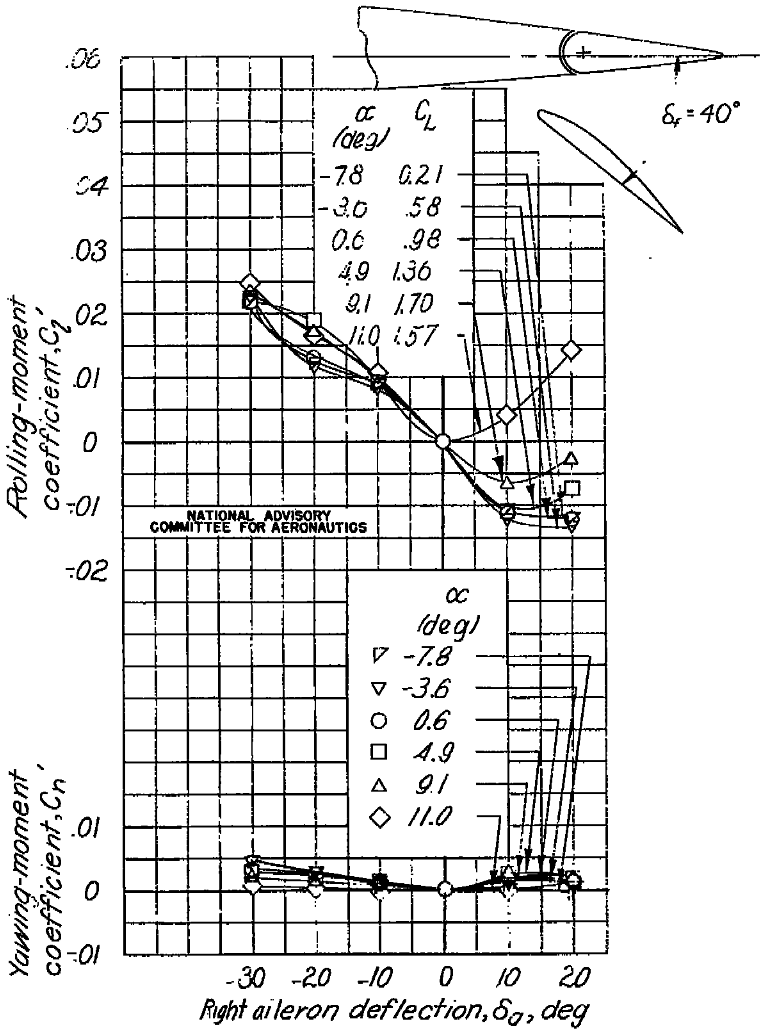

(b) δ_{f_1}, 45°; δ_{f_2}, 40°.

Figure C37.- Effect of right aileron deflection on the rolling- and yawing-moment characteristics of the model of a bomber-type airplane. Landing condition. δ_r, δ_e = 0°.

Figure C37.- Concluded.

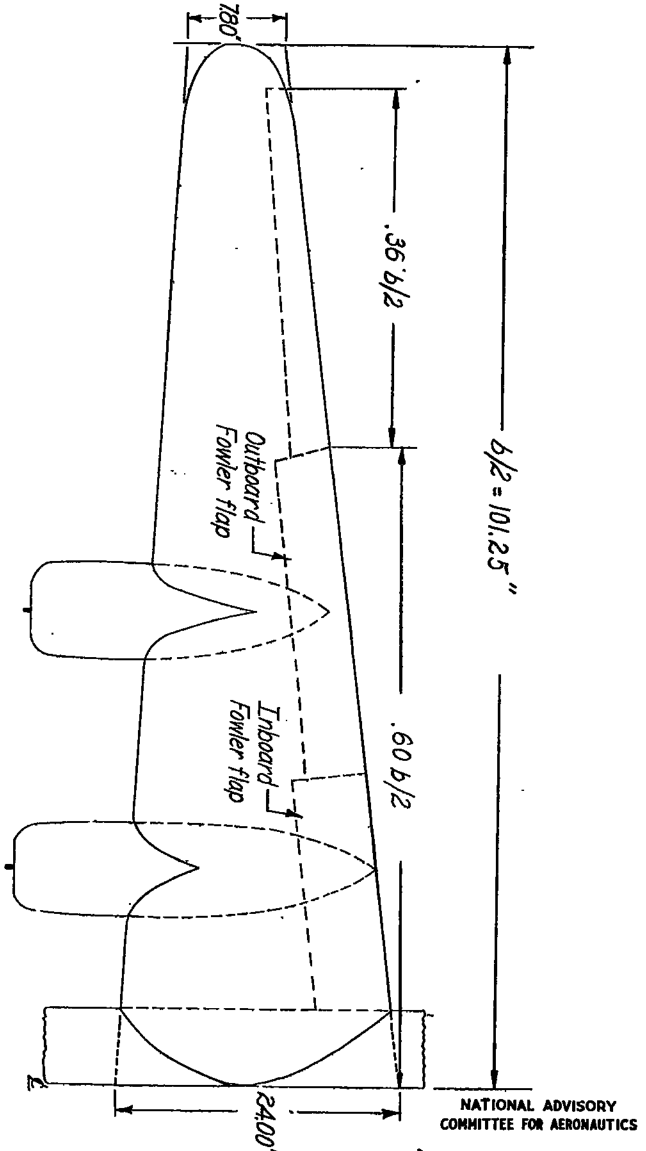

Figure C38.- Semispan wing of a $\frac{1}{8}$-scale model of a bomber type airplane tested in NACA 19-foot pressure tunnel.

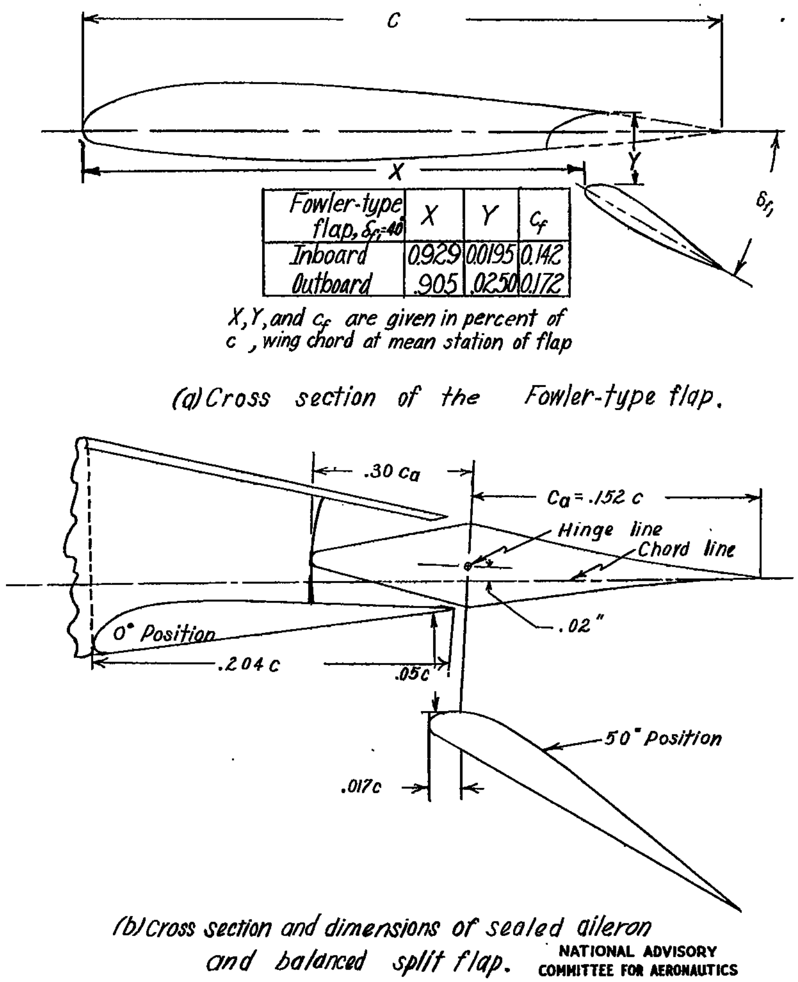

Fowler-type flap, δ_f=40°	X	Y	c_f
Inboard	0.929	0.0195	0.142
Outboard	.905	.0250	0.172

Figure C39.- Typical cross sections of the wing showing the Fowler type flap and the sealed aileron with a balanced split-flap on the $\frac{1}{8}$-scale model.

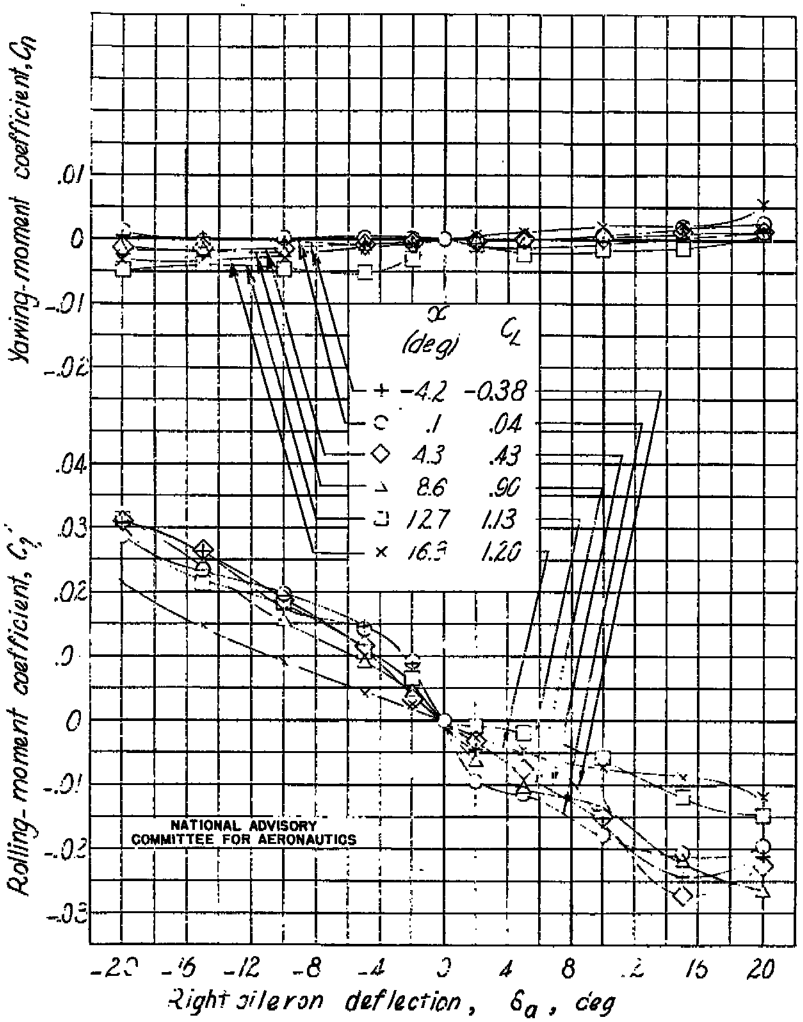

(a) δ_{f_1}, 0°; δ_{f_2}, 0°.

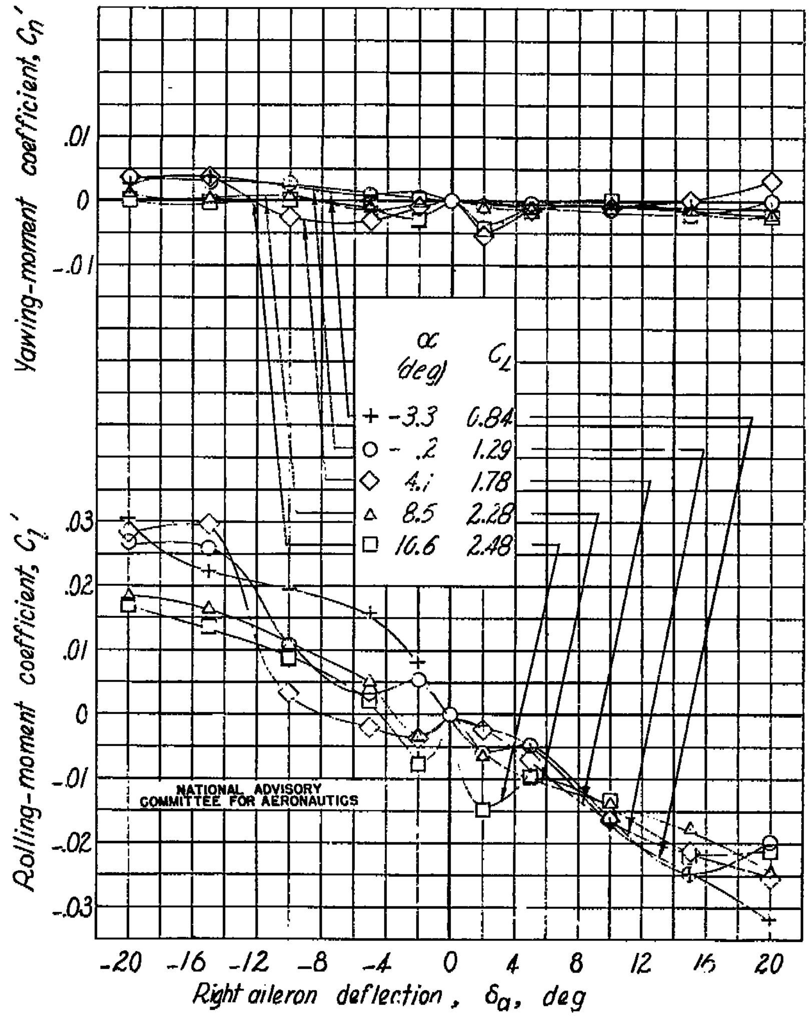

(b) δ_{f_1}, 40°; δ_{f_2}, 50°.

Figure [illegible].- Variation of the rolling- and yawing-moment coefficients with aileron deflection on the [illegible]-scale model.

Figure [illegible].- Concluded.

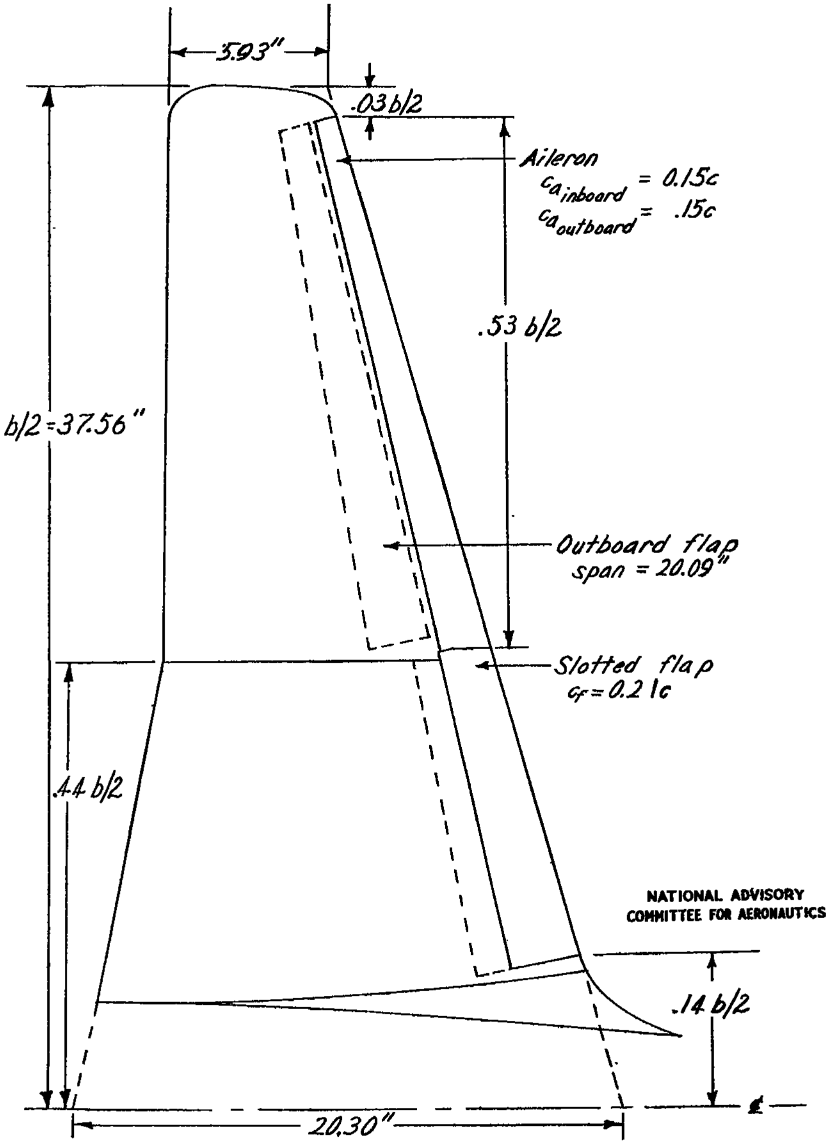

Figure C41.- Plan form of the semispan wing of a $\frac{1}{8}$-scale model of a torpedo-bomber-type airplane tested in the Langley 7- by 10-foot tunnel.

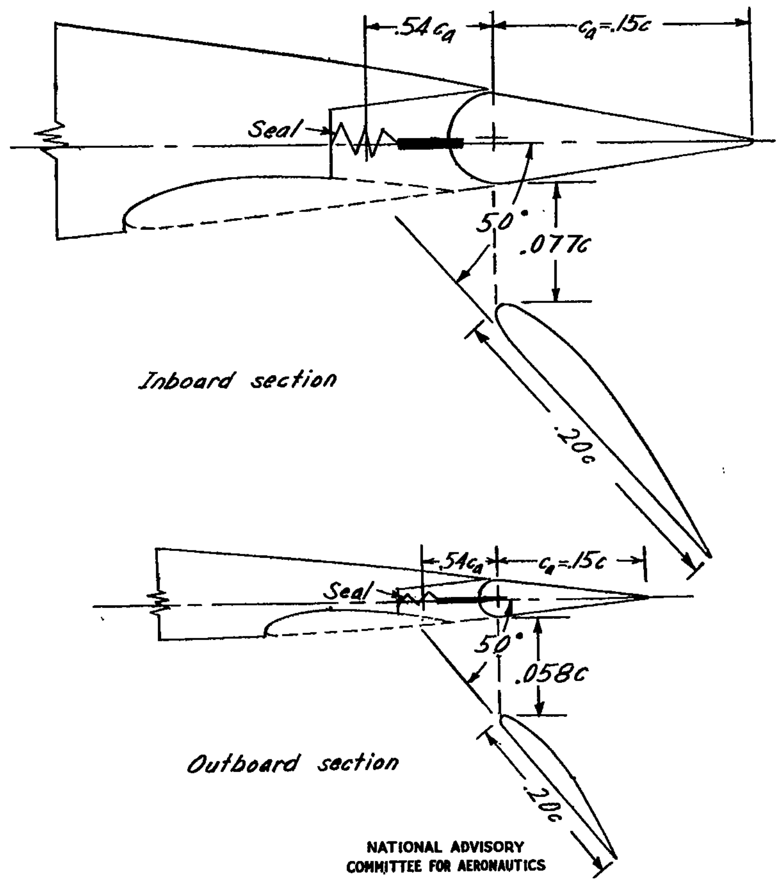

Figure C42.- Sections of the wing at the aileron section, showing the aileron and the outboard flap in the extended position.

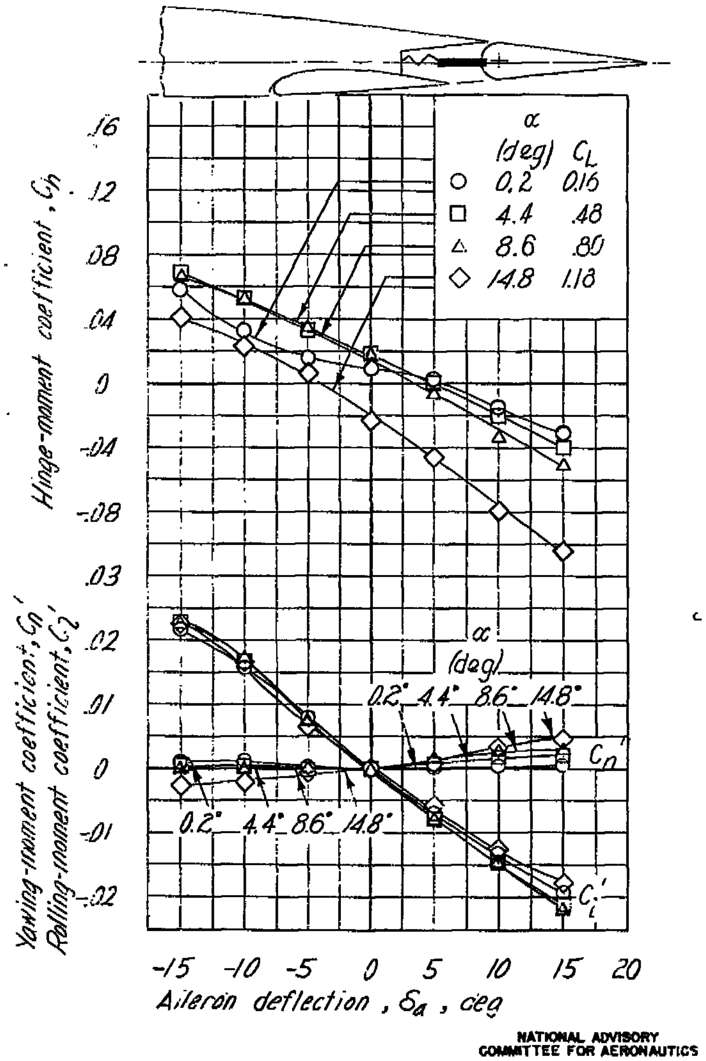

(a) δ_{f_1}, 0°; δ_{f_2}, 0°.

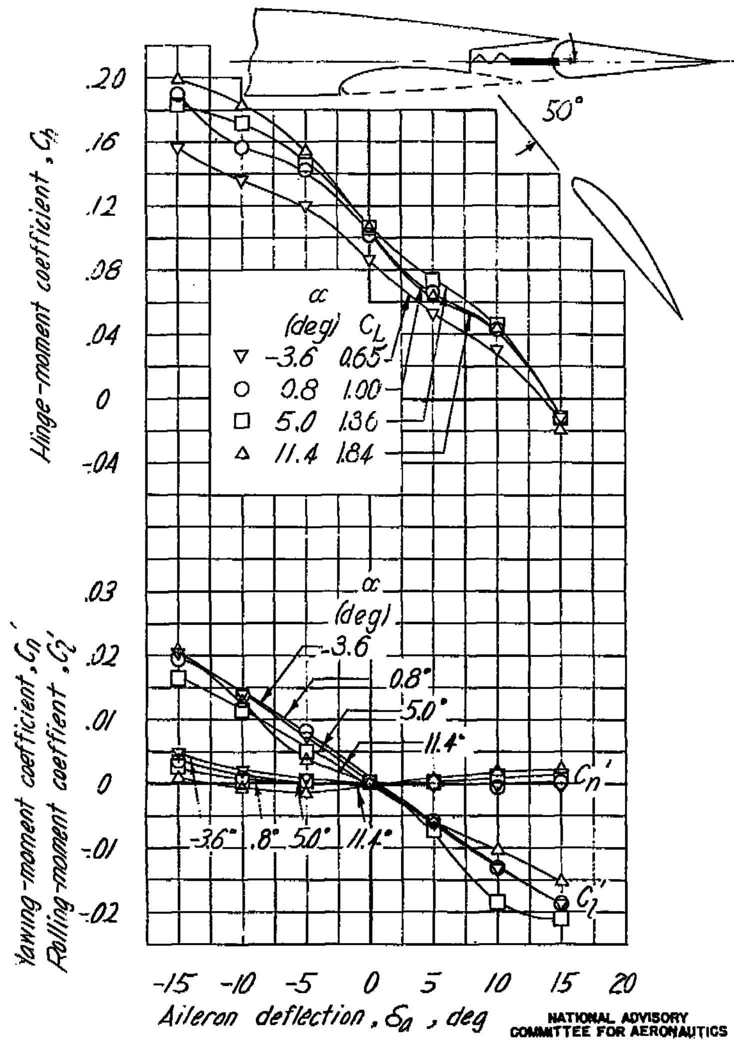

(b) δ_{f_1}, 50°. δ_{f_2}, 50°. Leading-edge slats extended.

Figure C43.- Variation of rolling-, yawing-, and hinge-moment coefficients with right aileron deflection on the $\frac{1}{8}$-scale model airplane.

Figure C43.- Concluded.

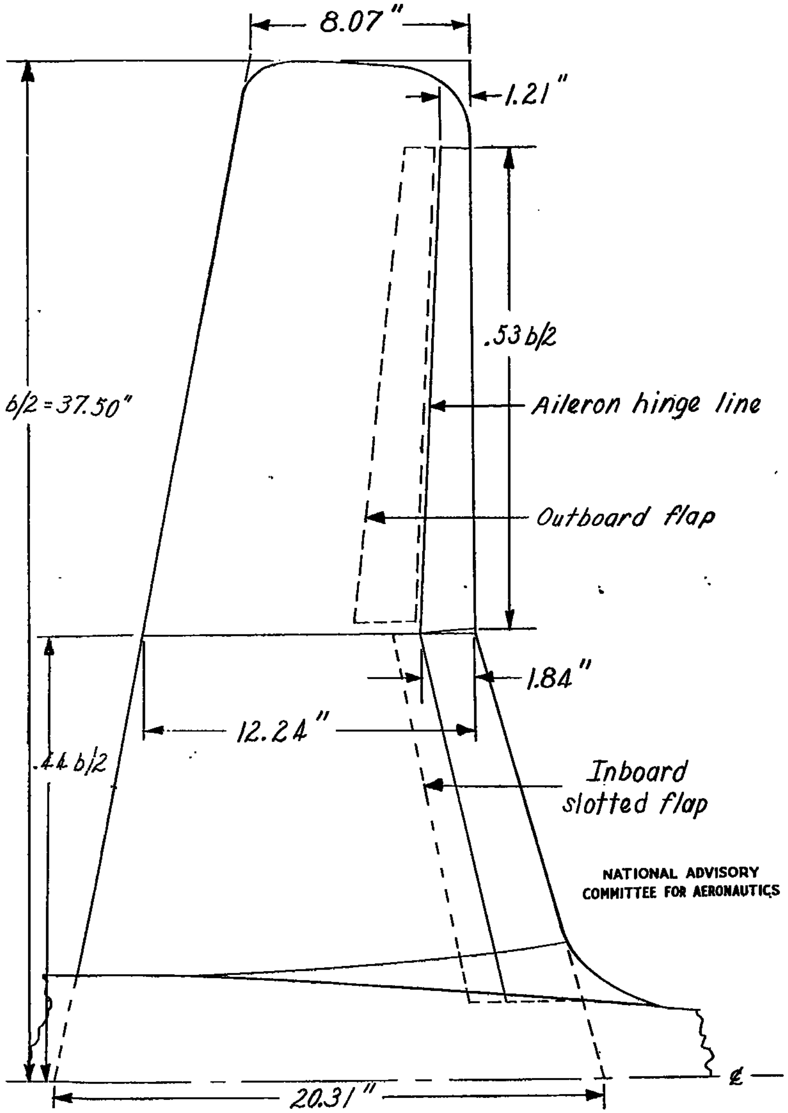

Figure C44.- Plan form of the $\frac{1}{8}$-scale model of the torpedo bomber-type airplane tested in the Langley 7- by 10-foot tunnel.

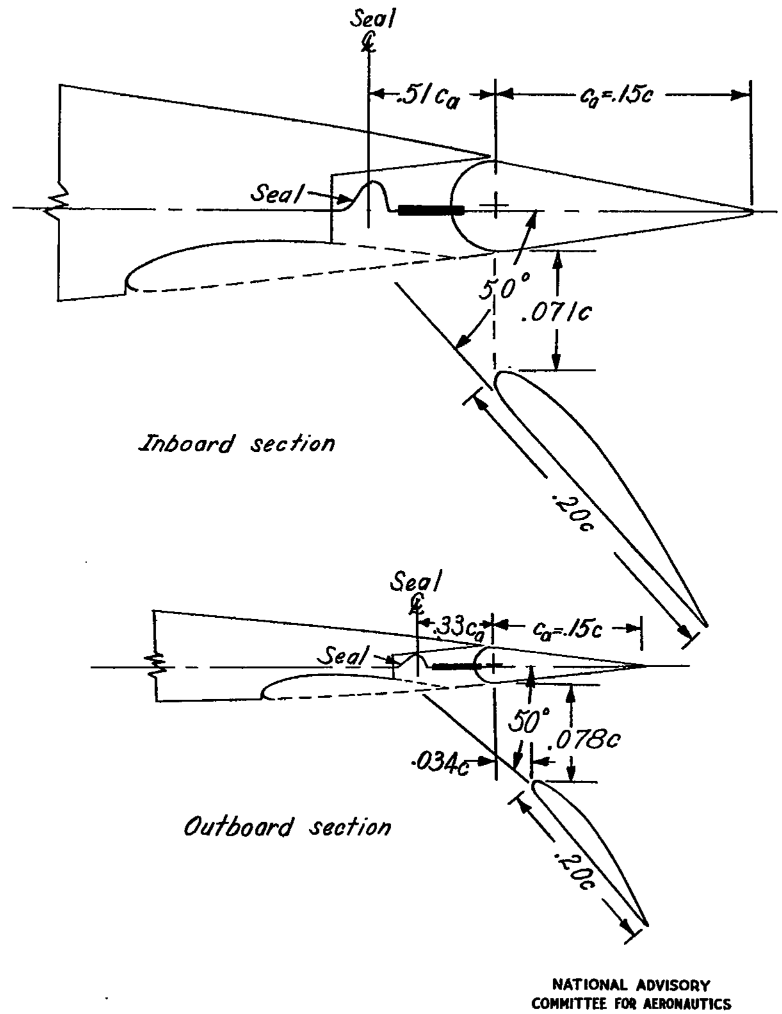

Figure C45.- Aileron sections of the $\frac{1}{8}$-scale model.

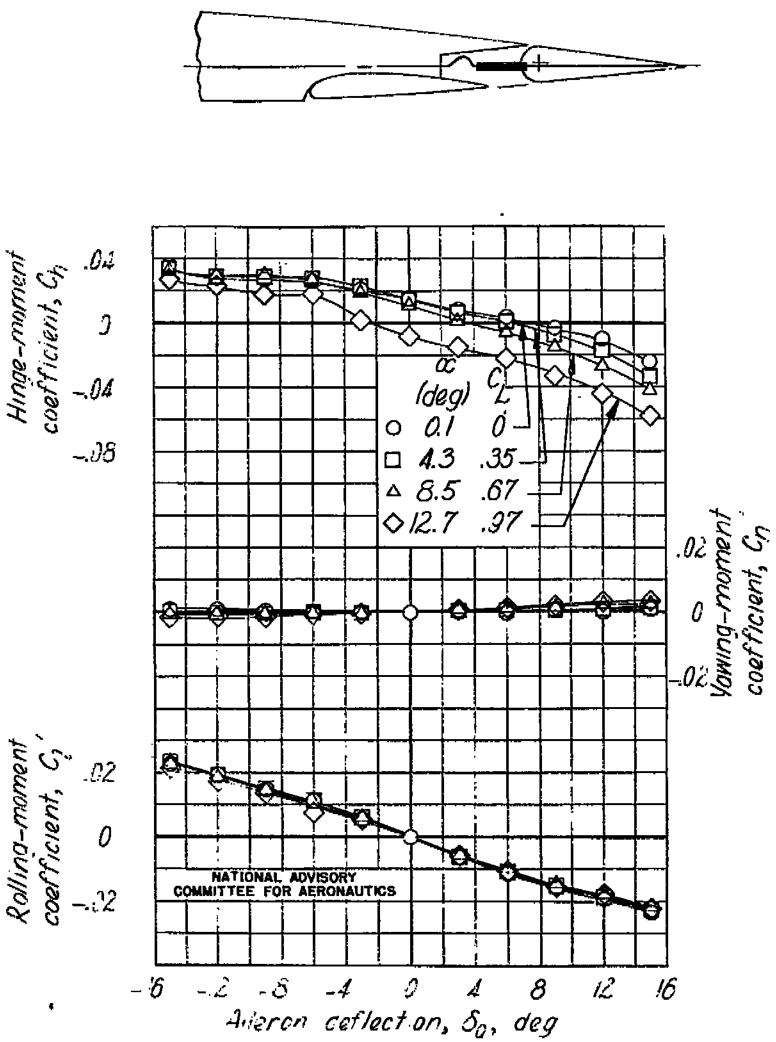

(a) Flaps neutral.

Figure C46.- Variation of the rolling-, yawing-, and hinge-moment characteristics with aileron deflection of the $\frac{1}{3}$-scale model.

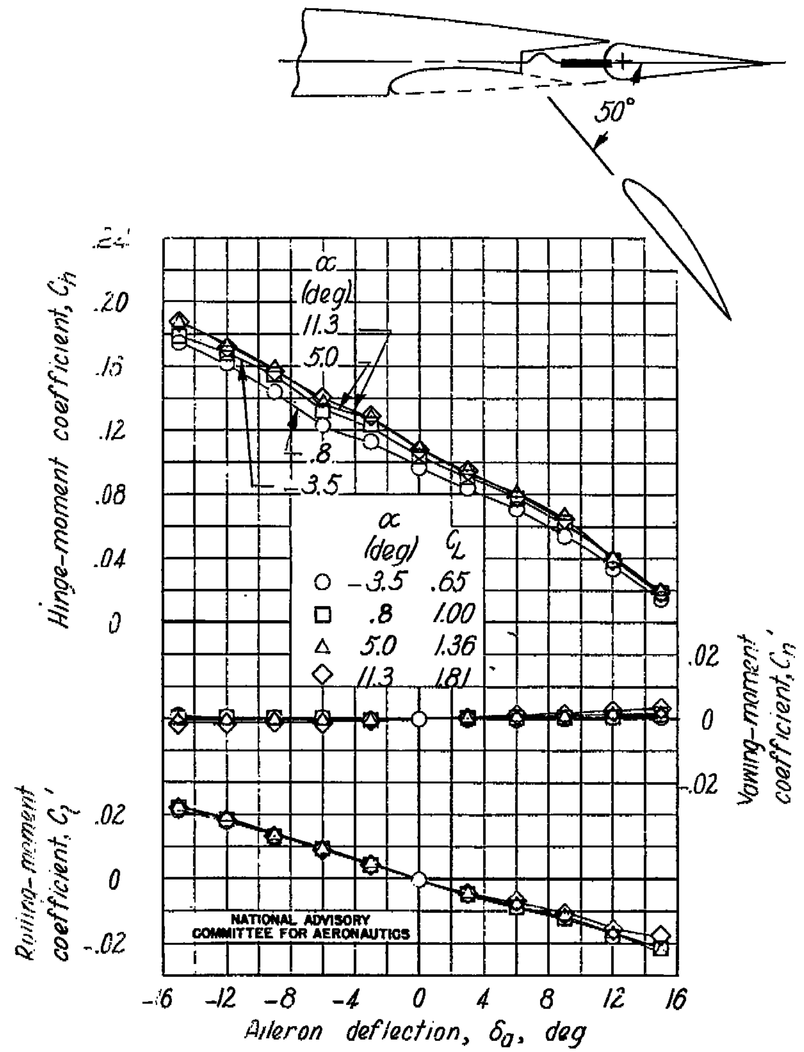

(b) δ_{f_1}, 50°; δ_{f_2}, 50°; leading-edge slats extended.

Figure C46.- Concluded.

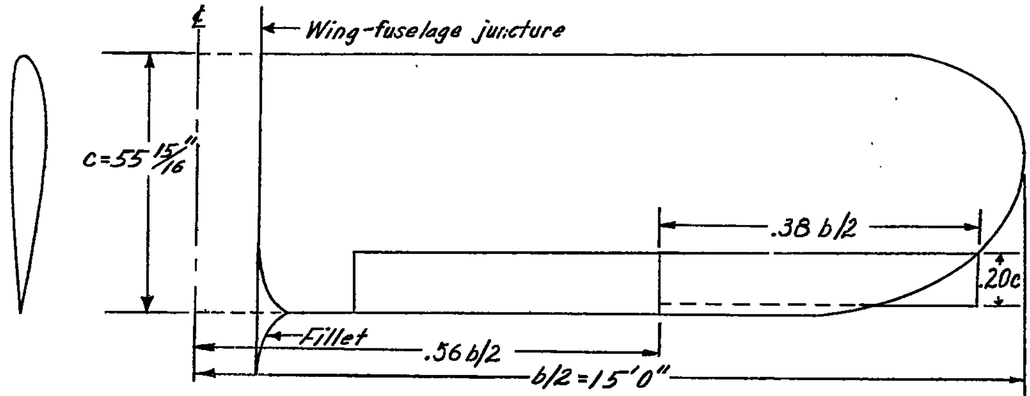

NATIONAL ADVISORY COMMITTEE FOR AERONAUTICS

Figure C47.- Plan form of the semispan wing of a personal-type airplane with fixed and balanced split flaps as tested in flight at Langley.

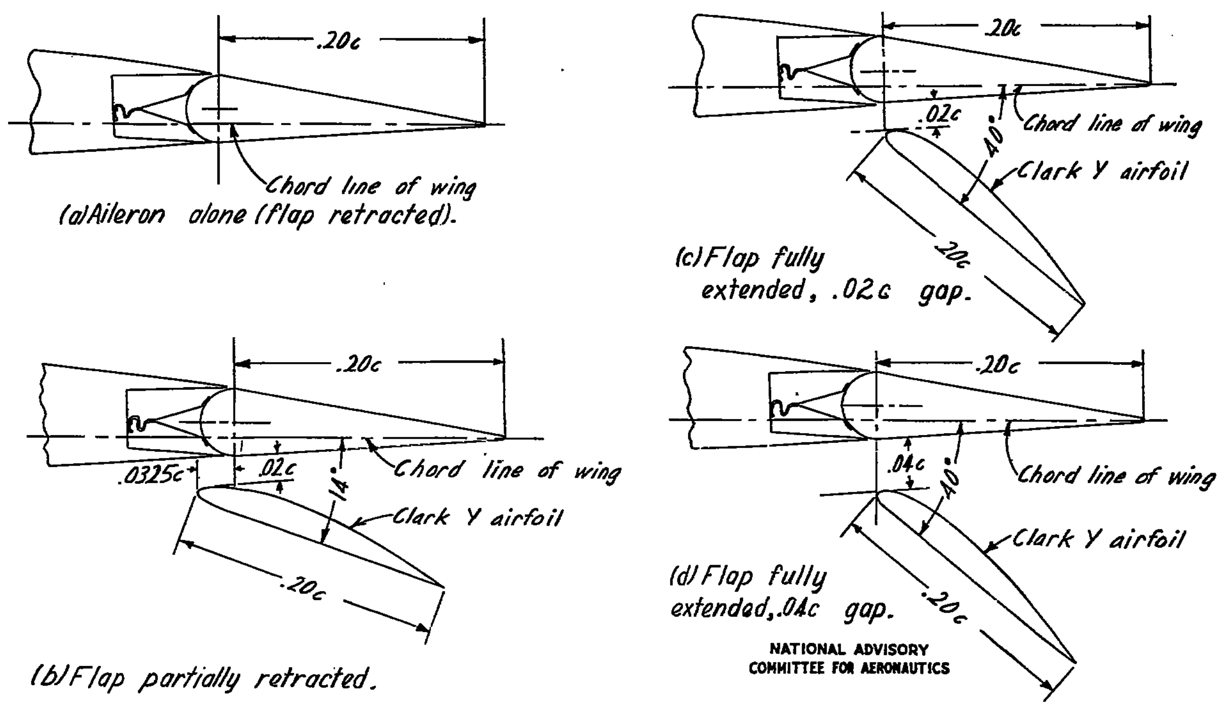

Figure C48.- Sections of internally balanced aileron and balanced split-flap arrangement as tested on a personal-type airplane.

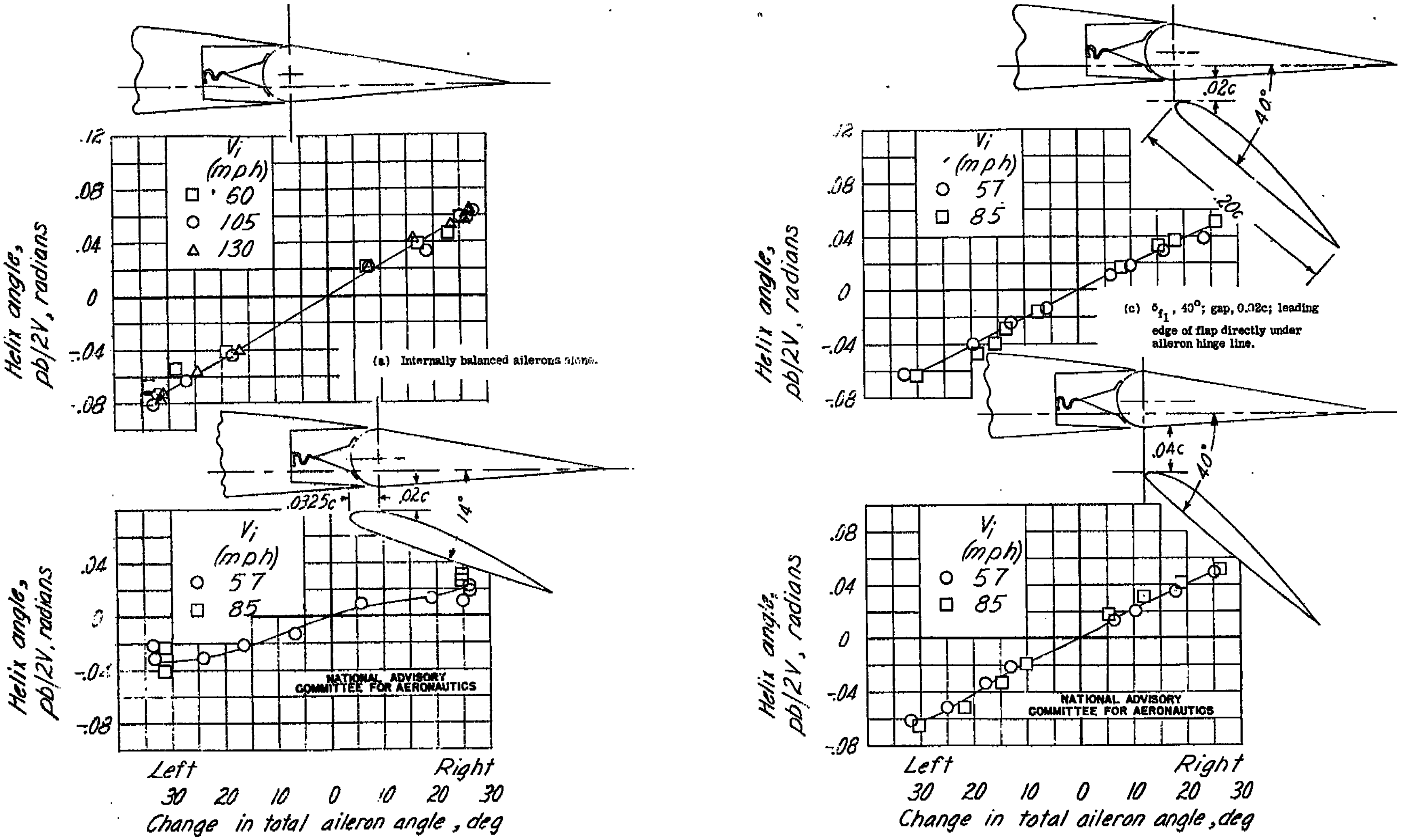

(a) Internally balanced ailerons alone.

(b) δ_{f_1}, 14°; gap, 0.02c; leading edge of flap 0.0325c ahead of aileron hinge line.

(c) δ_{f_1}, 40°; gap, 0.02c; leading edge of flap directly under aileron hinge line.

(d) δ_{f_1}, 40°; gap, 0.04c; leading edge of flap directly under aileron hinge line.

Figure C49.- Variation of helix angle [illegible] with [illegible] deflection [illegible] a personal-type airplane.